E-Proceedings
of
The 5th International Conference on Highway Engineering 2024

"Future-Proofing Roads for Asia and Beyond"

4 - 6 September 2024
Bangkok International Trade & Exhibition Centre (BITEC)
Bangkok, Thailand

Organised by
Department of Highways
and
Roads Association of Thailand

Edited by
Ponlathep Lertworawanich, Ph.D.
Auckpath Sawangsuriya, Ph.D.
Harutus Phoban, Ph.D.

Published by
Department of Highways
Ministry of Transport

E-Proceedings
of
The 5th International Conference on Highway Engineering 2024

"Future-Proofing Roads for Asia and Beyond"

4 - 6 September 2024
Bangkok International Trade & Exhibition Centre (BITEC)
Bangkok, Thailand

Organised by
Department of Highways
and
Roads Association of Thailand

Edited by
Ponlathep Lertworawanich, Ph.D.
Auckpath Sawangsuriya, Ph.D.
Harutus Phoban, Ph.D.

Published by
Department of Highways
Ministry of Transport

iCHE BANGKOK 2024

Published by the Department of Highways, Ministry of Transport
2/486 Si Ayutthaya Road,
Thung Phaya Thai, Ratchathewi,
Bangkok, 10400, Thailand.

ISBN (e-book) 978-616-7754-87-1

Preface

This E-proceedings contains papers from the **International Conference on Highway Engineering 2024 (iCHE2024)** with the theme of **"Future-Proofing Roads for Asia and Beyond"**, held in Bangkok, Thailand, on September 4-6, 2024. This conference is the 5th International Conference on Highway Engineering in this conference series which serves as the platform for national and global leaders, policy-makers, industry professionals, specialists, research scholars, and academia to attend and exchange knowledge, experience, and insights on roads and road transport in these following topics: (a) efficient, inclusive, and safe road management, (b) smart mobility, digital technology, and innovation for roads, and (c) sustainability and resilience of road networks.

This E-proceedings includes a collection of papers from three main tracks of the iCHE2024. **Track A** involves efficient, inclusive, and safe road management. 37 papers were collected in this track. These papers described a wide range of road administrator tasks from planning for effective road networks to managing road infrastructure and transportation system for promoting economic growth and social development as well as improving the lives of citizens across the country. In addition, they also covered road safety management, which is essential towards achieving social equity in accessibility in rural areas.

Track B is associated with smart mobility, digital technology, and innovation for roads. 12 papers were collected in this track. These papers summarized mobility on roads, which was a crucial aspect of modern society, enabling people to access essential services, to engage in economic activities, and to connect with others. The papers addressed the application of new technologies and digital transformation concept in road transport, which optimized the road network operations and enhance the intelligent transportation system. In addition, they also discussed the implementation of emerging technologies and innovations that could help supporting road agencies during the design, construction, operation, and maintenance of roads.

Track C involves sustainability and resilience of road networks. 16 papers were collected in this track. These papers described sustainable and resilient road infrastructure and networks to ensure the serviceability and reliability of road transportation systems. The papers also demonstrated that an increasingly significant global impact of climate change and natural hazards such as floods, landslides, and earthquakes had a devastating impact on road networks, disrupted transportation, and caused significant economic and social harm. The papers presented the resilience of road networks, the development of robust disaster management plans, the investment in resilient infrastructure to mitigate the impact of these events as well as the ongoing monitoring and adaptation to changing conditions. In addition, they also discussed about the decarbonization efforts e.g. the use of low-carbon materials and the adoption of sustainable construction practices, making transportation systems more resilient to the impacts of climate change, and reducing the carbon footprint of road construction and maintenance.

The Editors,
Ponlathep Lertworawanich, Ph.D., Department of Highways
Auckpath Sawangsuriya, Ph.D., Department of Highways
Harutus Phoban, Ph.D., Department of Highways

Acknowledgments

Thanks are due to the authors, reviewers, technical committees, scientific committees, and chairman of iCHE2024 without whom this publication would not be possible.

iCHE2024 Chairman

Dr. Piyapong Jiwattanakulpaisarn
Deputy Director-General for Engineering, Department of Highways

iCHE2024 Scientific Committees

Prof. Dr. Agachai Sumalee, Chulalongkorn School of Integrated Innovation, Thailand
Prof. Dr. Kasem Choocharukul, Chulalongkorn University, Thailand
Prof. Dr. Kunnawee Kanitpong, A sian Institute of Technology, Thailand
Assoc. Prof. Dr. Sorawit Narupiti, Chulalongkorn University, Thailand
Prof. Dr. Saksith Chalermpong, Chulalongkorn University, Thailand
Prof. Dr. Vilas Nitivattananon, Asian Institute of Technology, Thailand
Prof. Dr. Somnuk Tangtermsirikul, Sirindhorn International Institute of Technology, Thailand
Dr. Ponlathep Lertworawanich, Department of Highways, Thailand
Dr. Auckpath Sawangsuriya, Department of Highways, Thailand
Dr. Sumet Ongkittikul, Thailand Development Research Institute (TDRI), Thailand
Prof. Dr. Hiroaki Nishiuchi, Kochi University of Technology, Japan
Dr. John Calvin Milton, Washington State Department of Transportation, United States
Mr. Christos S. Xenophontos, Rhode Island Department of Transportation, United States
Ms. Caroline Evans, PIARC Strategic Theme 1 Coordinator, Australia

iCHE2024 Technical Committees

Attasit Sawatparnich	Advisor
Ponlathep Lertworawanich	Chairman
Jakraphob Watcharamonthian	Member
Auckpath Sawangsuriya	Member
Songrit Chayanan	Member
Tunwin Svasdisant	Member
Sukit Yindeesuk	Member
Gridsana Pensomboon	Member
Patthanapong Tongsuk	Member
Poranic Jitareekul	Member
Chairat Supachawarote	Member
Jutha Sunitsakul	Member
Bhanitiz Aursudkij	Member
Pattharin Sarutipand	Member
Apivat Jotisankasa	Member
Wasin Rujikietgumjorn	Member
Puttipan Seraneeprakarn	Member
Pichanan Aursudkij	Member
Kavalin Wangsiripaisal	Member
Rajwanlop Kumpoopong	Member
Harit Prasertsin	Member
Waritz Rattanasiriphan	Member
Harutus Phoban	Member and Secretary
Warit Chookate	Member and Assistant Secretary
Siwakorn Dumduang	Member and Assistant Secretary
Patra Sukmoung	Member and Assistant Secretary
Nattapong Nusrikaew	Member and Assistant Secretary
Wuttichai Amornprasitpol	Member and Assistant Secretary
Punnawat Siripatthiti	Member and Assistant Secretary

Acknowledgments

Local Reviewers

Ackchai Sirikijpanichkul
Agachai Sumalee
Ampol Karoonsoontawong
Apichai Issariyanukula
Apivat Jotisankasa
Arkhom Termpittayapaisith
Auckpath Sawangsuriya
Boonchai Sangpetngam
Chaiyut Charoenphon
Chakrapan Tuakta
Chutipong Paraphantakul
Dussadee Satirasetthavee
Harit Prasertsin
Jetthawee Mark
Jittichai Rudjanakanoknad
Jumrus Pitaksringkarn
Kasem Choocharukul
Kazuya Tomiyama
Kerkritt Sriroongvikrai
Kriangkrai Pattanapakdee
Kunnawee Kanitpong
Ladda Tanwanichkul
Manop Kaewmoracharoen
Monchai Chumintarajak
Muanmas Wichiensin
Nongnuch Poolsawad
Nopadon Kronprasert
Noppakun Boongrapue
Nuksit Noomwongs
Pakpoom Limtong
Paramet Luathep
Parinya Sanguansat
Pasan Kulvanit
Pattara Kiatisevi
Peeranut Jeammaneeporn
Peerapol Sittivijan
Piya Chotickai
Pongsun Bunditsakulchai
Ponlathep Lertworawanich
Pornpote Nusen
Puttipan Seraneeprakarn
Rapee Tangsongsuwan
Rattaphol Pueboobpaphan
Rosalind Amornpitakpun
Sarawut Jansuwan
Saroch Boonsiripant
Siradech Surit
Sittinun Tongbai
Sivach Kaewcharoen
Somnuk Tangtermsirikul
Songpol Charuvisit
Songrit Chayanan
Sruangsaeng Chaikasetsin
Sukit Yindeesuk
Suladda Subsin
Tanakorn Chaiyarungyos
Teerapong Panboonyuen
Teerapun Phumrattanaprapin
Thaned Satiennam
Thapat Silalertruksa
Thavatchai Tayjasanant
Treerapot Siripirote
Tunwin Svasdisant
Usanee Raha
Warit Wipulanusat
Waritz Rattanasiriphan
Wasin Rujikietgumjorn
Watchara Sattayaprasert
Wichuda Satiennam
Winai Raksuntorn
Wirat Chinnan
Withit Pansuk

Table of Contents

Track A - 1

Efficient, Inclusive and Safe Road Management

Measures of Improving Road Safety

M.R.C.U.Alwis, BSc.Eng., CEng., Senior Engineer
Central Expressway Project-IV, Road Development Authority, Sri Lanka.
cualwis@gmail.com

ABSTRACT

Road accidents have become one of the world's largest Public health and injury prevention problems. According to the World Health Organization (WHO), it is estimated that about 1.2 million people were killed and 50 million injured due to accidents on roads around the world each year. The WHO highlighted that road accidents are more severe in developing countries having a percentage of 90% of world's fatalities even though these countries have approximately 54 % of the World vehicles. Therefore, improving road safety is vital to reduce the number of crash fatalities and injuries over time in any country to achieve substantial increases in economic growth and national income. According to available worldwide road accident data and literature review, it has been identified that human behavior is one of leading factors to many road accidents. Apart from that, increased number of vehicles, poor maintenance of road network, ineffectiveness of authorities in penalizing road traffic offenses and lack of awareness regarding road safety are some of other common factors to increase road traffic injuries and higher fatalities. This crisis in South Asia has significantly increased due to rapid growth in vehicle ownership, speeds and inadequate protection for most vulnerable road users. In this paper, it has been proposed some possible road safety improving measures such as improving road way designs, accident data analysis and adoption of remedial measures, improving road users' behaviors, improvement of laws and regulations, adoption of new technologies, etc. Some of improvements can be incorporated during feasibility and detailed design stages and some of improvements during operation and maintenance stages by analyzing accident data and incorporating mitigation measures such as reducing speed, design modifications etc. Further, it is very important to aware road users regarding road safety. In this task, introduction of road safety into school curriculum plays a significant role to improve the road safety.

Keywords: Road safety, Road accidents, Improving measures, Road user, Awareness

1. INTRODUCTION

Road traffic deaths and injuries are major global health and development challenge. Many governments are grappling to ensure that transport safety and road safety have been accorded high priority on international development agenda because of their magnitude and impact on the society and economy. More than half of fatalities are among pedestrians, motorcyclists and cyclists and whereas occupants of four-wheel vehicles account for approximately one-third of fatalities; occupants of vehicles carrying more than ten people, heavy goods vehicles constitute one-fifth of all deaths (World Health Organization [WHO], 2023). Road traffic crashes are the leading killer of children and youth aged 5 to 29 years and are the 12th leading cause of death when all ages are considered (WHO, 2023). Two-thirds of deaths occur among people of working aged 18–59 years (WHO, 2023). In the Asia – Pacific region, three people in every two minutes are killed on roads, resulting more than fourteen thousand lives in the region being lost every week due to road accidents. This is nearly 60% of global total road traffic deaths of a year (Economic and social commission for Asia and the Pacific [ESCAP], 2016). Pedestrians and non-motorized transport users in many developing

countries are significantly exposed to road accidents compared with developed countries. It is about more than 26 % of total fatalities in the world (ESCAP, 2016).Thousands of hospital beds are being occupied by injured people involved in road accidents. Therefore, road accidents are considered as a global epidemic causing huge health, social and economic harm throughout the society.
Road safety is one of sustainable development goals to reduce the number of global deaths and injuries from road traffic accidents and to provide safe, affordable, accessible transport systems for everybody. To reduce road traffic accidents and to provide safe road systems, improving road safety plays an important role. Some of measures such as enforcing laws and regulations, adopting of new technologies, conducting road safety awareness programmes, road safety audit and adoption of remedial measures etc. are already being implemented in some countries to improve road safety. Objectives of this technical paper is to identify inadequacies and weaknesses of the present practices and to propose possible road safety improving measures to reduce road accidents.

2. MEASURES OF IMPROVING ROAD SAFETY

Road safety improvement can be started from feasibility stage and carried out up to operation and maintenance stages for a new road project and whereas for an existing road, it can be done by analyzing safety issues such as blackspots analysis and adoption of mitigation measures. Road safety improvement can be mainly done by enforcing or enhancing laws and regulations, incorporating safety standards into construction of road infrastructure facilities, adoption of new technologies, improving road safety awareness etc.
In this technical paper, a limited number of road accident data from various sources such as available publications from World Health Organization (WHO, 2023), The World Bank. (WB ,2023), as well as some of published road accident data in several countries including India (Ministry of Road Transport and Highways [MORTH], 2021), Sri Lanka (Ministry of Transport and Highways [MOTH], 2023), Australia (Department for Infrastructure and Transport [DIT], 2022), South Africa (International Transport Forum [ITF],2019) has been referred to identify common causes for road accidents. Some of identified key factors have been tabulated in table 1 .

Table 01 Major causes of road crashes in different countries

Country	Major cause(s)
Sri Lanka	Speeding, lack of awareness of road users, road infrastructures
India	Driver's fault, road infrastructures
Napal	Negligence by drivers
Australia	Speeding, influence of alcohol, seat belts and helmets
South Affrica	Speeding, influence of alcohol, road infrastructures
Mexico	Mobile phones, influence of alcohol
Cambodia	Helmets, seat belts
Bhutan	Speeding, influence of alcohol
Bangladesh	Helmets

It is obvious that human behaviors and road infrastructure facilities have caused significant impact to many road accidents. Most of accidents can be prevented if proper mitigation measures are adopted ensuring the road safety. In the process of proposing possible road safety improving measures, a comprehensive review has been done on existing laws and regulations regarding road users and vehicles, worldwide practicing road design guidelines and manuals such as Austroads, AASHTO and present published road safety manuals in different countries. Details of possible improvement measures that can be adopted to enhance road safety are discussed below.

2.1 Speed management

The speed at which a vehicle travel directly influences the risk of a road accident as well as the severity of injuries sustained or the death resulting from that accident. Therefore, adoption of a safe speed limit plays an important role in reducing road accidents. It is very important to reduce vehicle speeds in areas where the road user mix included a significant volume of vulnerable road users, such as pedestrians and cyclists. In many countries, it has been adopted national speed limit as 50 km/h for urban or built-up areas and whereas it is about 70 km/h in rural areas (Austroads, 2009). But it has been observed that some countries have adopted speed limit as 30 km/h for urban areas to reduce accident rate. By analyzing accident data, it has been revealed that nearly 50% of drivers have violated speed limits. A reduction of 5% of average speed can reduce the number of fatal accidents approximately by 30% (ESCAP, 2016). Therefore, it is necessary to take suitable measures to reduce speed specially in urban areas where there is a high concentration of vulnerable road users.

Reduction of speed can be done by imposing national speed limits together with adoption of traffic calming measures. Traffic calming is a combination of mainly physical measures that can reduce the negative effects of motor vehicle use, alter drivers' behaviors and improve the condition of non-motorized road users. Imposing a speed limit at a place should be aware of drivers with proper road signs and markings ahead of the location (American Association of State Highway & Transport Officials. [AASHTO], 2018). There shall be a sufficient distance and visibility to take reactions without any complication to drivers.

Adoption of traffic calming measures to improve road safety can be done either by speed control devices or volume control devices (Austroads, 2009). Speed control devices will be either vertical deflection, horizontal deflection or horizontal narrowing. Speed humps, speed tables, raised crosswalks, textured pavements can be adopted for vertical deflection and whereas traffic circles, roundabouts can be adopted for horizontal deflection. Median barriers can be adopted as a method of volume control device. Apart from these, full closer or half closure can be adopted whenever necessary. (eg. near school zones).

From literature review, it has been observed that only penalties in the form of fines are not much effective in improving drivers' attitudes. Therefore, it is necessary to introduce and enforce a method of merit system that is linked to the driving license. As an example , it can be suggested that higher speed beyond the posted speed, more merit points will be lost and at a certain stage temporary suspension of the driving license can be done. In this case, it is required to adopt new technologies in detecting high speed vehicles with aid of CCTV cameras. The use of speed cameras helps to enforce speed limits and also to identify penalties for offenders in the form of fines. Further, fixing of GPS for every vehicle can be used to monitor speed of vehicles apart from CCTV cameras. Therefore, enforcing speed laws and adoption of new technologies will play a significant role in speed management and thus these will result to reduce the number of fatalities and improving road safety.

2.2 Safe vehicle

Safe vehicles play an important role in reduction of road accidents. The current motor vehicle fleet has already exceeded one billion vehicles and is likely to double by 2030 (WHO, 2023). In many cases, vehicles are being produced and sold even without meeting minimum safety standards. This condition is worst in the middle-and low-income countries. Many manufacturers tend to produce vehicles at a low cost where regulations on manufacturing are weak. It has been reported that about 23 million used passenger vehicles during the period of 2015-2020 have been exported and out of 66% of them are to low-and middle-income countries without ensuring safety regulation of these vehicles (WHO, 2023). This has directly influenced to increase number of road accidents. Therefore, it is necessary to enforce laws and regulations on manufacturing new vehicles as well as exporting used vehicles.

Further, it is compulsory to enforce laws regarding safety equipment of vehicles, such as braking system, electronic stability control, front and side impact protection and pedestrian protection. Apart from these, it is essential to have regulations regarding periodic inspections and assessment of vehicles. It can be seen that most countries haven't proper regulations or standards to certify or pass assessments of vehicles. Further, in the case of fossil fuel vehicles, it is required to maintain emissions at acceptable standards. Emission of Carbon dioxide, Carbon monoxide and other toxic gases has caused significant threat to public health as well as fauna and flora. In most countries, when issuing revenue licenses for vehicles, fuel emission test reports and vehicle fitness certificates are normally considered (The World Bank, 2020). But other safety equipment of vehicles are not at all considered. Even in periodic service of vehicles, most vehicle owners/users concern regarding running conditions, but not all other safety aspects of vehicles.

Therefore, it is compulsory to fulfill at least minimum safety requirements prior to drive any vehicle. Further, importing of used vehicles to any country, it is required to satisfy mechanical and safety standards. But most countries especially in developing countries have only a few standards. Therefore, formulation of worldwide acceptable standards for a safe vehicle has become an essential requirement to reduce road accidents and to improve road safety. In the process of formulation of these standards, existing non-governmental organizations for road transport such as World Road Association, International Road Federation and International Road Transport Union can play a significant role in making arrangements to initiate an inter-governmental international technical organization to formulate required standards. Accordingly, vehicle production, exporting and importing can be carried out to satisfy the safety requirements of this organization. If this organization is established, it will result to reduce road accidents at considerable level due to safer vehicle fleet in the global road networks in the future.

2.3 Adoption of road safety audit

Presently, most of road networks have been designed and constructed to cater to traffic demands and to provide required infrastructure facilities for the development. But any road infrastructure facility also has to design, construct, operate and maintain to eliminate or reduce possible accident risks for all road users apart from its key objectives. Therefore, it is essential to conduct road safety audit to verify its safety adequacy.

The objectives of road safety audit are to minimize risk and severity of road accidents that might be affected by the road project at the site or nearby network, minimize the need for remedial work after construction, reduce the whole- life cycle costs of the project, improve the awareness of safe design practices by all of those involved in planning, design, construction and maintenance of roads. Road safety audit can be carried out during feasibility stage in selection of routes, selection of design standards, etc. to verify adequate level of safety. During the preliminary design stage safety audit, it can be further improved in selection of safe horizontal and vertical alignments, super elevations, sight distances, lane configuration etc. During the detailed design stage road safety auditing, further improvements can be made through road signs and lane markings, street lighting, providing adequate clearance to road side objects, provisions for road user groups with special requirements, guard rails, fencing, drainage etc. Further, safety improvements can be made prior to opening the road to traffic. This audit involves driving, riding and walking through the project area to check the adequacy for the needs of all road users in both wet and dry conditions, including night time inspections. If any modifications or alterations are required to assure standards as well as to improve safety, it can be adopted from the outcomes of road safety audit.

Final road safety auditing of a new road network can be done during operation followed by systematic examination of sections to assess the adequacy of the road, intersection, road site etc. From the findings of the audit, it can be incorporated any alterations or modifications required to improve the safety. On the other hand, safety audit for an existing road network can be done with a view of identifying safety related deficiencies. Identification of blackspots and adoption of remedial measures, improving road pavement conditions etc. are some of possible examples to improve road safety. Further, it is required to have national legislation on formal road safety auditing for existing roads and systematic programmes to upgrade higher risk locations to safer status by allocating required funds. Thus, findings from road safety auditing, provision of safe road infrastructure can be achieved by adopting safety standards.

A case study has been carried out in Sri Lanka on Colombo Kandy Highway (A-001) which is the first constructed road linking the city of Colombo to Kandy having a length of 116 km during the colonial period in 1820. This is one of highly traffic congested roads in Sri Lanka and many towns and commercial activities can be seen either side of the road. Due to reported high fatal accidents rate in each year throughout road sections, a road safety audit had been done in 2008. All necessary information and data required about the route had been collected from relevant authorities before going to the site for observations. The data set included available traffic counts, land use patterns, speed levels and accident blackspots if there were any. Particular accident data had been obtained from Sri Lanka police.

After gathering all road and environment information around, audit surveys of the route were started from Colombo which selected as a starting point and marked as 00 + 000 km and carried out both left and right sides separately. Features like lane width, shoulder width, median type and width, road side clear zones, traffic volume, posted legal speed limit, surroundings or land use and other elements were recorded and analyzed during the audit.

The existing geometric parameters of different cross sections on the audited road were compared with the Geometric Design Standards of Roads by Road Development Authority (RDA). This has been prepared based on AASHTO and Austroads Highway Design Manuals to suit national conditions in Sri Lanka. The results are displayed in Table 2.

Table 2. Available design comparisons with RDA Standards

No	Roadway Element	Standard Values	Observed Values
1	Design Speed	50-80 km/hr depending on the terrain	30-90 km/hr
2	Number of lanes	Two or more	Two lanes
3	Travel lane width	3.5 m (minimum)	2.8-3.3 m
4	Right hard shoulder width	2.4 m	0.3-2.0 m
5	Left hard shoulder width	2.4 m	0.4-2.0 m
6	Right soft shoulder width	0.6 m	0.0-0.5
7	Left soft shoulder width	0.6 m	0.0-0.75
8	Fill slope	1.5H:1V	1.5H:1V - 1H:3V
9	Cut Slope	1H:4V	1H:4V - 1H:7V
10	Min. bridge vertical clear	6.5 m	6.5 m -7.0 m
11	Bridge width	Full approach travelled way width	2/3 of traveled way width
12	Control of access	Partial/by regulation	Uncontrolled access
13	Alignment	Adequate & smooth flowing alignment	Poor alignment
15	Pedestrians crossing	Controlled	Uncontrolled
16	Foot walk	0.9 m (minimum)	Randomly provided
17	Drainage	0.9 m (minimum)	Randomly provided

The most common and dangerous hazards identified and classified were insufficient of lane configurations, missing shoulder, improper junction design, potholes, improper commercial activities layouts on road sides, improper bus stop locations, edge deterioration and missing signs, dangerous fixed objects on roadside etc. Majority of these hazards were associated with road side safety issues. Overall alignment features both horizontal and vertical were also found as inappropriate in many locations.

From findings of the study, it was recommended to have road improvements with aid of funding arrangement in 2010 and completed in 2012. The major improvements included modifications of horizontal and vertical alignments to cater 70 km/hr operating speed with standard two land configurations. Accordingly, 3.5 m wide dual carriageway, 2.4 m wide hard shoulder, 0.6 m wide soft shoulder were adopted with built up drains at suitable locations, pedestrian facilities specially at town areas, road signing and road marking, widening culverts and bridges, street lighting etc. Further, establishment of Right of Way boundary removing of unauthorized structures and other obstacles were also included as per the findings from the road safety audit. After analyzing accident data in consecutive years after the road improvement, it has been observed that a reduction of road accident rate is about 45% compared with previous accidents rates.

2.4 Strengthening legislation on drink-driving

Drink-driving is one of major causes of deaths in road accidents. Drink-driving has significantly increased risk and severity leading to fatal accidents. Studies carried out in low-and middle-income countries have shown that between 33%-69% of fatally injured drivers have consumed alcohol before accidents (WHO, 2023). Most counties have enacted national drink-driving legislation but out of them, only few countries have defined blood alcohol concentration. Countries such as Australia and New Zealand have set it as Zero level and some countries have defined levels between 0.02-1.0 grams per deciliter (ESCAP, 2016).

To reduce road accidents due to drink-driving, it is required to strengthen existing legislation of every country. In this event, it can make significant contributions through international organizations such as WHO to formulate worldwide acceptable legislation. Canceling drunk drivers' driving licenses for certain periods, making penalties in the process of relicensing after disqualification periods are some of possible measures to reduce drink-driving attitudes of drivers to improve road safety.

2.5 Introducing of legislation on driving with mobile phones

Driving with mobile phones has become a growing problem of drivers' distraction in the world contributing to road accidents (WHO, 2023). Usage of mobile phones while driving reduces the concentration of drivers on road signs and markings, behaviors of incoming vehicles, vulnerable road users and automatically loses control of vehicles resulting accidents. Therefore, it is required to prohibit the use of mobile phones while driving to ensure safety. To overcome this growing threat due to mobile phones, it is required to have proper legislation prohibiting usage of mobile phones while driving to enhance road safety.

2.6 Wearing quality helmets

Head injuries are the main cause of death in most motorcycle accidents. Quality helmets reduce the risk of death at least six times and reduce the brain injury risk up to 74% (WHO, 2023). However, helmet wearing rates for different countries vary from 7% - 99% around the world. Wearing helmet rates in urban areas are significantly higher than in rural areas. And also, wearing rate of motorcycle drivers is much higher than that of passengers. Studies carried out in Thailand have found that the helmet wearing rate of rural passengers is about 12% compared with 83% of urban drivers (ESCAP, 2016).

The use of life saving helmets often lags far behind specially in developing countries. This has mainly influenced availability and affordability of quality helmets. Low quality helmets may protect drivers and passengers from the police, but it is not protected the users from deaths and injuries. Therefore, to improve safety of wearing helmets, it is required to adopt best practice criteria that applies law on both drivers and passengers to all road types specifying helmet standards.

2.7 Seat belts and child restraints

Most of countries have adopted national laws on wearing seat belts to improve safety on passengers as well as drivers. Even though all occupants of vehicles are necessary to wear seat belts to minimize injuries in road accidents, it can be seen that wearing seat belts more than 90% of few countries such as Australia, Japan, New Zealand and countries such as India and China, it is less than 50% (ESCAP, 2016). This gives an indication that, it is required to adopt more strategies to improve seat belt wearing rates such as imposing more fines for offenders. In addition to seat belts, child restraint systems are very important to protect infants and children (up to age ten years) from injuries in road accidents. Therefore, enhancing national legislation on helmets, seat belts and child restraints for every country plays a significant role in improving road safety.

2.8 Restrictions on overloading and overhanging vehicles

Overloading of passengers in public transport has become an issue specially in developing countries. This has directly affected to increase number of victims in road accidents. Overloaded passenger vehicles, overloaded and overhung goods transport vehicles have caused to reduce their safe running conditions specially at higher speed creating lots of road accidents. On the other hand, overloaded vehicles damage the road pavement resulting higher maintenance cost. Therefore, in the absence of laws and regulations to control these issues, it is necessary to enact national legislation on overloaded and overhung vehicles to improve road safety.

2.9 Promoting of multimodal transport system

It has been forecast that the present vehicle fleet is to be double by the year 2030 (WHO, 2023) and many countries are still struggling to provide adequate road networks with required level of services. But due to economic situations in developing countries, it has become a difficult task. Further, about 60% of global population is expected to live in urban areas by the year 2030 (WHO, 2023) and it is expected that mobility demand will exceed the capacity of these areas. This will create traffic congestion on road networks, resulting more road accidents and air pollution.

Multimodal transport system is good solution to reduce traffic congestion. To promote multimodal transport system, many developed countries have empowered some rules and regulations to limit vehicles entering cities. Some of rules are permissions for vehicles to enter cities based on registration number plate basis only for several days per week, minimum number of passengers required in private vehicles to enter cities etc. But it is better to improve facilities on parking and riding, facilities public transport and introduce road taxes for private vehicles in urban areas to curtail private vehicles entering cities. Reduction of vehicle capacity in urban areas will enhance safety of vulnerable road users and reduce road accident rates.

2.10 Road safety into school curriculum

As discussed above, road traffic crashes are the leading killer of children and youth aged 5 to 29 years and the 12th leading cause of death when all ages are considered (WHO, 2023).This has given an indication to educate children and young generation regarding road safety to reduce road accidents.

Children are normally classified as anybody under the age of 14 years. Within this age group, there is a further difference between junior primary and senior primary, i.e., between aged 7 to 10 years and aged 11 to 14 years. It is generally accepted that children under age of 7 years should not be allowed unaccompanied in traffic (Transport Research Laboratory [TRL], 1997). These children behave significantly different from adults in traffic. They have physical and mental characteristics that limit their ability to handle complex traffic situations. Most children from aged 7 to 10 years can walk to school alone. Above 10 years, children can start riding bicycles where they share the road with vehicles in some cases.

Teaching about road safety to children requires a multi-medium approach over several years with a lot of repetitions. A multi-medium approach is necessary as a specific medium will be effective with one child, but not for others. It is most important of educating children through parents, older family members and teachers. Setting good examples and consistently adhering to the rules of road safety are very important.

Children need to be more aware of road safety and shall be taught survival skills appropriate to their ages and needs. Road safety education requires to provide necessary structures for acquisition of safety knowledge and skills. These need to include decision making skills, identification, assessment of risk and strategies to reduce these risks. Further, road safety education requires to prepare children for different tasks at each stage progressively and independently to use road network and later as adults.

Roads in developing countries are often more unsafe than roads in developed countries and traffic safety problems faced by children are greater in developing countries (TRL, 1997). In the absence of traffic education, children expose to unnecessary risk. Since traffic circumstances and problems faced by such children are very different from developed countries, it is inappropriate to simply use teaching materials from developed countries to teach road safety. Therefore, local curriculum needs to be developed using worldwide acceptable standards. It will need to reflect the needs, problems and circumstances of relevance to each country's children.

It is essential for long-term prospects of road safety education in schools that there will be adequate provision in the national curriculum. The curriculum content must of course be well defined, based on sound educational principles and should reflect local needs and accident problems. Road safety education can naturally fit into many topics such as within life skills, social studies or health education. Where ever possible, specific road safety lessons can be included in school time table, but it shall also be incorporated into other subjects throughout the year. Further, road safety lesson content shall be relevant to local conditions including practical roadside trainings and be reinforced on a regular basis. Initially, it will be necessary for school students in the age of 12 years to compulsorily study for a road safety certificate at junior level that covers pedestrian and two-wheeler safety. At the age of 16 years, students will require a road safety certificate at senior level that covers wider knowledge of road safety. Therefore, the possibility shall be looked to issue safety certificates to students who have sufficient knowledge in road safety. Further, its' validity shall be considered as a requirement to apply for driving licenses. This method will reduce road accidents considerably in the future.

2.11 Road safety awareness programmes

To improve road safety among the society, it is vital to conduct suitable awareness programmes targeting groups such as school children, drivers and vulnerable road users (The World Bank, 2020). Awareness programmes will be in the form of lectures, practical sessions, presentations depending on education levels of each group in the society. These progeammes shall include laws and regulations regarding road users, road signs and markings, accident preventive methods, post-crash consequences etc. Proper awareness among the society will help to reduce road accident rates and improve safety of road users.

3. CONCLUSION

From the findings of this study, it has shown that factors such as rapid growth rate of motor traffic fleet in global road networks, behaviors of road users, inadequate regulations, lack of road safety awareness have caused significant number of road traffic deaths and injuries at present causing global health and development challenges. To eradicate this global epidemic, improving of road safety measures plays an important role. As discussed above, there are several methods that can be adopted to improve road safety locally as well as internationally. In this task, intergovernmental and international organizations acting on road safety can play a significant role to take remedial measures to improve road safety. It is clear that during the Covid 19 epidemic situation every country, regions, governmental and non-governmental organizations of health came together under one flag to defeat the epidemic within a short period of time. Similarly, these best practices can be adopted in the process of improving road safety around the world.

It has shown from this study that speed management and provision of safe road infrastructure are mainly dependent on design aspects. Therefore, adoption of proper design standards followed with road safety auditing during design, construction and operation stages play a significant role to reduce road accidents and improve road safety. Drink driving, violation of speed limits, use of mobile phones while driving are some of identified drivers' behaviors in this study and changing drivers' attitudes directly will help to improve road safety. Changing attitudes can be done by proper awareness at a considerable extent but it is required to enact regulations to suit present driving behaviors. Introducing or enhancing existing regulations on drink-driving, usage of mobile phones while driving, wearing helmets and seat belts are some of other areas to be considered to improve road safety. Further, it is very important to teach road safety for school children to change their attitudes. This will directly relate to rapid improvement in road safety in the future. Therefore, it is compulsory to introduce road safety into school curriculum. Adoption of new technologies in the process of detecting speed limits violations and accidents are more effective than current conventional practices. All road safety violations are also needed to record digitally rather than present conventional recording practices carried out in some countries. This data base is very useful in deciding what kind of penalties shall issue to offenders for violations of safety rules and also avoid possible malpractices that exist in the present conventional practices. Further, prior to issuing of driving licenses, revenue licenses, insurance, etc. it will be very useful to refer this data base to detect previous accidents and violations of road safety and act accordingly. Adoption of these methodologies will also reduce accident rate in road networks significantly.

The existing non-governmental organizations for road transport such as World Road Association, International Road Transport Union, International Road Federations as well as road safety policymakers and designers can play a significant role giving their support to improve road safety measures as discussed above. Further, sharing knowledge of best practices among professionals, workshops and awareness campaigns, etc. can be effectively implemented through inter agencies such as WHO, Asian Development Bank, Global Road Safety Partnerships and United Nations Road Safety Collaborations to improve road safety.

Limited financial allocations to implement road safety improvement measures is one of issues faced by many countries including developing countries. Therefore, it is required to seek possible financing assistance from international donor agencies or need to have their own strategies. Such strategies will be in the form of taxes from revenue licenses, vehicle insurances and fuel to gather allocations for improvement of road safety. Further, in preparation of estimates for road construction, it is necessary to include at least 5% of the total civil work amount for road safety improvements.

In this paper, it has been discussed some possible key factors that should be considered to improve road safety.

Therefore, to mitigate present growing global threat due to road accidents, adoption of above discussed road safety improvement measures will play a significant role to reduce road accidents at a considerable level in the future.

4. ACKNOWLEDGEMENT

The author wishes to extend the gratitude to senior officers of Road Development Authority of Sri Lanka, regarding their encouragement to present this technical paper.

5. REFERENCES

American Association of State Highway & Transport Officials. [AASHTO]. (2018). *A policy on geometric design of highways & street* (7th ed.). https://store.transportation.org/Common/DownloadContentFiles?id=1776

Austroads. (2009). *Guide to road design*. https://austroads.com.au/safety-and-design/road-design/guide-to-road-design

Department for Infrastructure and Transport [DIT]. (2022). *Road crashes in South Australia: Statistical Summary of road crashes & casualties in 2022.* http://dpti.sa.gov.au/towardszerotogether.

Economic and social commission for Asia and the Pacific [ESCAP]. (2016, September 19). *Major issues in transport: Improving road safety*. https://www.unescap.org/sites/default/d8files/event-documents/7E_Improving%20road%20safety%20in%20Asia%20and%20the%20Pacific_0.pdf

International Transport Forum [ITF]. (2019). *Road Safety Annual Report -South Africa.* http://www.transport.gov.za/.

Ministry of Road Transport and Highways [MORTH]. (2021). *Road accident in India*. https://www.morth.nic.in.

Ministry of Transport and Highways [MOTH]. (2023). *Road Accidents 2019-2022 in Sri Lanka*. https://www.info@transport.gov.lk.

The World Bank. (2020). *Delivering road safety in Sri Lanka: Leadership Priorities and Initiatives to 2030*. https://documents1.worldbank.org/curated/en/976361582088610795/pdf/Delivering-Road-Safety-in-Sri-Lanka-Leadership-Priorities-and-Initiatives-to-2030.pdf

The World Bank [WB]. (2023). *Beyond the numbers: estimating the disability burden of road traffic injuries: Findings from six Low and Middle-Income countries*. http://www.worldbank.org/transport.

Transport Research Laboratory [TRL]. (1997). *Road safety education in developing countries: Guidelines for good practice in primary schools*. https://trl.co.uk/uploads/trl/documents/ORN017.pdf

World Health Organization [WHO]. (2023). *Global Status Report on Road Safety 2023*. https://www.who.int/publications/i/item/9789240086517

Fatigue Resistance Assessment of RC Bridge Deck Slabs

Nuttapong Kongwang[1,*] and Yasuhiko Sato[2]

[1]Graduate School of Creative Science and Engineering, Waseda University, Tokyo, Japan
Email: nuttapong.kong@fuji.waseda.jp
[2]Department of Civil and Environmental Engineering, Waseda University, Tokyo, Japan
Email: y.sato@waseda.jp

ABSTRACT

Knowing the fatigue life enables engineers to understand the current potential for maintaining the bridge in service with satisfactory safety. With the objective of ensuring bridge safety, this study presents the approach for fatigue resistance assessment of reinforced concrete (RC) bridge deck, specifically RC curved bridge deck slabs. The method involves investigating fatigue performance through fatigue life prediction maps. Based upon the results obtained from the proposed method, the remaining fatigue life of RC curved bridge deck slabs can be entirely evaluated for both individual slab panels and the overall bridge deck. Consequently, a precise fatigue damage assessment and proactive maintenance of the curved RC bridge deck slab can be performed thoroughly. Although the present study mainly focuses on the curved RC bridge deck, the authors believe that the methodology outlined herein can serve as a valuable guide for assessing the fatigue life of typical RC bridge deck slabs.

Keywords: Bridge performance assessment, Fatigue life prediction, Curved bridge decks, RC slabs

1. INTRODUCTION

Considering structural concrete bridge components, the reinforced concrete (RC) bridge deck slabs are the first element that is directly exposed to the repetitive concentrated wheel loads. Therefore, they are more prone to fatigue damage than other elements. Although the fatigue problem in RC bridge deck slabs has been recognized for decades, fatigue damage has been consistently observed in RC bridge deck slabs (Boothby & Laman, 1999; Fu et al., 2003; McCarten, 2022). As a result, a number of researchers have extensively done work related to this field covering experimental, numerical, and design approach studies (Matsui, 1984; Perdikaris & Beim, 1988; Fujiyama et al., 2013; Takeda & Sato, 2023).

Additionally, to prevent the fatigue problem from the design stage, several national design codes, e.g., JSCE, fib Model Code 2010, and Eurocodes, require shear fatigue strength verification in their provision. Meanwhile, AASHTO LRFD Bridge Design Specifications (AASHTO, 2020) provide provisions mainly related to steel reinforcement and structures. For the RC bridge deck slabs under the fatigue limit state conforming to AASHTO LRFD (2020), they do not need to be investigated for fatigue life. However, the deck potholes caused by fatigue loading (i.e., repeated moving loads) were observed in the deck slabs of an RC box girder bridge in the United States after a few years of use, as reported in Fu et al. (2003). Thus, the provision for fatigue life prediction is necessary when RC bridge deck slabs are being designed following the AASHTO LRFD (2020)

In recent years, high-capability measuring devices such as the weigh-in-motion (WIM) system could accurately obtain sufficient quantity and efficient quality of traffic data. By utilizing the data from the WIM system, Sivakumar et al. (2011) have reported that truck weight and volume increase and become more complex compared to the past truck configuration. This finding was then adapted and analyzed by Kulicki et al. (2014) to calibrate the concrete bridge design according to AASHTO LRFD specifications. They suggested that the load factors for fatigue live load in AASHTO LRFD should be upgraded to represent the current truck loads. As a consequence, the factor loads for fatigue limit state and fatigue threshold for steel reinforcement have been updated since the 8th edition of the AASHTO LRFD Bridge design specification (AASHTO, 2017). However, provisions for fatigue verification in concrete structures have not yet been established.

Nevertheless, assessing fatigue resistance when designing RC bridge deck slabs following AASHTO LRFD has been optional while bridges are maintained in service for increasingly extended periods. Therefore, the fatigue resistance assessment of RC bridge deck slabs has become even more critical. In this respect, this study aims to introduce an approach for assessing the fatigue life of the RC bridge deck slabs, which are designed to conform to AASHTO LRFD requirements. The approach employs the developed fatigue life prediction method, involving the S-N curve developed by Takeda & Sato (2023) and modified shear strength equations derived from the AASHTO shear design equation (Kongwang & Sato, 2024). This method can predict the fatigue life of RC deck slabs with various support conditions under moving wheel loads and failing in shear. A curved RC bridge deck is utilized to demonstrate fatigue life calculation following the proposed approach. Eventually, the fatigue resistance could be evaluated through the fatigue life prediction maps. Additionally, the study compares fatigue lives calculated using the old load factor (for existing bridges) and the updated load factor (for new bridges) to investigate the effect of load factor changes on the fatigue resistance of RC bridge deck slabs, highlighting the importance of fatigue resistance assessment in RC bridge deck design.

2. FATIGUE LIFE PREDICTION METHOD

2.1 Approach for Assessing Fatigue Resistance of RC Bridge Deck Slabs

Fatigue damage assessment of the bridge deck can be quickly started through the visual inspection, a method that involves a thorough examination of the bridge's physical condition, which is fast and easy to investigate bridge conditions. This is included as the first step for the approach presented in this study (Figure 1). Generally, fatigue damage could be observed with the sign of two directional cracks (grid-like cracking pattern) on the soffit of RC bridge deck slabs. More cycles due to moving loads (i.e., trucks) running on the bridge deck could propagate those cracks, leading to failure with the punch-off concrete blocks (PWRI, 2020; McCarten, 2022). To deal with fatigue damage rationally, the fatigue failure mechanism should be clarified. Some researchers (Matsui, 1984; Perdikaris & Beim, 1988) developed the traveling wheel-type loading machine to understand the failure mechanism of RC slabs under fatigue loading. Based on the experimental result, they unveiled that the typical cracking pattern of RC slabs that failed under moving wheel load is the grid-like cracking pattern, whilst slabs under fixed pulsating load fail in the radial-like cracking pattern (Batchelor et al., 1978). In addition to the grid-like cracking pattern, the cracks parallel to the main reinforcement (transverse cracks) suffer the reverse shear stress, which accelerates them to propagate upwards, ultimately forming a beam-formed cracking pattern and finally ending up with punching shear failure as illustrated in Figure 1. The cracks observed during the experiment closely resembled those found in operational concrete bridge decks (PWRI, 2020). This indicates that an experimental approach can be effectively utilized to develop the fatigue life prediction method.

As shown on the development of fatigue life prediction method in Figure 1, by adapting experimental results obtained from RC slabs tested under moving wheel loads, Takeda and Sato (2023) have successfully proposed the fatigue life prediction method, S-N curve-based method, that can estimate the fatigue life of RC slabs from Equations 1 which is used for fatigue life prediction in this study.

$$S = \frac{P}{2V_{bc}} = 1 - \mathrm{KlogN} \tag{1}$$

When using Equation 1 in predicting fatigue life, the ratio between shear force and strength ratio, S, can be calculated by dividing the applied load, P, with double shear strength of beam-formed member, V_{bc}. Factor 2 could be changed depending on the load position along the beam span. The constant K can be taken as 0.057 and 0.061 for slabs under dry condition and the wet condition, respectively, and N denotes the number of cyclic moving loads at failure. In the present study, the shear strength V_{bc} was replaced with V_{mc} (Equation 2) which was developed based on the AASHTO shear design equation to consider the effect of support condition on the shear strength of beam-formed member. Its capability in predicting fatigue life was validated with the experimental dataset that can be found in the previous study, Kongwang & Sato (2024).

$$V_{mc} = \alpha_{wc}\alpha_{sc}\beta_{dc}\sqrt{f_c'}\,b_v d_v \tag{2}$$

Where α_{wc}= 1.0 and 0.59 in the dry and wet condition, α_{sc} = 0.50, 1.00, and 1.30 for the slab supported by 2-side simple and 2-side free, 2-side simple and 2-side elastic, and 4-side simple, respectively. β_{dc}=2.0·[0.4/{1+(750-175$\rho_d/\rho_m)\varepsilon_s$}]·[1300/(1000+$S_{xe}$)], ρ_d and ρ_m denoted as the distribution and main reinforcement ratio respectively. ε_s, S_{xe}, b_v, and d_v can be taken as specified in AASHTO LRFD (2020) equations 5.7.3.4.2-1 to 4.

According to AASHTO LRFD (2020), to generate the potentially critical fatigue load, a design truck or axles should be placed both longitudinally and transversely on the bridge deck when fatigue resistance assessment is performed. For analysis, AASHTO permits the subdivision of the bridge deck into strips along the longitudinal axis. This strip method facilitates the assessment of fatigue resistance in the transverse direction of the bridge deck, using the aforementioned fatigue life prediction method. Ultimately, fatigue life prediction maps can be created by combining the results from each strip.

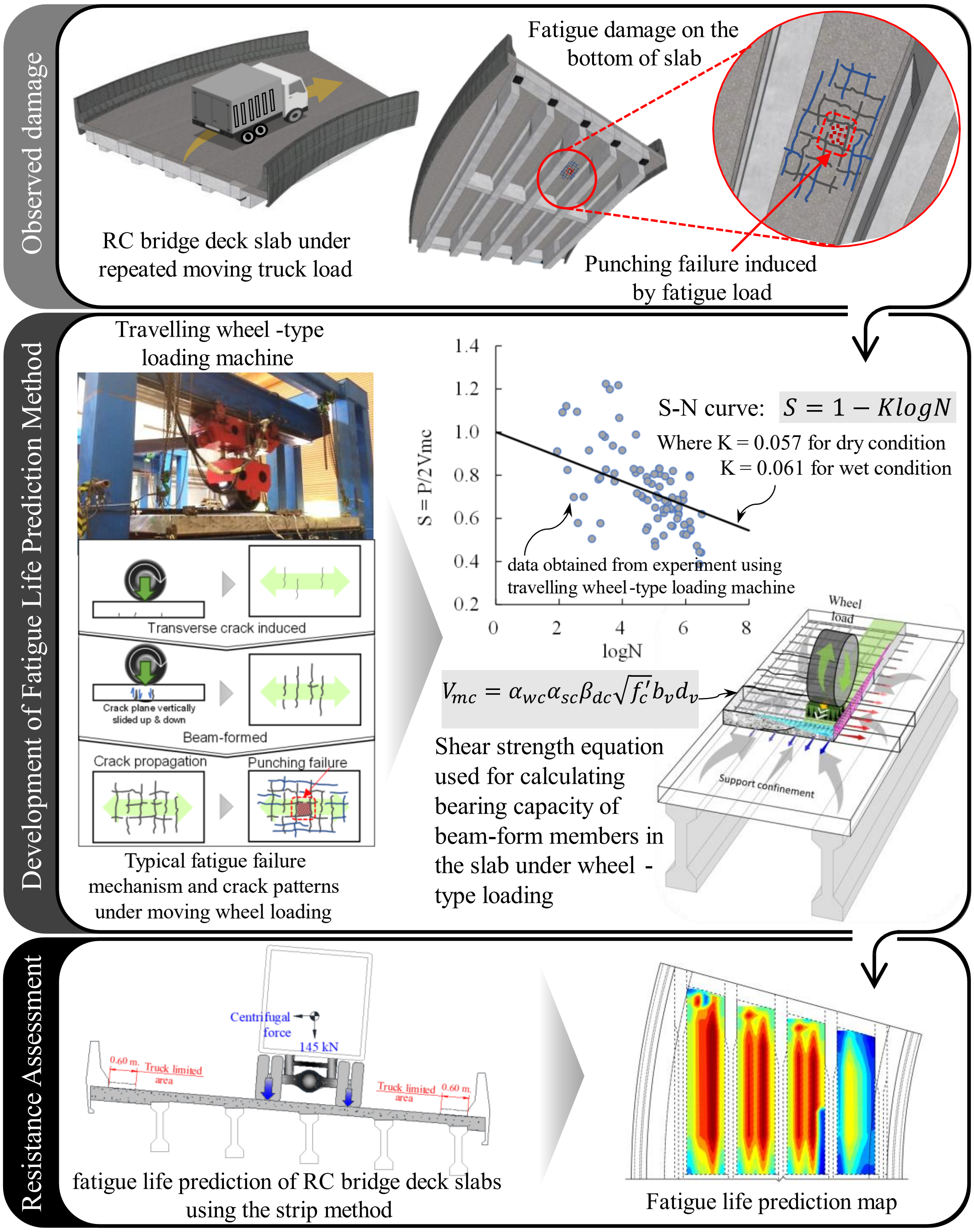

Figure 1 Fatigue resistance assessment of RC bridge deck slabs.

2.2 Details of Studied Curved RC Bridge Deck Slabs

To encompass the possible extreme wheel loads in estimating fatigue life, the curved RC bridge deck slabs were employed throughout this study because the curved bridge deck has the superelevation and curvature that could induce the centrifugal force affecting the load unequally transferred from the axle to the wheels, one significantly higher than another wheel. A plan and cross section views of the studied curved RC bridge deck are shown in Figure 2a. The bridge deck is 9.0 m wide including concrete barrier rail (8.0 m. roadway), and its radius of curvature and superelevation are 22.7 m. and 8% respectively. It is supported by five straight I-shaped concrete girders with different lengths varied between 10.35 and 14.0 m. Girders are arranged 1.665 m. apart. This spacing becomes the span length of interior RC deck slabs. For overhang slabs, the maximum and minimum length for 1) outside slab are 1.64 and 0.70 m. respectively and 2) inside slab are 1.40 m. and 0.70 m. respectively. Additionally, the thickness of slabs is 0.20 and 0.30 m. for interior and overhang slabs respectively (section 1-1 in Figure 2b).

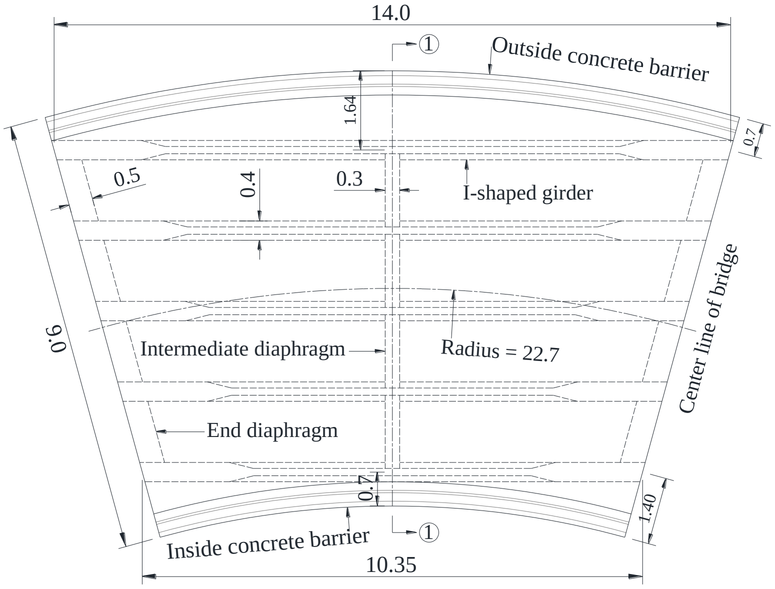

Unit: m. (unless otherwise specified)

(a) Plan views

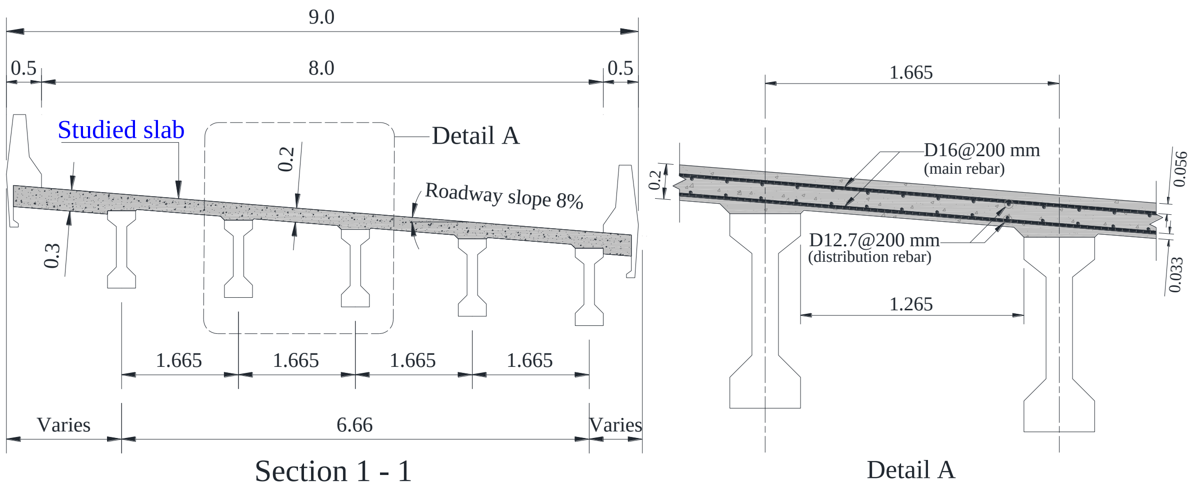

Unit: m. (unless otherwise specified)

(b) Cross section and typical reinforcement detail

Figure 2 Configuration of the studied RC curved bridge deck.

The slabs are steel-reinforced by deformed bars with 16-mm diameter (D16) transversely placed at 200 mm. spacing both top and bottom layers which are the main reinforcement. Meanwhile, a 12.7-mm diameter (D12.7) is used as the distributing reinforcement in both layers with identical spacing with the main rebars as illustrated in detail A (Figure2b). The yield strength of reinforcing steel is 420 MPa. In addition, the concrete cylinder compressive strength is 30 MPa. It should be noted that all properties are provided conforming to the AASHTO LRFD (2020) on the basis of ultimate and service limit states.

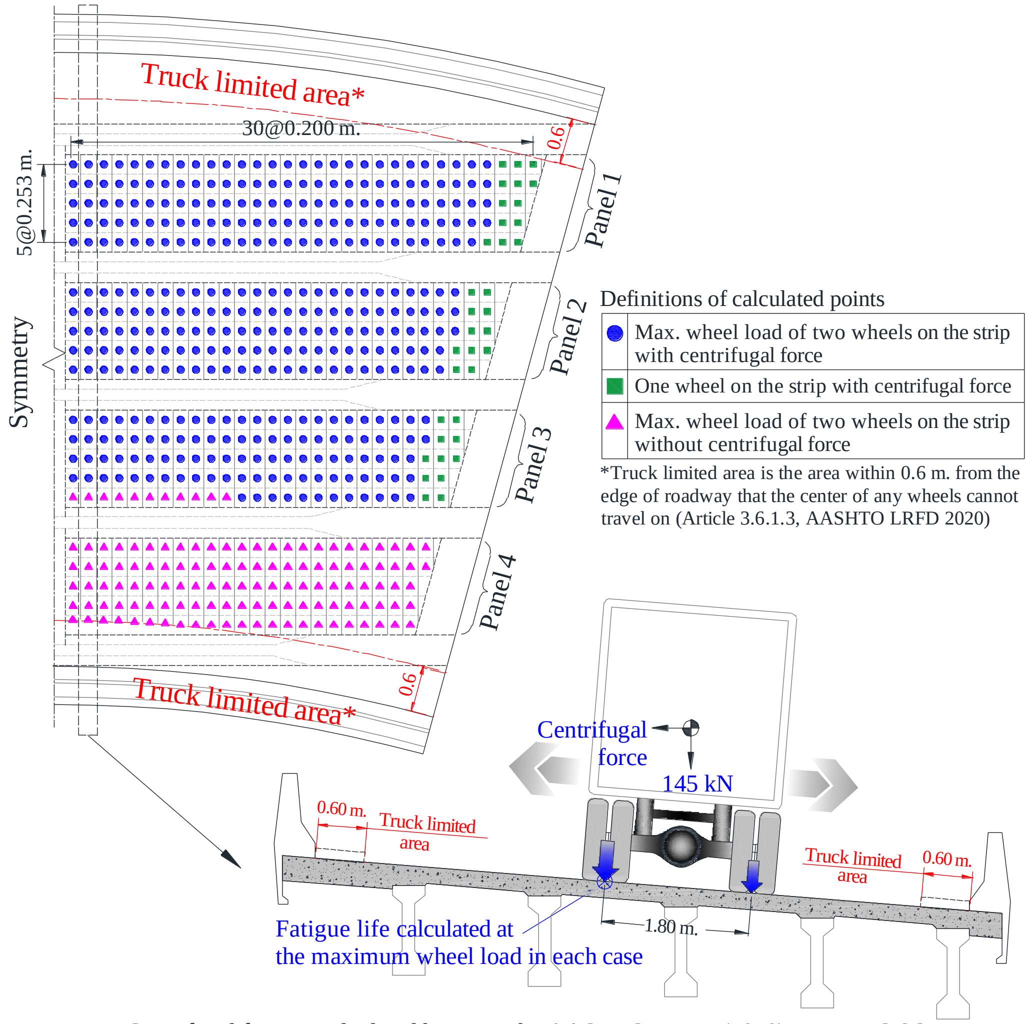

Note: Centrifugal force is calculated by using the AASHTO LRFD (2020) equation 3.6.3-1

Figure 3 Diagram of fatigue calculation points and applied fatigue loads.

2.3 Defined Calculation Points for Fatigue Resistance Assessment

To investigate the fatigue resistance according to AASHTO LRFD (2020), the design truck with an axle load of 145 kN, magnified by a dynamic load factor of 15% (i.e., IM = 1.15), is applied longitudinally and transversely over the bridge deck to produce the extreme fatigue load effect. The bridge deck is subdivided into several strips to facilitate longitudinal analysis, with each strip being 200 mm wide for the present study. These strips are then used for transverse analysis by applying the axle load along the strip. In this way, calculated points representing the maximum wheel load of the axle at the position being considered can be defined as illustrated in Figure 3.

Given the curvature of the bridge deck, the centrifugal force was included in the analysis. However, comparisons were also made to scenarios without the centrifugal force to determine the worst-case scenario for the fatigue shear force. Consequently, the envelope diagram of fatigue loads was obtained as shown in Figure 3, highlighting three different worst-case scenarios: 1) the maximum wheel load from the axle load including centrifugal force, denoted by a blue circle; 2) one wheel load including centrifugal force, with another wheel load on the adjacent deck slabs, denoted by a green square; and 3) the maximum wheel load from the axle without centrifugal force, denoted by a pink triangle. Additionally, the effect of superelevation on wheel load reactions was considered.

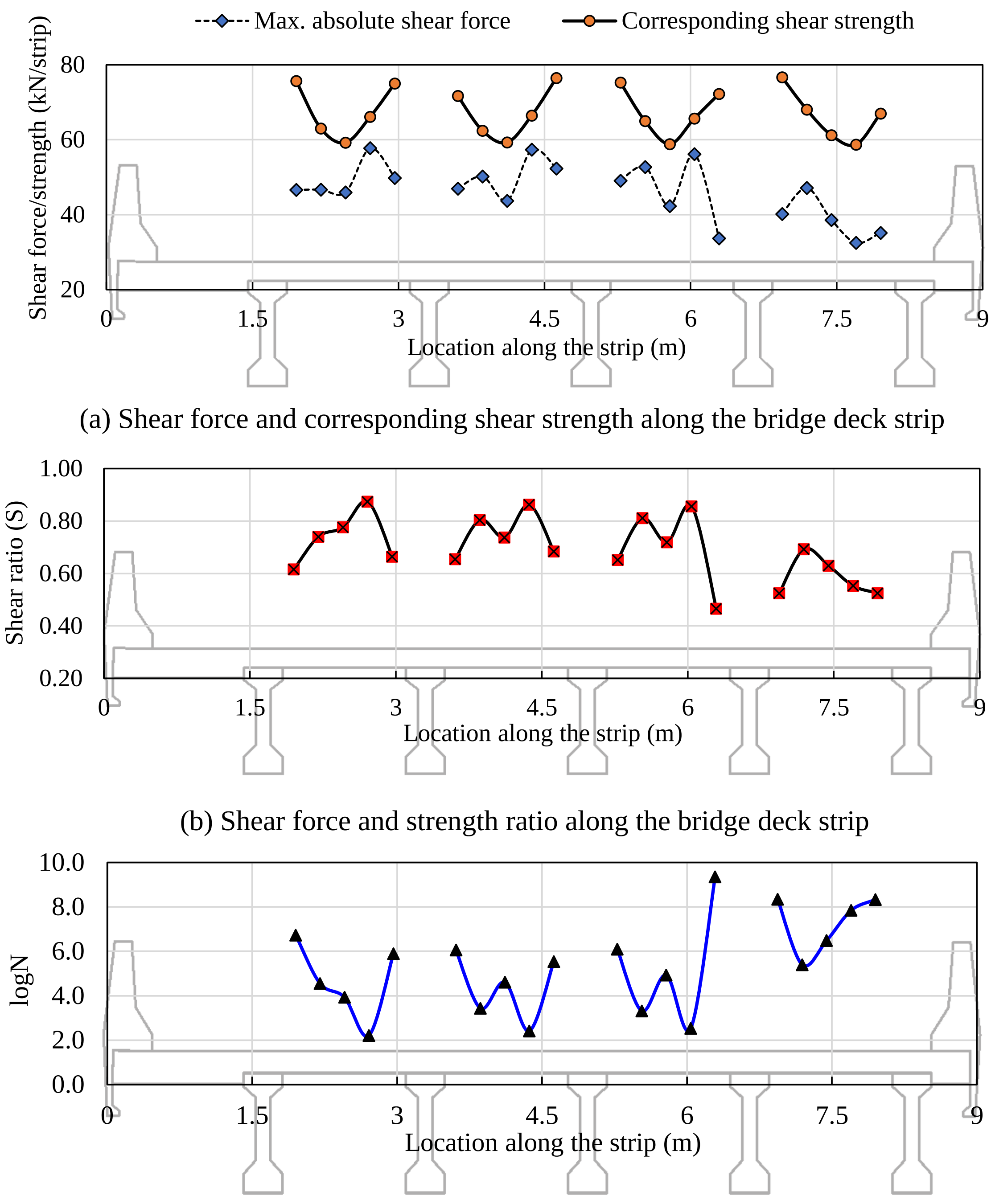

(a) Shear force and corresponding shear strength along the bridge deck strip

(b) Shear force and strength ratio along the bridge deck strip

(c) logarithmic number of cycles (logN) along the bridge deck strip

Figure 4 Typical fatigue life assessment of an RC bridge deck strip.

3. FATIGUE LIFE OF THE CURVED RC BRIDGE DECK SLAB

3.1 Fatigue Life Assessment of RC Bridge Deck Strips

Figure 4 illustrates a typical fatigue life assessment of an RC bridge deck slab using the strip method. By applying the method presented in section 2, the enveloped maximum absolute shear force at various locations along the strip can be obtained, as shown by the dashed line in Figure 4a. The envelope forces indicate that the lowest absolute shear force typically occurs at the middle span of the slab and gradually increases toward the support. However, it suddenly drops again at a certain length near the support due to the applied load (i.e., wheel load) being transferred directly to the supporting girder. Additionally, the envelope force on panel 4 shows lower values than the other panels because the presence of centrifugal force reduces the wheel reaction on this panel. Subsequently, the shear forces on panel 4 are governed by the axle load without centrifugal force, as identified in Figure 3. The shear strength was computed at corresponding locations to the maximum absolute shear force and is also plotted with a solid line in Figure 4a. The shear strength results show a similar tendency in all slab panels since the shear strength calculated using Equation 2 mainly depends on the strain of the main reinforcement (lower strain results in higher shear strength), which is proportional to the deformation of the slab member. As a result, the minimum strength appears at the mid-span of the slab panel. Referring to Equation 1, when the shear force and shear strength are known, the fatigue life (N) can be estimated from the shear force ratio (S), which is plotted in Figure 4b. This means that a lower shear force ratio corresponds to higher fatigue resistance, and vice versa as shown in Figure4c. Applying this strip method over the entire bridge deck in the longitudinal direction enables a comprehensive fatigue life assessment, as demonstrated through the contour maps in the following section.

3.2 Fatigue Resistance Assessment Using Fatigue Prediction Maps

Due to the non-symmetric shape of a curved RC bridge deck along the longitudinal axis, resulting in an unequal length of slab panels, fatigue life assessment based on one representative slab for the entire deck slab might be inadequate. Therefore, the present study proposes fatigue life prediction maps, as shown in Figure 5, to investigate the deck slab's fatigue life both in the local area of the slab panels and in the overall bridge deck. Following the previously mentioned fatigue life prediction method, fatigue life estimation needs the applied fatigue loads and shear strength. Figures 5a and 5b show the fatigue loads, excluding the load factor, and the shear strength contour maps of the studied curve RC bridge deck slab. These contour maps were generated corresponding to the calculated points in Figure 4. Figure 5a indicates that the shear force in panel 4 is significantly lower than that in panels 1 to 3. This result is due to the effect of centrifugal force induced by the curvature of the bridge deck, which causes significantly different wheel reactions. Specifically, in Figure 4, the left wheel reaction is relatively higher than the right wheel reaction. Figure 5b exhibits a similar tendency in the shear strength of each panel; however, different shear strength between the middle slab and the area close to the support can be obtained using the developed shear design equation (Equation 2).

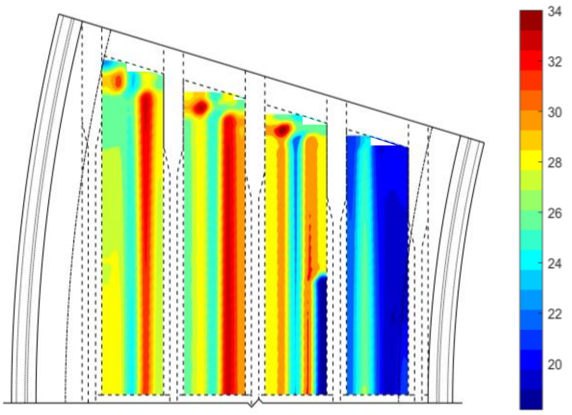

(a) Shear force map (kN/strip)

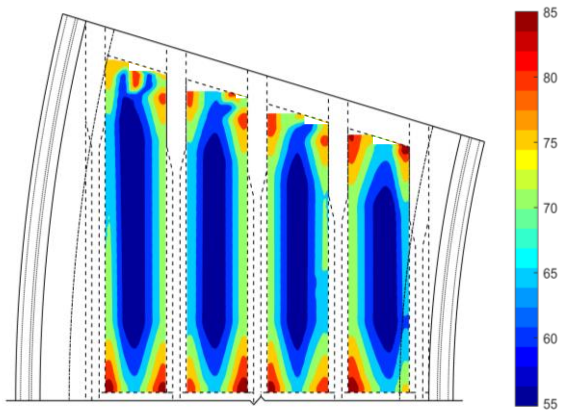

(b) Shear strength map (kN/strip)

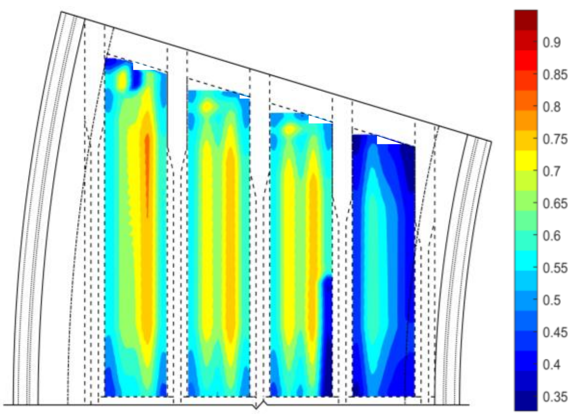

(c) Shear ratio map (Load factor 1.50)

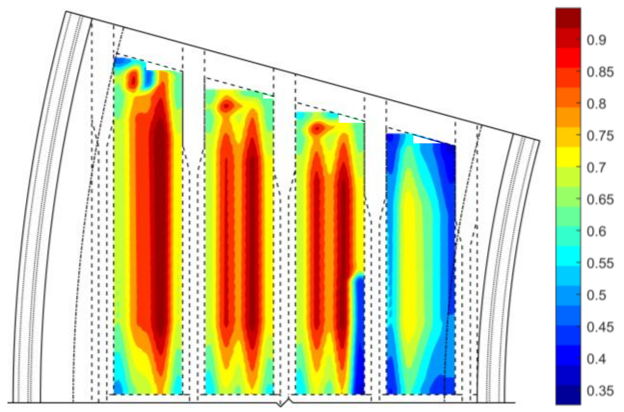

(d) Shear ratio map (Load factor 1.75)

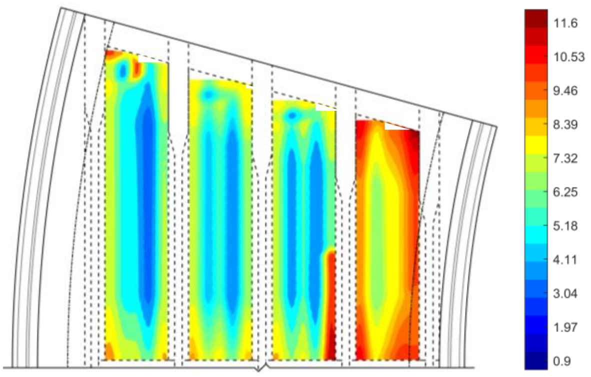

(e) logN (Load factor 1.50)

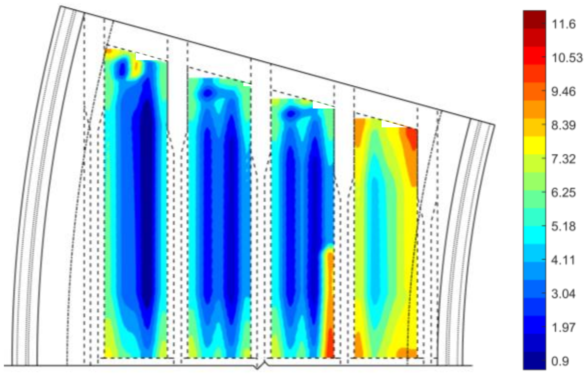

(f) logN (Load factor 1.75)

Figure 5 Fatigue life prediction maps.

Table 1 Summary of fatigue life prediction of the studied curved RC bridge deck slab.

Panel number of slab		1	2	3	4
Maximum shear force (kN/strip)		32.9	33.3	31.8	26.7
Corresponding shear strength (kN/strip)		62.3	62.4	61.3	63.9
Case 1: Old load factor, 1.50	Maximum shear ratio, *S*	0.807	0.790	0.781	0.630
	Cycle number, *N* (logN)	2432 (3.38)	4833 (3.68)	6952 (3.84)	3.1×10^6 (6.49)
Case 2: Updated load factor, 1.75	Maximum shear ratio, *S*	0.946	0.918	0.913	0.737
	Cycle number, *N* (logN)	9 (0.95)	27 (1.43)	34 (1.53)	4.1×10^4 (4.61)

According to the shear forces and strengths mentioned above, the shear ratio (S) for different live load factors was calculated and visualized using contour maps in Figures 5c and 5d. Case 1 uses a factor of 1.5, representing the old fatigue load factor (Figure 5c), and Case 2 uses a factor of 1.75, referring to the current fatigue load factor (AASHTO 2020) (Figure 5d). These shear ratios are then utilized to predict the fatigue life (number of cycles to failure, N) of each slab panel using Equation 1. Ultimately, the fatigue life (logN) regarding Cases 1 and 2 can be obtained as illustrated in Figures 5e and 5f respectively. The results are summarized in Table 1, where the maximum values picked up from each slab panel are demonstrated. Comparing the predicted cycle number between Case 1 and Case 2, the results reveal that the fatigue life could be significantly shorter, starting from 1/75 to 1/270, owing to the updated live load factor in AASHTO LRFD (2017). This substantial reduction suggests that a thorough fatigue life assessment of the RC bridge deck slab, particularly for shear failure, is essential when adapting to the AASHTO truck load. This assessment is crucial both for newly constructed bridges to ensure they meet the required design life and for existing bridges to evaluate their remaining lifetime.

Based on the fatigue life prediction maps, the fatigue life sensitivity of RC curved bridges can be clarified. The maps unveil that the slab panels closer to the outer curve, such as panel 1, are more prone to fatigue damage than others. This increased susceptibility is due to the higher centrifugal force when the radius of curvature increases, resulting in a higher wheel load reaction on these slabs. Moreover, when considering the panel closest to the overhang slab (panel 1) in the longitudinal direction, it is evident that its fatigue life decreases proportionally with the overhang length. This finding highlights the impact of the overhang slab on fatigue life prediction. These results underscore the importance of conducting a comprehensive fatigue resistance assessment using contour maps, as they emphasize the necessity of evaluating the entire bridge deck slab for fatigue damage.

4. CONCLUSIONS

(1) The fatigue life prediction method, integrating the shear design equation derived from AASHTO provisions and incorporating the S-N curve proposed by previous researchers (Takeda and Sato, 2023), offers a robust framework for assessing the fatigue life performance of RC curved bridge deck slabs through the fatigue life prediction maps. This approach enables comprehensive fatigue resistance assessment for both local and global regions of the bridge deck slab.

(2) The significant variance in predicted fatigue life resulting from updated fatigue load factors indicates the importance of thorough investigation into fatigue life performance when designing or evaluating RC bridge deck slabs according to AASHTO specifications. Thus, implementing the latest live load factors is crucial for accurate fatigue life estimation.

(3) The observed differences in fatigue lives among individual slab panels of the curved bridge deck highlight the influence of centrifugal forces induced by the bridge deck's curvature on fatigue life prediction. Accounting for these forces is essential for precise fatigue life assessments and ensuring structural integrity over the bridge's lifespan.

5. ACKNOWLEDGMENTS

The authors would like to express their gratitude for the research funding provided by JICA-SATREPS.

6. REFERENCES

ASHTO (2017), AASHTO LRFD bridge design specifications 8th edition, Washington D.C.
AASHTO (2020), AASHTO LRFD bridge design specifications 9th edition, Washington D.C.
Batchelor, B de V., Hewitt, BE., and Csagoly, P. (1978), An investigation of the fatigue strength of deck slabs of composite steel/concrete bridges, Transp Res Rec, 664, pp. 153–161
Boothby, T. E., and Laman, J. A. (1999), Cumulative Damage to Bridge Concrete Deck Slabs Due to Vehicle Loading, Bridge Engineering, 4, pp. 80-82
Fu, G. et al. (2003), Effect of Truck Weight on Bridge Network Costs, Washington D.C.
Fujiyama, C., Tang, X. J., Maekawa, et al. (2013), Pseudo-cracking approach to fatigue life assessment of RC bridge decks in service, Advanced Concrete Technology, 11(1), 7-21
Kongwang, N., and Sato, Y., Adaptation of MCFT-based shear design equation for fatigue life prediction of RC bridge deck slabs, In: Proceedings of the 46th Annual Conference of the Japan Concrete Institute, Ehime, Japan, 2024
Kulicki, J. M., Wassef, W. G., Nassif, H et al. (2014), Calibration of AASHTO LRFD concrete bridge design specifications for serviceability (No. 201)
Matsui, S. (1984), Study on Fatigue and Design Method of Concrete Deck Slabs for Road Bridge, Doctoral dissertation, Osaka University.
McCarten, P. S. (2022), Bridge deck fatigue: A case for proactive preventive bridge management, in Bridge Safety, Maintenance, Management, Life-Cycle, Resilience and Sustainability, CRC Press, pp. 449-457
Perdikaris, P. C. and Beim, S. R. (1988), RC Bridge Decks Under Pulsating and Moving Load, Structural Engineering, 114, pp. 591-607
PWRI (Public Works Research Institute). (2020). Examination for preventing disintegration of concrete beneath asphalt surfacing in highway bridge decks. Ibaraki, Japan: PWRI; Report No.: 4398. (In Japanese).
Sivakumar, B., Ghosn, M., and Moses, F. (2011), Protocols for collecting and using traffic data in bridge design, Transportation Research Board, 683
Takeda, K., and Sato, Y. (2023), Proposal for fatigue life prediction method for concrete slabs subjected to cyclic wheel-type loads, JSCE, 79(12), 23-00078

Innovative Analysis and Design Approach for Horizontally Curved Bridges

Wanakorn Prayoonwet[1,*] and Yasuhiko Sato[2]

[1] Graduate School of Creative Science and Engineering, Department of Civil and Environmental Engineering, Waseda University, Tokyo, Japan, wanakorn.p@fuji.waseda.jp
[2] Graduate School of Creative Science and Engineering, Department of Civil and Environmental Engineering, Waseda University, Tokyo, Japan, y.sato@waseda.jp

ABSTRACT

The implementation of dapped-end prestressed concrete I-girders in U-turn ramp bridges is a common practice in highway route constructions due to its simplicity and effectiveness. However, many researchers have observed signs of concrete deterioration and reinforcement corrosion induced by carbonation in existing dapped-end girders, particularly at the upper nib. These deterioration mechanisms lead to earlier degradation in overall structural performance than expected. Consequently, state authorities are required to replace existing deteriorated structures with new ones to ensure the sound functionality of the road network. This results in overutilisation of national resources and non-conformance with sustainable development goals. As a result, challenges have arisen for newly constructed facilities to achieve sustainable design and construction. Therefore, this study proposes an innovative analysis and design framework for the dapped-end connection in the main girders of the curved superstructure. By utilising this framework, the structural performance to withstand carbonation deterioration aimed at prolonging the structural working life can be ensured through the analysis of sectional forces and calculation of completion time for carbonation penetration, taking into account the effect of crack width and structural configuration. Ultimately, the structural performance of the designed dapped-end girder can satisfy not only the sectional force demand but also the target service life, promoting sustainable design and construction.

Keywords: Curved bridges, Parametric study, Live load, Dapped end, Finite element method

1. INTRODUCTION

Bridges with curved alignments, such as the U-turn ramps, are commonly used in urban developments. The design and construction of the superstructure of these U-turn ramps typically involve the curved edge reinforced concrete (RC) slab supported by straight dapped-end prestressed concrete (PC) I-girders. However, the unique configuration of this curved superstructure results in higher sectional forces in the main girders induced by live loads compared to straight superstructures, making it challenging to precisely determine the live load effects in the main girders, which compromises structural design and detailing. Additionally, the geometry of the upper nib in dapped-end girders has disadvantages related to the water tightness of the connection itself, creating beneficial environment for concrete deterioration and rebar corrosion (Desnerck et al., 2016). These deteriorations accelerate the degradation of overall structural performance, ultimately shortening the service life of the structure and demoting sustainable development goals.

To address these shortcomings, this paper proposes an innovative analysis and design approach for the horizontally curved superstructure, emphasising the dapped-end connection of the main girder. This framework is developed based on analytical investigations using both linear and nonlinear numerical analyses. The results from linear finite element analyses aim to provide a method to precisely determine the live load effects in the main girders, while the structural performance and inadequacies of the dapped-end connection, designed according to the current design codes, are investigated using the results obtained from nonlinear finite element analyses. To this end, the findings from this study serve as comprehensive guidance for the enhanced analysis and design towards sustainable and resilient horizontally curved bridges.

2. BRIDGE DESCRIPTION

Figure 1 summarises the overall plan details of the U-turn ramp bridge utilised in this study. In this paper, the curved superstructure located between pier 11 and pier 12, as denoted in Figure 1, was the targeted superstructure. This superstructure has a centreline radius of curvature equal to 22700 mm and a centre arc length equal to 12140 mm, as shown in Figure 2. The clear roadway width, measured between inner faces of barriers, is 8000 mm accommodating maximum two traffic lanes (AASHTO, 2020).

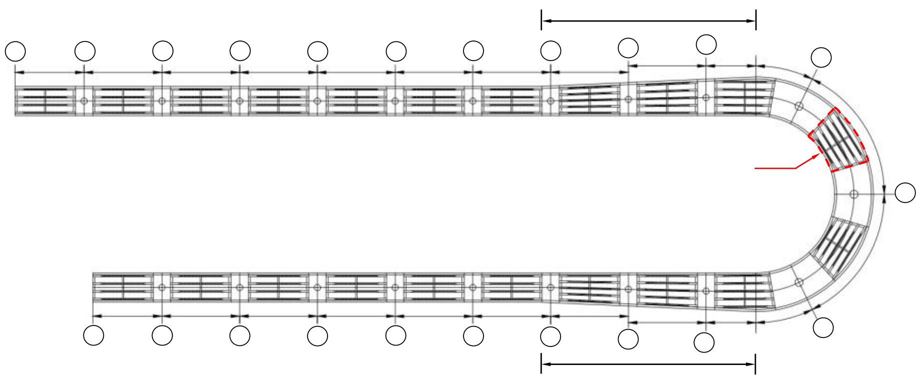

Figure 1 U-turn ramp bridge plan (unit: mm).

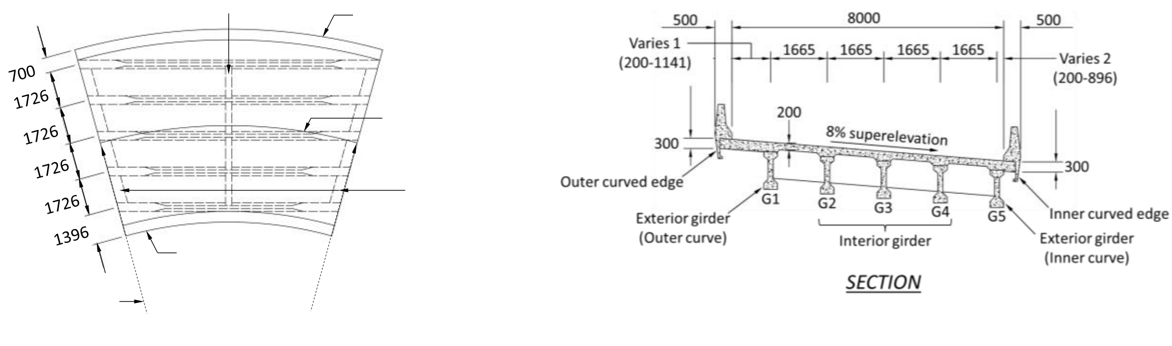

Figure 2 Details of the targeted superstructure (unit: mm).

According to Figure 2, the bridge superstructure consists of five straight PC I-girders supporting the curved edges RC slab. For this study, the main girder located next to the outer curved edge (outside radius) is denoted as G1, whilst the main girder located next to the inner curved edge (inside radius) is denoted as G5. For the RC slab, two different thicknesses of 200 mm and 300 mm are designed for the interior slab panels, spanning between the main girders, and the cantilever slab panels, respectively. Additionally, the superelevation of 8%, which is the slope in the transverse direction, is denoted on the curved RC slab. The cast in-place RC diaphragms are provided at the centre of the span and at both ends of the span. For the diaphragms at the centre of the span, a solid rectangle section with the dimension of 300 mm breadth and 1050 mm height is used, while the end diaphragms are constructed using a solid rectangle section having breadth and height of 500 mm and 510 mm, respectively.

Figure 3 shows the elevation and cross-section of the PC I-girder. The 7-wire low relaxation strands are implemented as prestressing reinforcements. The prestressing force is applied to the member using the pretensioning system. According to Figure 3, the PC I-girder is designed as a dapped-end girder, also referred to as a half-joint girder.

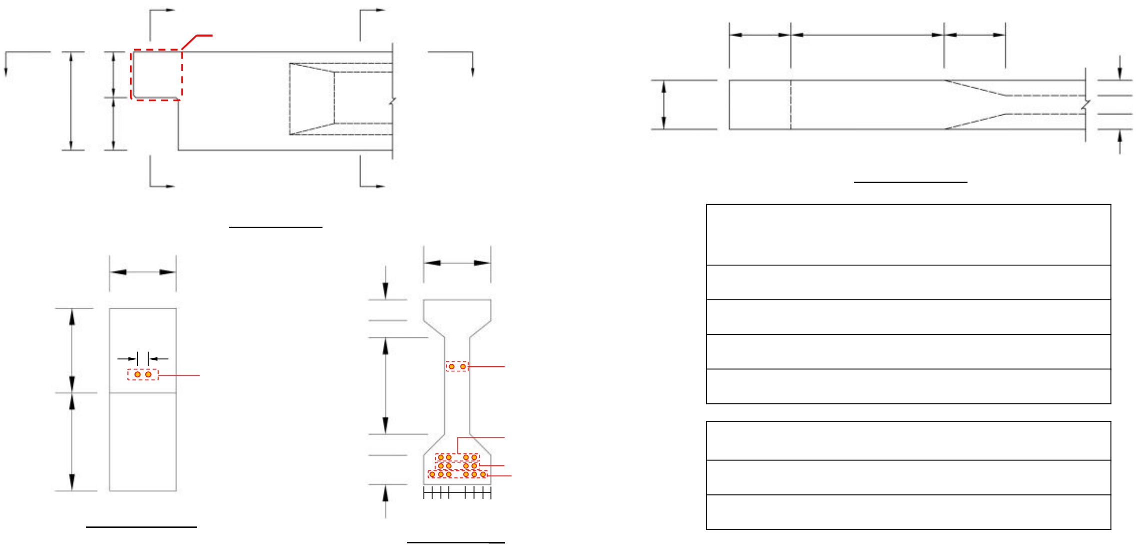

Figure 3 PC I-girder details.

Two different 28-day concrete cylinder strengths are specified for PC structural members or RC structural members. For the PC I-girders, the concrete cylinder strength (f_c') of 35 MPa is employed, resulting in concrete elastic modulus (E_c) of 30.38 GPa (AASHTO 2020), while f_c' utilised in the curved edge RC slab and RC diaphragms is 26 MPa, resulting in E_c of 26.29 GPa. For the reinforcements, yielding strength and modulus of elasticity for both ordinary and prestressing steels are summarised in Table 1. Based on the structural drawings, two different grades of ordinary steel bars are specified. For the normal steel bars with smaller diameters than 12 mm, the round bar with a minimum specific yield strength of 235 MPa, denoted as SR24 in Table 1, is used, and for the rebars with diameters equal to or greater than 12 mm, the SD30 deformed bar with a specific yielding strength of 295 MPa is implemented.

Table 1 Mechanical properties of reinforcements.

Types of reinforcements	Yielding strength (MPa)	Modulus of elasticity (GPa)
7-wire low relaxation prestressing strand	1581	197
SD30	295	200
SR24	235	200

3. OUTLINE OF ANALYTICAL APPROACH

3.1 Investigation on live load distribution mechanisms of curved superstructure

To precisely determine the effects of external loads such as flexural moments and shear forces developed in the main girders of the curved superstructure, a parametric study using a linear three-dimensional finite element method (3D-FEM) was carried out to examine the effect of significant curved bridge properties on the live load distribution responses. The summary of investigated parameters and their variations are tabulated in Table 2.

Table 2 Summary of considered parameters.

Parameters	Range of values (Considered condition)
Curvature angle, L_{arc}/R (rad)	0.273, 0.364, 0.571, 0.769
Girder spacing, S (mm)	1400, 1500, 1600
Superelevation, E (%)	4, 6, 8
Intermediate diaphragm	Absence of intermediate diaphragm
Boundary condition	Longitudinal restraint at roller support

Bridge Modelling

For all bridge models, PC I-girders and diaphragms were simulated via the two nodes Timoshenko beam element possessing six degrees of freedom (DOFs) at each node (Midas, 2022). For the RC deck, the Kirchhoff thin plate element, which has the in-plane axial and shear stiffnesses and the out-of-plane shear and bending stiffnesses, was implemented for the structural modelling (Midas, 2022). Figure 4 shows the geometry and mesh details of the numerical model. The simply supported boundary condition conforming to the actual details of the investigated superstructure was utilised. Note that the vehicle loads as per the AASHTO LRFD (AASHTO, 2020) were used.

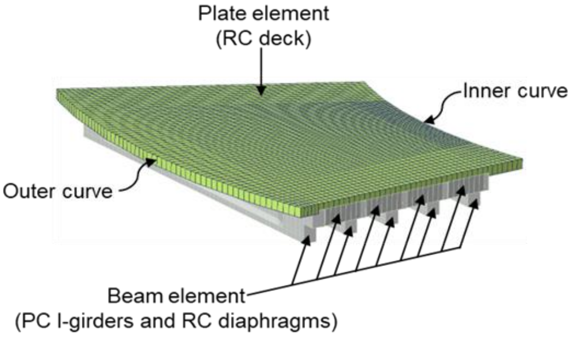

Figure 4 Finite element modelling and mesh detail of curved bridge superstructure.

3.2 Clarification on the structural performance of the dapped-end connection

Once the effects of actions on the main girders are determined, the structural design and detailing aimed at satisfying the design values from the effects of actions are conducted based on the current design codes. Then, the structural performance and drawbacks of the designed dapped-end girder can be investigated using the three-dimensional nonlinear finite element method (3D-NLFEM). Note that this paper delved into the behavioural examination of the dapped-end connection due to the complexity in the stress distribution within the disturbed region (D-region) and signs of advanced concrete deterioration and reinforcement corrosion in the nib reinforcements (Desnerck et al., 2016).

Finite Element Modelling

The 3D-NLFEM was performed using commercial software ATENA 3D. The structural concrete and steel plate were modelled using brick and tetrahedral elements, respectively, depending on the structural geometry constraints (Červenka et al., 2022). Ordinary reinforcements in D-regions and prestressing strands were modelled using discrete two-dimensional (2D) truss bar elements (Červenka et al., 2022). To optimise the numerical modelling, normal reinforcements located in other regions were modelled using smeared reinforcements (Červenka et al., 2022). It is worth to mention that the employed mesh size was 50 mm in all parts.

For material constitutive laws, the behaviour of concrete under tension and compression was modelled using the equivalent uniaxial stress-strain law, incorporating the Rankine failure criterion and the plasticity model based on the Menétrey-William failure surface (Červenka et al., 2022). A bi-linear stress-strain law, elastic-perfectly plastic, was employed for both discrete and smeared reinforcements. A perfect bond between concrete and reinforcements was assumed. For steel plates, the 3D-elastic isotropic constitutive law was employed in modelling.

Figure 5 shows the finite element model of the dapped-end girder. In the analysis, the applied loads were given in two stages. Initially, the girder's self-weight and prestressing force were applied to the girder. Then, a vertical load was incrementally applied using a displacement-controlled loading scheme at a distance of 1200 mm from the centreline of the pin support on the left side, as shown in Figure 5. The monitoring points to detect the predicted reaction force at the pin support and vertical displacement at the re-entrant corner, as depicted in Figure 5, were provided. A modified Newton-Raphson method was implemented in the nonlinear analysis.

Figure 5 Finite element model of dapped-end girder.

Studied Parameters and Investigated Structural Responses

To clarify the structural performance of the dapped-end connection aimed at enhancing the structural design methodology, the impacts of structural details on structural responses need to be investigated. In this research, the rebar layouts in the dapped-end connection and the concrete cover were the two key parameters emphasised in the analytical investigations. For the steel reinforcing schemes, the effects of different reinforcement arrangements, as illustrated in Figure 6, were examined consisting of orthogonal reinforcing scheme, diagonal reinforcing scheme, and combined diagonal and orthogonal reinforcing scheme. These three rebar layouts were designed conforming to the design standards (PCI, 2010; BS-EN 1992-1-1, 2004) where the number of reinforcements were basically determined to ensure adequate capacity against the required reaction force in the nib at the strength limit state. For the concrete cover, the structural responses of dapped-end connections with two different concrete covers, 25 mm and 35 mm conforming to the minimum allowable cover (AASHTO, 2020), were investigated.

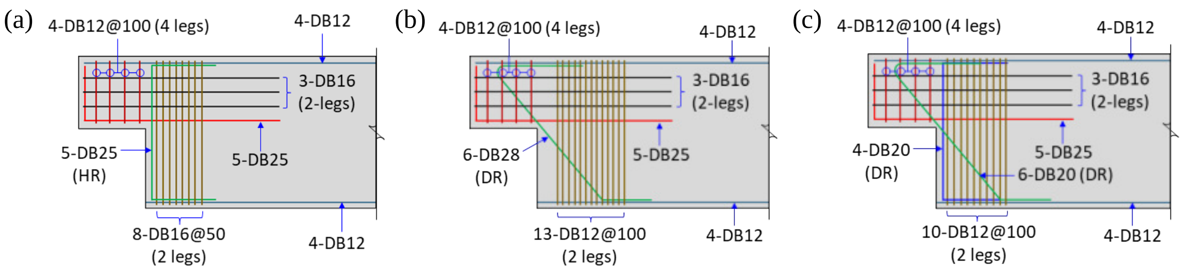

Figure 6 Investigated steel reinforcing schemes in dapped-end connection: (a) orthogonal reinforcing scheme; (b) diagonal reinforcing scheme; and (c) combined orthogonal and diagonal reinforcing scheme.

Throughout the analytical investigation, the effects of studied parameters on structural responses were clarified through the predicted reaction force-vertical displacement at the re-entrant corner and the maximum crack width at the service limit state. Moreover, the completion time for carbonation penetration taking into account crack width effects (Kwon & Na, 2011) was also predicted and compared against the repair-free service life of 30-year (DPT1332-55, 2012).

4. RESULTS AND DISCUSSION

4.1 Live load distribution mechanism

Based on the analytical results, the maximum flexural moment and shear forces at the critical sections in the main girders were obtained. Subsequently, these results were used to calculate the live load distribution factors (LLDF), representing the maximum ratio of live load effects resisted by the main girders. In this study, the beam-line method, as described in Equation (1), was employed to calculate the LLDF for both flexural moment and shear force (Zokaie et al., 1991).

$$LLDF = \frac{F_{refined}}{F_{beam}} \cdot m \tag{1}$$

where $F_{refined}$ is the maximum live load effects in the main girders analysed from the linear 3D-FEM of the superstructure; and F_{beam} is the maximum live load effects calculated from a single girder; and m is the multiple presence factor, defined by the AASHTO LRFD (AASHTO, 2020). The calculation of $F_{refined}$ and F_{beam} must be performed under the same live load models.

The results showed that LLDF was influenced by discrepancies in the considered parameters. Among all investigations, the curvature angle showed prominent effects on both moment and shear responses in the main girders, while spacing between girders and superelevation mainly contributed to variations in shear force. The effect of intermediate diaphragms and boundary conditions were pronounced on the occurrence of the flexural moment in the main girders. Figure 7 illustrates the example of variations in live load effects on the main girders induced by changes in curvature angles. Additionally, the predicted LLDF results using the codified equations (AASHTO, 2020), representing the live load distribution mechanism of a typical straight bridge with the same span length as the curved superstructure, were plotted alongside the 3D-FEM LLDF. The results indicated that live load effects predicted from the current practice tended to be smaller than those obtained from 3D-FEM, representing curved superstructures. This comparison highlights behavioural different between these two superstructures and emphasises the need for either linear 3D-FEM or specific equations to estimate LLDF in the main girders of the curved superstructure.

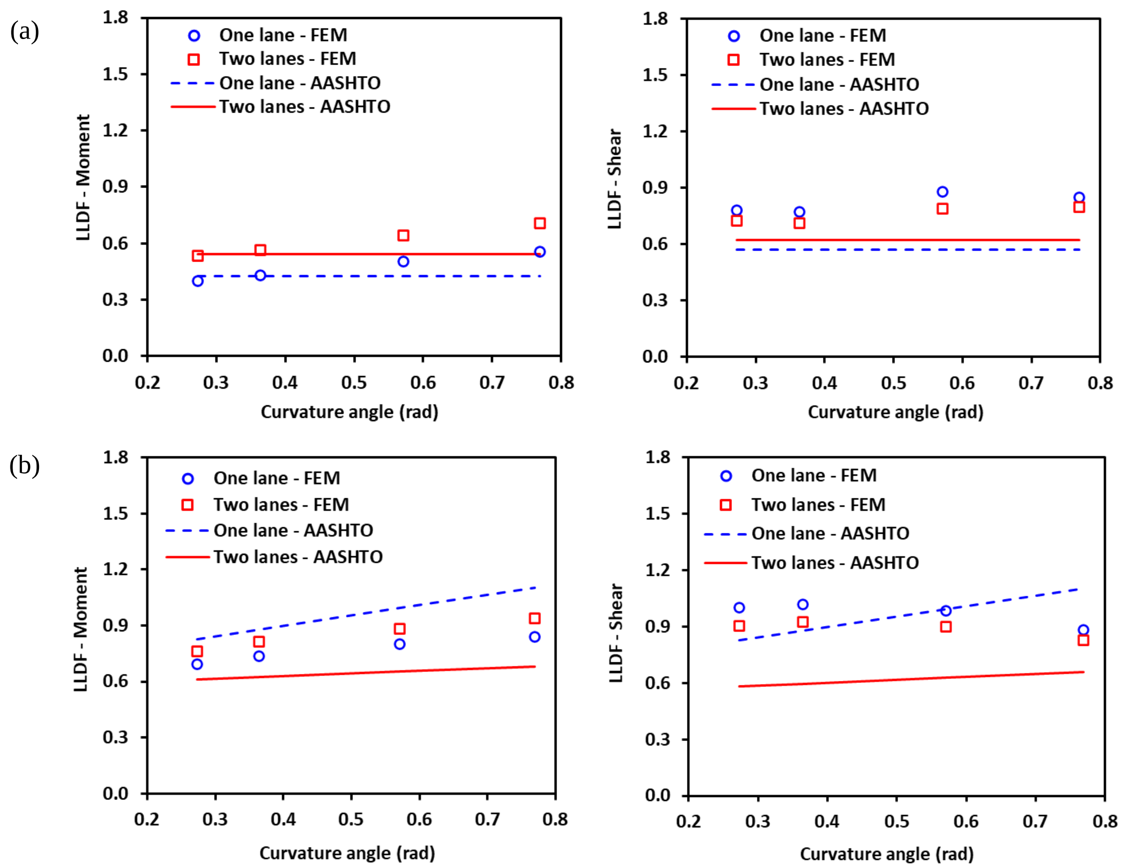

Figure 7 Variations in live load effects induced by curvature angle: (a) interior girder; and (b) exterior girder.

Based on the results of parametric study, the multiple linear regression analyses were performed to formulate the LLDF equations for the curved superstructure, aimed at providing an alternative approach to the linear 3D-FEM for analysing the live load effects on the main girders of the curved superstructure. The example of developed LLDF equations for the main girders of the targeted superstructure is described in Equations (2) to (9).

For one design lane (interior girder):

$$LLDF_m = 0.430 - 0.199\left(\frac{S}{4300}\right)^{0.4}\left(\frac{S}{L_{arc}}\right)^{0.3}\left(\frac{K_g}{L_{arc}t_s^3}\right)^{0.1} + 0.304\left(\frac{L_{arc}}{R}\right) - 0.003(E) \tag{2}$$

$$LLDF_s = 0.451 - 0.551\left(\frac{L_{arc}}{R}\right)^2 + 0.781\left(\frac{L_{arc}}{R}\right) + 1.013\times10^{-4}(S) - 0.007(E) \tag{3}$$

For two design lanes (interior girder):

$$LLDF_m = 0.430 + 0.100\left(\frac{S}{2900}\right)^{0.6}\left(\frac{S}{L_{arc}}\right)^{0.2}\left(\frac{K_g}{L_{arc}t_s^3}\right)^{0.1} + 0.335\left(\frac{L_{arc}}{R}\right) - 0.004(E) \tag{4}$$

$$LLDF_s = 0.357 - 0.172\left(\frac{L_{arc}}{R}\right)^2 + 0.402\left(\frac{L_{arc}}{R}\right) + 1.707\times10^{-4}(S) - 0.006(E) \tag{5}$$

For one design lane (exterior girder at outer curve):

$$LLDF_m = 0.499 - 0.253\left(\frac{L_{arc}}{R}\right)^2 + 0.521\left(\frac{L_{arc}}{R}\right) + 5.522\times10^{-5}(S) - 0.002(E) \tag{6}$$

$$LLDF_s = 2.727 - 0.772\left(\frac{L_{arc}}{R}\right)^2 + 0.650\left(\frac{L_{arc}}{R}\right) - 0.001(S) - 0.005(E) \tag{7}$$

For two design lanes (exterior girder at outer curve):

$$LLDF_m = 0.623 - 0.248\left(\frac{L_{arc}}{R}\right)^2 + 0.583\left(\frac{L_{arc}}{R}\right) + 1.060\times10^{-5}(S) - 0.003(E) \tag{8}$$

$$LLDF_s = 2.436 - 0.648\left(\frac{L_{arc}}{R}\right)^2 + 0.601\left(\frac{L_{arc}}{R}\right) - 0.001(S) - 0.005(E) \tag{9}$$

where $LLDF_m$ is the live load distribution factor for flexural moment; $LLDF_s$ is the live load distribution factor for shear force; L_{arc} is the centre arc length (mm); R is the centreline radius (mm); S is the spacing between girders (mm); E is the superelevation (%); t_s is the thickness of RC slab (mm); and K_g is the longitudinal stiffness parameter of the main girder (mm^4) calculated as per the equation suggested by the AASHTO LRFD (AASHTO, 2020). Additionally, since the proposed equations were derived from the results of the parametric study, it is vital to consider their range of applicability. Specifically, the values of L_{arc}/R shall be between 0.273 and 0.769 radians, S should range between 1400 and 1600 mm, and E should be within 4 and 8%.

The prediction accuracy of the proposed equations was also investigated by comparing the 3D-FEM results against the predictions using proposed equations, as illustrated in Figure 8. The comparison suggested that the predictions obtained from the developed formulae well fitted to those determined from the numerical analyses. These results imply that the proposed Equations (2) to (9) are more suitable for analysing the LLDF of the targeted superstructure compared to the current codified equations.

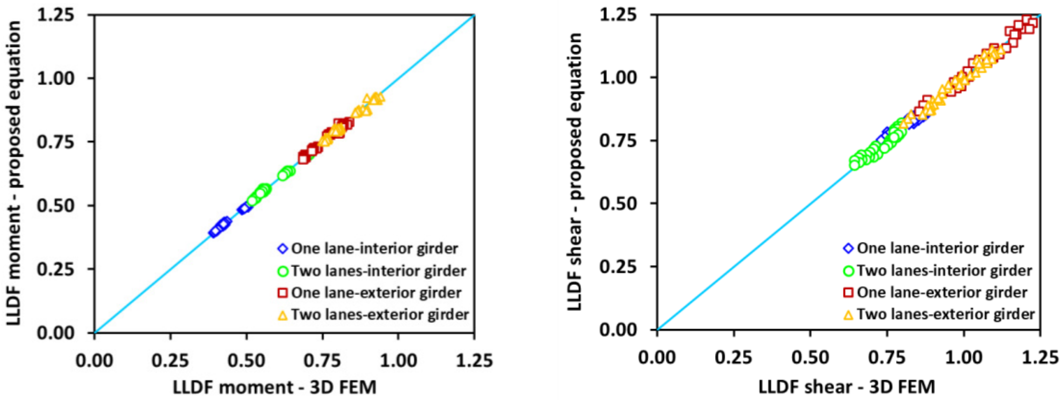

Figure 8 Variations in live load effects in the interior girder induced by curvature angle.

4.2 Structural performance of dapped-end connection

Once the live loads effects were identified using either the proposed equations or the linear 3D-FEM, the factored reaction forces applied to the upper nib at the considered limit states can be determined, taking into account the effect of all applied loads. Subsequently, analytical investigations can be conducted to examine the impacts of reinforcing schemes and concrete cover, as described in section 3.2, on the ultimate capacities and maximum crack width at the service limit state. Figure 9a shows the plots of the predicted reaction force versus vertical displacement at the re-entrant corner obtained from all analyses. In general, all analyses showed sufficient reserve capacity when compared to the required reaction force at the strength limit state (AASHTO, 2020), which is 911 kN. Based on the sensitivity study, the results implied that the peak load capacities and overall stiffnesses of the connections were more sensitive to the reinforcement arrangement than the concrete cover. The dap featuring diagonal reinforcements (Figure 6b) showed the highest ultimate capacities, followed by the one reinforced with combined orthogonal and diagonal reinforcements (Figure 6c), and then by the one reinforced solely with orthogonal reinforcements (Figure 6a). The predicted ultimate capacities are summarised in Figure 9b.

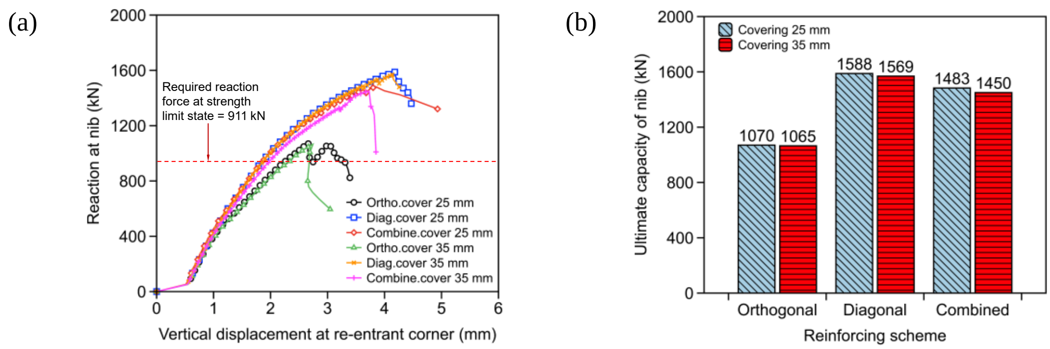

Figure 9 Effect of considered parameters on ultimate capacity and stiffness: (a) plot between reaction and vertical displacement at re-entrant corner; and (b) summary of ultimate capacity.

Table 3 tabulates the predicted maximum crack widths at the service limit state obtained from the analytical investigations. Consistent with the results for peak load capacities and stiffnesses, the dapped-end connection reinforced with diagonal reinforcements (Figure 6b) exhibited the narrowest corner cracks, suggesting the superior performance of this reinforcing scheme compared to other reinforcement details. Nevertheless, the results indicated that an increase in concrete cover led to widening of the predicted crack width.

Table 3 Summary of the predicted maximum crack width at the service limit state.

Reinforcement arrangement	Predicted maximum crack width (mm)	
	Concrete cover 25 mm	Concrete cover 35 mm
Orthogonal	0.147	0.209
Diagonal	0.098	0.136
Combined orthogonal and diagonal	0.120	0.158

Furthermore, to evaluate structural durability against the carbonation deterioration, the completion time for carbonation penetration was predicted, considering the impact of the maximum crack width at the service limit state, atmospheric carbon dioxide concentration, and variations in water-to-cement (w/c) ratios. It is worth nothing that the information related to w/c ratios was compiled from actual data used in the construction. The plots presenting the utilised w/c-ratios versus completion time for carbonation penetration are shown in Figure 10. According to these results, some predictions on the required completion time for the carbonation reaction were much faster than 30-year, implying possibility in future structural distresses and irregularities caused by the deterioration mechanism. These unsatisfactory results were detected in all daps with a concrete cover of 25 mm (Figure 10a).

When the concrete cover was increased to 35 mm, it was observed that the required completion time for carbonation penetration was delayed in all analyses. Eventually, some predictions gained from dapped-end connections featuring diagonal reinforcements and combined orthogonal and diagonal reinforcements could achieve the required service life of 30-year, as depicted in Figure 10b, despite the observed crack widths being wider than those yielded by daps with a concrete cover of 25 mm. To satisfy a 30-year repair-free service life, the w/c-ratio of concrete in daps reinforced with diagonal rebar layout and combined orthogonal and diagonal rebar layout should be smaller than 0.389 and 0.383, respectively. Although the applicable w/c ratios are lower than 0.39, this value is possible in practice since the construction processes of the PC I-girder are conducted in a factory, where quality control is precise and efficient. Additionally, to enhance workability while reducing the w/c ratio, the use of admixtures, such as superplasticisers, should be considered in practice. Furthermore, applying surface coating for carbonation protection can also be implemented.

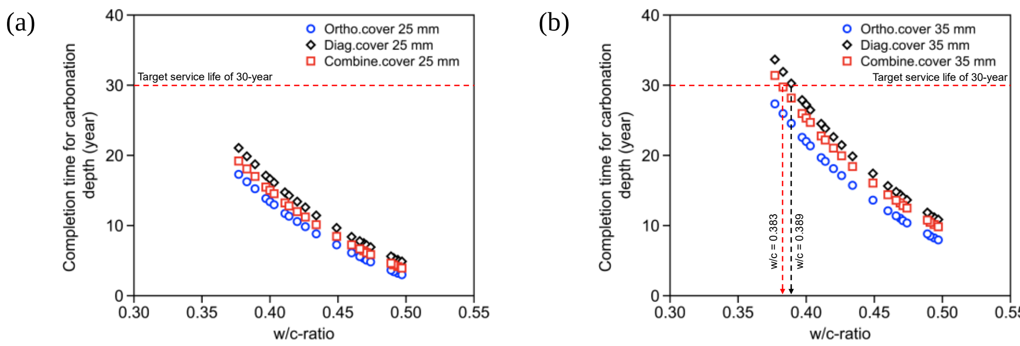

Figure 10 Completion time for the carbonation depth: (a) cover 25 mm; and (b) cover 35 mm.

5. FRAMEWORK FOR ANALYSIS AND DESIGN OF CURVE SUPERSTRUCTURE

Based on analytical investigations, the enhanced structural analysis and design framework for the main girders of curved superstructures, visualised in Figure 11, is proposed to accomplish sustainable and resilient highway infrastructure. This framework is designed as a general procedure compatible with the structural design of any structural members using any design regulations. Nevertheless, the concept illustrated in Figure 11 presents an example of the analysis and design of the dapped-end connection.

The framework includes the structural analysis for the effects of actions to determine the design values from the combination of actions. Subsequently, the required amount of reinforcement in the dapped-end connection is determined, considering the requirement of minimum concrete cover in accordance with the design codes. The rebar layout in the dapped-end connection can then be detailed. Additionally, the target service life (t_r) conforming to the codified regulations shall be selected at this design stage. Subsequently, the ultimate capacities (Q_r) and the maximum crack width (w_{cr}) induced by reaction force in the nib at the service limit state (Q_s) can be analytically clarified. Also, the required time for completing carbonation penetration (t), considering the effect of crack width, can be calculated.

Once Q_r and t are determined, the structural performance verification can be then performed. Based on the analytical investigations, the results showed that achieving the target service life is challenged when solely relying on the maximum allowable crack width limitation. Therefore, to enhance the structural design method aimed at improving durability performance, the completing time for deterioration mechanisms in the structure, such as the carbonation used in this framework, should be explicitly calculated. This calculation should consider the impact of crack width at the service limit state and other structural configurations, including utilised concrete covers and w/c-ratios. Ultimately, the appropriate structural configuration of the dapped-end connection, satisfying both structural capacity and the targeted service life, can be finalised.

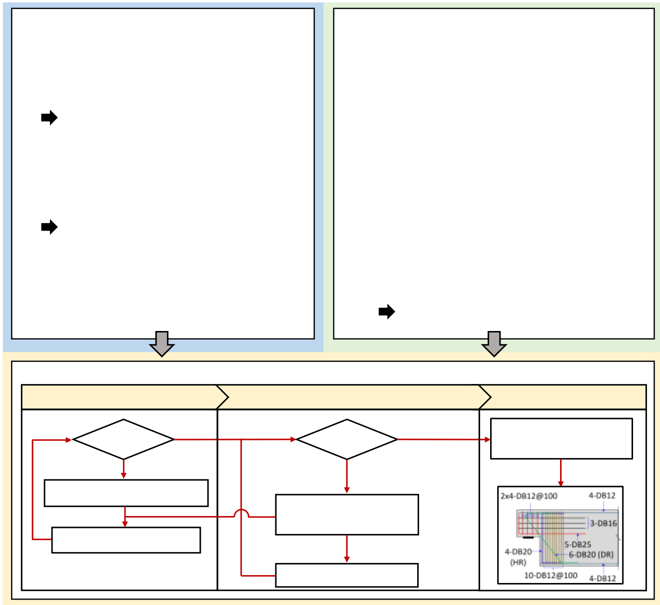

Figure 11 Framework for enhanced structural analysis and design of curved superstructure.

6. CONCLUSIONS

Based on the analytical investigations, the current research aims to propose the framework for innovative structural analysis and design of the main girders in the curve superstructures, targeted at improving durability performance towards sustainable structural design. The findings obtained from the overall analyses could be drawn as follows:

- Live load effects in the main girder of the curved superstructure were significantly influenced by its unique structural configurations. This result highlighted the importance of conducting the linear 3D-FEM or implementing the proposed LLDF equations to accurately determine the sectional forces induced by live load.
- All dapped-end connections exhibited sufficient ultimate strength compared to the force demand at the strength limit state. However, solely relying on the maximum crack width limitation was insufficient for ensuring structural durability and resistance to carbonation deterioration.
- The implementation of the proposed framework ensures adequate capacity and functionality of the structure throughout its design service life. This approach helps prevent the over-exploitation of resources caused by the rapid deterioration of existing structures, which often necessitates their replacement with new ones. Additionally, it promotes sustainable and resilient infrastructure development.

7. ACKNOWLEDGEMENTS

The authors would like to acknowledge the financial support provided by JICA-SATREPS for this research.

8. REFERENCES

American Association of State Highway and Transportation Officials (AASHTO). (2020). AASHTO LRFD bridge design specification. 9th Edition. Washington (DC).

BS EN-1992-1-1. (2004). Eurocode 2: Design of Concrete Structures.

Červenka, V., Jendele, L., & Prague, J. Č. (2022). ATENA Program Documentation Part 1-Theory.

Desnerck, P., Lees, J. M., & Morley, C. T. (2016). Impact of the reinforcement layout on the load capacity of reinforced concrete half-joints. Engineering Structures, *127*, 227–239. https://doi.org/10.1016/j.engstruct.2016.08.061

DPT1322-55. (2012). Durability design requirement of concrete structures (in Thai language).

Kwon, S-J., & Na, U-J. (2011). Prediction of durability for RC columns with crack and joint under carbonation based on probabilistic approach. International Journal of Concrete Structures and Materials, 5(11), 11-18. https://doi.org/10.4334/IJCSM.2011.5.1.011

MIDAS IT Corporation. (2022). Analysis for Civil Structures.

Precast/Prestressed Concrete Institute. (2010). PCI design handbook. Precast and prestressed concrete

Zokaie, T., Osterkamp, T.A., & Imbsen, R.A. (1991). Distribution of wheel loads on highway bridges. National Cooperative Highway Research Program, Report 12-26, Washington.

Analysis of Motorcycle Accidents at Signalized Intersections on National Highways in Thailand: Same-direction Collisions

Pasakorn Kuenpet[1], Thaned Satiennam[2],
Ponlathep Lertworawanich[1], Chaiwut Kanjanasantisuk[3]

[1]Department of Highways, Bureau of Road Research and Development, Bangkok, Thailand
[2]Department of Civil Engineering, Faculty of Engineering, Khon Kaen University, Khon Kaen, Thailand
[3]Department of Highways, Bureau of Highway Safety, Bangkok, Thailand

ABSTRACT

Motorcycles account for 52.5% of all registered vehicles in Thailand, and this percentage is increasing annually. This corresponds to the fatality rate of motorcycle riders, which accounts for 83.8% of all fatalities. Over the last three years, the number of highway accidents has increased, with a total of 58,751 incidents. Motorcycles were involved in 12,795 cases, which accounted for 14.3% of all accidents. Out of the total accidents, 5,668 (9.7%) occurred at intersections. The death rate for motorcycle accidents is alarmingly high at 33.4%. The aim of this study is to examine same-direction motorcycle collisions at signaled intersections along Thailand's national highways. The analysis focuses on accidents within the highway network under the Department of Highways between 2021 and 2023. It aims to identify the characteristics of same-direction crashes occurring at signalized intersections using the Multinomial Logistic Regression (MLR) method. The study classified motorcycle accidents into four categories: property damage, minor injuries, serious injuries, and fatalities, and collision characteristics into three categories: side swipe in a parallel lane, vehicle hit while changing lanes, and rear-end collision. The study results revealed that in 2022, the likelihood of fatalities was the highest, with the number of accidents increasing annually. Additionally, accidents involving large-sized vehicles had the highest probability of fatalities. All types of collisions were likely to cause serious injuries. However, side swipe in a parallel lane was found to have the highest likelihood of causing serious injuries.

Keywords: Motorcycle, Same-direction accidents, Signalized Intersections, Highways, Road safety

1. INTRODUCTION

The World Health Organization (WHO) reported that in 2021, the global road accident situation remained critical, with a death toll of 1.19 million people per year. An assessment of high-risk road users, such as pedestrians, cyclists, and motorcyclists, indicated that these groups still face significant risks, with 80% of all roads failing to meet minimum safety standards (World Health Organization, 2021). In Thailand, the mortality rate from road accidents involving motorcycles is the highest, accounting for 83.8% of all road accident fatalities (Department of Disease Control Ministry of Public Health, 2023).

Motorcycles are a popular mode of transportation in Thailand, with the registration rate for new motorcycles increasing every year, as shown in Figure 1. In 2023, the total number of registered motorcycles nationwide reached 22,569,593 accounting for 52.5% of all registered vehicles in Thailand (Department of Land Transport Transportation Statistics Group Planning Division, 2024). As the number of motorcycles on the road network increases, the likelihood of accidents also rises. The trend of accidents at intersections on highways has been increasing from 2019 to 2023, as shown in Figure 2 (Department of Highways Bureau of Highway Safety, 2023). Therefore, the problem of road accidents, especially motorcycles, is crucial. Currently, Thailand's highway network totals 52,288 kilometers, comprising 2,897 kilometers of concrete roads and 49,391 kilometers of asphalt roads (Department of Highways Bureau of Highway Maintenance Management, 2024). These highways serve as the primary transportation routes, linking various secondary road networks. The issue of motorcycle accidents at intersections in Thailand requires urgent attention. Studying the types of collisions and their impact on the severity of motorcycle accidents is essential. This research will enable relevant government agencies to formulate more effective policies and measures to address the problem.

In foreign countries, there have been numerous studies on the types of collisions affecting the severity of motorcycle accidents (Rifaat et al., 2012), (Jung et al., 2013), (Abrari Vajari et al., 2020). However, due to differences in Thailand's road infrastructure, urban layouts, traffic conditions, and driving behaviors, the types of collisions impacting the severity of motorcycle accidents in Thailand may differ from those in other countries.

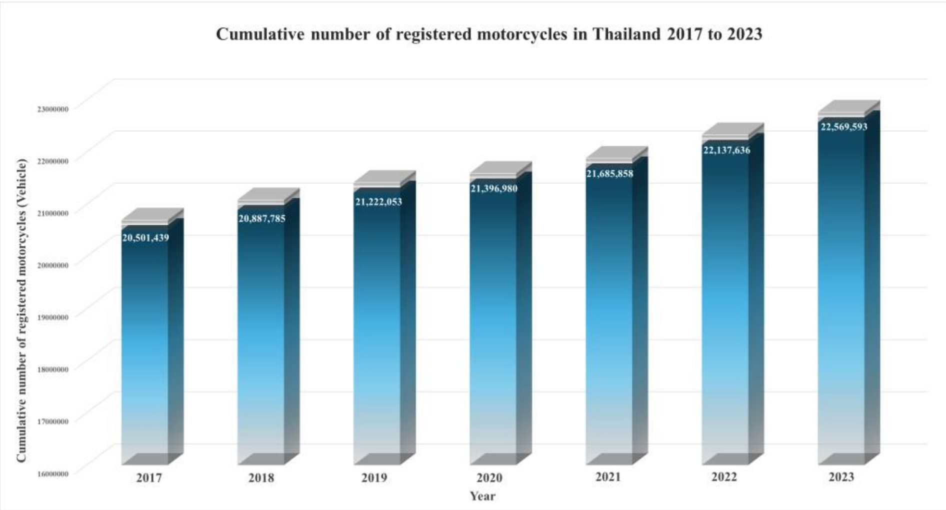

Figure 1 Cumulative number of registered motorcycles in Thailand (2017 to 2023)

In the past, related studies in Thailand have explored the factors influencing the severity of injuries sustained by motorcycle riders on main roads in the country (Se et al., 2021). It has been found that the nature of collisions is one of the factors impacting the severity of accidents. However, the variety of collision types encountered does not cover all potential accident scenarios, such as collisions occurring at intersections. This is because the physical characteristics of each road segment differ, potentially influencing the severity of motorcycle accidents.

Therefore, the objective of this research is to investigate same-direction collisions at signalized intersections that affect the severity of motorcycle accidents on national highways in Thailand. This will be done using accident data related to motorcycles on the national highway network of Thailand, spanning a period of 3 years (2021 - 2023), obtained from the Highway Accident Information Management System (HAIMS) of the Department of Highways, is to analyze the characteristics of collisions at signalized intersections in the same direction that affect the severity of motorcycle accidents, using Multinomial Logistic Regression, and to propose measures to reduce the severity of motorcycle accidents on Thailand's national highways.

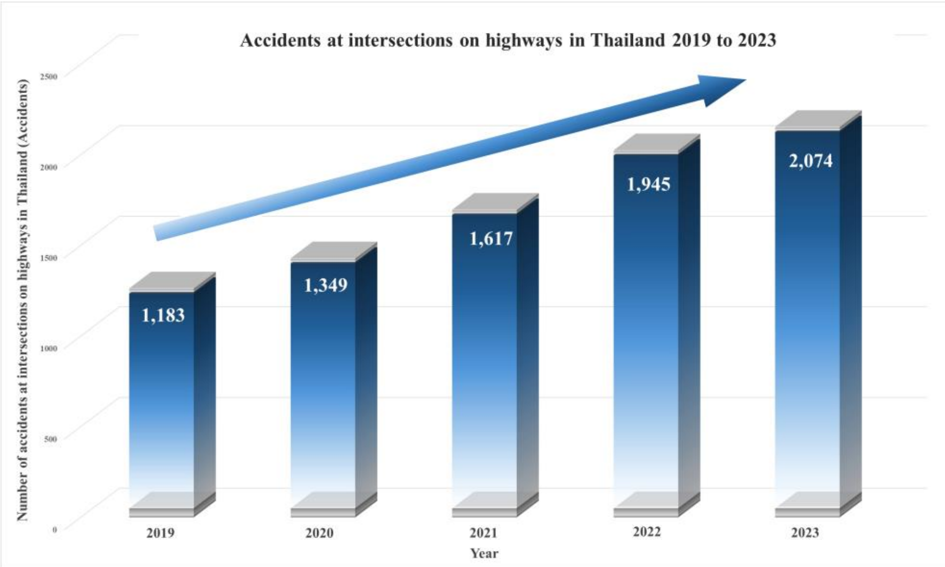

Figure 2 Accidents at intersections on highways in Thailand (2019 to 2023)

2. Literature review

Table 1 Summary of past studies on factors and analysis methods for motorcyclist injury severity. The study explores various factors influencing the severity of accidents, encompassing the utilization of statistical techniques for analysis. Multinomial Logistic Regression (MLR) is widely employed to analyze accident severity. This method is commonly used to examine factors related to motorcycle accident severity, as it efficiently predicts severity levels and allows for the analysis of variables across more than two groups (Abdulhafedh, 2017)(Rezapour & Ksaibati, 2018)(Abrari Vajari et al., 2020)(Shiran et al., 2021). Typically, accident severity is categorized into more than two levels, such as fatalities, serious injuries, minor injuries, and property damage (Rifaat et al., 2012), (Shiran et al., 2021). Therefore, Multinomial Logistic Regression is suitable for analyzing motorcycle accident severity. Previous studies have investigated numerous significant risk factors, including driver characteristics (gender (Se et al., 2021), age (Abrari Vajari et al., 2020), speeding behavior (Jung et al., 2013), (Rifaat et al., 2012), (Se et al., 2021)), road physical characteristics (intersections (Abrari Vajari et al., 2020), stopping points (Abrari Vajari et al., 2020), lane counts (Se et al., 2021),(Champahom et al., 2022), traffic control systems (Abrari Vajari et al., 2020)), collision characteristics (rear-end collisions, side collisions (Se et al., 2021), collisions with large vehicles such as trucks, buses, trailers (Rifaat et al., 2012), (Jung et al., 2013), (Se et al., 2021), collisions with medium-sized vehicles such as personal cars, pickups, vans (Rifaat et al., 2012), (Se et al., 2021), collisions with motorcycles, and collisions with other vehicle types (Jung et al., 2013), (Abrari Vajari et al., 2020), and temporal factors (nighttime visibility (Se et al., 2021), daytime conditions (Abrari Vajari et al., 2020)).

Table 1 Summary of previous studies on motorcyclist injury severity.

Authors	Area	Accident types	Methodology	Key findings

(Rifaat et al., 2012)	Canada	Intersection vehicle from adjacent approaches	Ordered logit model, heterogeneous choice model and partially constrained generalized ordered logit model	• Motorcycle riders are at greater risk and suffer more severe injuries than car drivers in the event of a crash.
				• Crash severity is categorized into three levels.
				• Injury severity tends to increase when:
				  • The crash involves a van.
				  • The rider is male.
				  • The rider is following too closely behind another vehicle.

(Jung et al., 2013)	United States of America	Head-on collisions and Broadside collisions	Multinomial logit (MNL)	• Motorcycle accidents evaluated by injury severity
				• Factors influencing the severity of accidents include:
				  • Collision characteristics
				  • Truck involvement

(Abdulhafedh, 2017)	United States of America	Motor vehicle collisions	Multinomial logistic regression (MLR)	• Effective in modeling injury severity
				  • As it does not require assumptions of normality, linearity, or homoscedasticity.
				• Transforms the dependent variable into a continuous form
				  • Yielding results in the form of log odds, ranging from negative infinity to positive infinity.
				  • These results can be interpreted using regression coefficients and odds ratios.

(Rezapour & Ksaibati, 2018)	United States of America	Collisions involving commercial vehicles	Multinomial and Ordinal logistic regression	• Driver behaviors such as failure to maintain proper lanes, tailgating, and speeding for road conditions account for approximately 40% of all truck accidents.
(Rezapour et al., 2019)	United States of America	Run-off-road Collision	Multinomial logistic regression (MLR)	• Severity of accidents associated with traffic barriers. • Driver behavior plays a significant role in determining the severity of these accidents.

Authors	Area	Accident types	Methodology	Key findings
(Abrari Vajari et al., 2020)	Australia	Intersection Crashes	Multinomial logistic regression (MLR)	• Motorcycle collisions at intersections pose a higher risk of fatality and severe injury compared to other vehicle types. • Intersection accidents are more likely to result in severe injuries or fatalities than non-intersection accidents. • Factors contributing to increased severity include time of occurrence, gender, and intersections where vehicles must stop.
(Shiran et al., 2021)	United States of America	Motorcycle accidents (unspecified collision type)	Multinomial logistic regression (MLR)	• Severity levels were classified into five categories: property damage only (PDO), fatality, severe injury, other visible injuries, and complaint of pain.
(Se et al., 2021)	Thailand	Motorcycle accidents (unspecified collision type)	Correlated random parameters ordered probit model with heterogeneity in means (CRPOPHM)	• Analyzing and comparing the impact of accidents in urban and rural areas on the severity of motorcycle rider injuries. • Vehicle type, law violations, time of occurrence, and collision type significantly influence injury severity.
(Champahom et al., 2022)	Thailand	Motorcycle accidents (unspecified collision type)	Multiple Correspondence Analysis (MCA) and Ordered Logistic Regression	• Factors influencing the severity of motorcycle accidents on main roads in Thailand include the number of lanes, gender, and road characteristics.
(Se et al., 2022)	Thailand	Motorcycle accidents (unspecified collision type)	Random Parameters Logit Model	• The severity of injuries sustained by motorcycle riders is evaluated and classified into three categories: minor injuries, severe injuries, and fatalities. • The differences in days significantly impact the severity level of accidents.
(Champahom et al., 2023)	Thailand	Motorcycle accidents (unspecified collision type)	Random parameters logit models with unobserved heterogeneity in means and variances	• Fatal motorcycle crashes on local roads involve four main components contributing to fatalities: rider characteristics, pre-collision actions, temporal and environmental factors, and road characteristics.

In summarizing the literature review, it was found that several factors influencing the severity of motorcycle accidents align with studies conducted in other countries. However, certain factors need further consideration, such as the collision characteristics of motorcycles at signalized intersections. This is because there is still ambiguity regarding the types of collisions in the same direction at intersections with traffic signals. Moreover, Thailand's road infrastructure, traffic conditions, and driving behaviors differ from those in other countries. Additionally, the use of lanes shared with other vehicle types, coupled with the smaller size of motorcycles compared to those in Europe or America, allows for greater maneuverability between traffic lanes. Consequently, the collision characteristics influencing the severity of motorcycle accidents in Thailand may differ from those in other countries. Thus, this study aims to investigate the characteristics of accidents at signalized intersections in the same direction that affect the severity of motorcycle accidents on Thailand's national highways.

3. METHODS

3.1 Data Collection and Screening

This research utilized data from the Highway Accident Information Management System (HAIMS), operated by the Department of Highways, for data management and accident analysis on national highways. (Department of Highways Bureau of Highway Safety, 2023) The accident data was collected through two methods: 1) Highway Department officials surveyed accident data at the accident locations, and 2) Highway Department officials copied accident data from police officers and visited the accident sites to gather additional information. The data was recorded according to the Highway Accident Report form and stored in the database of the Department of Highways. This research utilized accident data related to motorcycles on the national highway network covering a total distance of 52,288 kilometers across Thailand.

The data covers 2021 to 2023. 12,795 accident records involved with motorcycles. After screening the data for accidents occurring at signalized intersections and collisions in the same direction, 639 cases (N = 639) were used for further analysis.

3.2 Data Analysis

This research applied the Multinomial Logistic Regression model, a widely used analytical method in previous studies. (Jung et al., 2013)(Abdulhafedh, 2017)(Rezapour & Ksaibati, 2018)(Rezapour et al., 2019)(Abrari Vajari et al., 2020)(Shiran et al., 2021). With a 95 percent confidence level, this method was used to examine the characteristics of accidents that influence the severity of motorcycle accidents on Thai highways. The study categorized the severity of motorcycle related accidents into four levels based on the Highway Accident Information Management System: 1) Fatal Injury (FI) accounting for 19.7 percent of the data, where the driver or pillion rider succumbs to injuries at the scene or within 48 hours at the hospital, 2) Serious Injury (SI) representing 15.6 percent of the data, where the driver or pillion rider sustains injuries that cannot be cured within three weeks, 3) Minor Injury (MI) representing 51.3 percent of the data, where the driver or pillion rider sustains minor injuries that heal within a short period, and 4) Property Damage (PD) representing 13.3 percent of the data, where no injuries or fatalities occur. The property damage level was set as the reference group since it represents incidents without injuries or fatalities. In multinomial logistic regression analysis, selecting the group with the lowest severity as the reference group helps interpret the odds ratios of variables regarding accident severity in each level. This method is suitable for establishing standard criteria for comparing other groups with higher severity.

This research identified various factors expected to influence the nature of accidents at intersections with traffic lights in the same direction, affecting the severity of motorcycle accidents on highways. These factors were categorized into two groups: Temporal characteristics and Crash characteristics, as shown in Table 2

Table 2 Variable Codes and Descriptions

Variable
Injury severity
Fatalities Injury (FI)
Serious Injury (SI)
Minor Injury (MI)
Property Damage (PD)*
Temporal characteristics
Year of accidents
Categorical Variable (3 groups, including 2021*, 2022, 2023)
(V_1) Year of Incident, 2022, Coding (0 = Yes, 1 = Others)
(V_2) Year of Incident, 2023, Coding (0 = Yes, 1 = Others)
Crash characteristics
Type of involved vehicle
Categorical Variable (3 groups, including small-sized vehicle (Motorcycles)*, medium-sized vehicles (including, sedans/vans/pickup trucks), and large-sized vehicles (including, trucks/buses/public transport vehicles))
(V_3) Medium-sized vehicle, Coding (0 = Yes, 1 = Others)
(V_4) Large-sized vehicle, Coding (0 = Yes, 1 = Others)
Type of collision
Categorical Variable (4 groups, including rear end, side swipe in parallel lane, vehicle hit while changing lane and other types*)
(V_5) Rear end (Categorical Variable) (0 = Others, 1 = Yes)
(V_6) Side swipe in parallel lane (Categorical Variable) (0 = Others, 1 = Yes)
(V_7) Vehicle hit while changing lane (Categorical Variable) (0 = Others, 1 = Yes)

Note: *Reference group

4. RESULTS AND CONCLUSION

Results of the analysis of accidents occurring in the same direction at signalized intersections influencing severity are presented in Table 3. The table shows estimates, p-values, and odds ratios (OR) for statistically significant variables at the 0.05 level. From the analysis, significant influences on accident severity were found for both temporal characteristics and crash characteristics. These results will be elaborated upon in detail, categorized by the type of factor, namely serious injuries and fatalities.

Table 3 Results of Multinomial Logistic Regression Analysis Model

Variables	Estimated	P-value	Odd Ratio
Injury severity			
Intercept (FI)	-4.285	0.018*	
Intercept (SI)	-4.344	0.011*	
Temporal characteristics			
Temporal characteristics: Year of Incident, 2022 (FI)	1.142	0.002**	3.133
Temporal characteristics: Year of Incident, 2023 (FI)	0.880	0.013*	2.411
Temporal characteristics: Year of Incident, 2022 (SI)	0.932	0.015*	2.540
Temporal characteristics: Year of Incident, 2022 (MI)	0.722	0.022*	2.059
Temporal characteristics: Year of Incident, 2023 (MI)	0.647	0.026*	1.910
Crash characteristics			
Type of involved vehicle: other vehicle involved in motorcycle accident, large-sized vehicles (FI)	3.535	<0.001**	34.311
Type of involved vehicle: other vehicle involved in motorcycle accident, medium-sized vehicles (FI)	1.485	0.029*	4.415
Type of involved vehicle: other vehicles involved in motorcycle accident, large-sized vehicles (SI)	1.445	0.043*	4.242
Type of collision: Rear-end collision, Yes (SI)	1.503	0.050*	4.493
Type of collision: Side swipe in parallel lane, Yes (SI)	2.413	0.004**	11.165
Type of collision: Side swipe in parallel lane, Yes (MI)	1.555	0.043*	4.733
Type of collision: Vehicle hit while changing lane, Yes (SI)	1.648	0.050*	5.198
n = 639, Reference group: Property Damage (PD). Statistical values: Log Likelihood = 259.467, Chi-Square = 81.483, P-Value <0.001, Nagelkerke Pseudo R-Square: 0.131			

Note: 1) Fatalities Injury (FI) 2) Serious Injury (SI) 3) Minor Injury (MI), * Statistically significant at 5% level, ** Statistically significant at 1% level.

4.1 Analysis results of temporal characteristics

- In the years 2022 and 2023, the likelihood of fatalities is greater compared to property damage, with odds ratios of 3.133 and 2.411 respectively, when compared to the year 2021.
- In the year 2022, the likelihood of serious injuries is greater compared to property damage, with an odds ratio of 2.540 when compared to the year 2021.
- In the years 2022 and 2023, the likelihood of minor injuries is greater compared to property damage, with odds ratios of 2.059 and 1.910 respectively, when compared to the year 2021.

In summary, in the years 2022 and 2023, the likelihood of fatalities was greater compared to the year 2021, with the odds of fatalities increasing in sequence. The highest odds of fatalities were observed in the year 2022 at 3.133 times. Additionally, in the year 2022, the likelihood of serious injuries was greater compared to the year 2021, with an odds ratio of 2.540. Moreover, in the years 2022 and 2023, the likelihood of minor injuries was greater compared to the year 2021, with the highest odds of minor injuries observed in the year 2022 at 2.059 times.

4.2 Analysis results of crash characteristics

- At signalized intersections, same-direction motorcycle accidents involving large-sized vehicles and medium-sized vehicles are more likely to be fatal at 34.311 and 4.415 times (OR = 34.311 and 4.415) compared to property damage, when compared to accidents involving Motorcycles.
- At signalized intersections, same-direction motorcycle accidents involving large-sized vehicles are more likely to be seriously injured at 4.242 (OR = 4.242) compared to property damage, when compared to accidents involving Motorcycles.
- At signalized intersections, same-direction rear-end accidents are more likely to be seriously injured at 4.493 (OR = 4.493) compared to property damage, when compared to accidents of other types.
- At signalized intersections, same-direction side swipe in parallel lane accidents are more likely to be seriously injured and minorly injured at 11.165 and 4.733 times (OR = 11.165 and 4.733) compared to property damage, when compared to accidents of other types.
- At signalized intersections, same-direction Vehicle hit while changing lane accidents are more likely to be seriously injured at 5.198 (OR = 5.198) compared to property damage, when compared to accidents of other types.

In summary, regarding crash characteristics, motorcycle accidents involving large-sized vehicles have the highest likelihood of fatalities, with an odds ratio of 34.311 (OR = 34.311) when compared to accidents involving Motorcycles. Additionally, Side swipe in parallel lane, Vehicle hit while changing lane, and Rear-end accidents, as shown in Figure 3, 4 and 5 have a higher likelihood of serious injuries compared to all others when compared to property damage, ranked in descending order: 11.165 (OR = 11.165), 5.198 (OR = 5.198), and 4.493 (OR = 4.493), respectively.

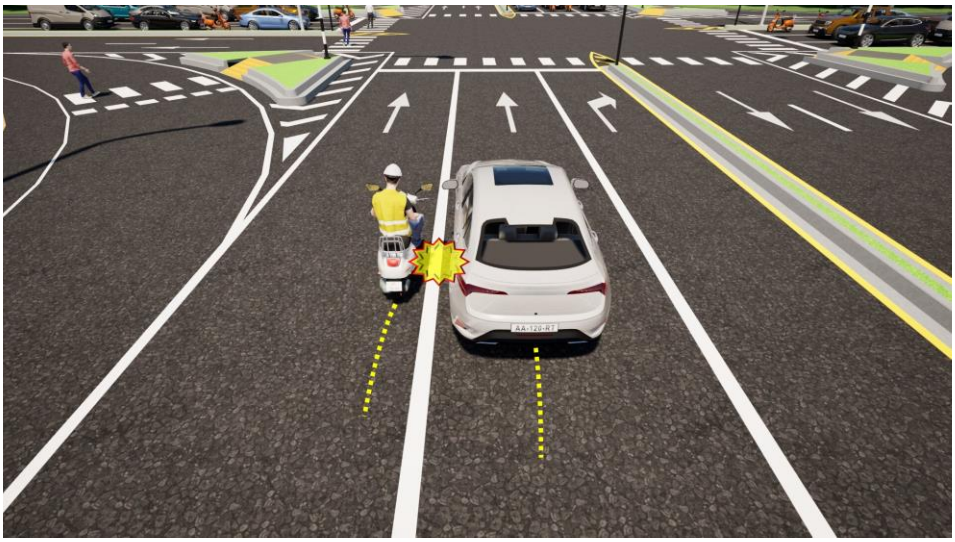

Figure 3 Side swipe in parallel lane

Figure 4 Vehicle hit while changing lane

Figure 5 Rear-end collision

Future studies should consider incorporating factors that may influence the severity of motorcycle accidents, such as traffic volume and road speed limits. This approach aims to comprehensively analyze accidents at signalized intersections that affect the severity of motorcycle accidents on highways in Thailand. Additionally, safety measures that can reduce the likelihood of same-direction collisions at signalized intersections should be considered, such as the installation of Exclusive Stopping Space (ESS) for Motorcycles at Signalized Intersections. These dedicated areas separate motorcycles from other vehicles stopped at red lights, reducing the chance of being squeezed or hit when starting simultaneously. It is also essential to continuously evaluate the effectiveness of these measures.

6. REFERENCES

Abdulhafedh, A. (2017). Incorporating the Multinomial Logistic Regression in Vehicle Crash Severity Modeling: A Detailed Overview. *Journal of Transportation Technologies*, *07*(03), 279–303. https://doi.org/10.4236/jtts.2017.73019

Abrari Vajari, M., Aghabayk, K., Sadeghian, M., & Shiwakoti, N. (2020). A multinomial logit model of motorcycle crash severity at Australian intersections. *Journal of Safety Research*, *73*, 17–24. https://doi.org/10.1016/j.jsr.2020.02.008

Champahom, T., Se, C., Jomnonkwao, S., Boonyoo, T., Leelamanothum, A., & Ratanavaraha, V. (2023). Temporal Instability of Motorcycle Crash Fatalities on Local Roadways: A Random Parameters Approach with Heterogeneity in Means and Variances. *International Journal of Environmental Research and Public Health*, *20*(5). https://doi.org/10.3390/ijerph20053845

Champahom, T., Wisutwattanasak, P., Chanpariyavatevong, K., Laddawan, N., Jomnonkwao, S., & Ratanavaraha, V. (2022). Factors affecting severity of motorcycle accidents on Thailand's arterial roads: Multiple correspondence analysis and ordered logistics regression approaches. *IATSS Research*, *46*(1), 101–111. https://doi.org/10.1016/j.iatssr.2021.10.006

Department of Disease Control Ministry of Public Health. (2023). *Road Traffic Death Data Integration(RTDDI)*. https://dip.ddc.moph.go.th/rtddi/public/?page=std01

Department of Highways Bureau of Highway Maintenance Management. (2024). *Highway Statistics*. https://stat.doh.go.th/

Department of Highways Bureau of Highway Safety. (2023). *Highway Accident Information Management System*. https://haims2.doh.go.th/

Department of Land Transport Transportation Statistics Group Planning Division. (2024). *Number of Vehicle registered*. https://web.dlt.go.th/statistics/

Jung, S., Xiao, Q., & Yoon, Y. (2013). Evaluation of motorcycle safety strategies using the severity of injuries. *Accident Analysis and Prevention*, *59*, 357–364. https://doi.org/10.1016/j.aap.2013.06.030

Rezapour, M., & Ksaibati, K. (2018). Application of multinomial and ordinal logistic regression to model injury severity of truck crashes, using violation and crash data. *Journal of Modern Transportation*, *26*(4), 268–277. https://doi.org/10.1007/s40534-018-0166-x

Rezapour, M., Molan, A. M., & Ksaibati, K. (2019). Application of Multinomial Regression Model to Identify Parameters Impacting Traffic Barrier Crash Severity. *The Open Transportation Journal*, *13*(1), 57–64. https://doi.org/10.2174/1874447801913010057

Rifaat, S. M., Tay, R., & De Barros, A. (2012). Severity of motorcycle crashes in Calgary. *Accident Analysis and Prevention*, *49*, 44–49. https://doi.org/10.1016/j.aap.2011.02.025

Se, C., Champahom, T., Jomnonkwao, S., Chaimuang, P., & Ratanavaraha, V. (2021). Empirical comparison of the effects of urban and rural crashes on motorcyclist injury severities: A correlated random parameters ordered probit approach with heterogeneity in means. *Accident Analysis and Prevention*, *161*(August), 106352. https://doi.org/10.1016/j.aap.2021.106352

Se, C., Champahom, T., Jomnonkwao, S., & Kronprasert, N. (2022). Analytic Methods in Accident Research The impact of weekday , weekend , and holiday crashes on motorcyclist injury severities : Accounting for temporal influence with unobserved effect and insights from out-of-sample prediction. *Analytic Methods in Accident Research*, *36*, 100240. https://doi.org/10.1016/j.amar.2022.100240

Shiran, G., Imaninasab, R., & Khayamim, R. (2021). Crash severity analysis of highways based on multinomial logistic regression model, decision tree techniques and artificial neural network: A modeling comparison. *Sustainability (Switzerland)*, *13*(10). https://doi.org/10.3390/su13105670

World Health Organization. (2021). *WHO. Global status report on road safety*.

Adapting the Macroscopic Fundamental Diagram for Motorcycle-Dependent Cities: A Case Study of Cần Thơ City, Vietnam

Siti Raudhatul Fadilah[1], Hiroaki Nishiuchi[2,*], and An Minh Ngoc[3]

[1] Kochi University of Technology, Kami City, Kochi, Japan, 258003k@gs.kochi-tech.ac.jp
[2] Kochi University of Technology, Kami City, Kochi, Japan, nishiuchi.hiroaki@kochi-tech.ac.jp
[3] Ritsumeikan University, Kusatsu, Shiga, Japan. anngoc@fc.ritsumei.ac.jp

ABSTRACT

The dominance of motorcycles in traffic demands a specialized analytical approach that extends beyond conventional methods designed for homogeneous vehicles. This study explores the traffic dynamics in areas heavily reliant on motorcycles, specifically focusing on Ninh Kiều District, Cần Thơ City, Vietnam, to understand the implications of such vehicular prevalence. Addressing the shortcomings of traditional analysis techniques, the research redefines the macroscopic fundamental diagram (MFD) to better accommodate the mixed and non-lane-based nature of motorcycle-centric networks. By integrating motorcycle equivalent units and area occupancy into the standard MFD framework, this approach facilitates a detailed exploration of traffic flow and concentration in mixed traffic settings. This refined approach not only fills a notable research gap but also enhances the reliability of traffic analysis. The recalibrated MFD yields a more precise representation of network performance, unveiling key operational behaviors and potential bottlenecks. The broader implications of this research are extensive, as the proposed MFD serves as an instrumental tool for traffic evaluation in motorcycle-dependent regions, aiding efforts to mitigate congestion.

Keywords: Mixed traffic, Motorcycle-dependent traffic, Macroscopic fundamental diagram.

1. INTRODUCTION

Traffic analysis traditionally hinges on the assumption of homogeneity, expecting predictable movements expecting similar-sized vehicles adhering to lane discipline. However, this paradigm proves inadequate for motorcycle-dependent regions, such as Vietnam—the focus of this study—where motorcycles make up about 86% of all vehicles, marking the highest rate of motorcycle ownership globally (Tonko & Gidwani, 2018). These challenges to conventional traffic models are set against a backdrop of such regions, characterized by lower income, high-density land use, and a predominance of motorcycle traffic (Minh et al., 2007). As M. and Verma (2016) pointed out, traffic models and theories designed toward homogeneous traffic fall short in these settings, prompting the need for tailored approaches.

Herein lies the significance of the Macroscopic Fundamental Diagram (MFD)—an analytical construct that correlates vehicle volume with the rate of reaching destinations within a network. Utilizing the MFD helps assess traffic conditions and pinpoint areas for improvement. Daganzo (2007) proposed the MFD to model traffic on a broad scale, yet its application to mixed traffic remains scarcely examined. This study aims to customize the standard MFD to better represent areas dominated by motorcycles, which frequently deviate from strict lane adherence, unlike their four-wheeled counterparts. Thus, the applicability and utility of the MFD in motorcycle-heavy traffic environments can be enhanced.

The remainder of the article is organized as follows: Section 2 provides a literature review setting the theoretical framework. Section 3 outlines the methodology, followed by Section 4 on traffic micro-simulation model development, and Section 5 presents a refinement of the MFD. Finally, the paper concludes in Section 6 with a summary of the findings.

2. LITERATURE REVIEW

2.1 Mixed traffic

Mixed traffic environments are characterized by the coexistence of multiple vehicle types, creating a complex traffic flow that is markedly different from homogeneous traffic conditions, where similar vehicles exhibit predictable patterns. M. and Verma (2016) describes these heterogeneous conditions as arising from various vehicle types with differing static and dynamic characteristics sharing the same road space. In such conditions, smaller, more agile vehicles like motorcycles can adeptly maneuver through tight spaces and rapidly adjust their trajectories and speeds quickly, often bypassing larger, slower-moving vehicles. This ability to exploit smaller gaps significantly alters the overall flow dynamics and interaction patterns among vehicles. Furthermore, the variability in driver behavior, vehicle size, and the general lack of strict lane discipline, which are common in many urban areas, especially in developing countries, contribute to the complexity of managing mixed traffic.

2.2 Challenges of applying homogeneous traffic flow models to mixed traffic

In regions where motorcycles dominate the roads, mixed traffic conditions pose some challenges for traffic modeling. The literature underscores the limitations of conventional homogeneous traffic models when applied to such contexts, as highlighted by Khan and Maini (1999). Their review advocated for models that are tailored to account for the intricate aspects of mixed traffic, such as vehicle interactions, driver behaviors, and road configurations. It also noted the dynamic nature of motorcycles, particularly their ability to navigate congested roads by exploiting gaps and adjusting speeds, stressing the importance of developing analytical frameworks capable of accommodating the diverse behaviors found in these environments.

The critique extends to the use of Passenger Car Units (PCU) for modeling traffic conditions in India, as discussed by Chandra and Sikdar (2000) and Chandra and Kumar (2003). Their approach, while innovative, has been noted for not fully capturing the complexities of mixed traffic settings, especially in areas heavily trafficked by motorcycles. As traffic composition fluctuates, the effectiveness of PCUs varies, often failing to represent the distinct mobility characteristics of motorcycles, as observed by Arasan et al. (2008). This issue was further underscored by Kov and Yai (2010) in their study on Phnom Penh traffic, where motorcycles made up 70% of traffic. They noted that PCU metrics lose relevance in areas where light vehicles constitute less than 25% of the traffic mix, as the increase in light vehicles tends to reduce overall speeds and capacity, thereby impacting the maneuverability and lateral positioning of motorcycles. Tan et al. (2018) observed similar challenges in Vietnam, where the low car-to-motorcycle ratio complicates traffic modeling using PCUs.

Another significant challenge is the measurement of traffic concentration. In mixed traffic systems, traditional density metrics, which count the number of vehicles per unit length per lane, fail to capture the true dynamics of the road. Unlike homogeneous environments with similar vehicle sizes and strict lane discipline, mixed traffic involves more complex spatial dynamics. As Lee (2007) notes, in motorcycle-heavy traffic, interactions are not only longitudinal but also lateral, with motorcycles often filtering, weaving, and maintaining shorter headways. This behavior, which allows multiple vehicles to occupy the same lane space simultaneously, is not typically observed in car-dominated traffic and complicates traditional traffic analyses by challenging the effectiveness of standard density measurements.

2.3 Macroscopic Fundamental Diagram (MFD)

The MFD marks a significant leap in traffic studies, mapping the relationship between traffic flow and density, to the network performance. Initially introduced by Daganzo (2007) and expanded by Geroliminis & Daganzo (2007, 2008), the MFD extends the scope of the fundamental diagram from individual road segments to an aggregated network. In contexts with relatively uniform congestion levels, a well-defined MFD emerges (Geroliminis & Daganzo, 2007), showing that average flow increases with rising density up to a critical point, indicative of the peak sustainable flow rate (Knoop et al., 2014). Beyond this threshold, the network experiences congestion, potentially leading to gridlock as density continues to rise.

The shape and stability of the MFD are influenced by a wide array of factors, such as network structure (Ambühl et al., 2018), route preferences (Geroliminis & Daganzo, 2008), inhomogeneity in traffic distribution (Ambühl et al., 2018), traffic management strategies (Ambühl et al., 2018), and time periods (Knoop et al., 2014). The MFD quantifies network conditions by correlating trip production—the number of vehicles in the network—with vehicle accumulation—the rate at which vehicles reach destinations (Geroliminis & Daganzo, 2008). The peak of trip production rate (q_{MFD}) signifies the network's capacity, whereas the corresponding accumulation (k_{MFD}) denotes critical. It calculates the parameters by weighting the link flow (q_i) and density (k_i) of each link i by its length (l_i), reflecting aggregate traffic states, as shown in Equations (1) and (2) by Geroliminis and Daganzo (2008).

$$q_{MFD} = \frac{\sum_i q_i \cdot l_i}{\sum_i l_i} \tag{1}$$

$$\mathrm{k}_{\mathrm{MFD}} = \frac{\sum_\mathrm{i} \mathrm{k}_\mathrm{i} \cdot \mathrm{l}_\mathrm{i}}{\sum_\mathrm{i} \mathrm{l}_\mathrm{i}} \tag{2}$$

Despite the chaotic traffic conditions prevalent in Southeast Asian countries, there is a notable gap in network performance analyses. A pertinent study by Suwanno et al. (2021) assessed the impact of floods on traffic in Bangkok's Sukhumvit District using the MFD. Utilizing 2019 Thailand open data (i.e., vehicle and mobile probe data), the study analyzed taxi movements on weekdays and excluded freeway data. Although it provided insights into how flood levels and network operations shape the MFD, the study did not consider the mixed traffic conditions crucial in Thailand, where motorcycles constitute about 87% of traffic

(Tonko & Gidwani, 2018), an oversight that compromises the reliability of the findings.

3. METHODOLOGY

3.1 Workflow

In an effort to enhance the understanding of mixed traffic in motorcycle-dependent regions, this study follows a systematic flowchart depicted in Figure 1, employing AIMSUN Next 23 software to model and simulate traffic dynamics in Ninh Kiều District.

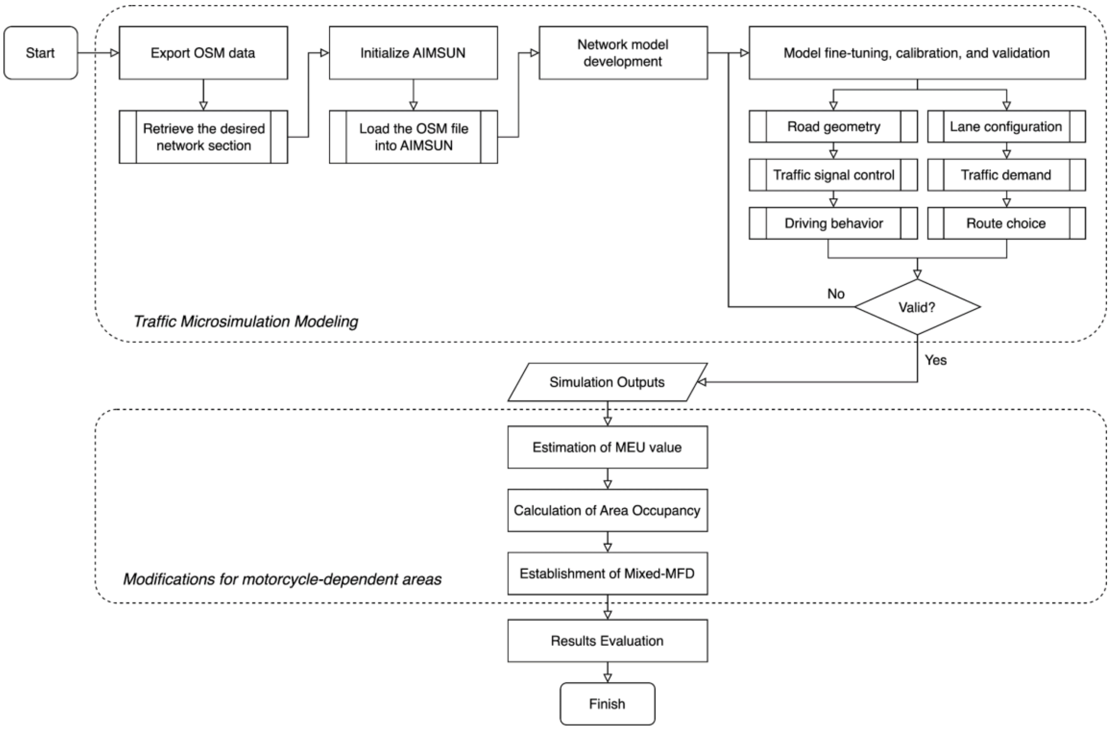

Figure 1 Methodological framework for simulation modeling and analysis of mixed traffic.

3.2 Case study

Cần Thơ City, situated in southern Vietnam, is the third most populous city with approximately 1.25 million residents, spread over an area of 331,212 km² with a density of 870 individuals/km² (Vietnam General Statistics Office, 2022). Motorcycles are the primary mode of transport, comprising 80–85% of traffic, with cars and taxis accounting for 7–10%. The study specifically targets Ninh Kiều District due to its high population density and significant traffic volumes among all districts in the city, making it a focal point of the study.

This research leverages both secondary and primary data to investigate traffic patterns in the district. Primary data was gathered on March 2, 2024, through field observations that recorded traffic signal timing and phase configurations at 27 intersections in Ninh Kiều District. A survey on March 2, 2024, gathered empirical data on signal cycles and timings at 27 intersections in Ninh Kiều District. The majority of these intersections operate with two and four signal phases; the busier ones employ four phases to accommodate extended green times for left turns, in accordance with Vietnam's right-hand driving rules. Meanwhile, secondary data encompasses traffic counts from 12 key intersections recorded from February

24–26, 2020, complemented by a seven-day activity diary survey engaging 5,841 participants. The survey documented the purpose of each trip, with details on the mode of transportation, distance, speed, and trip duration. Analysis of these data showed that motorcycles were the primary mode of transportation, accounting for 87.84% of the 11,465 recorded trips. Other modes included cars (1.57%), walking (5.00%), bicycles (5.40%), and other modes (0.19%). For analytical purposes, each journey entry was treated as a separate trip, irrespective of multiple daily trips by individuals. These data sources are integrated to construct calibrated origin-destination matrices, as summarized in Figure 2. The analysis identifies trends in Ninh Kiều District, with Monday emerging as the peak traffic volume day.

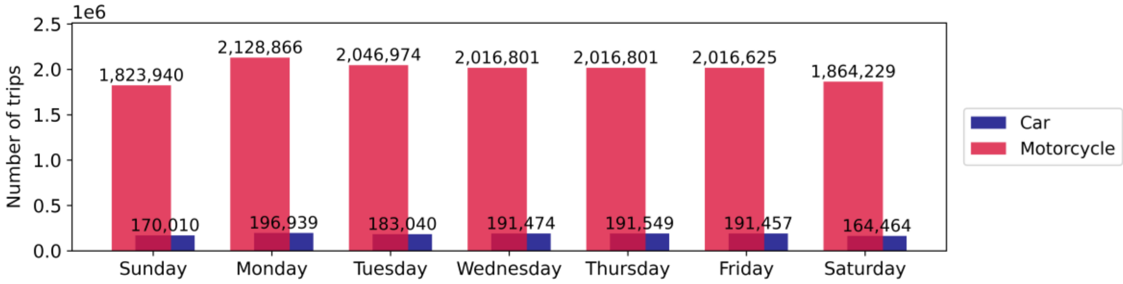

Figure 2 Daily traffic volume comparison by vehicle Type in Ninh Kiều District.

4. DEVELOPMENT OF TRAFFIC MICROSIMULATION MODEL

Figure 3 displays the simulation model for Ninh Kiều District, leveraging geographic configurations from OpenStreetMap. Further adjustments are made to reflect actual geometries, converting the map into a simulated environment where links, nodes, and zones correspond to road segments, intersections, and trip origins and destinations, respectively.

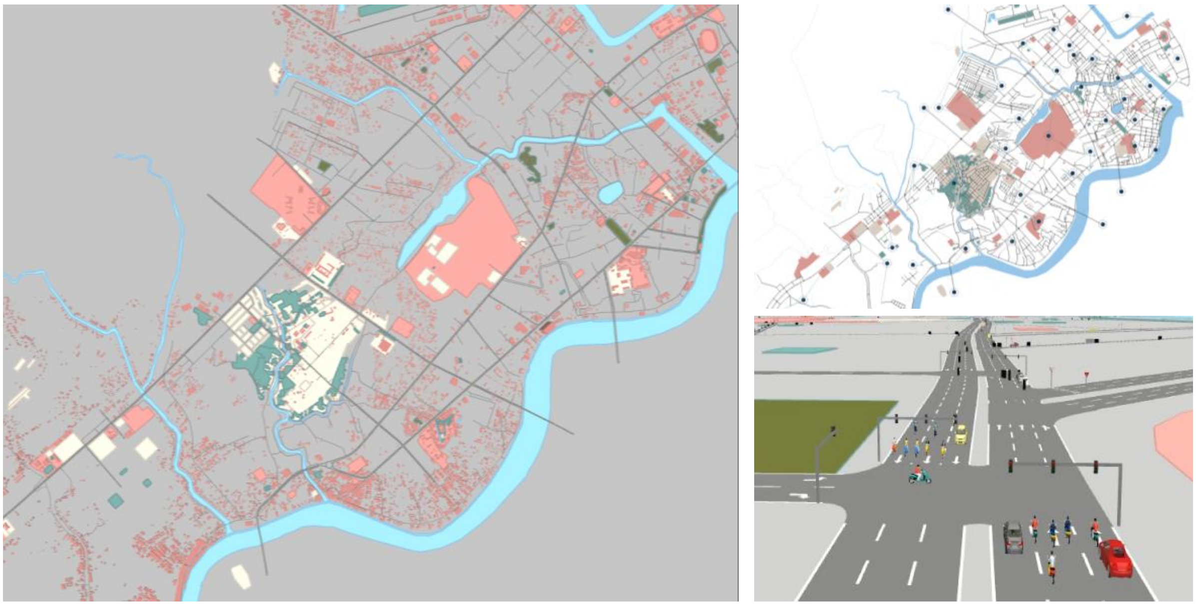

Figure 3 AIMSUN traffic simulation model of the Ninh Kiều District.

Although AIMSUN provides default parameters, customizing these to mirror the specific traits of the case study is essential. This process entails a rigorous calibration process, adjusting simulation parameters iteratively to align closely with empirical data. Special emphasis is placed on calibrating behavioral models that account for cognitive processes in route selection, especially important in motorcycle-dependent settings. First, the calibration process begins by refining network configurations, modifying road segments, intersections, and integrating traffic signal control schemes. Subsequently, traffic demand calibration utilizes secondary data to form origin-destination matrices, as summarized in Figure 4.

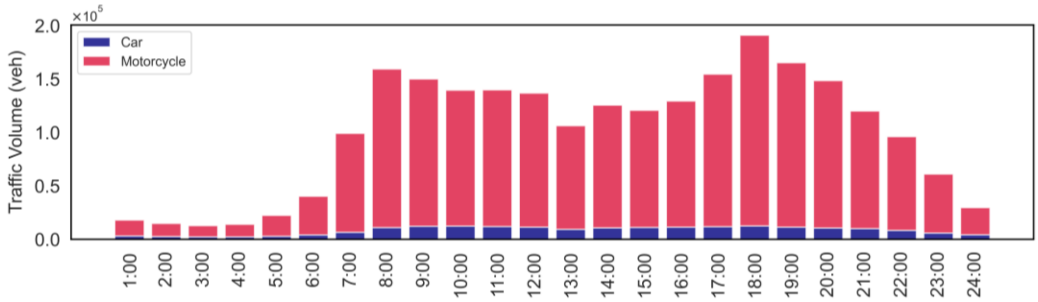

Figure 4 Hourly distribution of traffic demand.

AIMSUN enhances these efforts by incorporating dynamic traffic assignment models, crucial for handling time-variant flows and route choices. It integrates stochastic route choice and dynamic user equilibrium algorithms, fine-tuned to reflect the routing decision process and adapt to current traffic conditions. The final phase of the calibration process emphasizes driver behavior, specifically targeting the non-lane-based and aggressive driving patterns prevalent among motorcycle riders, as shown in Figure 5. Turn parameters were also modified to describe their gap acceptance behavior at unsignalized intersections, contrasting with the more cautious driving styles typically observed in developed countries.

Figure 5 Field observations of traffic conditions in Ninh Kiều District.

In essence, the efficacy of a simulation model depends on its capability to replicate observed conditions. Model validation entails a trial-and-error calibration process, comparing simulated outcomes to actual behaviors to identify and rectify discrepancies. This study conducts validation at the network level by examining aggregate flow across different spatial and temporal contexts, quantified using the GEH statistic. Detailed in Equation (3), the GEH formula calculates deviations where m represents the model's hourly traffic volume and o is the real-world count. GEH thresholds classify model accuracy as follows: values below 5 indicate a well-calibrated model; values between 5 and 10 suggest potential errors requiring further investigation; and values above 10 necessitate recalibration or model rejection.

$$GEH = \sqrt{\frac{2(m-o)^2}{(m+o)}} \tag{3}$$

Table 1 presents validation indicators, including speed and total traffic volume, along with their relative differences and GEH values. With all GEH below 5, the model is deemed statistically validated, affirming its reliability in representing traffic in Ninh Kiều District.

Table 1 Validation of the overall network simulation against empirical data

Indicators	Observed	Simulated	Rel. Difference (%)	GEH
Mean speed - cars (km/h)	23.97	25.26	5.38	0.26
Mean speed - motorcycles (km/h)	24.19	24.39	0.83	0.04
Throughput - cars (veh)	35,837	36,120	0.79	1.49
Throughput - motorcycles (veh)	350,415	353,373	0.84	4.99

5. MACROSCOPIC EVALUATION FOR MIXED TRAFFIC

5.1 Adaptation for motorcycle-heavy traffic: The MEU approach

The analysis of mixed traffic conditions necessitates a specialized approach, leading to the development of the Motorcycle Equivalent Unit (MEU) concept, an evolution from the PCUs. It assesses the relative speed and spatial occupancy of different transportation modes, using motorcycles as the baseline. Building upon the PCU calculation method by Chandra and Kumar (2003), further refined by Minh et al. (2005), this study utilizes Equation (4) to compute MEU_{car}, where V_{mc} and V_{pc} represent the mean speeds of motorcycles and cars, respectively, while A_{mc} and A_{pc} denote their projected rectangular areas on the road.

$$MEU_{car} = \frac{V_{mc} \,/\, V_{pc}}{A_{mc} \,/\, A_{pc}} \tag{4}$$

MEU computations consider the mean stream speed crucial in heterogeneous traffic, where speed consistency is absent. Traditional speed measurements like spot speed or space mean speed are not suitable due to speed disparities between vehicle types. To overcome this, Cao et al. (2009) introduced an adjusted formula to compute the mean stream speed (V_m) that better reflects the collective mobility of mixed traffic flows. This is represented by Equation (5), which calculates a weighted average that accounts for the speed of each vehicle type k (v_k) and the quantity of each type (n_k), across all vehicle categories in the traffic stream (N).

$$V_m = \frac{\sum_{k=1}^{N} n_k \cdot v_k}{\sum_{k=1}^{N} n_k} \tag{5}$$

To further refine the model and represent the variability of speeds across different segments of the traffic network, Equation (6) is employed. This equation calculates the weighted speed for each vehicle type (v_k) across various segments of the road network, where v_{ik} indicates the mean speed of vehicle type k at link i while l_i is the length of that link i.

$$v_k = \frac{\sum_i v_{ik} \cdot l_i}{\sum_i l_i} \tag{6}$$

Furthermore, Chandra and Kumar (2003) provide essential data on the average dimensions and projected areas for each vehicle category, as listed in Table 2.

Table 2 Classification of vehicle types and rectangular area projection size.

No	Type	Vehicles included	Average dimensions (m)	Rectangular area (m^2)
1	Motorcycle	Scooter, Motorbike, Mopeds	1.87 x 0.64	1.20
2	Car	Car, Jeep, Van	3.72 x 1.44	5.36

With motorcycles being predominant, their MEU is standardized at 1, serving as a baseline for evaluating network influence. For cars, MEUs are calculated for each road segment using Equation (4) to evaluate their relative impact, with their distribution depicted in Figure 6. Across 1,533 road segments, MEUs for cars range from 3.20 to 6.14, with an average of 4.78, indicating that the road space occupied by one car is nearly equivalent to five motorcycles. This information is vital in networks where the sheer volume of motorcycles vastly differs from that of cars, enabling the development of traffic models and management strategies that effectively address unique composition and behavior in such settings.

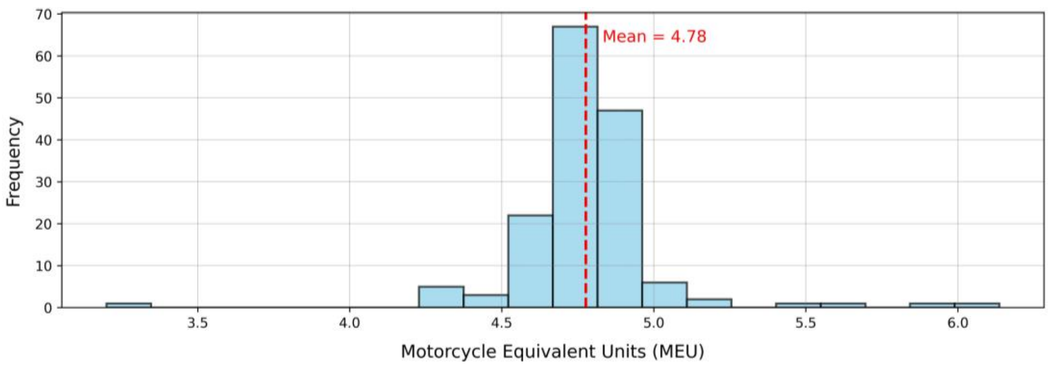

Figure 6 Distribution of MEU values across road sections in Ninh Kiều District.

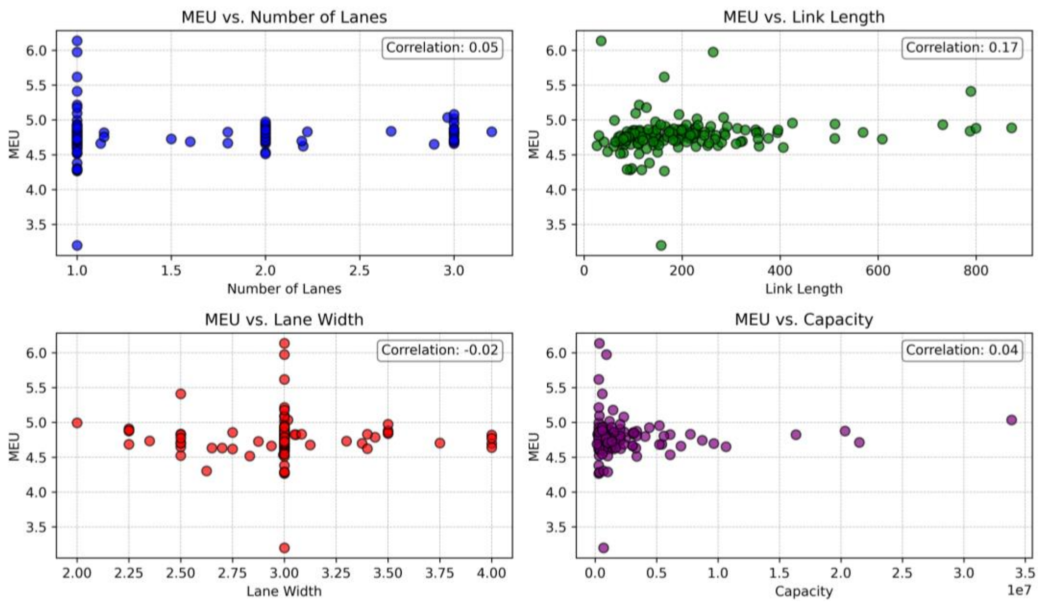

Figure 7 Correlation analysis of MEU values with road geometry attributes.

This study further examines the relationship of MEU values with road geometry attributes such as length, width, capacity, and lane count for each link. Figure 7 shows scatter plots that illustrate the correlation between MEUs and these geometric factors. The strength and direction of these relationships are then quantified using Pearson's correlation coefficient. It is observed that the low correlation coefficients indicate a weak linear relationship between the MEU values and network attributes such as the number of lanes, link length, lane width, and road capacity within Ninh Kiều District. This suggests a general independence of the MEUs from these geometric characteristics. Further research is necessary to determine if the applicability extends beyond this case study, as local driving behaviors, infrastructure conditions, and regional differences may influence its relevance and utility. In conclusion, the MEU metric is significant for macroscopic traffic analysis of motorcycle-dependent areas.

5.2 Accounting for spatial utilization: The role of area occupancy

In contexts where standard density metrics are inadequate, especially in environments with irregular or absent lane discipline, the concept of 'area occupancy' becomes pivotal. It offers a more precise measure of traffic concentration and spatial utilization, accurately reflecting the complex dynamics of mixed traffic by accounting for the actual space occupied by each vehicle type. This metric, introduced by Mallikarjuna and Rao (2006) and built upon observations by Chandra and Sikdar (2000), considers the actual space occupied by vehicles. It offers a comprehensive view of traffic flow in mixed traffic where different vehicle types—from motorcycles to larger vehicles—interact and use road space differently. This shift to area occupancy (ρ_A), as expressed in Equation (7) by Mallikarjuna and Rao (2006), marks a significant shift in traffic analysis. This formula provides a measure of how much space each vehicle type occupies in the study area over the specified observation period (T).

$$\rho_A = \frac{1}{T \cdot W \cdot L} \cdot \sum_{k=1}^{N} (O_k \cdot w_k \cdot l_k) \tag{7}$$

where,

W, L	: width and length of the study area,
w_k , l_k	: width and length of vehicle type k,
O_k	: occupancy time of vehicle type k (in seconds), and
N	: the set of vehicles.

The above formula helps to ascertain the thorough utilization of road space by different vehicle types in mixed traffic conditions. It takes into account the dimensional and operational characteristics of each vehicle to offer an in-depth perspective of their spatial impact on traffic flows. Introducing area occupancy as a measure marks a paradigm shift in the approach to understanding and analyzing heterogeneous traffic dominated by motorcycles. For the specific case of Ninh Kiều District, area occupancy at the link i (ρ_{A_i}) is determined as follows.

$$\rho_{A_i} = \frac{1}{T_i \cdot W_i \cdot L_i} \cdot \sum_t \sum_{k \in N_t} (w_k \cdot l_k) \tag{8}$$

where,

T_i	: observation period,
N_t	: index of the set of vehicles that appeared at the time t,

5.3 Enhancing macroscopic analysis for motorcycle-dependent traffic

Considering the issues highlighted in subsections 5.1 and 5.2, the standard MFD is no longer relevant in scenarios involving mixed traffic with a significant presence of non-lane-based vehicles and requires refinement to analyze such environments. Equations (1) and (2) are then transformed to include MEU-based traffic properties and substitute density metrics with area occupancy. This adaptation adjusts the counts of larger vehicles into motorcycle-equivalent numbers and incorporates spatial utilization measures.

These modifications improve the MFD's utility as a tool for delivering a holistic view of network performance and accurately depicting transitions between free-flow and congested states. New equations, presented in Equations (9) and (10), refine the model further. Here, q_{MFD_t} denotes the network-scale traffic flow, weighted by the flow of cars ($q_{pc_{it}}$) and motorcycles ($q_{mc_{it}}$) on the link i during time interval t and adjusted by MEU factors. Similarly, traffic concentration is then measured by area occupancy ($\rho_{A_{MFD_t}}$), which is also weighted across the network to provide a macroscopic perspective on traffic performance.

$$q_{MFD_t} = \frac{\sum_i \left[\left(q_{pc_{it}} \cdot MEU_{car}\right) + q_{mc_{it}}\right] \cdot l_i}{\sum_i l_i} \tag{9}$$

$$\rho_{A_{MFD_t}} = \left(\sum_i \left(\frac{1}{T_i \cdot W_i \cdot L_i} \cdot \sum_t \sum_{k \in N_t} \left(w_k \cdot l_k\right) \cdot l_i\right)\right) / \sum_i l_i \tag{10}$$

As a result, Figure 8 contrasts network performance using two metrics for vehicle accumulation: density and area occupancy. The blue data plot, labeled as 'before adjustment' MFDs, utilizes density—suitable for homogeneous traffic but less effective in mixed traffic contexts. The orange data plot, labeled 'after adjustment' MFDs, employs area occupancy, refined to better represent traffic systems predominantly composed of motorcycles.

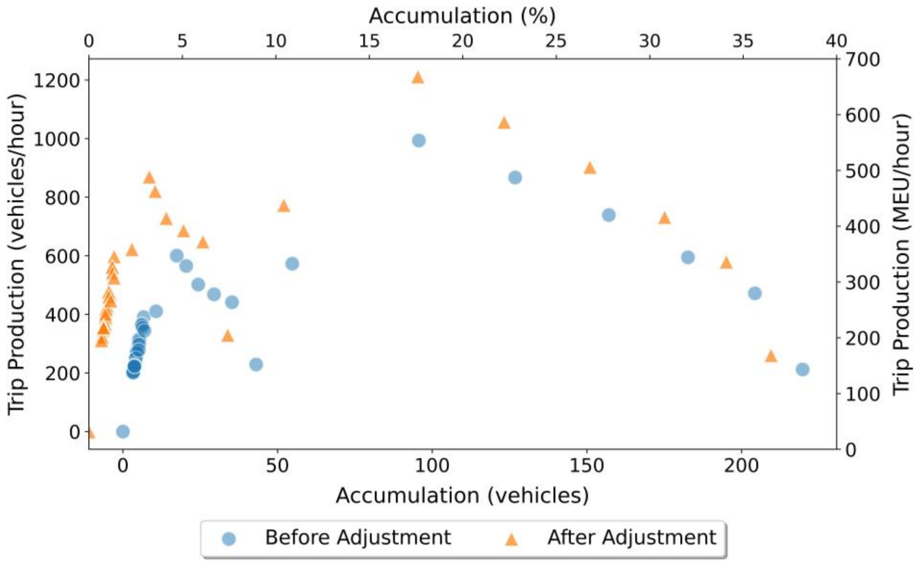

Figure 8 Comparative analysis of MFD using traffic density and area occupancy.

5.4 Refined results of the mixed traffic MFD

Network performance in Ninh Kiều District is evaluated with a modified three-dimensional MFD that also accounts for the proportion of motorcycles. This modified MFD, which captures trip production and accumulation tracked at 10-minute intervals over a 10-hour simulation using the AIMSUN microscopic simulation model, is illustrated in Figure 9.

The MFD initially exhibits a positive trend where increased trip production correlates with rising accumulation, signifying efficient network usage, known as the free-flow state. However, upon reaching a critical point of accumulation, the network hits its capacity limit where further vehicle presence ceases to aid flow efficiency. The peak of trip production, occurring at 614.99 MEU per hour at 07:10 a.m., marks the maximum volume manageable before the onset of congestion. Secondary data analysis indicates that the network's throughput capacity is reached early due to notable morning commuter trends. Specifically, 61.2% of employed individuals begin their work between 3 a.m. and 7 a.m., and 60.6% of students travel to school primarily between 6 a.m. and 7 a.m., making up 85.6% of all school-related trips. This leads to a significant spike in traffic volume, increasing by 146.37% from 6 a.m. to 7 a.m. Consequently, the capacity threshold is reached when 16.39% of the network is occupied by vehicles, leading to a decline in the MFD curve and marking a transition to a congestion state. Further accumulation then results in decreased trip production and a potential gridlock. The relatively low accumulation threshold can be attributed to the fact that 74.65% of the roads in Ninh Kiều District are local and residential types. It is also observed that motorcycles enhance trip production at low to moderate accumulation levels due to their compact size and higher maneuverability, allowing efficient space utilization. Nonetheless, as vehicle volume approaches and exceeds the capacity, the advantageous impact of motorcycles diminishes, signaling a drop in overall traffic system performance.

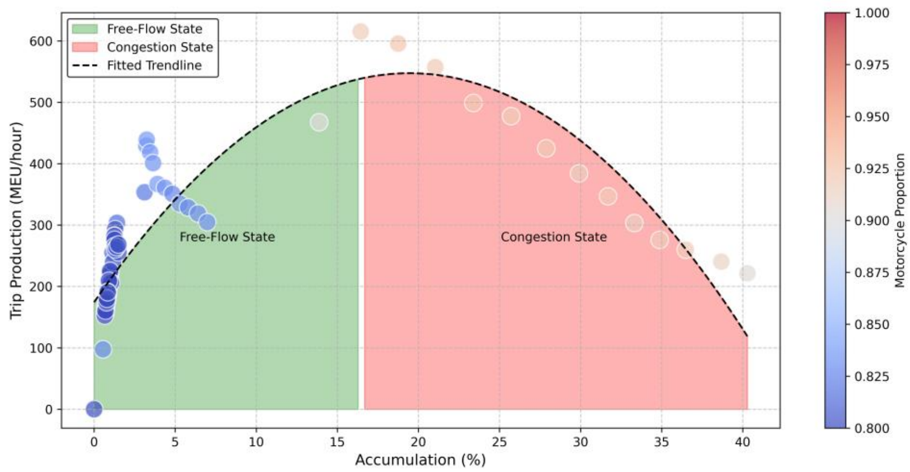

Figure 9 Three-dimensional recalibrated MFD for mixed traffic with motorcycle dominance.

6. CONCLUSIONS

This study investigates mixed traffic dynamics in Ninh Kiều District, highlighting the inadequacy of traditional traffic flow models designed for homogeneous, lane-disciplined settings when applied to areas where motorcycles dominate and frequently disregard lane markings. To address these complexities, a recalibrated MFD incorporating MEU metrics and area occupancy has been introduced, moving beyond standard density-based measurements.

This MFD offers a refined macroscopic perspective of traffic flow and concentration, better reflecting the spatial patterns in this context. The MEU metric, which acknowledges the smaller size and greater maneuverability of motorcycles compared to standard PCUs, offers a more appropriate measure for evaluating their impact in motorcycle-dependent settings.

The novelty of this research lies in its significant progress in adapting the MFD for mixed traffic with a high prevalence of motorcycles. This approach introduces a shift from density metrics to area occupancy, addressing a gap in analytical tools and providing a more accurate representation of these systems. Notably, alongside the effort to develop an MFD tailored for such context, the study also marks a seminal contribution to establishing the MFD for traffic patterns in Southeast Asia. The recalibrated MFD, validated against empirical data, effectively highlights key operational patterns and potential bottlenecks in traffic networks.

Despite its contributions, the study scope is inherently limited by focusing exclusively on the Ninh Kiều District. This specific network and the geographical extent may not fully represent other urban or rural settings, which could differ significantly in terms of traffic behavior, infrastructure, and regulatory frameworks. Consequently, while the findings are relevant to the study area, their generalizability to different contexts may not be straightforward, necessitating prudent consideration and caution when applying them to other regions. Moreover, although the AIMSUN model is useful for detailed simulations, it may include modeling assumptions that do not perfectly capture the complex interactions found in highly heterogeneous traffic environments. Future research should address these limitations by extending the study to include diverse locations with varying traffic compositions and infrastructure conditions to test the applicability of the findings. Additionally, comparative studies employing different simulation software or integrating empirical field data could enhance the validity of the modeling approach. Investigating the impacts of different management strategies within these mixed traffic settings would also be valuable.

7. ACKNOWLEDGMENTS

The authors would like to express gratitude to the "*Sustainable Urban Public Transport and Central Area Traffic Management Study for Can Tho City*" project, conducted by Sustainable Urban Development JSC, for their support with secondary data.

8. REFERENCES

Ambühl, L., Loder, A., Bliemer, M. C. J., Menendez, M., & Axhausen, K. W. (2018). Introducing a re-sampling methodology for the estimation of empirical macroscopic fundamental diagrams. Transportation Research Record, 2672(20), 239–248. https://doi.org/10.1177/0361198118788181

Arasan, T., & Arkatkar, S. S. (2008). Estimating passenger car units for vehicles of heterogeneous traffic using computer simulation. Presented at the Transportation Research Board 87th Annual Meeting, Washington D.C., January 2008.

Cao, N., Sano, K., Minh, C. C., & Matsumoto, S. (2009). Motorcycle equivalent units at road segments under mixed traffic flow in urban road. Proceedings of the Eastern Asia Society for Transportation Studies, 7.

Chandra, S., & Kumar, U. (2003). Effect of lane width on capacity under mixed traffic conditions in India. Journal of Transportation Engineering, 129(2), 155–160.

https://doi.org/10.1061/(ASCE)0733-947X(2003)129:2(155)
Chandra, S., & Sikdar, P. K. (2000). Factors affecting PCU in mixed traffic situation on urban roads. Road and Transport Research, 9(3), 40–50.
Daganzo, C. (2007). Urban gridlock: Macroscopic modeling and mitigation approaches. Transportation Research Part B: Methodological, 41(1), 49–62. https://doi.org/10.1016/j.trb.2006.03.001
Geroliminis, N., & Daganzo, C. F. (2007). Macroscopic modeling of traffic in cities. Technical Report. The National Academies of Sciences, Engineering, and Medicine: Washington, DC, USA.
Geroliminis, N., & Daganzo, C. F. (2008). Existence of urban-scale macroscopic fundamental diagram: Some experimental findings. Transportation Research Part B: Methodological, 42(9), 759–770. https://doi.org/10.1016/j.trb.2008.02.002
Geroliminis, N., Sun, J. (2011). Properties of a well-defined macroscopic fundamental diagram for urban traffic. Transportation Research Part B: Methodological, 45(3), 605–617. https://doi.org/10.1016/j.trb.2010.11.004
Khan, S. I., & Maini, P. (1999). Modeling heterogeneous traffic flow. Transportation Research Record, 1678(1), 234–241. https://doi.org/10.3141/1678-28
Knoop, V. L., Jong, D., & Hoogendoorn, S. P. (2014). The influence of the road layout on the network fundamental diagram. Transportation Research Record, 2421(1), 22–30. https://doi.org/10.3141/2421-03
Kov, M., & Yai, T. (2010). Traffic characteristics of motorcycle-dominated urban street considering the effect of light vehicle. Journal of the Eastern Asia Society for Transportation Studies, 8, 1806–1821. https://doi.org/10.11175/eastpro.2009.0.337.0
Lee, T. C. (2007). An Agent-Based Model to Simulate Motorcycle Behaviour in Mixed Traffic Flow. Doctoral Dissertation, Imperial College London, London.
M., S., & Verma, A. (2016). Review of studies on mixed traffic flow: perspective of developing economies. Transportation in Developing Economies, 2(5). https://doi.org/10.1007/s40890-016-0010-0
Mallikarjuna, C., & Rao, K. R. (2006). Area occupancy characteristics of heterogeneous traffic. Transportmetrica, 2, 223–236. https://doi.org/10.1080/18128600608685661
Minh, C. C., Sano, K., & Matsumoto, S. (2005). The speed, flow, and headway analyses of motorcycle traffic. Journal of the Eastern Asia Society for Transportation Studies, 6, 1496–1508. https://doi.org/10.11175/easts.6.1496
Minh, C. C., Sano, K., & Nguyen, C. Y. (2007). Acceleration and deceleration models of motorcycle at signalized intersections. Journal of the Eastern Asia Society for Transportation Studies, 7, 2396–2411. https://doi.org/10.11175/easts.7.2396
Nguyen, D. T., & Kajita, Y. (2018). Traffic congestion and impact on the environment in Vietnam: Development of public transport system - experience from actual operation of bus in Hanoi. Journal of Civil & Environmental Engineering, 8(3).
Suwanno, P., Kasemsri, R., Duan, K., & Fukuda, A. (2021). Application of macroscopic fundamental diagram under flooding situation to traffic management measures. Sustainability, 13, 11227. https://doi.org/10.3390/su132011227
Tan, D. T., Tu, T. V., & Sano, K. (2018). Estimation of motorcycle equivalent units on urban streets. Asian Transport Studies, 5(2), 243–255.
Tonko, M., & Gidwani, M. (2018). Motorcycle Growth Prospects in Southeast Asia: Rise of Business Use Two-Wheelers. Roland Berger GmbH: Munich, Germany.
Vietnam General Statistics Office (2021). Vietnam Statistical Yearbook (Niên giám thống kê Việt Nam). Retrieved from https://www.gso.gov.vn/wp-content/uploads/2022/08/Sach-Nien-giam-TK-2021.pdf. Accessed March 7, 2024.

Pedestrian Safety in Indonesian Urban Areas: A Walkability Index for Indonesian Urban Areas

Alfa A Ash-Shiddiqi[1], Jany Agustin[2]

[1]DG of Highways Indonesia, adibalfa@gmail.com/adibalfa@pu.go.id
[2] Environment and Road Safety Specialist, KIAT

ABSTRACT

WHO's Global Status Report on Road Safety 2023 stated that pedestrians account for 21% of fatalities on the road. Indonesian Police Report on Road Accident 2021 also reports around 12,614 accidents are involving pedestrian. This phenomenon leads to President Decree No.1 2022 on the General Plan for National Road Safety 2021-2040 that explicitly states under Pillar 2 Road Safety that there is a requirement for pedestrian facility provision on urban roads. To implement that decree, a set of indexes is important to be developed. In 2023, The Directorate General of Highways (DGH) issues The Guideline for Determining the Walkability Index in Urban Areas. This paper explores this index and emphasize the practicability and advantages of this index. The results demonstrate that there are parameters underrepresented from the DGH's walkability index. This work contributes mostly by discussing and offering suggestions for the index. It also provides critics and suggestions for further development.

Keywords: Pedestrian facility, pedestrian level of service, road safety, walkability index

1. INTRODUCTION

The WHO's Global Status Report on Road Safety 2023 highlights the critical issue of pedestrian safety on a global scale, revealing that pedestrians account for 21% of all road fatalities. This statistic underscores the high vulnerability of pedestrians in traffic environments, often due to inadequate infrastructure, lack of pedestrian-friendly policies, and insufficient enforcement of traffic laws. The report calls for enhanced safety measures, such as better road designs, improved crosswalks, and stringent speed limits, to protect pedestrians and reduce fatalities. The global focus on pedestrian safety is crucial for achieving the broader goal of reducing overall road traffic deaths and injuries.

In Indonesia, the situation mirrors this global concern, as evidenced by the Indonesian Police Report on Road Accident 2021, which recorded approximately 12,614 accidents involving pedestrians. Around 15% of the victims are involving pedestrians. This significant number of pedestrian-related incidents highlights the urgent need for comprehensive road safety strategies in the country. Measures such as improved pedestrian infrastructure, public awareness campaigns, and stricter enforcement of traffic regulations are essential to address this issue. By prioritizing pedestrian safety, Indonesia can make significant strides in reducing road traffic fatalities and creating safer environments for all road users.

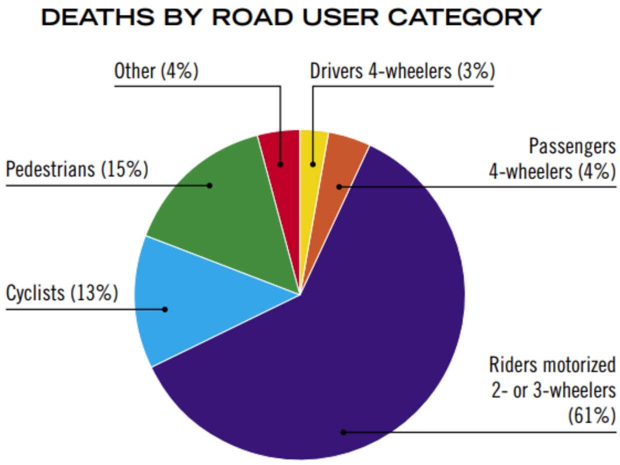

Figure 1 Deaths by Road User Category (Source: National Police Reports 2021)

In response to these alarming statistics, the Indonesian government has taken proactive steps to enhance pedestrian safety through legislative measures. President Decree No. 1 of 2022, known as the General Plan for National Road Safety 2021-2040, explicitly mandates the provision of pedestrian facilities on urban roads under Pillar 2 of Road Safety. To effectively implement this decree, the development of a standardized index is crucial. Consequently, in 2023, the Directorate General of Highways (DGH) issued The Guideline for Determining the Walkability Index in Urban Areas. This guideline aims to provide a practical and measurable framework for assessing and improving the walkability of urban environments, emphasizing the importance of safe, accessible, and well-designed pedestrian infrastructure.

This paper aims to explore this Index and compared with other measurement system such as The Global Walkability Index, Walk Scores ®, Neighborhood Environment Walkability Scale, and Pedestrian Level of Service. The paper will explain the Indonesian Walkability Index. It also analyzes other measurement system based on literature. The result and discussion section will make comparison, and suggest addition and critique into the Index.

2. INDONESIAN WALKABILITY INDEX

2.1 Basic Concept of Walkability

Walking is the most fundamental and important mode of transportation, serving as the primary means of travel for people across various settings. It is the most accessible form of mobility, requiring no special equipment or training, and it plays a critical role in daily activities such as commuting, shopping, and exercising. Walking not only supports physical health and well-being but also promotes social interaction and community engagement. By providing a foundation for other modes of transportation, such as cycling and public transit, walking contributes to a more sustainable and efficient transportation system.

Walkability, or the ease with which people can walk in an area, is a key criterion in assessing the livability of cities. This concept encompasses the availability and quality of walking facilities, such as sidewalks and crosswalks, as well as the overall environment, including safety, accessibility, and aesthetics. High walkability is associated with numerous benefits, including improved public health, reduced traffic congestion, and lower environmental impact. Cities that prioritize walkability often see increased economic activity and a higher quality of life for their residents. Thus, walkability has become a critical measure in urban planning and development, influencing policies and investments aimed at creating more livable and vibrant communities (Frank et al., 2021; Giles-Corti et al., 2014; Maghelal & Capp, 2011).

Pedestrian facilities that are safe, comfortable, secure, interesting, and continuous are essential for encouraging people to walk more. Safety features such as well-lit streets, visible crosswalks, and traffic calming measures reduce the risk of accidents and injuries. Comfort is enhanced through amenities like benches, shade trees, and clean, well-maintained pathways. Security involves ensuring that pedestrians feel protected from crime, which can be achieved through proper lighting and surveillance. An interesting walking environment might include diverse and attractive scenery, public art, and active storefronts. Continuity ensures that walking routes are uninterrupted and direct. Together, these elements create an inviting and practical walking experience, increasing the likelihood that people will choose walking over other modes of transportation.

The walkability index utilizes a set of parameters to calculate a score that reflects the walkability of an area. These parameters typically include factors such as sidewalk quality, pedestrian crossing safety, connectivity of walking routes, and the presence of amenities and destinations within walking distance. By systematically evaluating these components, the walkability index provides a quantitative measure that can be used to compare different areas, identify strengths and weaknesses, and guide improvements. Urban planners, policymakers, and community advocates use walkability indices to prioritize investments, design interventions, and monitor progress towards creating more walkable environments. The index serves as a valuable tool in promoting pedestrian-friendly urban design and encouraging a shift towards more sustainable transportation practices.

2.2 Indonesian Walkability Index

The Indonesian Walkability Index is a comprehensive tool designed to assess the walkability of urban areas through the evaluation of seven critical parameters (Directorate General of Highways, 2023). These parameters provide a detailed understanding of the pedestrian environment and help in identifying areas for improvement to enhance the overall walking experience (Tanan et al., 2017; Wibowo et al., 2015).

First, the condition of the walkway is assessed. This parameter examines the physical state of the pathways, including their surface quality, width, and continuity. A well-maintained walkway that is free from cracks, holes, and other hazards is crucial for ensuring the safety and comfort of pedestrians.

Figure 2 Condition of Walkways parameter

Second, the amenities available along the walkways are evaluated. Amenities such as benches, shade, drinking fountains, and public restrooms contribute significantly to the comfort and convenience of pedestrians. These features encourage people to walk longer distances and make walking a more enjoyable and practical mode of transportation.

Figure 3 Amenities parameter

Third, the index considers the care for disability, focusing on the accessibility of walkways for people with disabilities. This includes the presence of ramps, tactile paving for the visually impaired, and other facilities that ensure that walkways are usable by all individuals, regardless of their physical abilities.

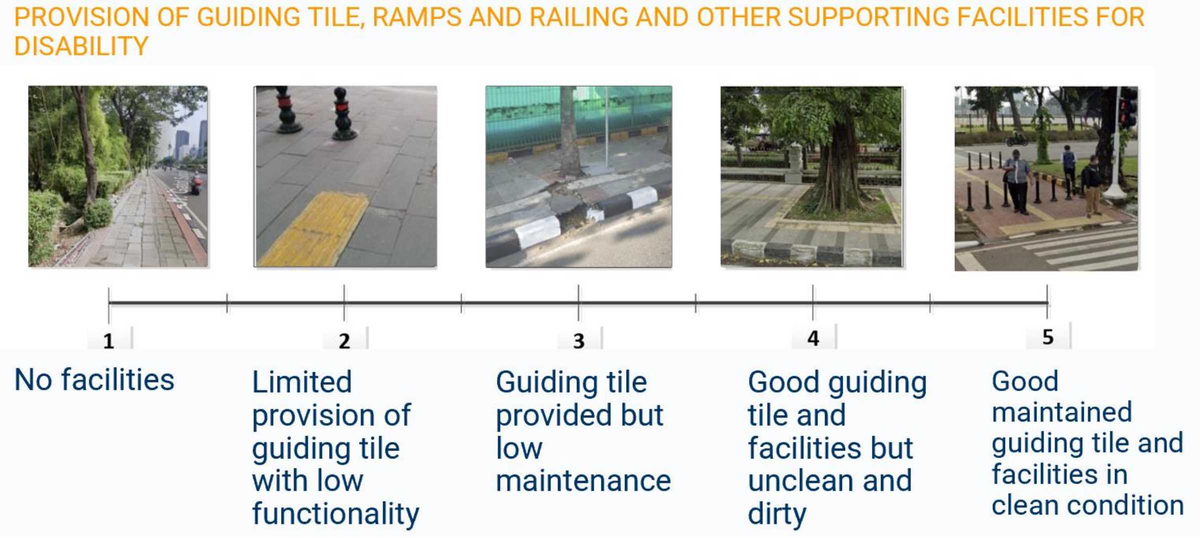

Figure 4 Supporting Disabilities parameter

Fourth, the amount of obstruction on the walkways is measured. Obstructions can include parked vehicles, street vendors, construction materials, and other items that block the path and force pedestrians to navigate around them. A high level of obstruction can significantly reduce the walkability of an area by making walking inconvenient and potentially unsafe.

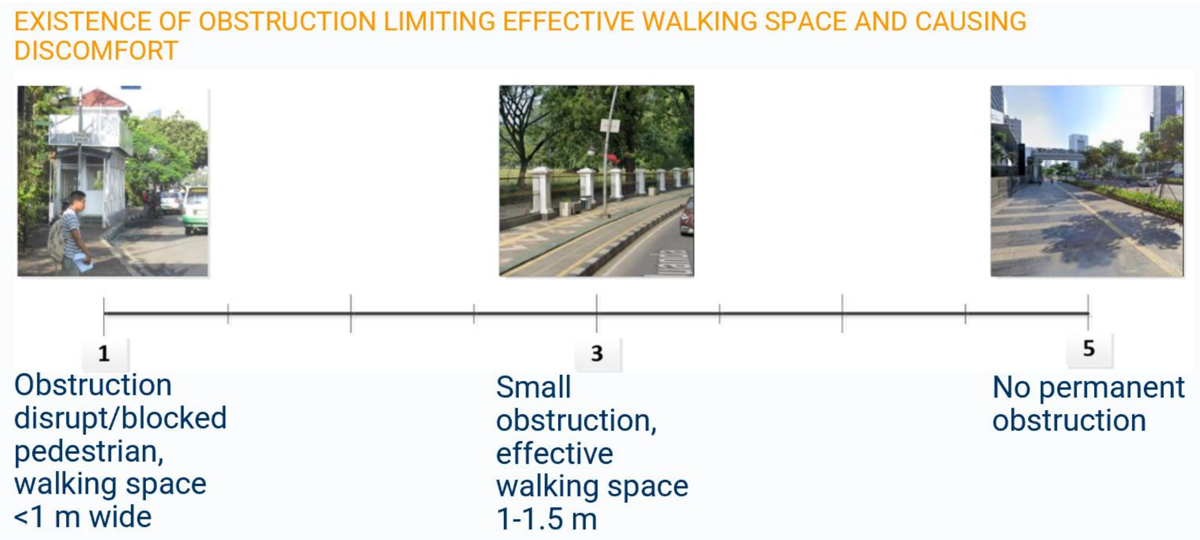

Figure 5 Obstruction parameter

Fifth, the ease and safety of crossing streets are examined. This parameter looks at the availability and condition of crosswalks, pedestrian signals, and pedestrian overpasses or underpasses. Safe and convenient crossing points are essential for ensuring that pedestrians can navigate urban areas without undue risk from vehicle traffic.

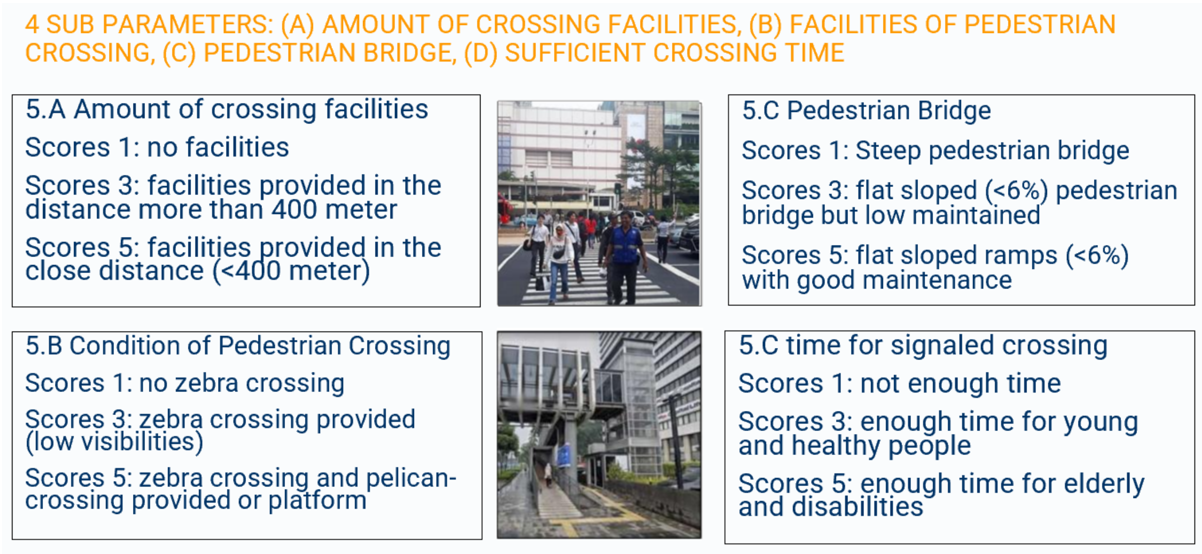

Figure 6 Crossing parameters

Sixth, the conflict with vehicles is assessed. This involves analyzing areas where pedestrian pathways intersect with vehicular traffic and the potential risks these intersections pose. Effective measures, such as traffic calming, dedicated pedestrian phases at traffic lights, and physical barriers, can reduce conflicts and enhance pedestrian safety.

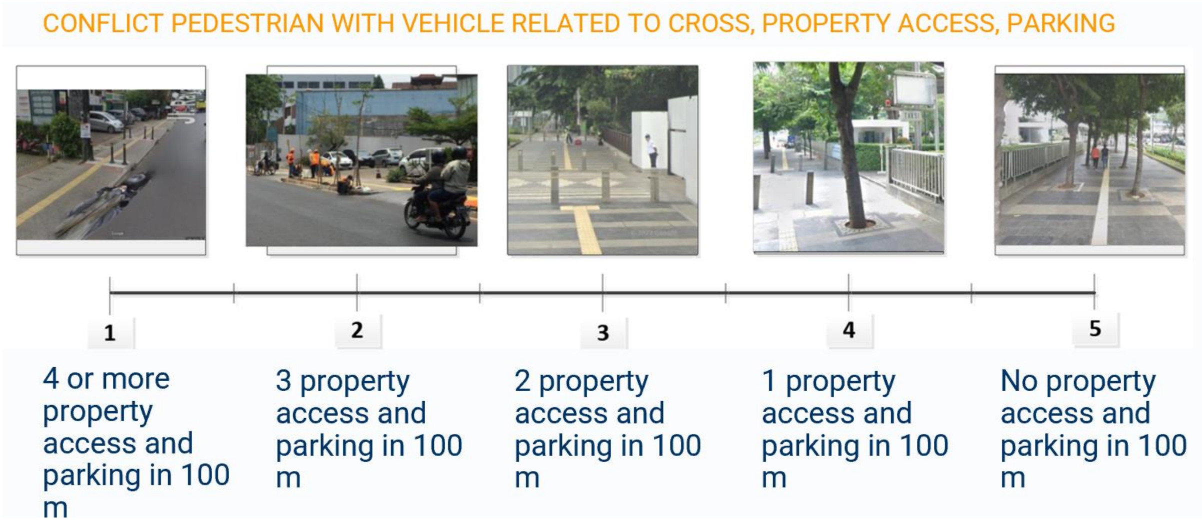

Figure 7 Conflict with vehicle parameters

Seventh, security is a crucial parameter in the walkability index. This encompasses both the perceived and actual safety of pedestrians from crime and harassment. Well-lit and well-patrolled walkways, along with community engagement, contribute to a sense of security, encouraging more people to walk.

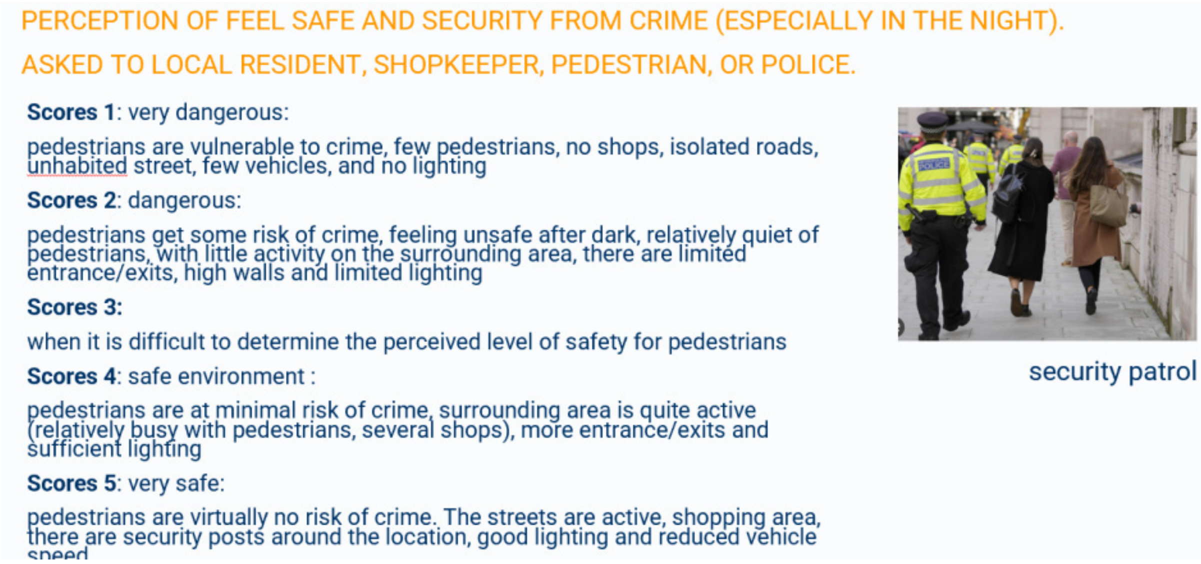

Figure 8 Security perception parameters

By utilizing these seven parameters, the Indonesian Walkability Index provides a robust framework for evaluating and improving the walkability of urban areas, ultimately promoting healthier, more active, and more sustainable communities (Tanan et al., 2017; Wibowo et al., 2015).;

3. WALKABILITY MEASUREMENT SYSTEM

International literatures develop several measurement systems which has similar purpose of the Indonesian Walkability Index. This section briefly elaborates popular measurement systems which are The Global Walkability Index, Walk-Score ®, The Walkability Scales and Pedestrian Level of Service.

3.1 The Global Walkability Index

The Global Walkability Index is a comprehensive metric designed to evaluate and compare the walkability of cities worldwide. This index assesses the pedestrian-friendliness of urban environments based on various criteria, including the availability and quality of pedestrian infrastructure, safety, accessibility, and the proximity to essential amenities. The primary goal of the Global Walkability Index is to provide a standardized method for measuring how conducive an area is for walking, thereby promoting more sustainable and healthy urban living (Frank et al., 2010; Krambeck & Shah, 2006; Maghelal & Capp, 2011).

The Global Walkability Index developed by Krambeck (2006), comprises three components: safety and security, convenience, and degree of policy support. It includes 22 indicators:

1. Pedestrian Fatalities and Injuries
2. Modal Conflict
3. Crossing Safety
4. Crossing Exposure
5. Traffic Management at Crossings
6. Security

7. Safety Rules and Laws
8. Pedestrian Safety Education
9. Motorist Behavior
10. Trees
11. Cleanliness
12. Quality and Maintenance of Walking Path Surface
13. Disability Infrastructure
14. Coverage
15. Obstructions
16. Availability of Crossings
17. Walking Path Congestion
18. Pedestrian Amenities
19. Connectivity
20. Overall Convenience
21. Planning for Pedestrians
22. Relevant Design Guidelines

The Global Walkability Index (GWI) is a valuable tool for assessing urban walkability, but it has several critiques. One major criticism is its lack of context sensitivity. The GWI often applies a standardized approach that may not account for the unique cultural, social, and economic contexts of different cities. This can result in assessments that do not reflect the real needs and priorities of various regions, particularly in developing countries where reliable data on pedestrian infrastructure and safety might be scarce.

Another critique is the GWI's emphasis on physical infrastructure over pedestrian behavior and societal attitudes toward walking. The index may not fully consider the impact of safety concerns, cultural preferences, and local behaviors on walking habits. Additionally, the GWI's weighting system for different walkability factors can be subjective and may not align with local priorities. This standardized approach can lead to skewed assessments that do not accurately represent the ground reality in diverse urban environments. Lastly, the GWI may overlook long-term urban planning and development goals, focusing primarily on current conditions. This can result in insufficient consideration of environmental factors such as air quality and green spaces, which significantly influence the walking experience. Moreover, the reliance on quantitative metrics can overshadow qualitative aspects of walkability, such as the aesthetic appeal of walking routes and the presence of social interactions. While the GWI is useful for promoting pedestrian-friendly urban design, it is essential to recognize its limitations and supplement it with context-specific insights to create a comprehensive picture of walkability.

3.2 Walk-Scores ®

Other popular measurement to quantitate the quality of pedestrian is Walk Score ®. Walk Scores are determined by calculating the walking distance from a specific origin to various amenities across nine crucial daily life categories. For categories where having multiple options is important, multiple amenities are considered. The categories are also weighted based on their relative importance. After the initial calculation, the score may be adjusted down if the area has poor pedestrian-friendly features, such as long blocks or a low density of intersections. Walk Score is then calculated for comparable spatial units by applying selected radii for network searches of the desired destinations and a buffer to assess connectivity. This method ensures that the score reflects not only proximity to amenities but also the overall pedestrian infrastructure and ease of navigation in the area (Frank et al., 2021; Hall & Ram, 2018; Horak et al., 2022).

Walk Score®	Description
90–100	**Walker's Paradise** Daily errands do not require a car.
70–89	**Very Walkable** Most errands can be accomplished on foot.
50–69	**Somewhat Walkable** Some errands can be accomplished on foot.
25–49	**Car-Dependent** Most errands require a car.
0–24	**Car-Dependent** Almost all errands require a car.

Figure 9 Walk Score description

Since the method evaluates the proximity and importance of various amenities and facilities, it also proves to be a valuable tool for assessing land and property values. The presence of nearby amenities, such as grocery stores, schools, parks, restaurants, and healthcare services, significantly enhances the desirability of a location. Therefore, properties in areas with higher Walk Scores often command higher market values due to the convenience and lifestyle benefits they offer. Real estate investors, developers, and homebuyers can use Walk Scores to make informed decisions. For investors and developers, a higher Walk Score indicates a potentially lucrative investment, as properties in walkable neighborhoods tend to appreciate more rapidly and attract higher rental income. Homebuyers, on the other hand, may prioritize Walk Scores when choosing a property, as a high score suggests a neighborhood where daily needs can be met without reliance on a car, contributing to a more sustainable and healthier lifestyle. Furthermore, urban planners and policymakers can use Walk Scores to identify areas in need of infrastructure improvements. By enhancing walkability, they can boost property values and attract new residents and businesses, stimulating economic development.

3.3 The Walkability Scale

The Neighborhood Environment Walkability Scale (NEWS) is a comprehensive survey tool designed to measure various aspects of the built environment that influence walkability in neighborhoods. It is to assess the impact of neighborhood characteristics on physical activity, particularly walking, NEWS evaluates factors such as (a) Types of residences in the neighborhood, (b) Stores, facilities, and other things in the neighborhood, (c) Access to services, (d) Streets condition in the neighborhood, (e) Places for walking and cycling, (f) Neighborhood surroundings, (g) Safety from traffic, (h) Safety from crime, (i) Neighborhood satisfaction (Almeida et al., 2021) .

3.4 Pedestrian Level of Service (PLOS)

Walkability performance can also be measured by pedestrian level of service terms. In China, the current approaches for evaluating pedestrian levels of service have been modeled after vehicle assessment methods and primarily focus on pedestrian flow operations. These methods use pedestrian space occupancy and sidewalk capacity as key parameters to measure changes in walking congestion and the level of freedom pedestrians experience (Raad & Burke, 2018; Tan et al., 2007). By using these parameters, the assessments aim to gauge changes in walking congestion and the degree of freedom pedestrians experience while navigating urban environments. However, this vehicle-centric approach may not fully capture the unique aspects of pedestrian experiences. Pedestrian space occupancy measures how much of the available space is being used by pedestrians, which can indicate levels of congestion. Sidewalk capacity refers to the maximum number of pedestrians that can be accommodated on a sidewalk at a given time. While these metrics are important, they predominantly address physical crowding and movement efficiency, potentially overlooking other critical factors such as safety, comfort, accessibility, and sociability. To develop a more holistic understanding of pedestrian service quality, it is essential to incorporate a broader range of parameters that reflect the diverse needs and experiences of pedestrians.

Traditionally, these methods do not take into account the user's perspective regarding the input variables. However, there is evidence suggesting that pedestrians' direct interaction with their environment warrants an investigation into how their perceptions contribute to these assessments. Studies from Bogota also suggest the effectiveness of user perceptions in explaining sidewalk quality of service (QoS), as compared to traditional measurable inputs like physical characteristics and traffic data (Rodriguez-Valencia et al., 2020; Vallejo-Borda et al., 2020).

A literature from Portugal suggests attributes for defining pedestrian quality of service are Rapidity, Comfort, Convenience, Reliability, Safety, Security, and Sociability (Florez et al., 2014). Rapidity focuses on the efficiency and speed of pedestrian movement, ensuring minimal delays and direct pathways. Comfort involves the physical and psychological ease of walking, enhanced by well-maintained surfaces, shade, and aesthetic appeal. Convenience relates to the ease of navigation and availability of amenities, facilitating smooth and intuitive movement. Reliability ensures that pedestrians can reach their destinations without unexpected interruptions, providing a predictable and consistent walking experience. Safety addresses the protection from traffic-related accidents through well-designed infrastructure like crosswalks and traffic calming measures, while security pertains to protection from crime, achieved through good lighting and surveillance. Sociability reflects the potential for social interactions within the pedestrian environment, supported by features such as wide sidewalks, public squares, and street furniture that encourage community engagement. Together, these attributes create a comprehensive framework for assessing and enhancing pedestrian quality of service, making walking a more attractive, safe, and enjoyable mode of transport. By focusing on these aspects, urban planners can design pedestrian-friendly environments that promote walking, improve public health, and foster vibrant, connected communities.

4. DISCUSSION

Each of measurement set have different indicators/parameters. Each of them has its own advantage and limitation. However, all of measurement set is aiming to quantify the performance of pedestrian mobilities. To analyze, matrix is developed to compare and finding the point could be added to enhance the Indonesian Walkability Index.

Table 1 Comparison of measurement set

	Indicator	**Factors/indicators not included in Indonesian Walkability Index**	**Description**
Indonesian Walkability Index	7 parameters	*baseline*	Physical and objective parameters
The Global Walkability Index	22 indicators	Policy support indicators Trees indicator	More comprehensive index since add policy support
Walk Scores ®	9 amenities	More detailed concern to amenities for living hood/welfare	Usually use for determining the value of properties
Walkability Scale	9 factors	Added satisfaction overall Land use/type of surrounding area	More subjective and perception-based method It evaluates how the built environment influences walking behavior and supports general health and physical activity.
Pedestrian Level of Service	7 attributes	Sociability attributes	General concern about the flow of pedestrian mobilities

Comparing the Indonesian Walkability Index with the Global Walkability Index (GWI) reveals that the GWI is more comprehensive. The Indonesian Walkability Index focuses on the physical aspects of pedestrian areas, assessing parameters such as walkway conditions, amenities, accessibility for people with disabilities, obstructions, crossing quality, vehicle conflict, and security. These factors primarily address the immediate convenience and safety of pedestrians within urban environments.

In contrast, the GWI extends beyond physical infrastructure to incorporate broader aspects of walkability, including policy support for pedestrians. This means the GWI not only evaluates the condition and quality of sidewalks, crosswalks, and pedestrian signals but also considers the presence of policies and regulations that promote pedestrian-friendly urban planning. These policies might include traffic calming measures, zoning laws that encourage mixed land use, and initiatives that prioritize pedestrian safety and accessibility. By including policy considerations, the GWI provides a more holistic view of walkability. It recognizes that sustainable and effective pedestrian environments are not solely the result of physical infrastructure but also depend on supportive policies and governance. This comprehensive approach enables the GWI to better capture the multifaceted nature of walkability, making it a more robust tool for assessing and promoting pedestrian-friendly cities worldwide.

Walk Scores ® measures walkability based on the walking distance to various amenities across nine categories essential for daily life, such as grocery stores, schools, parks, and restaurants. The score is adjusted based on the density and availability of these amenities. Walk Scores also consider pedestrian friendliness factors like block length and intersection density, applying penalties for poor pedestrian infrastructure. Meanwhile, Indonesian Walkability Index relies on a mix of on-site assessments, surveys, and data from local authorities to evaluate the specific parameters. It assessments tailored to the Indonesian urban environment. Walk Scores ® uses a mapping algorithm to calculate the walking distance from a specific location to nearby amenities. The score is then normalized and adjusted based on pedestrian infrastructure metrics. This method relies heavily on GIS data and is designed to be broadly applicable across different urban contexts.

The Indonesian Walkability Index and the Neighborhood Environment Walkability Scale (NEWS) both aim to assess walkability but differ in their purpose and scope. The Indonesian Walkability Index is specifically designed to evaluate and improve walkability within Indonesian urban areas. In contrast, the Neighborhood Environment Walkability Scale (NEWS) is developed to measure how neighborhood characteristics impact physical activity, particularly walking, across diverse urban settings. NEWS evaluates residential density, land use mix, street connectivity, pedestrian infrastructure, traffic and personal safety, aesthetics, and proximity to amenities. It uses detailed surveys to gather both objective measures and subjective perceptions from residents, providing a comprehensive view of how the built environment influences walking behavior and supports general health and physical activity.

Integrating Pedestrian Level of Service (PLOS) into the Indonesian Walkability Index can significantly enhance its comprehensiveness and accuracy. The current index already evaluates essential parameters such as walkway conditions, amenities, accessibility for disabilities, obstructions, crossing quality, vehicle conflict, and security. Adding PLOS will expand these criteria to include more detailed aspects of pedestrian experience, like pedestrian density and flow, sidewalk width and continuity, buffer zones between sidewalks and roads, and crosswalk safety and accessibility. Additionally, PLOS evaluates the surface quality of sidewalks and the availability of shade and weather protection, which are critical for pedestrian comfort and safety.

To further enhance the index, incorporating user perceptions and comfort is crucial. Conducting surveys and interviews with pedestrians can provide valuable insights into their experiences, capturing qualitative data that purely quantitative measures might miss. Evaluating the environment for social interactions and visual appeal will also help understand how aesthetics and sociability impact walkability. These aspects are essential as they directly affect the willingness of people to walk in urban areas.

Additionally, assessing traffic conditions and speed management is vital. The presence and effectiveness of traffic calming measures, such as speed bumps, reduced speed limits, and road narrowing, can significantly impact pedestrian safety. Monitoring traffic volumes and speeds on roads adjacent to pedestrian pathways ensures that these areas are conducive to safe pedestrian movement. Incorporating technological tools like GIS mapping and mobile apps can provide detailed spatial analysis and real-time data on pedestrian movement, density, and environmental conditions. This data can offer a comprehensive view of walkability and help identify specific areas that need improvement.

Finally, integrating policy and planning considerations into the index will ensure a more holistic approach. Evaluating the presence and effectiveness of policies that support pedestrian infrastructure, such as zoning laws and urban design guidelines, is crucial. Long-term urban planning considerations, like developing pedestrian zones, greenways, and public transportation connectivity, will help create a more pedestrian-friendly environment. By incorporating these elements, the Indonesian Walkability Index can become a more robust tool for assessing and improving walkability in Indonesian cities.

5. CONCLUSION

This paper set out to examine this Indonesian Index and compare it with other measurement systems, including the Global Walkability Index, Walk Scores®, the Neighborhood Environment Walkability Scale, and the Pedestrian Level of Service. As highlighted in this study, there remain significant parameters underrepresented in the current walkability index, suggesting ongoing opportunities for refinement and improvement to better align with international standards and local realities.

In conclusion, while the Indonesian Walkability Index focuses on essential physical aspects crucial for pedestrian safety and accessibility within urban settings, its scope remains narrower compared to the Global Walkability Index (GWI). The GWI's comprehensive approach, encompassing not only physical infrastructure but also policy support for pedestrian-friendly urban planning, sets a benchmark for evaluating and promoting walkability on a global scale. Incorporating elements such as policy frameworks and broader environmental factors enhances the GWI's applicability and effectiveness in fostering sustainable, pedestrian-friendly cities worldwide. As Indonesia continues to refine its approach to walkability assessment, integrating insights from global standards like the GWI could further enhance the Indonesian Walkability Index's utility and impact in improving urban pedestrian environments.

The limitation of this study as follows: the scope of this study primarily focuses on documented indices and may not fully capture evolving methodologies or recent innovations in walkability assessment that could be relevant to current urban challenges in Indonesia. Lastly, the study relies on published literature and may not encompass unpublished reports or local initiatives that could provide additional insights into effective strategies for enhancing walkability. These limitations underscore the need for future research to complement literature reviews with empirical data and local case studies to provide a more comprehensive understanding of walkability assessment and improvement strategies tailored to Indonesian cities.

Further studies can focus on three critical areas to advance pedestrian-friendly environments in Indonesian cities. Firstly, conducting a comparative analysis between the Indonesian Walkability Index and international counterparts can offer insights into effective strategies and best practices for enhancement. This approach involves examining various indices to identify gaps and opportunities for improving Indonesia's assessment framework, ensuring alignment with global standards. Secondly, qualitative studies can capture pedestrian perceptions and experiences to understand safety, comfort, and convenience issues. Engaging with urban populations through surveys and interviews will inform infrastructure improvements that prioritize pedestrian needs. Thirdly, integrating GIS mapping and mobile apps for real-time data collection could enhance assessment accuracy, evaluating pedestrian infrastructure, traffic patterns, and environmental conditions effectively. This data-driven approach supports evidence-based urban planning and policy decisions.

6. ACKNOWLEDGEMENT

We gratefully acknowledge the Directorate General of Highways for their essential support and resources, which were crucial for this study on pedestrian infrastructure and walkability in Indonesian cities. We also extend our appreciation to fellow researchers Natalia Tanan and Dr. Sony Sulaksono for their invaluable contributions and collaborative efforts. Their expertise and dedication significantly enhanced the quality and depth of our research, shaping our understanding of creating pedestrian-friendly urban environments in Indonesia.

7. REFERENCES

Almeida, D. P., Alberto, K. C., & Mendes, L. L. (2021). Neighborhood environment walkability scale: A scoping review. *Journal of Transport & Health*, *23*.

Florez, J., Muniz, J., & Portugal, L. (2014). Pedestrian Quality of Service: Lessons from Maracanã Stadium. *Procedia - Social and Behavioral Sciences*, *160*(Cit), 130–139. https://doi.org/10.1016/j.sbspro.2014.12.124

Frank, L. D., Appleyard, B. S., Ulmer, J. M., Chapman, J. E., & Fox, E. H. (2021). Comparing walkability methods: Creation of street smart walk score and efficacy of a code-based 3D walkability index. *Journal of Transport and Health*, *21*(March), 101005. https://doi.org/10.1016/j.jth.2020.101005

Frank, L. D., Sallis, J. F., Saelens, B. E., Leary, L., Cain, L., Conway, T. L., & Hess, P. M. (2010). The development of a walkability index: Application to the neighborhood quality of life study. *British Journal of Sports Medicine*, *44*(13), 924–933. https://doi.org/10.1136/bjsm.2009.058701

Giles-Corti, B., Macaulay, G., Middleton, N., Boruff, B., Bull, F., Butterworth, I., Badland, H., Mavoa, S., Roberts, R., & Christian, H. (2014). Developing a research and practice tool to measure walkability: A demonstration project. *Health Promotion Journal of Australia*, *25*(3), 160–166. https://doi.org/10.1071/HE14050

Hall, C. M., & Ram, Y. (2018). Walk score® and its potential contribution to the study of active transport and walkability: A critical and systematic review. *Transportation Research Part D: Transport and Environment*, *61*(March 2017), 310–324. https://doi.org/10.1016/j.trd.2017.12.018

Horak, J., Kukuliac, P., Maresova, P., Orlikova, L., & Kolodziej, O. (2022). Spatial Pattern of the Walkability Index, Walk Score and Walk Score Modification for Elderly. *ISPRS International Journal of Geo-Information*, *11*(5). https://doi.org/10.3390/ijgi11050279

Krambeck, H., & Shah, J. J. (2006). *The Global Walkability Index*.

Maghelal, P. K., & Capp, C. J. (2011). Walkability: A review of existing pedestrian indices. *URISA Journal*, *23*(2), 5–19.

Directorate General of Highways, M. of P. W. and H. R. of I. (2023). *Penentuan indeks kelayakan berjalan (walkability index) di kawasan perkotaan*. *05*.

Raad, N., & Burke, M. I. (2018). What are the most important factors for pedestrian level-of-service estimation? A systematic review of the literature. *Transportation Research Record*, *2672*(35), 101–117. https://doi.org/10.1177/0361198118790623

Rodriguez-Valencia, A., Barrero, G. A., Ortiz-Ramirez, H. A., & Vallejo-Borda, J. A. (2020). Power of User Perception on Pedestrian Quality of Service. *Transportation Research Record*, *2674*(5), 250–258. https://doi.org/10.1177/0361198120914611

Tan, D., Wang, W., Lu, J., & Bian, Y. (2007). Research on Methods of Assessing Pedestrian Level of Service for Sidewalk. *Journal of Transportation Systems Engineering and Information Technology*, *7*(5), 74–79. https://doi.org/10.1016/S1570-6672(07)60041-5

Tanan, N., Wibowo, S. S., & Tinumbia, N. (2017). Pengukuran Walkability Index pada Ruas Jalan di awasan Perkotan (Walkability Index MMeasurement on Road Links in Urban Area). *Jurnal Jalan-Jembatan*, *34*(2), 115–127.

Vallejo-Borda, J. A., Cantillo, V., & Rodriguez-Valencia, A. (2020). A perception-based cognitive map of the pedestrian perceived quality of service on urban sidewalks. *Transportation Research Part F: Traffic Psychology and Behaviour*, *73*, 107–118. https://doi.org/10.1016/j.trf.2020.06.013

Wibowo, S. S., Tanan, N., & Tinumbia, N. (2015). Walkability Measures for City Area in Indonesia (Case Study of Bandung). *Journal of the Eastern Asia Society for Transportation Studies*, *11*(2006), 1507–1521. http://dx.doi.org/10.11175/easts.11.1507%255Cnhttps://trid.trb.org/view/1378398

Investigating the Impact of COVID-19 on Speed Profiles: A Case Study of Rama2 Road, Thailand

Somsiri Siewwuttanagul[1], Phosawee Kettreekorn[2]*, Puttipan Seraneeprakarn[3], Natachai Wongchavalidkul[1]

[1]Faculty of Engineering, Mahidol University, Thailand,
Email: somsiri.sie@mahidol.ac.th, natachaiw@gmail.com
[2]Faculty of Business Administration Program in Logistics and Supply Chain Management,
Rajapruk University, Thailand, phkett@rpu.ac.th
[3]Inter-city Motorway Division, Department of Highways, Thailand, puttipan.doh@gmail.com

ABSTRACT

This study focuses on the impact of the COVID-19 pandemic on the speed profile of Rama2 road, employing a spatial-temporal analytical approach. Utilizing data extracted from TomTom databases, the study examines the change in average hourly speed spanning the years 2019 to 2022, discerning three pivotal periods of road usage: pre-COVID-19 (2019), and During-COVID-19 (2020). Each section of Rama2 road is compared to illustrate the variations in speed profiles.

The spatial-temporal analysis is analyzed in terms of both free-flow conditions and congestion patterns. Specifically, spatial analysis investigates the distribution of speed variations along different segments of Rama2 road, while temporal analysis assesses the fluctuations in average hourly speed within each identified period.

Furthermore, the research integrates a comprehensive timeline of significant COVID-19-related events, government interventions (e.g., lockdowns, restrictions, relaxations), and road construction and maintenance activities. This inclusion facilitates the identification of significant factors influencing changes in hourly average speed.

The study's findings offer a thorough explanation of the patterns of change in speed profiles during the COVID-19 period on Rama2 road. Additionally, the research underscores the importance of leveraging big data for highway planning and management, highlighting implications for future transportation policy and infrastructure development initiatives in Thailand.

Keywords: COVID19, Road speed, TomTom traffic data, Highway management

1. INTRODUCTION

RAMA2 Road, a critical transportation artery in Thailand, has long been plagued by severe traffic congestion (Maneesrikham, 2012). This thoroughfare is not only a major route connecting the central region to the southern parts of the country but also accommodates a substantial volume of traffic driven by its inter-regional transport connectivity (Moya-Gómez & García-Palomares, 2017). The high traffic volume is further compounded by dense activities along the road, including industrial operations, logistics facilities, and rapid urbanization. These factors contribute to the persistent and often severe congestion problems that RAMA2 Road experiences.

The strategic importance of RAMA2 Road for both local and long-distance travel means that it carries a heavy load of vehicles daily. This includes commuter traffic, freight transport, and inter-city travel, all of which are vital for the economic integration and mobility between central and southern Thailand. The road's capacity, however, has been insufficient to meet these demands, leading to chronic congestion (Jonathan & Yaakov, 2002). Efforts to improve and expand the road have been ongoing for decades, but these construction activities themselves have become a source of significant traffic bottlenecks Moya-Gómez & García-Palomares, 2017; Christidis & Rivas, 2012. The construction zones, often stretching over long sections of the road, disrupt the traffic flow and exacerbate congestion, particularly during peak travel times Litman, 2023; Aftabuzzaman, 2007.

To address these issues, this study leverages detailed historical traffic data from TomTom, a global leader in traffic analytics. TomTom data provides comprehensive insights into traffic speeds and travel times, allowing for a precise assessment of road performance and congestion points. By analyzing this data, we can identify specific locations where traffic slows down or bottlenecks occur, and evaluate the overall traffic flow along RAMA2 Road.

This study aims to compare the traffic speed data from two distinct periods: pre-COVID-19 and during the COVID-19 pandemic. The COVID-19 pandemic has had a significant impact on travel behaviors worldwide, and RAMA2 Road is no exception. During the pandemic, lockdowns and social distancing measures reduced traffic volumes significantly (Siewwuttanagul & JittrapiromPeraphan, 2023). By comparing data from these two periods, we can assess how traffic performance on RAMA2 Road changed in response to the pandemic and the resulting shifts in travel patterns.

Additionally, the analysis takes into account the locations of ongoing road construction projects. Understanding the impact of these construction activities on traffic congestion during the COVID-19 timeline is crucial for developing effective traffic management strategies. The study will pinpoint how these constructions have influenced congestion and whether reduced traffic volumes during the pandemic mitigated or exacerbated these impacts.

To provide a comprehensive picture of traffic dynamics on RAMA2 Road, the study also distinguishes between weekday and weekend traffic patterns. This distinction is essential because travel behaviors often differ significantly between weekdays and weekends, with varying implications for traffic congestion and speed profiles (Burris et al., 2016). By examining both sets of data, we can offer a nuanced understanding of how traffic on RAMA2 Road has evolved throughout the pandemic and identify patterns that may inform future infrastructure and traffic management policies (Cortright, 2010).

In summary, this study uses TomTom traffic data to investigate the impact of the COVID-19 pandemic on traffic speed profiles on RAMA2 Road. By comparing pre-pandemic and during-pandemic data, considering the effects of road construction, and differentiating between weekday and weekend traffic, we aim to provide a detailed analysis of the changes in traffic performance and identify strategies to alleviate congestion on this critical transportation route.

2. METHODOLOGY

This study investigates the impact of COVID-19 on speed profiles on Rama2 Road, which has complex road usage and is considered one of the most unreliable highways in Thailand. The methodology mainly applies TomTom traffic data to track the historical hourly speed data on Rama2 Road, observing the mobility impact at road sections affected by construction sites. This study focuses on the impact of COVID-19 on the target road section; therefore, a comparison between pre-COVID-19 and during-COVID-19 periods is made to identify changes in average speed. This analysis can potentially help the Highway Department precisely identify locations and times that need deep investigation, leading to the development of mobility improvement plans.

2.1 TomTom data

TomTom's real-time and historical traffic data encompass a vast geographic range, enabling analysis across a multitude of highway segments. The data provide detailed insights into traffic speed and travel time for specific highway sections. The greater precision of historical data facilitates the evaluation of traffic patterns over time, allowing the study to assess the impact of past interventions and predict future trends in highway mobility.

In this research, TomTom data will be employed to analyze historical 24-hour hourly data to understand existing traffic patterns and identify changes in average traffic speed on RAMA2 Road.

The one-year average speed data for each small road section is used in this study. Two datasets, from the years 2019 and 2020, are presented. Each dataset represents the 24-hour hourly data. The data are retrieved over Highway Number 35 (RAMA2 Road) from sections 9+887 to 83+948, which include all the RAMA2 Road sections.

By leveraging TomTom's datasets, this research aims to provide a comprehensive evaluation of highway mobility performance and inform data-driven strategies for optimizing the mobility improvement plan.

2.2 Construction timeline

The elevated highway construction on RAMA2 Road has been carried out in two main sections. The first section, between Bang Khun Thian interchanges (km. 9+731) and Ekachai Road (km. 20+295), as shown in **Figure 1**, has seen elevated highway construction throughout the year 2019 to the present, covering a distance of 10.567 kilometers. This section features 6 lanes and includes two entry and exit points: Phanthai Norasing Checkpoint and Mahachai Checkpoint 1

(**Figure 2**).

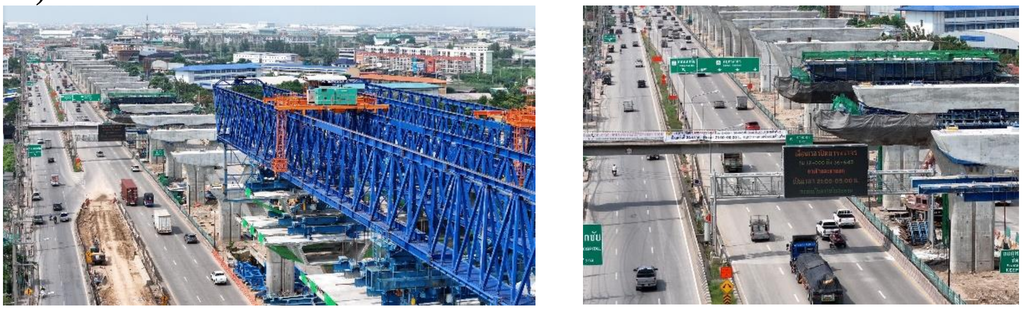

(a) (b)

Figure 1. Elevated highway construction site activities (a) and signage indicate the road closure due to the construction (b)

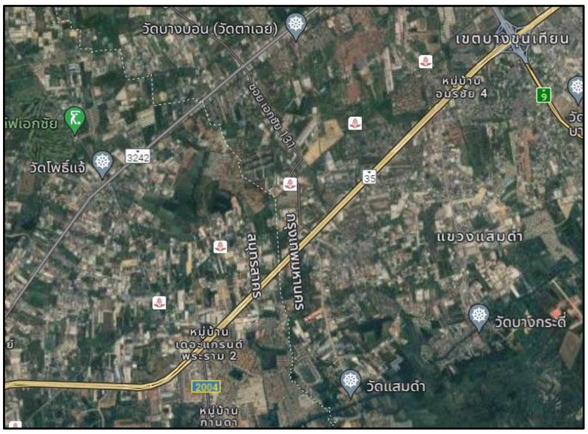

Note:
BKT refers to Bang Khun Thian interchanges (km.9+731)
EKC refers to Ekachai Road (km.20+295)
KL refers to Kalong (km.44+659)
WMN refers to Wang Ma Now (km.83+948)

Figure 2. Map of Elevated highway construction section between Bang Khun Thian interchanges (km.9+731) to Ekachai Road (km.20+295)

The second section, between Ekachai Road (km. 20+295) and Ban Phaeo (km. 36+645), as shown in **Figure 3**, is undergoing elevated highway construction from 2019 to 2025, covering a distance of 16.350 kilometers with 6 lanes and 4 entry and exit points: Mahachai Checkpoint 2, Samut Sakhon Checkpoint 1, Samut Sakhon Checkpoint 2, and Ban Phaeo Checkpoint. Additionally, road improvement constructions have been made to the section between Bang Khun Thian interchanges (km. 9+731) and Ekachai Road (km. 20+295). These improvements were conducted from 2018 to 2020, expanding the road from 10 lanes to 14 lanes over a distance of 10.567 kilometers.

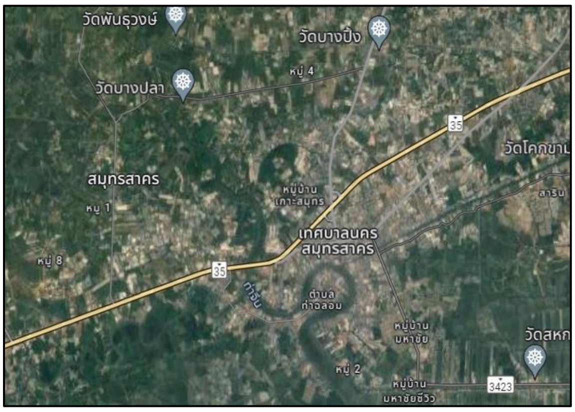

Note:
BKT refers to Bang Khun Thian interchanges (km.9+731)
EKC refers to Ekachai Road (km.20+295)
KL refers to Kalong (km.44+659)
WMN refers to Wang Ma Now (km.83+948)

Figure 3. Map of Elevated highway construction section between Ekachai Road (km. 20 + 295) to Ban phaeo (36 + 645)

3. RESULTS

The speed profile throughout the observation is illustrated in **Figure 4**. The overall average speed result shown that weekend during 09:00 to 15:00, the average speed has decreased significantly by discarding the impacts of COVID19.

The speed profile throughout the observation period is illustrated in Figure xx. The overall average speed results show that, on weekends during 09:00 to 15:00, the average speed decreased significantly, excluding the impacts of COVID-19.

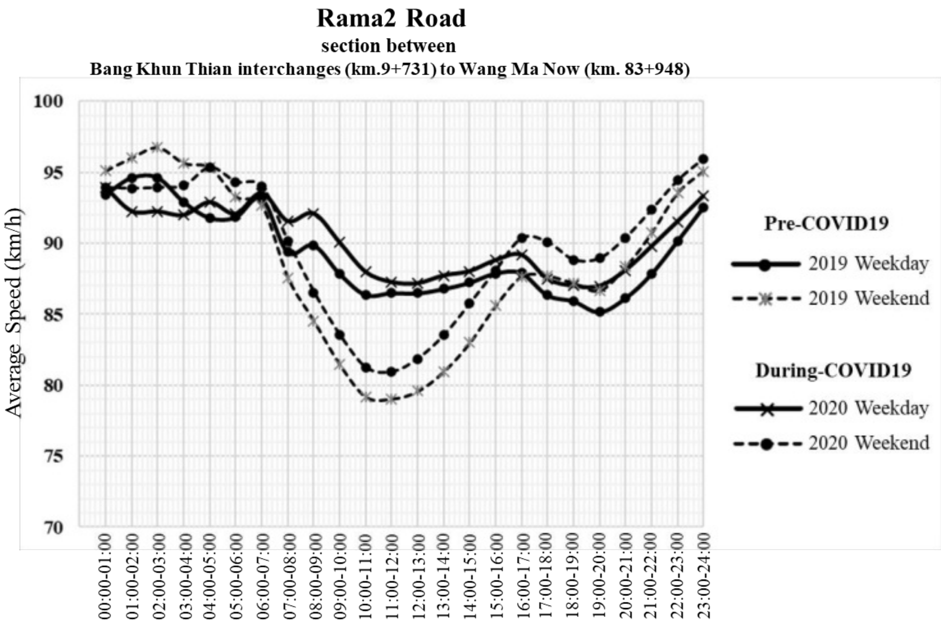

Figure 4. Speed profile of Rama2 Road section between
Bang Khun Thian interchanges (km.9+731) to Wang Ma Now (km. 83+948)

Comparing the change in average speed between pre-COVID-19 in 2019 and during-COVID-19 in 2020, the results indicate that COVID-19 affected the average speed on RAMA2 Road in terms of both location and time, as shown in **Figure 5**. Changes in weekday and weekend speeds report a similar trend and degree of change, but with slight differences in timing.

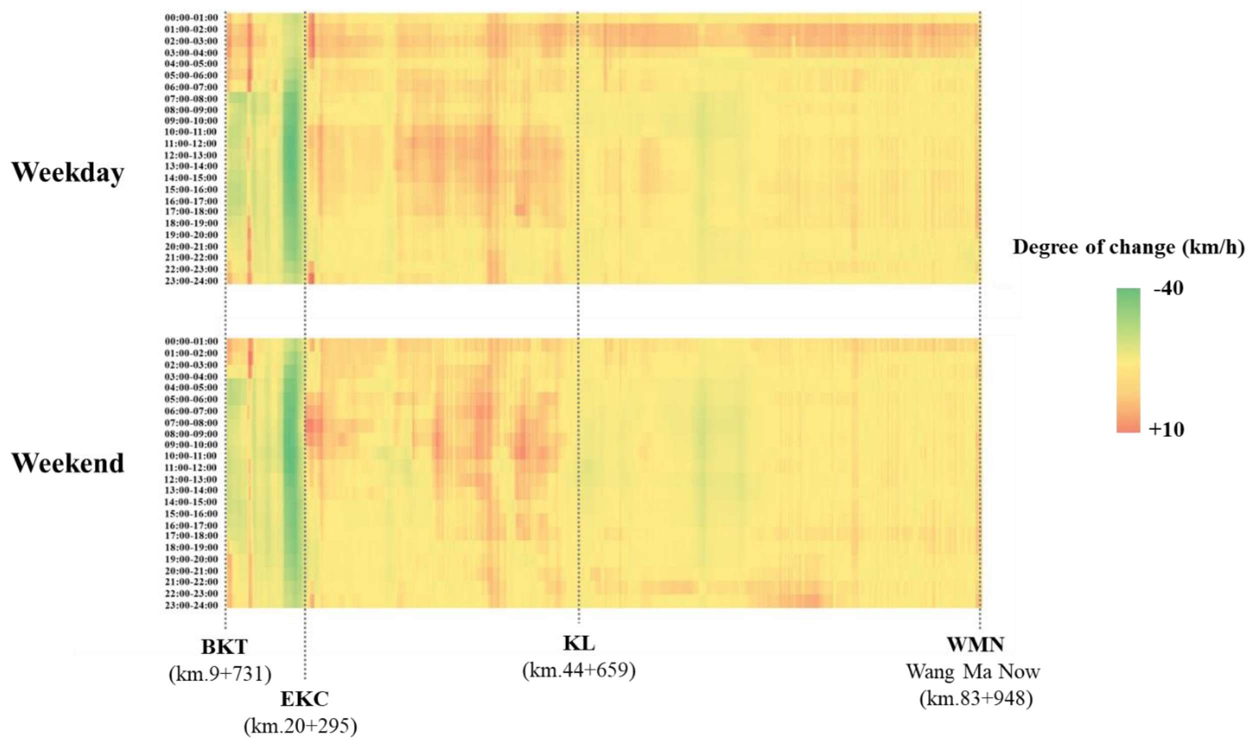

Note:
BKT refers to Bang Khun Thian interchanges (km.9+731)
EKC refers to Ekachai Road (km.20+295)
KL refers to Kalong (km.44+659)
WMN refers to Wang Ma Now (km.83+948)

Figure 5. Degree of change in average speed from 2019 to 2020 based on the location of road section

The characteristics of the speed profile on RAMA2 Road can be divided into three areas, indicating different speed patterns and impacts caused by COVID-19:

1. The road section between Bang Khun Thian interchanges (km. 9+731) and Ekachai Road (km. 20+295), which had ongoing road construction throughout 2019 and 2020.
2. The road section between Ekachai Road (km. 20+295) and Kalong (km. 44+659), which passes through Samut Sakhon city and Mahachai district, areas with dense industrial and logistics activities.
3. The road section between Kalong (km. 44+659) and Wang Ma Now (km. 83+948), which has less urbanization and indicated a higher average speed than the other sections.

On weekdays, the difference in weekday average speeds throughout RAMA2 Road in 2020 compared to 2019 increased by 12.60 km/h. Throughout the observation period from 2019 to 2020: The road section from Bang Khun Thian interchanges (km. 9+731) to Ekachai Road (km. 20+295) had an average speed of 66.5 km/h. The section from Ekachai Road (km. 20+295) to Kalong (km. 44+659) had an average speed of 83.9 km/h. The road section between Kalong (km. 44+659) and Wang Ma Now (km. 83+948) had an average speed of 95.9 km/h.

The most significant changes in speed were indicated at the Bang Khun Thian interchanges (km. 9+731) to Ekachai Road (km. 20+295) section, where the average speed increased from 64.35 km/h in 2019 to 68.57 km/h in 2020. This dramatic increase occurred during 07:00 to 09:00 and 14:00 to 18:00, as shown in **Figure 6**.

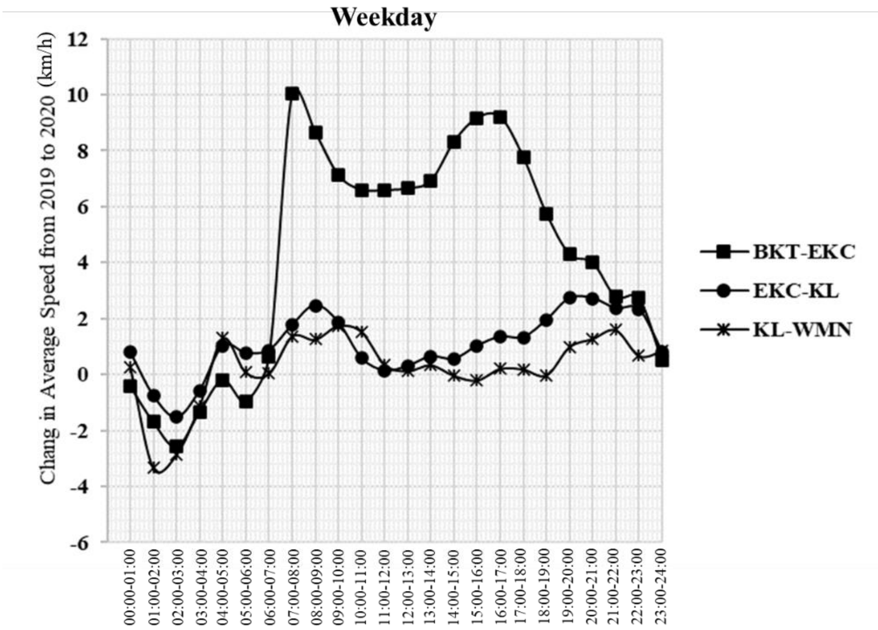

Note:
BKT refers to Bang Khun Thian interchanges (km.9+731)
EKC refers to Ekachai Road (km.20+295)
KL refers to Kalong (km.44+659)
WMN refers to Wang Ma Now (km.83+948)

Figure 6. Change in weekday hourly average speed from 2019 to 2020

On weekends, the difference in weekend average speeds throughout RAMA2 Road in 2020 compared to 2019 increased by 12.28 km/h. Throughout the observation period from 2019 to 2020: The road section from Bang Khun Thian interchanges (km. 9+731) to Ekachai Road (km. 20+295) had an average speed of 69.2 km/h. The section from Ekachai Road (km. 20+295) to Kalong (km. 44+659) had an average speed of 82.9 km/h. The road section between Kalong (km. 44+659) and Wang Ma Now (km. 83+948) had an average speed of 95.1 km/h.

Similar to the weekday average speeds, during the weekend, the most significant changes in speed were observed at the Bang Khun Thian interchanges (km. 9+731) to Ekachai Road (km. 20+295) section, where the average speed increased from 66.9 km/h in 2019 to 71.5 km/h in 2020. This dramatic increase occurred during 07:00 to 19:00, as shown in **Figure 7**.

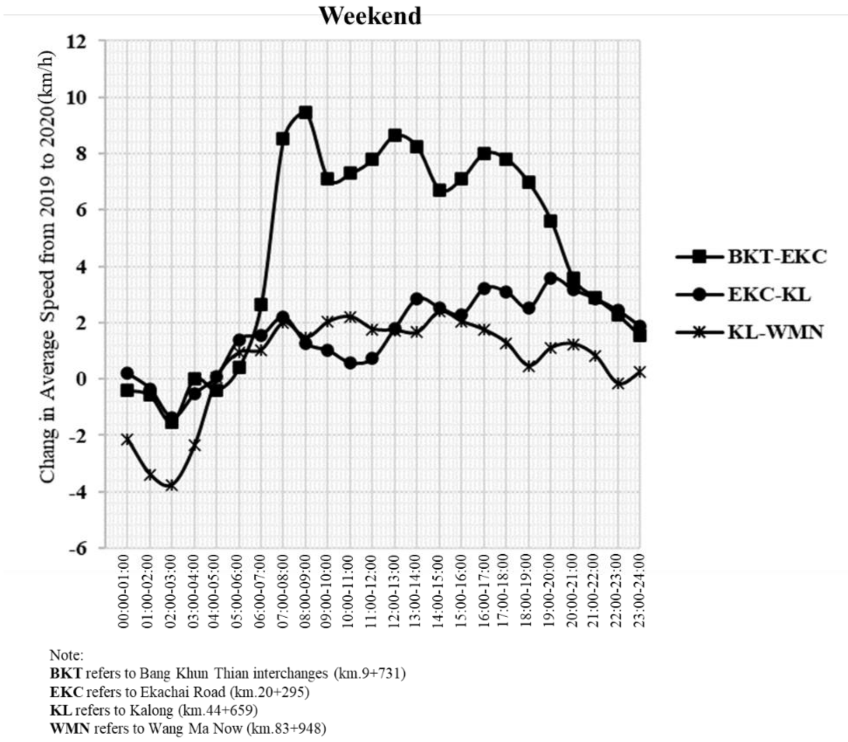

Figure 7. Change in weekend hourly average speed from 2019 to 2020

4. CONCLUSIONS AND DISCUSSIONS

TomTom data can identify road speeds more precisely than existing methods due to its high resolution, recording data in small road section formats as well as providing 24-hour hourly recordings. This speed data also reflects road flow. Comparison between pre-COVID-19 and during-COVID-19 shows notable differences. The bottleneck in the road section from Bang Khun Thian (BKT) to Ekachai (EKC) was caused by the limited capacity of the road during construction. This is clearly determined by the average speed during COVID-19, which increased significantly due to reduced traffic volume. This indicates that road construction needs to account for the spare capacity of the road to avoid bottlenecks. The severity of congestion differs between weekdays and weekends due to varying traffic volumes. Additionally, the fact that road construction operates at night on weekdays is related to the drop in speed compared to weekend nighttime speeds.

During COVID-19, although travel was restricted, the average road speed on RAMA2 Road decreased significantly between 23:00 and 04:00 on weekdays. This suggests a change in RAMA2 road users' behavior, potentially driving slower due to higher traffic volume or other obstacles that slow down traffic at night. The road section between EKC and Kalong (KL) also indicated lower speeds during COVID-19 on both weekdays and weekends, especially during the daytime. Evidence from this road section clearly shows different patterns of speed decline between weekdays and weekends. During COVID-19, the average road speed declined significantly from 11:00 to 19:00 on weekdays, while the same low-speed pattern occurred from 05:00 to 15:00 on weekends. The decline in speed during COVID-19 could be due to various factors such as government travel lockdown measures that restricted cross-city transportation to prevent the spread of disease, resulting in higher travel demand during the daytime, changes in roadside activities leading to higher urban density, or poor road visibility causing users to slow down and drive more cautiously.

Therefore, to investigate the precise causes of road performance issues, deeper analysis considering other factors is needed. However, the micro speed data introduced in this study can help narrow down specific times when problems occurred, providing insightful information for the Highway Department to speculate on faults and conduct detailed investigations.

5. REFERENCES

Aftabuzzaman, M. (2007). Measuring Traffic Congestion- A Critical Review. *30th Australasian Transport Research Forum*.

Burris, M., Spiegelman, C., Abir, A., & Lee, S. (2016). *Travelers' Value of Time and Reliability as Measured on Katy Freeway.* Texas: Texas A&M Transportation Institute.

Christidis, P., & Rivas, J. (2012). *Measuring road congestion.* European Commission, Joint Research Centre, Institute for Prospective Technological Studies.

Cortright, J. (2010). *MEASURING URBAN TRANSPORTATION PERFORMANCE.* CEOs for CITIES.

Jonathan, L., & Yaakov, G. (2002). Congestion pricing's conditional promise: promotion of accessibility or mobility? *Transport Policy 9*, 179-188.

Litman, T. (2023). *Smart Congestion Relief: Comprehensive Evaluation of Traffic Congestion Costs and Congestion Reduction Strategies.* Victoria Transport Policy Institute.

Maneesrikham, C. (2012). *Enhance the development process of the road safety network in the Rama 2 road area.* Bangkok: ThaiHealth Promotion Foundation.

Moya-Gómez, B., & García-Palomares, J. (2017). The impacts of congestion on automobile accessibility. What happens in large European cities? *Journal of Transport Geography 62*, 148-159.

Siewwuttanagul, S., & JittrapiromPeraphan, P. (2023). Impacts of COVID-19 and associated containment measures on Bangkok's Public Transport Ridership. *Transportation Research Interdisciplinary Perspectives 17*, 100737.

Effectiveness of Early Rehabilitation of Pavement and Development of FWD Prediction Model

Keizo Kamiya[1,*] and Kazutaka Suzuki[2]

[1] Engineering department, NEXCO Central, Nagoya, Japan, k.kamiya.ab@c-nexco.co.jp
[2] Kanazawa regional head office, NEXCO Central, Kanazawa, Japan, k.suzuki.ad@c-nexco.co.jp

ABSTRACT

Early rehabilitation is considered an ideal strategy for managing road pavements, as it is expected to ensure longer durability to minimize the life-cycle cost. However, such a practice has not much been adopted, so its effectiveness is even difficult to understand. In this paper the effectiveness was examined through analysis of repair history using NEXCO-PMS, which collects not just road surface and FWD data but also all segments of pavement repair projects for decades. When comparing problematic sections having their three layers replaced again, earlier dates of rehabilitation showed a longer durability, as bearing capacity of the porous pavement deteriorates fast. For the purpose of developing an FWD prediction model, a Machine Learning method was applied. As a result, between measured and predicted FWD values, coefficient of determination of the model 0.616 was confirmed. When the model was applied in a case study, the effectiveness of earlier date of rehabilitation was also confirmed. Moreover, it was revealed that keeping the bearing capacity of pavement in a good condition will in effect lead to assuring longer durability of pavement.

Keywords: Rehabilitation, Repair history, Porous asphalt, Durability, Machine learning

1. INTRODUCTION

Japanese nationwide toll expressways are regionally managed by three companies, NEXCO East, Central and West Nippon Expressway Companies (hereinafter referred to as NEXCO) on behalf of the Transport Ministry. For upgrading serviceability for road users, porous asphalt has already become NEXCO's face as it is covered with over 80% of its road surface (Figure 1).

Figure 1 Visibility of porous asphalt on a rainy day.

While greatly reducing traffic accidents on rainy days as well as absorbing traffic noise, porous pavement needs more rehabilitation costs than dense-graded asphalt. As depicted in Figure 2, damage of the porous asphalt is to occur in the underlying layers as rainwater is retained on the binder layer. Therefore, replacing two layers with new materials is becoming a standard rehabilitation for the pavement since a decade ago. Recently, rehabilitation of three layers is reportedly on the increase gradually.

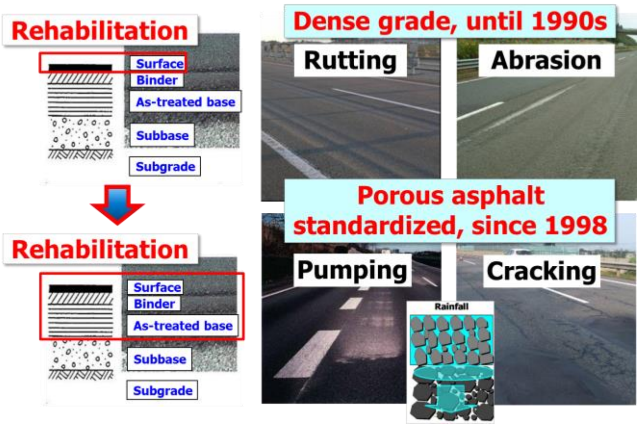

Figure 2 Pavement damage in dense-graded and porous asphalt pavements.

We have confirmed that distress mechanism of porous asphalt is generally explained as depicted in [0] to [6] of Figure 3. Early years of the pavement begins with surface defects that include de-bonding [1] of surface and binder layers. The loosened two layers [2] are to be rehabilitated with two new layers [3] as long as underlying layers can support them substantially. Then after repeating the process of [0] to [3] for years, fatigue crack may possibly emerge from the bottom of the bituminous base layer [4] at some problematic sites. Despite rehabilitation [5] again, in a worst case at fewer sites, the bottom-up crack further develops and combines with the top-down cracks later years, permanent deformation [6] is to take place on the subbase as final life stage of the pavement. Note that during the whole process underlying layer's bearing capacity is going to reduce gradually.

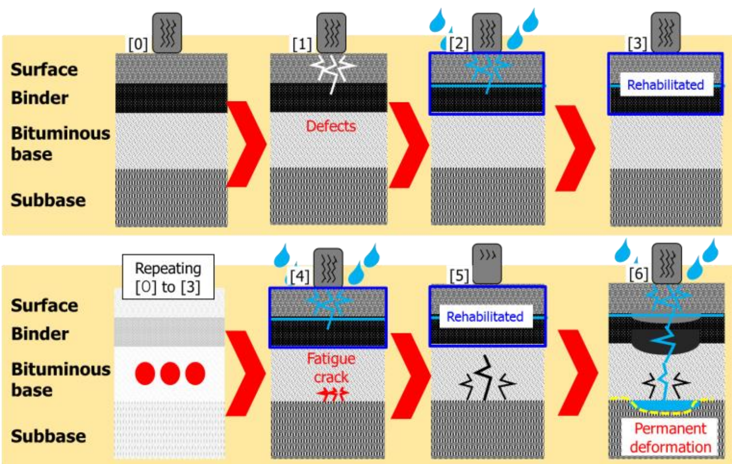

Figure 3 Distress mechanism of porous asphalt.

To avoid deeply rooted rehabilitation, early rehabilitation seems to be a right answer. However, as it means simply spending a budget for repairing not damaged pavements, or segments before reaching surface criterion, such case studies have not been done much so far. Therefore, it has remained difficult even to understand the effectiveness practically in the field.

This paper tries to examine the effectiveness of early rehabilitation by using a PMS owned by NEXCO, and to find a practical guide to achieving longer life of pavement.

2. NEXCO-PMS

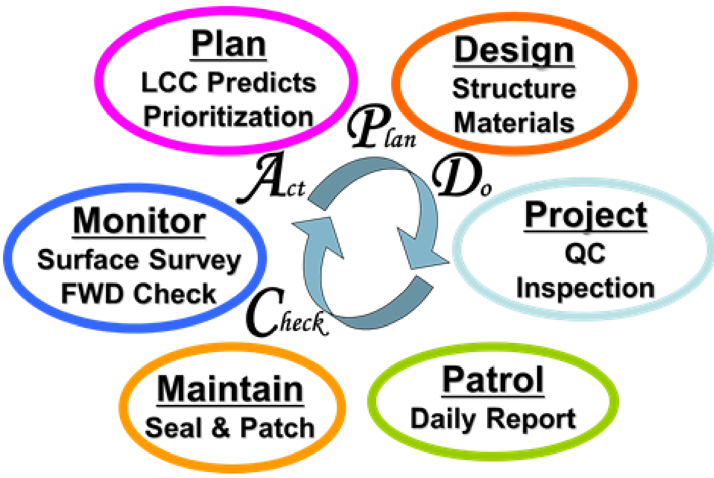

Figure 4 Job stages of pavement life cycle.
(Kamiya_1, 2024)

Figure 4 illustrates pavement job stages being adopted at NEXCO. For example, to begin with "Monitoring" stage, conditions of the in-service pavements are to be scrutinized. Second, depending on the level of distress, prioritization of pavement repair projects and analysis of life cycle costs are carried out at the next "Planning" stage. Then a set of specific layer structures and materials to be used for newly replacing layers is determined on a project basis at the following "Designing" stage. At the next "Project" stage, sufficient quality is to be maintained as a prerequisite for achieving the design concept of the project. Daily patrols are to begin immediately after the project is completed, to keep the road surface safe at the "Patrolling" stage. If necessary, routine maintenance like sealing cracks and patching potholes remedies is to be carried out in the years-long "Maintaining" stage. In several years, both road surface and structural conditions will be diagnosed again at the "Monitoring" stage.

In the course of the entire pavement management cycle, if there is some problem at either of the stages, longevity expected in the design cannot be achieved. Indeed every stage is equally important, but more weight should be placed on "Planning" and "Designing" stages, as they practically determine most of the life cycle cost of the pavement; the planning stage is responsible for strategic budget allocation for repair projects by appropriately assessing the condition of the pavement, and then the designing is in charge of specific repair methods that can minimize the life cycle cost of the pavement by finding the best way to solve the problem in the field. "Rehabilitation" as referred in this study belongs to the designing stage.

The PMS owned by NEXCO (NEXCO-PMS) contains comprehensive pavement data arising from 'Project' and 'Monitor' stages of the figure. In short, NEXCO-PMS stores not just road surface data like rutting, cracking and IRI as well as FWD data but also projects data such as when, where and how every rehabilitation was done all over the net-work. All such rehabilitation data over 30 years have been recorded in one-meter basis and in structure-basis, such as a bridge, tunnel or earthwork, on which pavement performance completely differs.

In this paper, sustained days until the next rehabilitation are used to assess the quality of project on earthwork; the longer sustainable days of a project, the better (Kamiya_1, 2024).

3. EARLY REHABILITATION

3.1 Current procedure

Like many road agencies overseas, rehabilitation at NEXCO is annually conducted according to the criteria authorized by the government. Since its road budget is restricted, NEXCO cannot afford to apply a seemingly unnecessary procedure like early rehabilitation, as it means spending for repairing seemingly not much damaged pavements.

However, all pavements will not be rehabilitated in completely the same condition, because repair reasons may vary. For example, some 100-meter sections are not much cracked but rutted, but the next continuing 100-meter sections are no defected in surface but may have structural problems. However, both sections might be repaired in the same procedure by field engineers for their other views such as keeping safety, project continuity and so on. Therefore, among repair projects, there could be some inclusion of early rehabilitation cases or segments not reaching surface criterion of rutting, cracking or IRI. Such cases might eventually end up with longer durability.

To properly evaluate quality of a rehabilitation project and its ensuing pavement performance, all target projects were categorized into groups that have the same rehabilitation history in this paper. All data were extracted from the NEXCO-PMS.

3.2 Effectiveness

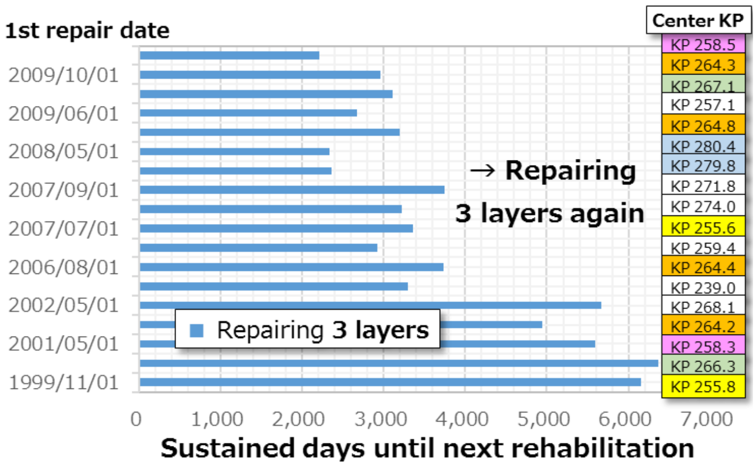

Figure 5 Chronological lineup of problematic sections (Hokuriku Expressway). (Kamiya_1, 2024)

Figure 5 is a lineup of spotted problematic earthwork sections that had to be rehabilitated by replacing three layers twice on the Hokuriku Expressway. With very curiosity, despite no necessity, there is a tendency that earlier dates of first repair give longer durability. However, the center Kilo post of each project site is a bit informative about the cause of the tendency. Focusing on every same colored KP group, which is within one kilometer range, effectiveness of earlier rehabilitation dates becomes more remarkable. This can also be more understandable, as the pavement's bearing capacity deteriorates drastically in such nearby problematic sections, as above mentioned in Figure 3.

Broadly viewing in a decade scale, this indicates that recent projects in problematic areas are going to be shorter lived. In other words, however, if each project had been rehabilitated some more years earlier, each sustained days might have been longer. In this way, the effectiveness of early rehabilitation can be seen from a macro view.

The above phenomenon is not just limited to two times of three layers rehabilitation but also to other problematic cases where pavement rehabilitation was repeated with huge spending (Kamiya_1, 2024). Before moving onto a more detailed case study, how to evaluate the bearing capacity of pavement is to be discussed in the next chapter.

4. MACHINE LEARNING

4.1 Prototype model

To assess the structural strength of underlying layers, Falling Weigh Deflectometer has been used over 15 years at NEXCO. However, since the measure is point-basis, which requires a traffic control of lane-closure, it is impossible to cover 9,000km long for monitoring objectives. Moreover, it also poses a question to develop a relationship between 100m-basis road surface data and point-basis FWD data.

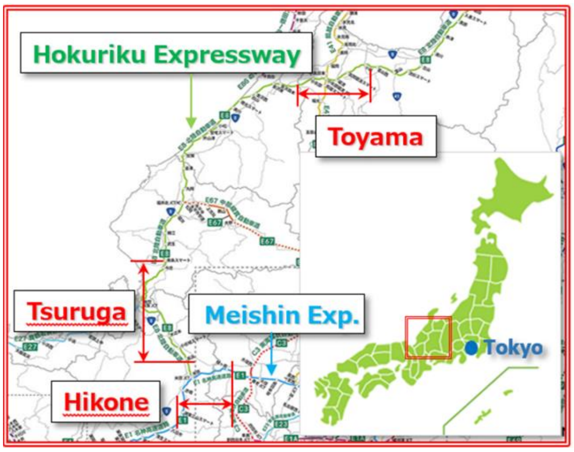

Figure 6 Targeted three expressway sections in this study.
(MLIT_1, 2024)

To deal with such a conundrum, we focused on a Machine Learning methodology to develop a FWD prediction model so that structural value can be substantially estimated from key elements including road surface indices of crack ratio, rutting and IRI on 10-meter basis. However, data stock of existing FWD data so far recorded is far less in quantity compared with entirety of road surface data. Thus, we specifically targeted three expressway earthwork sections that hold relatively many more FWD data records and accordingly rehabilitations many times. They are Hikone on heavily trafficked Meishin Expressway and Tsuruga and Toyama on Meishin's connecting Hokuriku Expressway, as above shown in Figure 6.

In evaluation of the bearing capacity of pavement at NEXCO, its originally developed bituminous layer's distress index (hereafter called "*D*i") has been utilized. After years-long FWD measurement and laboratory tests, it was concluded that the *D*i value, as defined in Figure 7, correlates to the indirect tensile strength of AC core samples taken from the FWD loading point (Kamiya_2, 2010, Kamiya et al., 2012). In reality, it has been confirmed in the field that lower *D*i values assure longer durability of pavement.

Figure 7 shows a feature of the prediction model, based on the Multi-Layer Perception, a user-friendly method. Fifteen explanatory factors we selected as we judged as important here include three surface indices of each 10-meter-basis crack ratio, rutting and IRI, thickness of base and sub-base layers, repair times and elapsed days from the latest rehabilitation date and others. Of 1,160 data sets of the three sections, 128 train data, 16 validation data and 16 test data were randomly selected respectively with almost 8:1:1 ratio, as shown in the left figure. On the right, *D*i value was used here for comparison between prediction and measured values. In spite of big differences in pavement performance between the three sections, *D*i's coefficient of determination was 0.616, which is seemingly a good result.

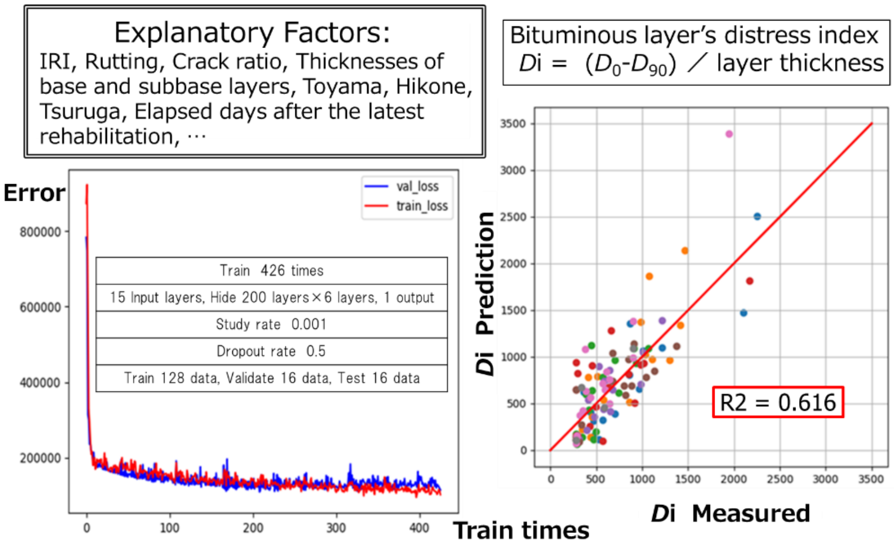

Figure 7 FWD prediction model based on the Multi-Layer Perception method.
(Kamiya_4, 2023)

4.2 Explanatory features

Figure 8 compares SHAP feature importance (DataCamp_1, 2023) as impact on model output magnitude, or our selected explanatory factor's magnitude to the objective *D*i value.

Of the whole fifteen explanatory factors, 10-meter-basis crack ratio is found to be the biggest importance in magnitude. This is practically acceptable. So are the second and third factors, which are respectively of the thickness of upper and lower layers. The reason of Toyama's fourth position is that larger *D*i values were more extendedly measured due to the section's thinner pavement thickness than the other two sections. The fifth ranked IRI and the sixth rutting are a surface movement either longitudinally or transversely. The seventh is elapsed days after the latest rehabilitation, followed by repair times as the eighth. The ninth 'Hikone' is probably the opposite reason of Toyama, as lesser *D*i values were more recorded due to the thicker pavement thickness. If the section names of 'Toyama, Hikone and Tsuruga' had been replaced with other quantitative values, the coefficient of determination might have been a bit higher than 0.616.

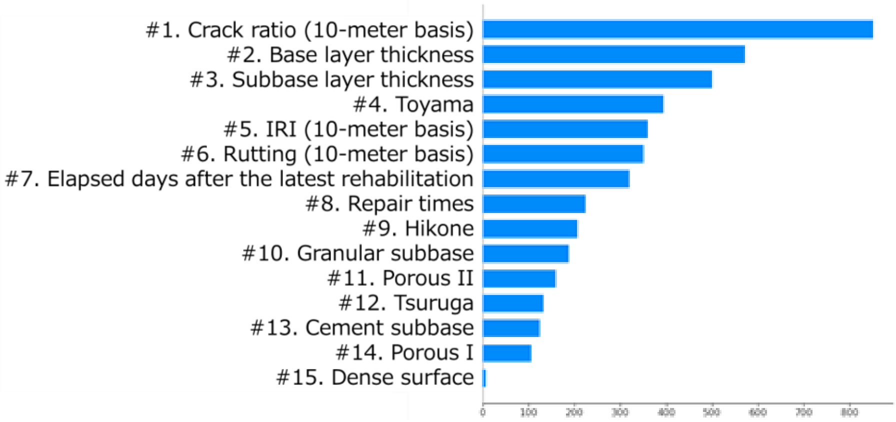

Figure 8 SHAP feature importance - Impact on model output magnitude.
(Kou, 2023)

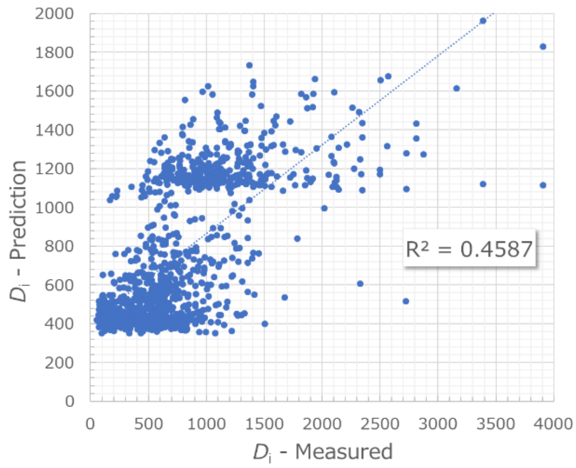

Figure 9 Conventional approach of multi-regression analysis.

For reference, Figure 9 is a result of the multi-regression analysis, so far having been used conventionally. Despite the same top six explanatory factors applied here, however, prediction Di values were obviously polarized at around 900 levels. This suggests that the regression analysis be made separately. As above mentioned, at least, a higher *D*i range group of Toyama with thinner AC thickness and the opposite group of Hikone having thicker AC are better to be separated. As one of the reasons, this is why coefficient of determination is just 0.4587, which is much lower than the above mentioned Machine Learning method.

5. CASE STUDY

As a representative of problematic sections, Figure 10 compares two projects with the heavy rehabilitations: surface and binder layers first repaired on 2005/5/1 or 2006/10/1, top three layers repaired in 2013, and then replaced again later with new three layers. Note that both earthwork sections have the same pavement structure and are located several kilometers apart. The earlier date of first rehabilitation gives longer days of durability. But why?

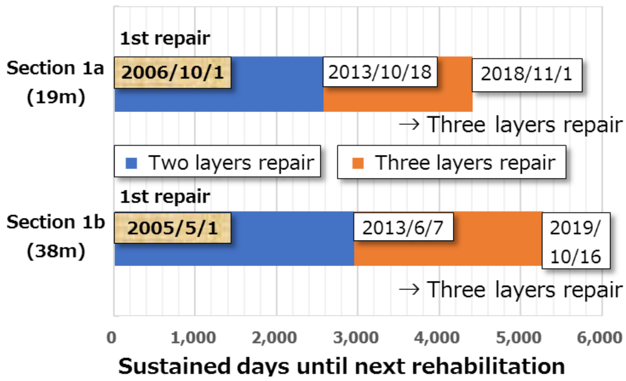

Figure 10 Comparison of two sections with a rehabilitation pattern (2 layers → 3 layers→ 3 layers).

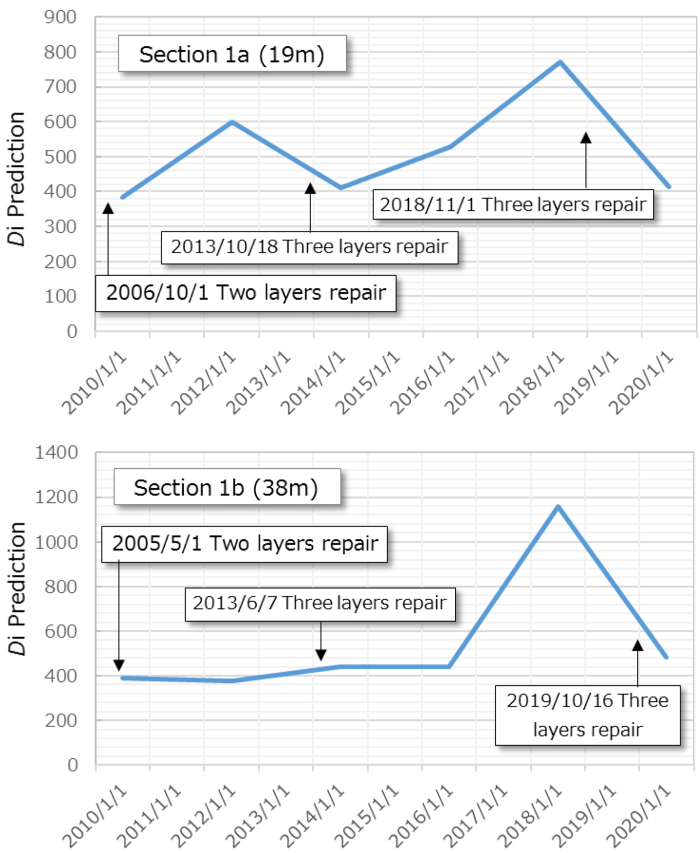

Figure 11 Comparison of progress of Di prediction values (Sections 1a and 1b).

(Kamiya_4, 2023)

To answer to the question, it is possible to see the relationship between the predicted *D*i values and the effect of rehabilitations in the past. Figure 11 plots predicted *D*i values in time series for every section, based on the 15 explanatory features. Note that as road surface data is inputted every two years, *D*i prediction values can be calculated for the same interval.

The predicted *D*i value in the upper section increased repeatedly after rehabilitation was made. Meanwhile the *D*i generally remained stable in the lower section until mid of 2016. This is the substantial reason of the lower section's longer durability. However, the value had since increased more dramatically until its rehabilitation on 2019/10/16. At the time of rehabilitation year of 2013, it is noted that the *D*i levels were considerably different between the two sections; the upper section's value was expected to reach 700 level, while the lower section's sustained 400 level.

This is significant because the lower section can be regarded as early rehabilitation in terms of *D*i level. As the Section 1b was rehabilitated earlier days, this effect was substantially reflected as longer durability. However, the lower section probably may not again win longer sustainably at the next rehabilitation; instead the upper section would be superior. Compare each *D*i value just before the third rehabilitation; the upper section may be around 900 level, whereas the lower section may exceed much higher up to over 1,200 level, meaning that the upper can be an earlier rehabilitation case next time (Kamiya_4, 2024).

In conclusion, the importance of keeping *D*i constantly in lower levels is a key to longer sustainability.

6. CONCLUSION

For the purpose of avoiding increase of rehabilitating three layers, effectiveness of early rehabilitation was examined by extracting repair history data from NEXCO-PMS.

To properly evaluate quality of a project and its ensuing pavement performance, all earthwork projects were categorized into groups that have the same rehabilitation history. Below are the findings of this study.

Between problematic sections with three layers rehabilitation twice on the Hokuriku Expressway, earlier dates of rehabilitation showed longer durability. As time goes by, bearing capacity of porous asphalt decreases very fast. This indicates the importance of developing an FWD prediction model that can assess structural strength of pavement.

Next, for the purpose of developing an FWD prediction model, a Machine Learning method based on the Muti-Layer Perception method was applied in this study. So that the model can be substantially used at a certain time and place, explanatory factors include road surface indices of 10-meter-basis crack ratio, rutting and IRI and other key elements. Using 1,160 data sets from three expressway sections having relatively many FWD measurements, a prediction model of bituminous layer's Distress index was successfully developed. As a result, the prototype's coefficient of determination 0.616 was confirmed between measured and predicted Di values.

When compared with the conventionally used multiple-regression analysis method by applying the same top six explanatory factors, the model's coefficient was found much higher than 0.4587 of the conventional approach.

In a case study for analyzing two problematic sections, effectiveness of earlier date of rehabilitation was also confirmed. By applying the *D*i prediction model in time-series for both sections, it was revealed that keeping the *D*i lower level will in effect lead to assuring longer durability of pavement.

Although the importance of keeping road defects at a lower level is revealed, specific criterion of road surface is yet to be developed. The extension of case studies is needed for further confirmation and towards development of road surface criterion for early rehabilitation.

Finally, the Transport Ministry of Japan published the Pavement Inspection Manual (MLIT_2, 2017) with the main focus being on protection of the base course of a pavement through preventative maintenance. This concept is not just applicable in Japan, but also all parts of the world. The author appreciate it if a bit of this paper's findings would be beneficial with other agencies or field practitioners.

7. REFERENCES

Kamiya, K. (2024). Effectiveness of Early Rehabilitation of Pavement Confirmed on a Japanese Expressway. The 10th International Conference on Maintenance and Rehabilitation of Pavements (MAIREPAV10)

Kamiya, K., Kazato, T. (2010). Study on How to Determine Repair Thickness of Damaged Layers for Porous Asphalt. The 11th International Conference on Asphalt Pavements, Volume I, pp.587-596 (ISAP Nagoya)

Kamiya, K., Kazato, T. (2012). A study on repair design method of porous asphalt for the Japanese motorwaysy. The 2nd International Conference on Transportation Geotchnics (IS-Hokkaido)

Kamiya, K. (2023). Validation of Effectiveness of Early Rehabilitation of Pavement Using NEXCO-PMS (in Japanese). The 7th Conference of Japan Association Asset Management

Kou, S. (2023). Selection of Repair Priorotization Based on Prediction of FWD Deflation and Road Surface Deterioration Levels (in Japanese). The 28th Conference of the Committee on Pavement Engineering

DataCamp. (2023). An introduction to Shap values and Machine Learning Interpretability. https://www.datacamp.com/tutorial/introduction-to-shap-values-machine-learning-interpretability

The Ministry of Land, Infrastructure, Transport and Tourism. (2024). Expressway Numbering Route Map. https://www.mlit.go.jp/road/sign/numbering/en/map/index.html

The Ministry of Land, Infrastructure, Transport and Tourism. (2017). Pavement Inspection Manual (in japanese). https://www.mlit.go.jp/road/sisaku/yobohozen/tenken/yobo3_1_10.pdf

Safety Impact for Average Speed Control in Taiwan

PIN-YI TSENG[1], YOU-ZONG SHI[2]

[1] Department of Traffic Science, Central Police University, Taoyuan, Taiwan, una139@mail.cpu.edu.tw
[2] Department of Traffic Science, Central Police University, Taoyuan, Taiwan, cyc51201@yahoo.com.tw

ABSTRACT

In recent years, several countries have installed average speed control (ASC) systems to improve road traffic safety through speed management. In Taiwan, 45 ASC systems have been installed since January 2022 in various locations, including urban roads (single-lane and multilane), urban and suburban tunnels (single-lane and multilane), suburban highways (single-lane and multilane), and intercity expressways (multilane), with speed limits ranging between 30 and 90 km/h. In this study, despite the highly complex and diverse road environments and speed limits of these ASC systems, we ensured a meticulous data collection process. This process involved collecting individual vehicle speed data from 15 ASC systems in the month before these systems were activated and in the four quarters after they were activated. The process also involved compiling full-year accident data in the year before and after the systems were activated. Speed measures included the average speed of traffic flow and its standard deviation, the 85th percentile speed, and the average free-flow speed and its standard deviation. Accident measures included the number of accidents and accident severity indicators. The results indicated that approximately 70% of the ASC systems reduced various speed measures of traffic flow, whereas 88% of the ASC systems effectively controlled the average speed below the speed limit, thereby indicating their major effect on road safety. In terms of accident prevention, the number of accidents decreased in 11 locations. In addition, the number of accidents and casualties exhibited a downward trend in 13 locations 1 year after the systems were activated. Despite the diversity and randomness of the accidents, accident prevention was not entirely achieved in all locations where the ASC systems were installed. Nevertheless, the majority of the ASC systems reduced vehicle speed and improved road safety, particularly in tunnels.

Keywords: Average speed control, Sectional speed control, Technology enforcement, Road type, Accident characteristics.

1. INTRODUCTION

From a theoretical and practical viewpoint, traffic speed management on highways is essential for controlling the incidence and severity of accidents. To achieve this goal, many countries tend to prioritize highway speed management strategies, such as setting speed limits and enforcing speeding regulations. Among the traditional methods of speeding regulation enforcement are police-operated radar or laser guns for fixed-point enforcement of vehicle speeds. In 1997, the Netherlands started using average speed control (ASC) systems (Soole *at al*., 2013).

In April 2018, Taiwan installed its first ASC system for traffic law enforcement in Wanli Tunnel on Highway No. 2 in New Taipei City. Automated vehicle identification cameras were installed at the beginning and end of a specific road section. The system records the entry and exit times of each vehicle passing through this road section and automatically calculates the difference between these times to determine the vehicle's speed. Vehicles exceeding the speed limit receive a fine. The system differs from traditional fixed-point or moving-point speed control systems. ASC systems enhance the speed control of passing vehicles on a road section by extending the speed control range from points to lines while mitigating the difference between vehicle speeds. This approach facilitates uniform and stable traffic flow. ASC systems are effective in reducing average speeds, standard deviations of speed, and vehicle speeding ratios. ASC systems also have a positive effect on the number of accidents and casualties. Therefore, several ASC systems have been installed across Taiwan, particularly in locations such as tunnels (urban or suburban), urban roads (two-lane or multilane), suburban highways (two-lane or multilane), and intercity expressways (Tseng & Tsai, 2021). As of 2023, Taiwan had 45 ASC systems, among which, 10 were in tunnels, 4 were on urban roads, 22 were on suburban highways, and 9 were on intercity expressways. In this study, we examined the effectiveness of these systems in terms of speed and safety.

2. LITERATURE REVIEW

Vehicle speed affects traffic safety, with higher speeds exhibiting a greater effect on the incidence and severity of road traffic accidents. Many studies indicate that speeding is a critical factor associated with traffic safety hazards. Higher speeds are typically associated with a longer vehicle stopping distance and a higher risk of accidents. Higher speeds are also associated with higher kinetic energy generated by collision, which increases the probability of casualties (Howard *et al*., 2008). Differences in vehicle speeds in traffic flow affect road safety. According to Mohammed (2013), variations in vehicle speed positively correlate with the rate of accidents. If the variation in vehicle speed increases by 1%, the rate of accidents increases by 0.3% (Figure 1).

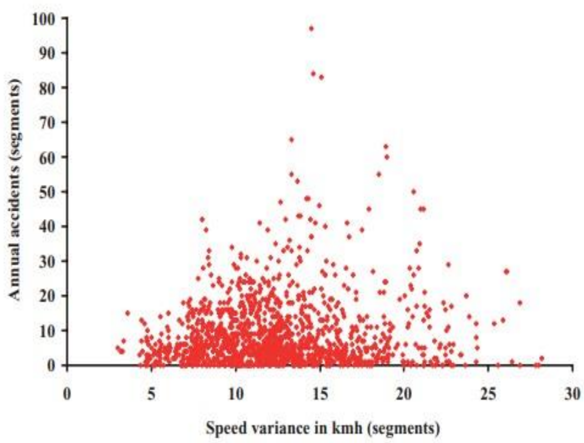

Figure 1. Relationship between vehicle speed variation and accident rate.

(Mohammed, 2013)

Speeding directly influences not only the incidence but also the severity of accidents. According to Nilsson (2004), changes in average speed positively correlate with the probability of death, injury, or severe injury in an accident (Figure 2), indicating that higher speeds are associated with greater accident severity. When the average speed increases by 10%, the probability of death, injury, or severe injury increases by 20% to 40% (Figure 2).

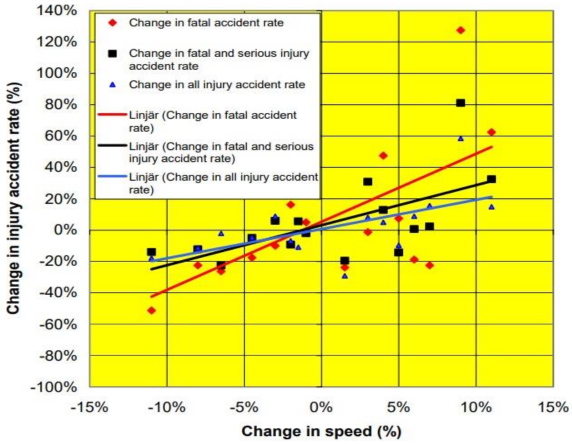

Figure 2. Relationship between average speed change and accident severity.

(Nilsson, 2004)

In ASC systems, cameras are installed at the beginning and end of a road section to identify license plates. When a vehicle passes through this road section, the system records the entry and exit times of the vehicle and calculates the vehicle's speed by dividing distance by time. Figure 3 illustrates the operation principle of an ASC system. ASC systems control the average speeds of vehicles on the road, force drivers to comply with speed regulations, and mitigate the burden placed on traffic law enforcement. In addition, their rate of reporting traffic violations is close to 100% (Aarts *et al*., 2009; Montella *et al*., 2011).

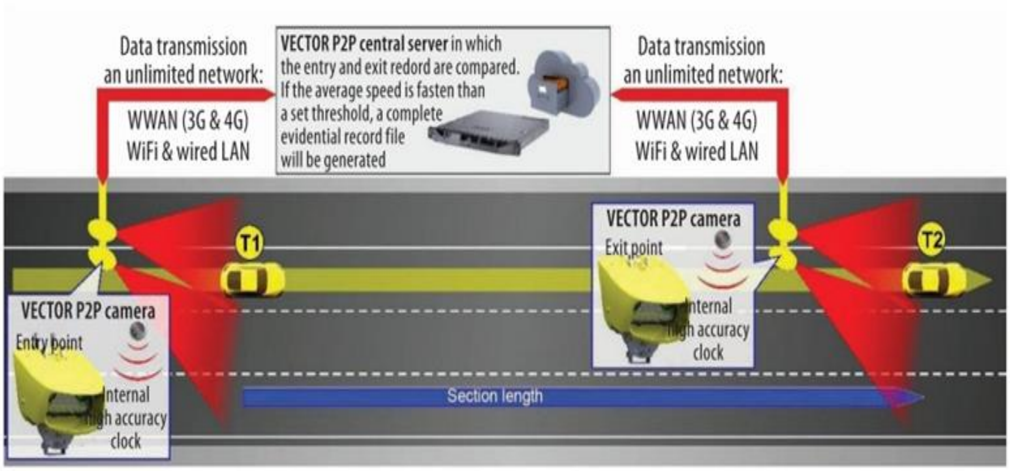

Figure 3. ASC system operating principles.

(Gaveniene *et al.*, 2020)

In 1997, the Netherlands installed the world's first ASC system (Soole *et al.*, 2013). After this system was installed, vehicle speeds, accident rates, and travel times decreased, increasing traffic safety. Despite being more expensive than other speed control measures, this ASC system proved more cost-effective in scenarios involving large road sections. Therefore, countries such as Norway, the United Kingdom, Finland, Lithuania, Switzerland, and Italy decided to install their own ASC systems.

In Italy, after an ASC system was installed on the A56 urban expressway, the speed difference between vehicles and the speeding behavior of drivers decreased (Alfonso *et al*., 2015). The standard deviation of vehicle speed also decreased by 26%, and a 20% reduction in speeding patterns was observed. In addition, the percentages of speeding small and heavy vehicles decreased by 84% and 77%, respectively, and the frequency of traffic accidents decreased by 32%. Mattia et al. (2019) argued that increasing the coverage of sectional speed enforcement effectively increases road safety. In Italy, increasing the coverage of sectional average speed enforcement by 30% reduced the frequency of accidents by an average of 3%.

Montella et al. (2012) reported that after an ASC system was installed on the A1 Milan–Naples highway in Italy in 2007, the number of accidents and casualties decreased by 31.2% to 55.6%. ASC systems considerably influence the curve rate caused accidents. Vanlommel *et al.* (2015) examined the effect of an ASC system installed in a road section on the Belgian E40 highway on the driving speed of vehicles. They reported that the system reduced the average speed of vehicles by 15 km/h, making the flow of traffic more uniform. Gaveniene *et al.* (2020) compared the speed data of 25 road sections over a period of 16 months in Lithuania. They reported that after an ASC system was installed, the number of accidents decreased by 16.67%. In addition, the number of vehicles exceeding the speed limit by 20 km/h decreased from 20.84% to 9.91%, representing a reduction of 10.93%. Similarly, the number of vehicles exceeding the speed limit by more than 20 km/h decreased from 2.10% to 0.20%, representing a reduction of 1.9%. Taken together, these findings confirm the efficacy of ASC systems in controlling vehicle speeds.

Liu *et al.* (2019) examined the effects of an ASC system installed in Wanli Tunnel in New Taipei City, Taiwan. They reported that the system effectively reduced the speeds of vehicles while stabilizing the differences in speed in traffic flow. Specifically, the average speed of traffic flow decreased from 57.89 to 46.57 km/h, and the difference in speed decreased from 11.92 to 5.74 km/h (Figure 4). Before the system was activated, the maximum traffic flow in the tunnel was approximately 1,800 pcu/h. However, after the system was activated, the maximum traffic flow in the tunnel reached approximately 2,100 pcu/h, indicating an increase of 17%. In addition, after the system was activated, the number of speeding tickets considerably decreased from nearly 1,800 in July 2018 to nearly 600 in February 2019. The percentage of violations also substantially decreased from 10.56% to 0.56%, and the number of traffic accidents decreased from 7 to 1.

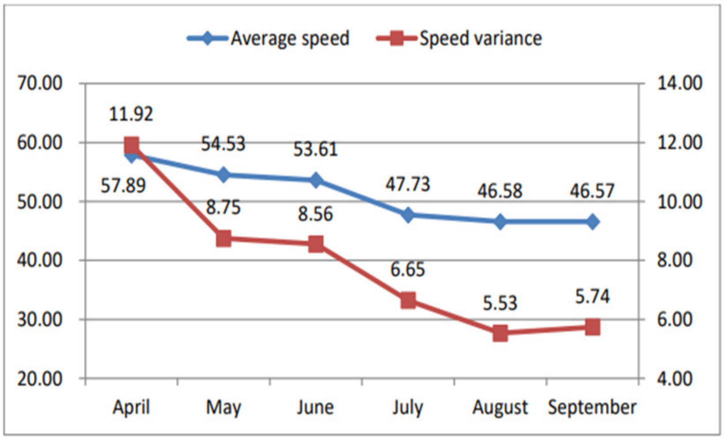

Figure 4. Change in vehicle speeds after installation of ASC system in Wanli Tunnel.

(Liu *et al.*, 2019)

Hu *et al*. (2020) explored the same ASC system in Wanli Tunnel. They examined the effects of the system on vehicle speeds and speeding conditions in the east–west direction of the tunnel. Their results indicated that, after 6 months of its installation, the system considerably reduced the average speed, standard deviation of speed, and 85th percentile speed of all vehicles (Table 2). Specifically, the average speed decreased by 9.2% and 25.6%, the standard deviation of speed decreased by 41.7% and 36.7%, and the 85th percentile speed decreased by 28.2% and 22.7%. In addition, the probability of speeding decreased by more than 90%.

Overall, reviewing the aforementioned literature revealed the following:

1. Many countries consider speed management to be an essential strategy for preventing road traffic accidents. In Taiwan, speed management is included as a countermeasure in the Road Traffic Order and Traffic Safety Improvement Plan enacted by the government. According to experience and academic theories, the main purpose of speed management is to ensure road safety and efficiency, indicating the importance of speed management as a countermeasure for preventing road traffic accidents.
2. Many countries have invested major resources to determine how to control the driving speeds of vehicles on the road. ASC systems are an effective approach for reducing vehicle speeds and road accidents and mitigating accident severity. Many countries have gradually implemented these systems to control traffic flow.
3. In both Taiwan and other countries, various performance indicators have been identified, and multiple comparisons before and after system implementation have been conducted to determine the effectiveness of ASC systems. These performance indicators include average speed, speed variation or standard deviation, 85th percentile speed, speeding proportion, and number of accidents or severe accidents. A literature review indicates that almost all studies employ the change in average rate before and after an ASC system is activated as their main evaluation index.

3. DATA COLLECTION AND CLEANING

In this study, data were collected from two primary sources. The first source of data was vehicle speeds recorded at controlled road sections, as identified by the ASC system of each police unit. These data were collected before the system was activated and in the first, second, third, and fourth quarters, represented by Q1, Q2, Q3, and Q4, respectively, after its activation. The second source of data was fatal accidents during the year before and after the ASC system was activated. A total of 15 sets of speed data were obtained (Table 1), with fatal accident data obtained from the accident database of the Police Department, Ministry of the Interior.

Table 1. ASC systems examined in this study.

No.	location of the ASC system	classification	activation date	speed limit (kph)	number of one-way lanes
A1	Guanyin Shan Tunnel, New Taipei City	tunnel	2022.5.1.	80	2
A2	Caopu Senyong Tunnel, Pingtung County	tunnel	2022.3.1.	70	2
B1	Huanhe Road, New Taipei City	urban road	2022.1.24.	60	3
B2	Xiwan Road, New Taipei City	urban road	2022.5.1.	40	1
B3	Shang Xiang Road, Taichung City	urban road	2022.2.16.	50	4
B4	Songyi Road, Kaohsiung City	urban road	2022.2.25.	50	2
C1	Provincial Highway No.7B, Taoyuan City	suburban highway	2022.2.28.	40	1
C2	County Highway 182, Tainan City	suburban highway	2022.1.28.	50	2
C3	Provincial Highway No.3, Kaohsiung City	suburban highway	2022.2.25.	60	2
C4	Provincial Highway No.21, Nantou County	suburban highway	2022.4.25.	60	2
C5	Provincial Highway No.9E, Taitung County	suburban highway	2022.1.29.	40	2
D1	Provincial Highway No.61, Taoyuan City	expressway	2022.2.24.	90	2
D2	Provincial Highway No.61, Changhua County	expressway	2022.3.1.	90	2
D3	Provincial Highway No.62, Keelung City	expressway	2022.4.1.	80	2
D4	Provincial Highway No.62A, Keelung City	expressway	2022.4.1.	40	2

3.1 Collection and cleaning of speed data

Daily individual vehicle speed data were obtained from 15 ASC systems over a period of 13 months, starting from 1 month before system activation until 12 months after system activation. Certain difficulties or limitations were observed during the process of data collection:

1. The management unit refused to provide information to protect personal data.
2. The data provided by the property management unit differed from those available on all vehicles, with the exception of speeding vehicles. Therefore, these data were discarded.
3. Some systems were suspended for specific reasons, resulting in a lack of data.
4. A high discrepancy was observed in the number of daily data samples. Therefore, these data were discarded.

Various performance measures, including average vehicle speed and standard deviation over a day, average free-flow speed (FFS) and standard deviation, and 85th percentile speed, were used to evaluate the effectiveness of individual ASC systems. In terms of the speed data of free-traveling vehicles, we conservatively selected vehicles whose headway from the previous vehicle exceeded 10 seconds while passing through the starting point of the speed-controlled road section as our sample.

Speed data were analyzed as follows:

1. To enable an objective comparison and analysis, complete 24-hour weekday data were uniformly selected for analysis.
2. During the speed data cleaning process, average values ± three standard deviations were used to detect outliers and mitigate the effect of extreme values on average speed.
3. The speed data recorded during the month before the ASC system was activated and in the first to fourth quarters after its activation were selected as performance indicators for comparison.

3.2 Collection of accident data

Traffic accident data were collected from the records of the Police Department, Ministry of the Interior, on each road section where an ASC system was installed for 1 year before and after its activation. These data included the number of accidents, the number of casualties on the scene and within 24 hours of the accident, and the number of individuals injured in the accident.

After the accident data were examined, data on the equivalent number of accidents were obtained from the Institute of Transportation, Ministry of Transportation and Communications (1993), to determine the differences in the number of accidents before and after each ASC system was activated:

$$\mathrm{ETAN} = (9.5 \times F) + (3.5 \times J) + \mathrm{TAN} \quad (1)$$

where ETAN is the equivalent number of accidents, *F* is the number of casualties in the accident, *J* is the number of individuals injured in the accident, and *TAN* is the total number of accidents.

4. RESULTS

In this section, we discuss the effects of various ASC systems on the speeds of vehicles (Section 4.1) and the frequency of accidents (Section 4.2) in Taiwan and provide a comprehensive evaluation of these effects (Section 4.3).

4.1 Impact on vehicle speed

For the sake of brevity, only one system with four patterns (Table 1) for tunnels (Type A), urban roads (Type B), suburban highways (Type C), and expressways (Type D) was selected in this study to determine its effect on vehicle speed (Table 2).

Comparison of the effects of various ASC systems on vehicle speed in each quarter (Q1 to Q4) before and after system activation revealed that most of the systems reduced the average speed or speed difference in general or free traffic flow. After 1 year of their activation, these ASC systems controlled the average speed of traffic flow within the speed limit. Varying speed reductions were achieved depending on the location and traffic conditions. In case the 85th percentile speed exceeded the speed limit, data were submitted to the relevant authorities to review the speed limit. Overall, the majority of the ASC systems reduced the number of speeding vehicles. In summary, the ASC systems effectively reduced the driving speed and speed difference of vehicles, thereby increasing the uniformity of traffic flow.

Table 2. Examples of effects of various ASC systems on vehicle speed.

A2：Caopu Senyong Tunnel, Pingtung County (S.L. = 80 kph)					
measure of effectiveness	**before**	**Q1**	**Q2**	**Q3**	**Q4**
average speed (kph)	65.1	64.5	63.5	65.2	64.6
standard deviation (kph)	4.3	4.5	5.1	4.3	4.7
average FFS (kph)	65.6	64.9	64.0	65.4	65.1
the standard deviation of FFS (kph)	4.7	4.7	5.1	4.5	4.9
85th percentile speed (kph)	69	69	68	69	69
speeding vehicle ratio (%)	9.8	8.4	6.4	9.9	9.9
B4：Songyi Road, Kaohsiung City (S.L. = 50 kph)					
measure of effectiveness	**before**	**Q1**	**Q2**	**Q3**	**Q4**
average speed (kph)	41.5	41.0	40.8	41.4	42.3
standard deviation (kph)	4.6	4.3	4.5	4.5	4.9
average FFS (kph)	41.8	41.4	41.1	42.2	43.2
the standard deviation of FFS (kph)	5.0	4.8	4.8	5.0	5.5
85th percentile speed (kph)	46	45	45	46	47
speeding vehicle ratio (%)	3.9	2.5	2.5	3.5	5.8
C3：Provincial Highway No.3, Kaohsiung City (S.L. = 60 kph)					
measure of effectiveness	**before**	**Q1**	**Q2**	**Q3**	**Q4**
average speed (kph)	58.9	58.4	56.0	59.6	55.7
standard deviation (kph)	7.3	7.4	6.7	7.1	6.9
average FFS (kph)	58.8	58.6	55.9	59.6	55.6
the standard deviation of FFS (kph)	7.6	7.3	6.7	8.5	7.2
85th percentile speed (kph)	66	65	62	68	62
speeding vehicle ratio (%)	7.3	7.4	6.7	7.1	6.8
D3：Provincial Highway No.62, Keelung City (S.L. = 80 kph)					
measure of effectiveness	**before**	**Q1**	**Q2**	**Q3**	**Q4**
average speed (kph)	80.7	75.1	75.6	73.6	75.5
standard deviation (kph)	7.9	5.5	5.7	6.7	5.6
average FFS (kph)	82.2	76.3	76.9	74.8	76.4
the standard deviation of FFS (kph)	8.6	5.8	5.7	6.2	5.8
85th percentile speed (kph)	88	80	81	80	81
speeding vehicle ratio (%)	49.6	14.5	17.5	11.5	16.8

4.2 Effect on accidents

Police data were analyzed to determine the number of accidents and identify severity indicators 1 year before and after the activation of each ASC system (Table 3). If the value of ETAN after system activation was lower than that before activation, a positive ETAN difference was obtained, indicating improved road safety.

Table 3 lists the locations of 15 ASC systems installed in Taiwan. At three locations, the number of accidents in the year before system activation was less than or equal to five. The ASC systems installed at these three locations were presumably not installed to prevent traffic accidents. We discarded the data obtained from these three locations (B2, C5, and D4). Among the remaining 12 locations, 9 experienced fewer accidents after the ACS systems had been installed (Table 3), and 3 (A2, C4, and D3) experienced more accidents after the ASC systems had been installed. Among the three locations that experienced more accidents, two experienced a decrease in accident severity (A2 and C4). In summary, the majority of the ASC systems effectively reduced the number of accidents and mitigated their severity (Table 3). Taken together, these findings underscore the importance of installing ASC systems.

Table 3. Effectiveness of various ASC systems in preventing accidents.

Sites	Number of accidents and ETAN in the year								
	Before (number)			After (ETAN and number)				Comparison (ETAN)	
	all accidents	fatal accidents	injury accidents	(1) ETAN	all accidents	fatal accidents	injury accidents	(2) ETAN	(3) = (1) – (2)
A1	36	0	5	53.5	14	0	5	31.5	22.0
A2	18	0	9	49.5	23	0	4	37.0	12.5
B1	22	0	9	53.5	15	0	1	18.5	35.0
B2*	5	0	5	22.5	1	0	1	4.5	18.0
B3	63	1	49	244.0	58	0	37	187.5	56.5
B4	36	1	30	150.5	15	0	12	57.0	93.5
C1	142	0	93	467.5	92	2	93	436.5	31.0
C2	49	2	56	264.0	45	3	50	248.5	15.5
C3	21	0	24	105.0	5	0	6	26.0	79.0
C4	19	1	9	60.0	23	0	10	58.0	2.0
C5*	3	0	4	17.0	4	0	4	18.0	-1.0*
D1	29	0	20	99.0	10	1	5	37.0	62.0
D2	42	1	14	100.5	40	1	7	74.0	26.5
D3	24	0	2	31.0	27	0	5	44.5	-13.5
D4*	2	0	1	5.5	1	0	2	8.0	-2.5*

4.3 Comprehensive analysis

Given the effectiveness of ASC systems in controlling vehicle speed, we expected the speeds of vehicles to decrease and the degree of road safety to increase after ASC systems had been installed. We collected and analyzed vehicle speed data and accident data and converted these data into equivalent values. Figure 5 depicts the effects of various ASC systems on different road categories.

Figure 5 depicts the effects of each ASC system on vehicle speed and road safety through an importance-and-performance comparison in management instead of an average speed index or an accident data index. The *x*-axis in the figure illustrates the effect on average speed after the ASC system was activated, with positive values indicating that the ASC system reduced vehicle speed, and vice versa. The *y*-axis in the figure illustrates the effect of accident severity after the ASC system was activated, with positive values indicating that the ASC system mitigated accident severity, and vice versa. Figure 5 shows the effects of various ASC systems on vehicle speed and accident severity in four road patterns (Types A1 to D4).

In Figure 5, the first quadrant illustrates a decrease in average speed and accident severity after ASC systems had been installed, representing the optimal scenario for the ASC system. The second quadrant illustrates an increase in average speed but a decrease in accident severity after the ASC systems had been installed. The third quadrant illustrates an increase in average speed and accident severity after the ASC systems had been installed. The fourth quadrant illustrates a decrease in average speed but an increase in accident severity after the ASC systems had been installed.

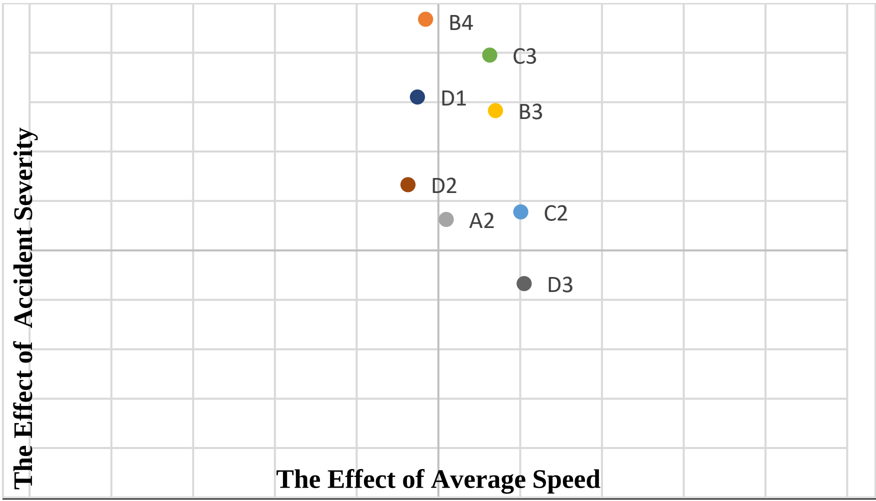

Figure 5. Effectiveness of ASC systems in Taiwan.

Figure 5 depicts the results of each ASC system. These results can be summarized as follows:

1. The majority of the ASC systems fell within the first quadrant, indicating that significant reductions in average speed and accident severity were achieved in most of the locations after the ASC system was activated.
2. Although three ASC systems fell within the second quadrant, a slight increase in average speed was observed, with an amplitude of approximately 2 km/h. Nevertheless, a significant reduction was observed in the severity of accidents.
3. None of the ASC systems fell within the third quadrant.
4. Only one ASC system (D3) fell within the fourth quadrant. Despite the significant effect on vehicle speed, an increase was observed in the severity of accidents. After further analysis, D3 was installed on Expressway No. 62 in Keelung City. This expressway has several curved sections and is characterized by high traffic volumes, high proportions of large vehicles, and rainy weather, suggesting that vehicle speed may not be the leading cause of accidents on this expressway. Taken together, these findings suggest that strategies other than ASC systems may be more effective in preventing accidents.

5.CONCLUSIONS

In this study, actual vehicle speed data were used to determine the effectiveness of ASC systems in reducing vehicle speed and accident severity on various highways or road types in Taiwan. Our findings can be used as a reference in the transportation field:

1. Most of the ASC systems installed in Taiwan reduce vehicle speed and increase road safety. In terms of vehicle speed, 93% of the systems effectively reduced the average traffic speed to less than the speed limit, 67% of the systems reduced the average speed, and 60% of the systems reduced the standard deviation of vehicle speed. In terms of safety, 67% of the systems reduced the number of accidents, and 91% of the systems mitigated the severity of accidents.

2. Given the diversity and randomness of accidents, not all accidents can be prevented through speed management in all locations. Both driver-related factors (e.g., fatigue and driving under the influence) and vehicle-related factors (e.g., tire tread wear, low road visibility, and insufficient turning radius) play a role in the occurrence of accidents. In this study, although the ASC systems reduced the number of traffic accidents in the majority of road sections, the number of accidents increased in three sections. These findings indicate that ASC systems may not be effective in all road sections.
3. After the ASC systems were activated, their effectiveness in reducing vehicle speed gradually decreased over time. According to our analysis, the greatest reduction in average vehicle speed was observed in the first quarter after an ASC system was activated. However, the average speed of 11 out of 16 systems was higher in the third or fourth quarter than in the first quarter. As indicated by the systems' pre-activation values, the effectiveness of the ASC systems presumably decreased over time after their activation.
4. Overall, we recommend extending the adaptation period and conducting a professional and objective evaluation before an ASC system is installed. In this study, challenges were experienced during data collection. Challenges included insufficient data collection instances, a small number of vehicles monitored, and other unstable conditions that hindered comparisons before and after system activation. Consequently, determining whether to implement ASC systems in the future is recommended. When a speed control system is installed, a comprehensive assessment of road geometric conditions, traffic characteristics, road types, and accident causes should be conducted. In addition, an objective and professional evaluation should be conducted to determine whether the target area is suitable for installing an ASC system.
5. In general, we recommend monitoring the effectiveness of ASC systems on a regular basis. According to our findings, certain systems achieve significant effects during the first 3 months of use. However, after 6 months, their effectiveness in reducing average vehicle speed or its standard deviation decreases, even below the values observed before their activation. To the best of our knowledge, no inspection mechanism has yet been established for the currently available systems. This lack of data suggests that certain systems are presumably still used although they are no longer effective. Hence, relevant units should establish performance indicators (average rate, standard deviation, etc.) and regularly monitor the effectiveness of ASC systems to ensure that these performance indicators meet their expected requirements.

6. ACKNOWLEDGMENTS

This study was partly funded by the National Science Council (project no. NSTC 112-2410-H-015-008), Executive Yuan, Taiwan. This manuscript was edited by Wallace Academic Editing.

7. REFERENCES

Aarts, L., van Nes, N., Wegman, F., Van Schagen, I., & Louwerse, R. (2009). "Safe Speeds and Credible Speed Limits： A New Vision for Decision Making on Speed Management," Transportation Research Board, pp.11–15.

Alfonso, M., Vincenzo, P., Salvatore, C., Filomena, M., & Marcello, M. (2015). "Point-to-Point Speed Enforcement Systems: Speed Limits Design Criteria and Analysis of Drivers' Compliance," Transportation Research Part C, Vol. 53, pp.1-8.

Gaveniene, L., Jateikiene, L., Cygas, D., & Kasperaviciene, A. (2020). "Impact of Average Speed Enforcement Systems on Traffic Safety Evidence from the Roads of Lithuania." The Baltic Journal of Road and Bridge Engineering, 15(3), pp1-18.

Howard, E., Mooren, L., Nilsson, G., Quimby, A. & Vadeby, A. (2008). "Speed Management: A Road Safety Manual for Decision-Makers and Practitioners," In Global Road Safety Partnership (Eds), Road Traffic Crashes and Injury Involving Speed, Geneva: Switzerland, pp.1–20.

Hu, S. R., Li, W. C. & Chang, C. W. (2020). "The impact of interval average speed enforcement on intercity highway driving speeds," Proceedings of Conference of Chinese Transportation Institute, Vol.5, pp.1–16.

Liu, C. P., Shieh, M. H., Hung, Y. Z., Li, H. C. & Wu, K. L. (2019). "Analysis on the Effectiveness of Implementing Sectional Speed Enforcement," Proceedings of Conference of Chinese Transportation Institute, Vol.4, pp.237-246.

Mohammed, Q. (2013). "Exploring the Relationship Between Average Speed, Speed Variation, and Accident Rates Using Spatial Statistical Models and GIS." Journal of Transportation Safety & Security, 5(1), pp.27–45.

Montella, A., Punzo, V., & Montanino, M. (2011). "Design and evaluation of speed limits for an automated section speed control system. In： 90th" Annual Meeting of the Transportation Research Board, pp.1–17.

Montella, A., Persaud, B., DApuzzo, M., & Imbriani, L. L. (2012). "Safety evaluation of an automated section speed enforcement system." Transportation Research, 2281, pp.16-25.

Nilsson, G. (2004). "Traffic Safety Dimensions and the Power Model to Describe the Effect of Speed on Safety." Department of Technology and Society, Lund Institute of Technology, Lund, Sweden, pp.69–85.

Soole, D. W., Watson, B. C. & Fleiter, J. J. (2013). "Effects of Average Speed Enforcement on Seed Compliance and Cashes: A Review of the Literature," Accident Analysis & Prevention, Vol.54, pp.46-56.

Tseng, P. Y. & Tsai, C. W. (2021). "A Study on Planning Procedure of Sectional Speed Enforcement for Pei-Yi Highway," Journal of Chinese Transportation Institute, Vol. 33, No. 4. pp, 447-474.

Vanlommel, M., Houbraken, M., Audenaert, P., Logghe, S., Pickavet, M., & Maeyer, D. P. (2015). "An Evaluation of Section Control Based on Floating Car Data," Transportation Research, part C, 58, pp.617–627.

Institute of Transportation of MOTC (1993)， Sustainable Transportation Information System - Traffic Accident Data Analysis and Research.

Study on countermeasure for traffic congestion on expressways by utilizing the Directional Loudspeaker

Taichi Kumagai[1*], Dai Tamagawa[2], Keisuke Ota[3]

[1] Planning Department / Hanshin Expressway Company Limited, Japan, E-mail/ taichi-kumagai@hanshin-exp.co.jp

[2] Planning Department / Hanshin Expressway Company Limited, Japan, E-mail/ Dai-Tamagawa@hansin-exp.co.jp

[3] Engineering Department / Hanshin Expressway R&D Company Limited, Japan, E-mail/ keisuke-ota@hanshin-tech.co.jp

ABSTRACT

Hanshin Expressway is an urban expressway located in the Osaka metropolitan area in Japan, and one of the significant issues is traffic congestion caused by heavy traffic. In study, an experiment of such voice guidance using the Directional Loudspeaker was also carried out on the Hanshin Expressway at a congestion point to verify its effectiveness.

The experiment was carried out on a section of road with an 8% uphill gradient, where the longitudinal gradient also changes dramatically. This section also has merging and branching points and is more complicated than other sections where the same countermeasures have already been implemented in Japan.

The results show that there was a slight improvement in traffic speed, traffic volume, and traffic capacity during congestion hours. As for the behavior of individual vehicles, the vehicle headway time was also slightly reduced. However, the effect to reduce traffic congestion was not significant. These results suggest that the effectiveness of this countermeasure depends on the road structure conditions and not so effective for the section with complex road structure, such as the sections which have merging and branching points. Therefore, appropriate locations for voice guidance using the Directional Loudspeaker should be selected when implementing as a traffic congestion countermeasure.

Keywords: Sag, the Directional Loudspeakers, Traffic congestion measures, Traffic management

1. Introduction

The Hanshin Expressway is an urban expressway located in the Osaka metropolitan area in Japan, and traffic congestion due to traffic concentration is chronic at various areas. To realize the safe, secure, and comfortable service that Hanshin Expressway has always aimed to provide, immediate countermeasures are desirable. Several countermeasures against traffic congestion have been implemented. For example, the Moving Light Guide System has been installed on the road at uphill gradient and uphill sections where traffic congestion due to reduced driving speed is a concern. The system visually prevents speed reduction, and has been confirmed to be effective in alleviating traffic congestion to a certain extent. In addition to visual countermeasures against traffic congestion that have been implemented in Japan as described above, in recent years, an auditory countermeasure against traffic congestion using voice guidance with directional loudspeakers has been implemented as a new method to deal with traffic congestion. Directional loudspeakers have the capability of reaching greater distances and a smaller sound spread than conventional speakers, so they can deliver voice guidance to drivers. Countermeasures against traffic congestion using directional loudspeakers have been implemented on various basic road sections on expressways, and have proven to be effective to a certain extent in alleviating traffic congestion. This paper describes an experiment that was conducted to verify the effectiveness of a new countermeasure against traffic congestion using voice guidance with directional loudspeakers at a section of the Hanshin Expressway with a complex road structure (Sambo JCT) where chronic traffic congestion is occurring.

2. Information on the section where the experiment was conducted (Sambo JCT)

2.1 Traffic conditions of the relevant section

This section was put into service in 2017. The road width of the travel lane is approximately 2.5 m, and the passing lane is approximately 0.6 m. The mixing rate of large vehicles is 40%, which is relatively high. The mixing rate of large vehicles is high at approximately 40%, making it a relatively busy section for large vehicles. Although traffic volume was low when it was first opened, traffic congestion became chronic with the opening of connecting lines. Traffic congestion usually occurs on weekdays, with the most congestion occurring between 7:00 and 9:00 a.m. The road structure is characterized by varying longitudinal gradients, as well as the presence of branch and confluence roads in the vicinity, which makes the road structure extremely complex. Specifically, as shown in Fig. 1, there is a 6% downhill section between the branch to the exit and the confluence from the entrance, and an 8% uphill gradient section between the confluence from the entrance and the branch, making the section prone to speed reduction (Fig.2). In addition, this section is a two-lane road with continuous merging from the entrance and branching off to other lines both northbound (toward the city center) and southbound (toward the suburbs).

Furthermore, since June 2022, large-scale construction work involving long-term road closures has started on other lines, and this section has been affected by increased demand for detouring traffic due to the road closures, resulting in frequent traffic congestion due to traffic concentration. Traffic demand, including from large vehicles, increases especially in the morning hours, resulting in frequent speed reductions starting from the uphill section after the confluence from the entrance. Also, the lane share ratio is extremely high in the first lane, with the first lane heading toward the city center and the second lane heading toward the suburbs.

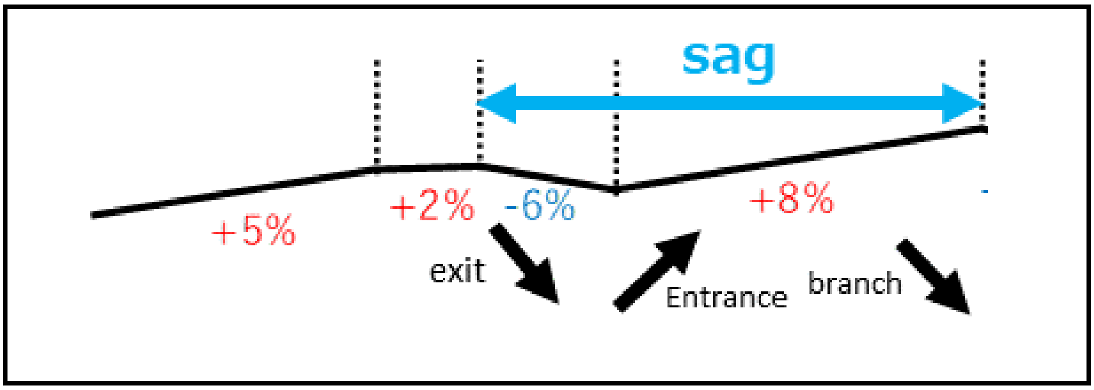

Figure 1 longitudinal gradient (congestion point)

2.2 Current countermeasures and issues in the relevant section

A number of traffic signs and signboards have already been installed in the relevant section in response to the fact that the road structure in the relevant section is prone to traffic concentration congestion due to reduced speed as mentioned earlier. However, the installation of additional signs providing visual information may cause confusion for drivers and is considered difficult to implement.

Therefore, we examined countermeasures against traffic congestion that can provide pinpoint guidance without providing visual information. As a result, we decided to implement a countermeasure against traffic congestion that uses directional loudspeakers, which have been used by other expressway companies, to broadcast information that encourages drivers not to slow down.

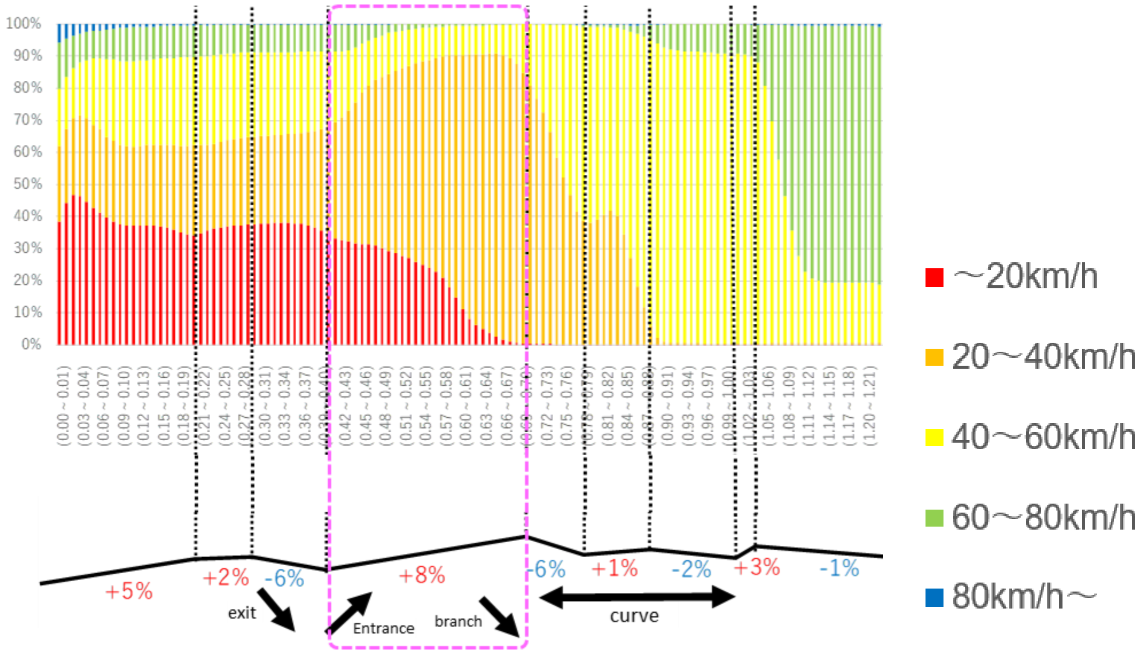

Figure 2 speed configuration

3. Purpose and method

This chapter describes the purpose and expected effects of an experiment of the aforementioned countermeasure against traffic congestion using directional loudspeakers, as well as the details and results of the experiment.

3.1 Purpose and expected effects

The purpose of this experiment is to test the countermeasure against traffic congestion using directional loudspeakers to encourage drivers not to slow down, verify the effectiveness of the countermeasure, and help facilitate the implementation of the countermeasure.

The expected effects are explained based on a mechanism that assumes an uphill section. The case where directional loudspeakers are not installed (Fig. 3) and the case where they are installed (Fig. 4) are compared in the three levels of traffic flow in the Q-V diagram: uncongested traffic flow zone (point A), maximum traffic volume zone (point B (B')), and congested flow zone (point C (C')). Differences can be seen at points B and C. Specifically, since the traffic volume is the highest at point B, a slight slowdown triggers the occurrence of a traffic congestion. Therefore, at point B, audio broadcasting to prevent a slowdown is delivered to restore the speed to the point B' state, thereby expanding the traffic capacity. In addition, since traffic congestion has already occurred at point C, eliminating the traffic congestion as soon as possible should be a goal. Therefore, at point C, audio broadcasting to restore the speed is delivered to restore the speed to that at point C', thereby increasing the queue discharge flow. Based on the above effects, the installation of directional loudspeakers could realize an increase in traffic capacity by restoring the driving speed.

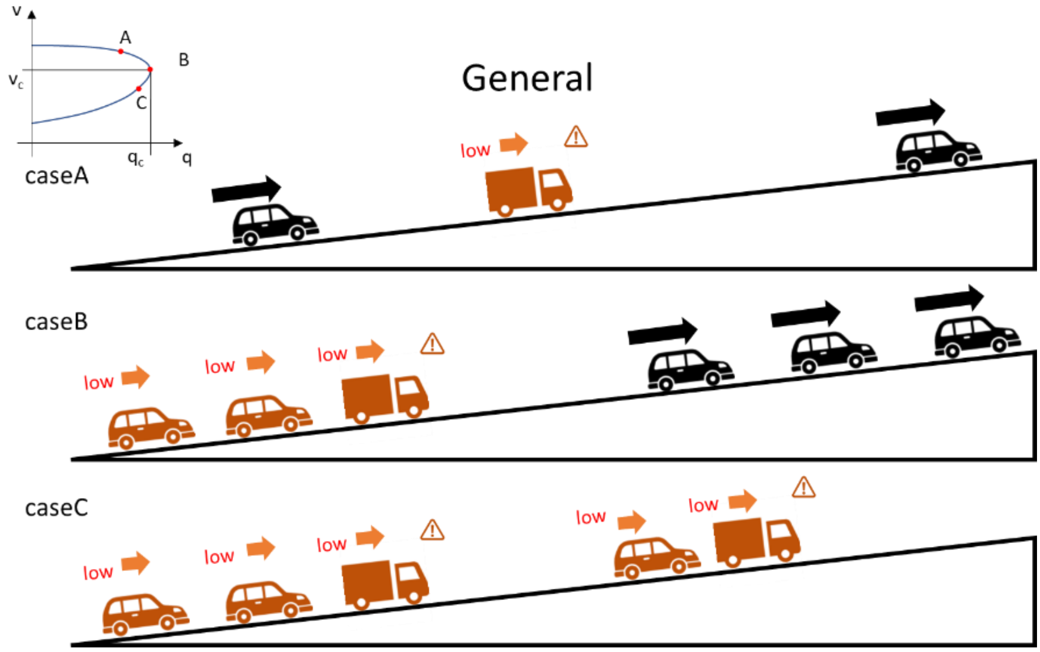

Figure 3 The case where directional loudspeakers are not installed.

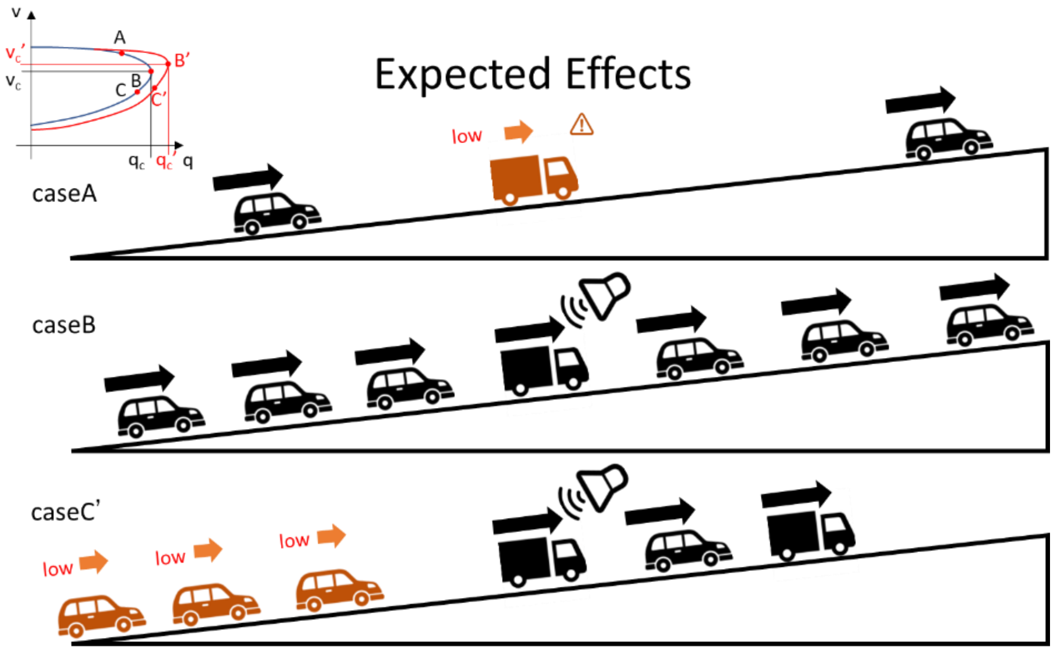

Figure 4 The case where directional loudspeakers are installed.

3.2 Details of the experiment

3.2.1 Period

Broadcasting was carried out from around 6:00 a.m. to 5:00 p.m. over eight days from Monday, November 27, 2023 to Friday, December 1, 2023 and Monday, December 4, 2023 (only in the afternoon and in the morning on the first day and the last day, respectively).

3.2.2 Location

The pinpoint countermeasure was implemented targeting vehicles driving on the uphill portion of the uphill gradient section by delivering broadcasting in an area of approximately 50 m from the area after the confluence from the entrance to the branch to the other line.

3.2.3 Traffic conditions and broadcasting patterns

As shown in the Q-V diagram above, broadcasting was delivered to encourage the prevention and early elimination of traffic congestion. Specifically, Pattern ①, "Please be careful not to slow down (approx. 3 seconds)," was repeatedly broadcast until immediately before the occurrence of a traffic congestion (when a queue is observed in the vicinity of the confluence from the Sambo entrance), and Pattern ②, "Please cooperate in restoring your speed (approx. 3 seconds)," was repeatedly broadcast after the occurrence of a traffic congestion. The above broadcasting patterns were switched onsite as necessary by checking traffic congestion on the road using camera images.

3.2.4 Installation equipment

The directional loudspeakers shown were installed on temporary scaffolding to provide effective broadcasting points for the uphill portion of the uphill gradient. During the experiment period, the experiment was made known to drivers through neighboring electronic bulletin boards and signs at the entrance.

4. Effectiveness verification results

This chapter describes the policy for verifying the effectiveness of the directional loudspeaker system in alleviating traffic congestion, and then describes the results in accordance with the policy and discusses the results.

4.1 Effectiveness verification method

The verification items determined prior to this experiment were roughly classified as ① verification of the feasibility of the countermeasure in reducing traffic congestion using directional loudspeakers, and ② verification of the effectiveness of the countermeasure in reducing traffic congestion using directional loudspeakers. In this chapter, we focus on item ② to organize traffic conditions based on vehicle detector data and verify the effectiveness of the countermeasure. In addition, we conducted a separate, more precise effectiveness verification using probe data and vehicle detector pulse data to determine the driving speed and behavior of individual vehicles .

4.2 Effectiveness verification results

4.2.1 Traffic volume based on vehicle detector data

Fig. 5 and Fig 6 summarize the section traffic volume between the confluence from the entrance and the branch, and the traffic volume at the entrance and exit. The section traffic volume decreased by 1 to 8% and 2 to 10% compared to the all-vehicle average (22,626 vehicles/day) and the average of tall vehicles (8,802 vehicles/day) on weekdays before the experiment (November 1 to 24), respectively. The traffic volume at the entrance increased by approximately 1 to 6% and approximately 2 to 14% compared to the all-vehicle average (3,215 vehicles/day) and the average of tall vehicles (1,541 vehicles/day) on weekdays during the same period, respectively. Compared to the all-vehicle average on weekdays during the same period (1,232 vehicles/day), the traffic volume at the exit increased by approximately 1 to 6% on November 28 and December 1 and decreased by approximately 3 to 11% on other days. Compared to the average of tall vehicles (554 vehicles/day), it increased by approximately 4 to 6% on November 28 and December 1 and decreased by approximately 2 to 10% on other days.

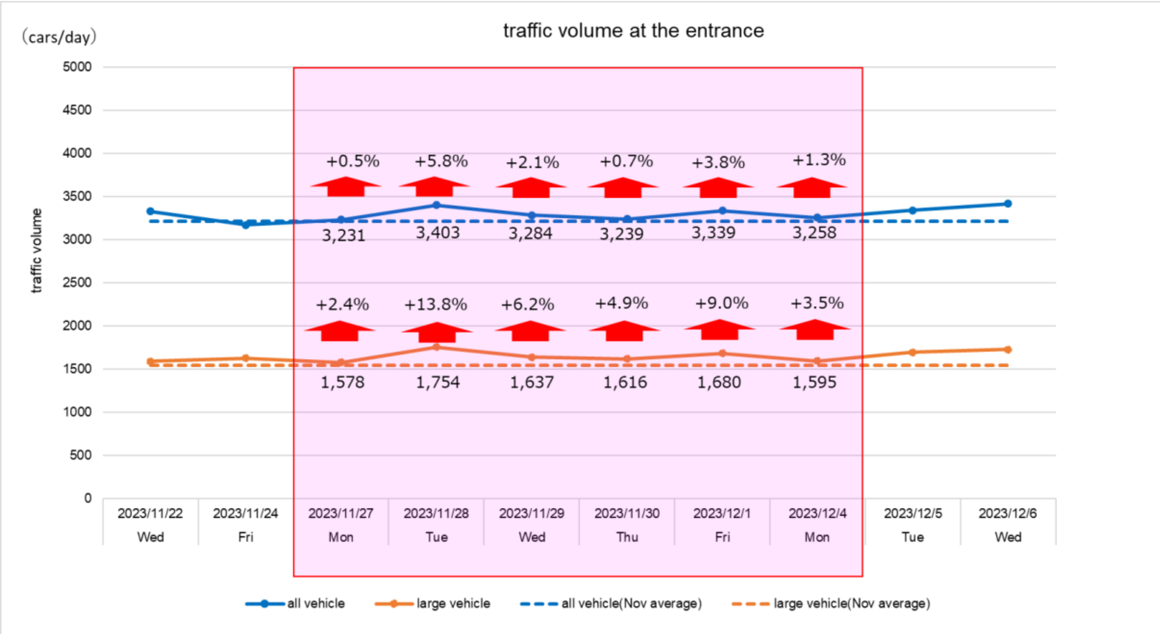

Figure 5 traffic volume at the entrance

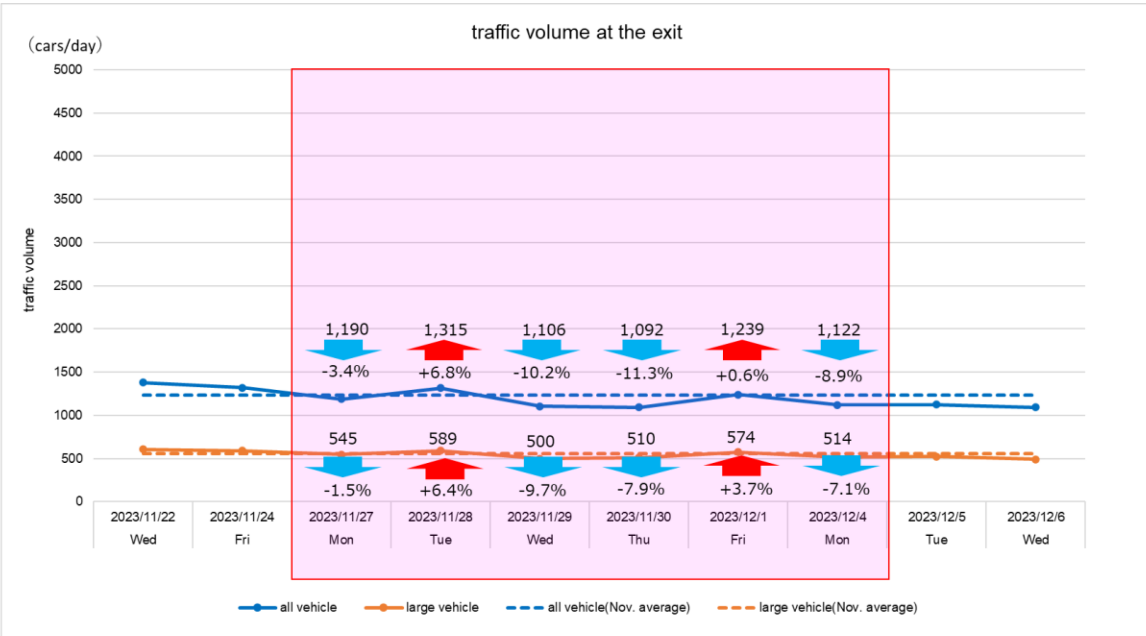

Figure 6 traffic volume at the exit

4.2.2 Traffic congestion organized based on vehicle detector data

Fig. 7 organizes the amount and duration of traffic congestion. Compared to the weekday average before the experiment (8.3 km/h/day), the overall amount of traffic congestion decreased by 1% (8.19 km/h/day) while it increased by 10 to 30% from November 27 to 29 and decreased by approximately 20 to 40% from November 30 to December 4. Compared to the average duration of traffic congestion during the same period (136 min/day), the overall duration of traffic congestion decreased by approximately 1 minute (135 min/day) while it decreased by 20 to 30 minutes on November 27, November 30, and December 1, and increased by approximately 10 to 50 minutes on November 28, November 29, and December 4.

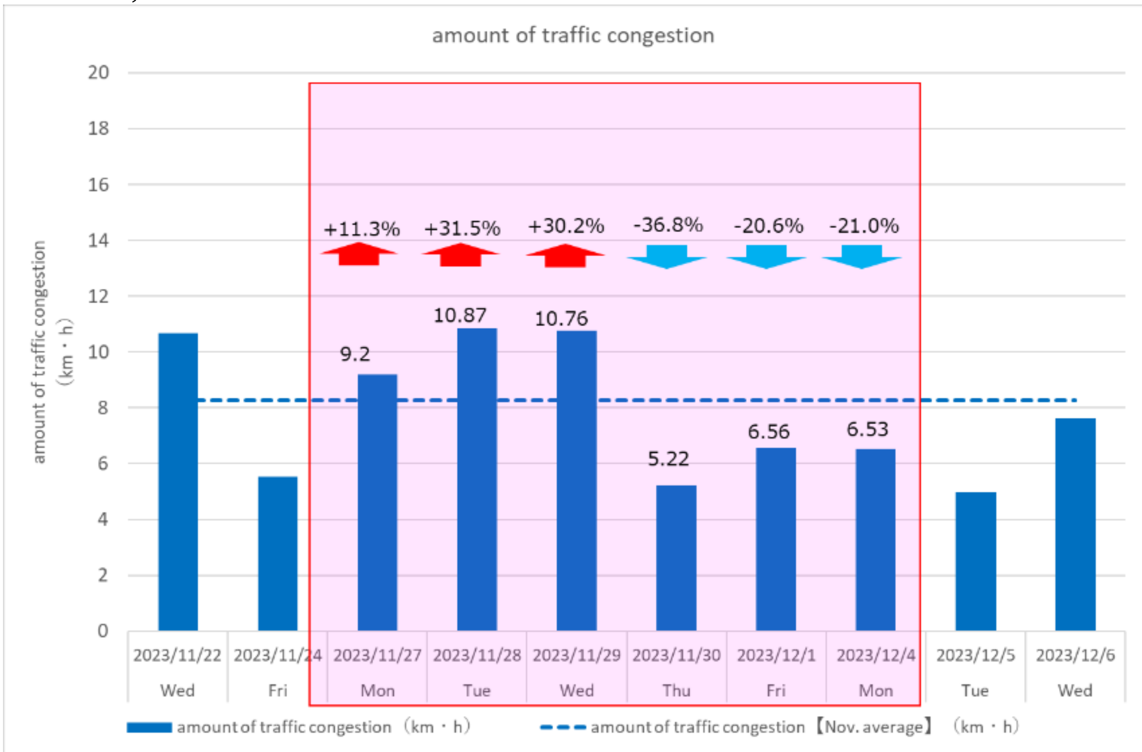

Figure 7 amount of traffic congestion

4.2.3 Queue discharge flow based on vehicle detector data

Fig. 8 shows the relationship between traffic volume and speed in the first lane during the experiment period and before the experiment. As for the comparison during the entire period, the traffic capacity during the experiment period (162.4 pcu/5 min) was higher than that before the experiment period (161.8 pcu/5 min). The traffic capacity during the experiment period except for November 29, November 30, and December 1 was higher than that before the experiment period, albeit slightly. When the tree is landed in detail on the pink and blue points, there are more plots due to the low velocity zone than on the blue points. Since the duration of the experiment was short, we believe that this is due to daily fluctuations and other factors. In order to improve these results, we believe it is necessary to conduct the experiment for a longer period of time and collect more samples.

Fig. 9 shows the queue discharge flow. Queue discharge flow is defined as the amount of traffic flow for a certain period of time after the occurrence of a traffic brake. This enables the evaluation of the smoothness of traffic flow after the occurrence of a traffic brake.During the experiment period, it generally showed an increasing trend, with all but the smallest values exceeding the values before the experiment. In addition, the average speed during traffic congestion in the same figure also showed a trend of general improvement, with the average value improving slightly from 21.8 km/h to 22.6 km/h.

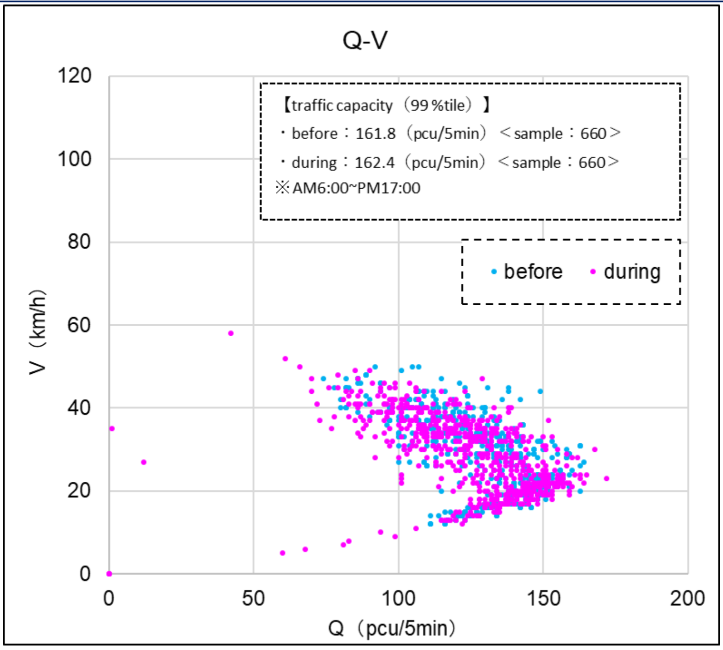

Figure 8 Q-V diagram

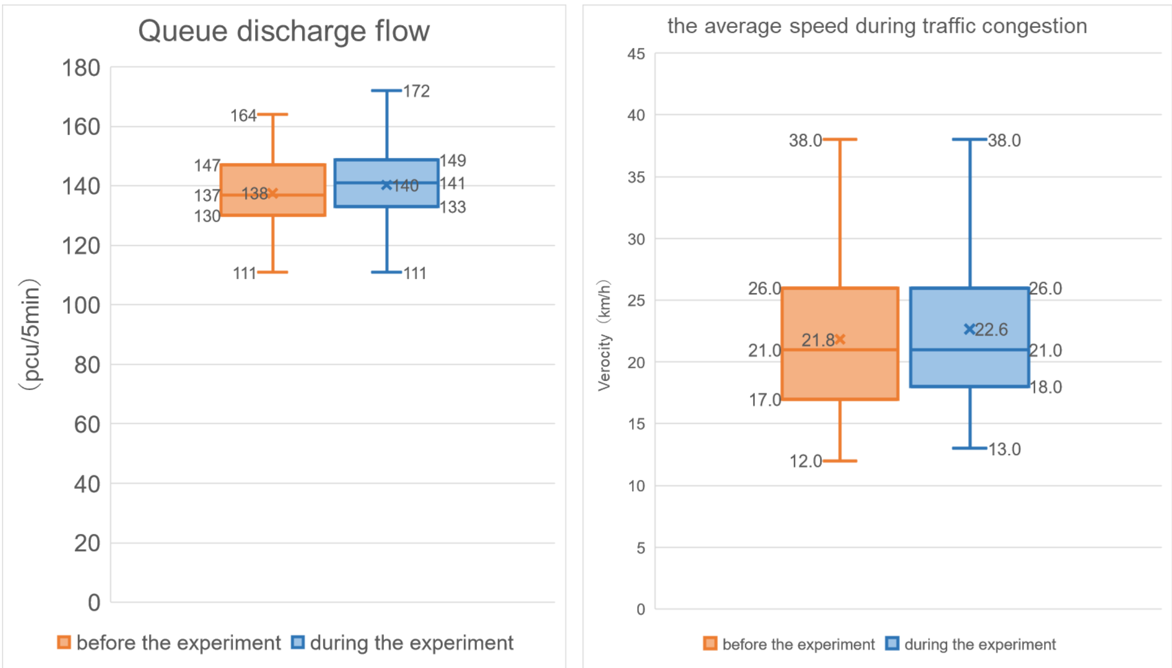

Figure 9 Queue discharge flow and the average speed during traffic congestion)

4.2.4 Driving speed during traffic congestion based on probe data

The probe data shows the distribution of driving speeds near the experiment period, as shown in Fig. 10 and Fig 11. This figure shows that the percentage of speeds below 20 km/h in the red boxed area decreased by approximately 2 points compared to the period before the experiment.

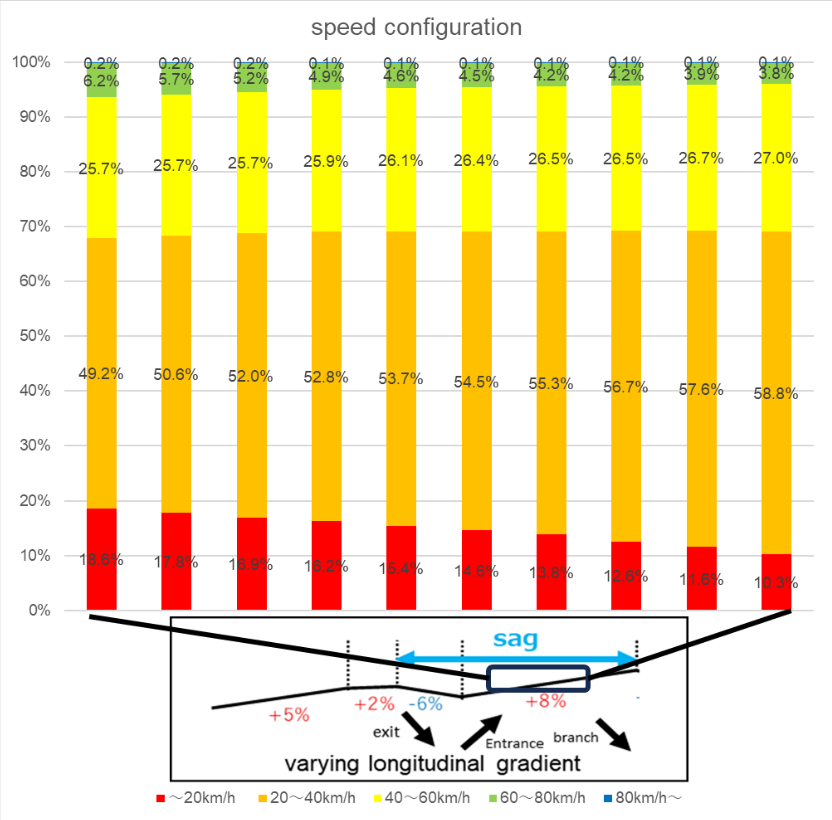

Figure 10 speed configuration (before the experiment)

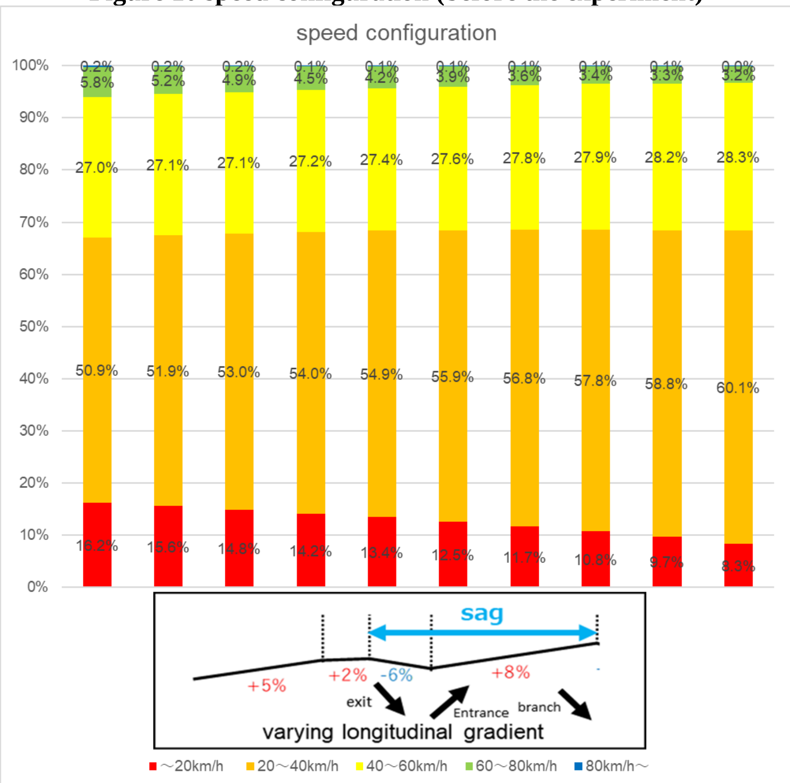

Figure 11 speed configuration (during the experiment)

4.2.5 Time headway based on vehicle detector pulse data

The vehicle detector pulse data records whether or not and when a vehicle is present, and the time headway can be calculated from the difference in the vehicle gap times. Fig 12 showed that the time headway was reduced during traffic congestion during the experiment period compared to that before the experiment.

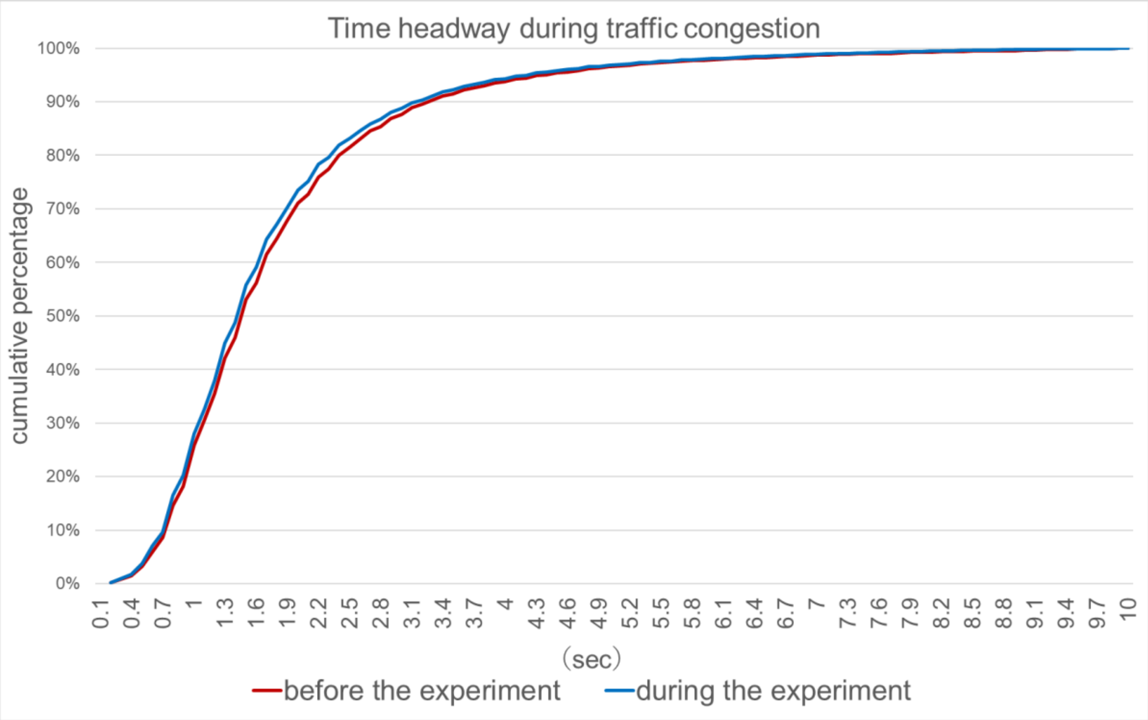

Figure 12 Time headway

These results indicate that there was a slight improvement in driving speed and traffic capacity during traffic congestion. However, these results are not considered significant as effects of reducing traffic congestion. In this study, the effects of the countermeasure is considered to be much smaller than that on basic road sections of other expressways, due to the complexity of the structure of the road where the experiment was conducted. This suggests that the countermeasure against traffic congestion using directional loudspeakers is dependent on the road structure and is not effective in the area studied here.

5. Summary and future actions

5.1 Summary

In this experiment, a countermeasure against traffic congestion using directional loudspeakers was implemented at the Sambo JCT, where traffic congestion has been confirmed to occur due to its complex road structure on the uphill section, with the purposes of preventing vehicle slowdown, reducing the occurrence of traffic congestion, and eliminating traffic congestion as soon as possible by restoring speed during traffic congestion. As a result, the speed at the time of traffic congestion became higher than that before the experiment, and the queue discharge flow also became higher than that before the experiment. Also, regarding the behavior of individual vehicles, the effect of reducing the headway time was observed. Therefore, we believe that using voice guidance to alert drivers to lower speeds is significant and that it is effective to consider auditory congestion countermeasures. However, as a countermeasure against traffic congestion, it is considered to be dependent on the road structure, and is unlikely to be effective at the section where this study was conducted and other locations with a complex structure where there are branch and confluence roads in the vicinity and the road gradient changes significantly. In the test area, where there are mergers, turnouts, and curves, many vehicles slow down for safety reasons, making it difficult to increase speed for the purpose of easing traffic congestion. If similar measures were to be implemented at locations with complex road structures, it would be possible to announce that the road is congested earlier than the congestion point or provide destination guidance.

5.2 Future actions

Based on the results of this experiment, since it is believed that this auditory countermeasure against traffic congestion can be effective, it is necessary to implement the countermeasure by selecting locations with simple road structures where it will be more effective. If the road structure is simple with few mergers, branches, and curves, and if the congestion occurs at locations with gentle uphill gradient, there is little vehicle deceleration except for uphill gradient, and it is possible to increase speed through aural congestion control measures. In addition, since the system uses physical voice guidance, it is considered necessary to ensure sufficient safety before implementing the system.

6.References

Analysis of the effectiveness of voice guidance utilizing speakers for the provision of recovery information, Japanese Journal of JSCE D3,ol.77,o.1,p.4-44,021.

A Study on Bottleneck Capacity on Divided Two-lane Expressways, Japanese Journal of JSCE, ol.22,p.839-845

Investigation and Analysis of Traffic Lane Overlapping Driving Behavior at Combined Curves on Multi-Lane Highways

Napon Srisakda[1,*], Sorawit Narupiti[2]

[1] School of Engineering, University of Phayao, Phayao, Thailand, napon.pon87@gmail.com, napon.sr@up.ac.th
[2] Faculty of Engineering, Chulalongkorn University, Bangkok, Thailand, sorawit.n@chula.ac.th

ABSTRACT

Because driving behaviors differ in each country, road safety impacts may differ despite using the same geometric design of highway manual, especially at the sharp curve that is a high-risk position of accidents due to traffic lane overlapping of vehicles on multi-lane highways expanded from 2-lane highways. However, most countries use the same geometric design from the highway manual without consideration of different driving behaviors. Previous studies have considered only lane-keeping performance variability, using driving tests only in the simulation regardless of realistic driving. Moreover, information on driving behaviors was received from spot speed measurements from each curve position (i.e. beginning, middle, and ending) without sufficient resolution and floating vehicle information. Therefore, this research aims to investigate and analyze driving behaviors when drivers drive through combined curves (horizontal and vertical alignment at the same curve) on a 4-lane highway, particularly traffic lane overlapping of drivers. To investigate driving behaviors, GPS devices, which were able to record in 1-second intervals and were installed in vehicles, collected driving behaviors using coordinate, speed, and direction information from vehicle movement. The 2.4-kilometer length of a 4-lane roadway with 7 combined curves in Phayao Province, Thailand was selected as the study site. The results investigated that lane overlapping can be seen at the middle and the ending position in each curve. Most drivers of personal vehicles (sedans, SUVs, and pick-ups) overlapped traffic lanes at curves due to high approaching and following speeds. They attempted to cut shorter alignment to avoid high lateral acceleration. Importantly, lane overlapping at the curve has a significant effect in cases where the vehicles are moving at the downslope and the long curve length. The findings in this research can consider lane widening for lane overlapping prevention and can adjust it which the design manual did not consider.

Keywords: Driving Behaviors, Traffic Lane Overlapping, Geometric Design of Highway, Combined Curves

1. INTRODUCTION

Road accidents, especially in a developing country, Thailand, have been a major problem due to an excessive number of accidents, and injured and dead travelers. This information approaches the top of the world in road traffic accident damages. Certainly, the biggest factor affecting road accidents is drivers, whereas; the second and third factors are vehicle and environment (PIARC, 2019). Thus, solving road accidents caused by drivers from their behaviors is a challenging issue.

Driving behaviors can be shown in the pattern of longitudinal vehicle speed, speed changes, and lateral acceleration when turning and affecting lane changing and overlapping because of unstable steering wheel catching (Said et.al, 2009). So, aggressive or bad driving behaviors can be investigated by high-speed driving, rapid speed changes, and frequent lane changing and overlapping. However, because driving behaviors differ in each country based on personal characteristics and traffic law enforcement ability (Ozkan et.al, 2006), road safety impacts may differ despite using the same geometric design of highway manual, especially on muti-lane highways at sharp curves and combining horizontal and vertical curves. Drivers driving through sharp combined curves with less or narrow radii cannot well control lane-keeping performance, and vehicles have opportunities to overlap with another lane. So, this driving behavior occurring at sharp combined curves is a high risk for road accidents due to lane changing or overlapping (Torbic et al., 2004).

The expansion of many roadways from 2-lane to multi-lane highways, especially in Thailand, has affected more lane changing or overlapping at the sharp curve because the operating speeds of multilane highways are higher than the original design speeds of 2-lane highways. Although some previous studies (Dijksterhuis et al., 2011; Jeong, H. & Liu, 2019) considered lateral measurement affecting lane overlapping, they analyzed only lane-keeping performance variability in different driving behaviors and focused on one lane direction.

The components of the curve include curve length and radius, slopes, transition length at both the beginning and end of the curve, lane and shoulder width, and median types (Gong and Stamatiadis, 2008). Then, these components were implemented to identify factors affecting traffic characteristics, especially speed (Gong and Stamatiadis, 2008). Although previous studies considered several components of curves related to operation speed and speed changes (Abele and Molter, 2011; Dijksterhuis et al., 2011; Nama et al., 2016; Wang & Wang, 2018; Jeong, H. & Liu, 2019; Sil et al., 2019; Wang et al., 2019), drivers were not tested on highways only in the simulation regardless of realistic driving. So, collecting driving data from real situations should also be considered.

There were using traffic data collection for finding factors affecting traffic characteristics (Gong and Stamatiadis, 2008; Wang & Wang, 2018). Nevertheless, information received from spot speed measurement from each curve position (i.e. beginning, middle, and ending) did not have sufficient resolution without floating vehicle and reflect driving behaviors, particularly lane-keeping performance.

From previous studies above, (1) driving behavior differences in each country, despite using the same geometric design of highway manual, especially at sharp curves and combined curves on muti-lane highways, (2) expansion of many roadways from 2-lane to multi-lane highways affecting more lane changing or overlapping at the sharp curve, and (3) considering only lane keeping performance variability, using driving tests only in the simulation regardless of realistic driving, receiving from spot speed measurement from each curve position without floating vehicle and driving behaviors, particularly lane-keeping performance, are limitations.

Therefore, this research aims to investigate and analyze driving behaviors using data from floating vehicles installed by GPS devices, particularly traffic lane overlapping of drivers on multi-lane highways. Drivers were asked to drive through combined curves (horizontal and vertical alignment at the same curve) on a multi-lane highway. Then, the relationship between lane overlapping and the factors affecting it was analyzed.

2. METHODOLOGY

For how to investigate and analyze driving behavior in this research, the methodology is illustrated in Figure 1. Firstly, GPS devices were installed in tested vehicles, including sedans, buses, SUVs, vans, and pick-ups. Secondly, drivers were asked to drive through combined curves at the selected study site. Then, driving behaviors can be collected and investigated from coordinates, speed, and direction information from vehicle movement. Because coordinates received from the GPS devices are subject to error, they must adjust by several tests of lane maintaining driving. Finally, driving behaviors were investigated by traffic characteristics including approaching and following speed, speed change, lateral acceleration, and lane overlapping. Then, they were analyzed by the relationship between lane overlapping and traffic characteristics, vehicle types, and components of curves.

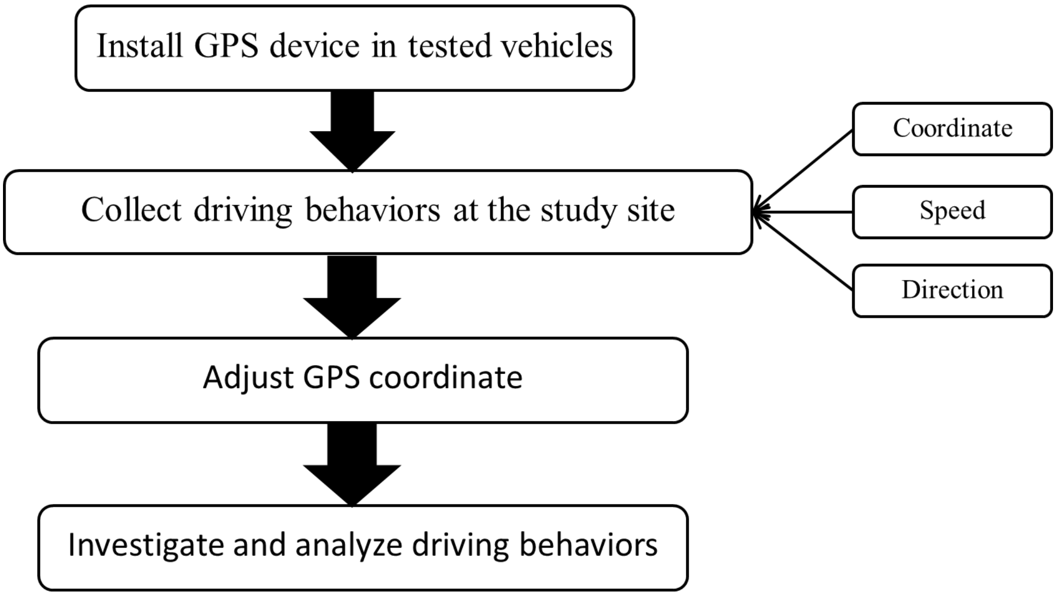

Figure 1 Research methodology.

2.1 Site Selection

The entrance road to the University of Phayao, Phayao Province, Thailand was selected as the study site. This roadway was originally a 2-lane highway under the operation of the Department of Rural Roads, Ministry of Transport. Then, it was transferred to the University of Phayao in 2010 and was expanded to a 4-lane highway with the same alignment.

It has a 2.4-kilometer length, 7 combined curves (C1-C7), and 2 lanes in each direction divided with a raised median. 7 curves have a curve radius from 36 to 62 meters which is a low and narrow curve. Because the distance from the entrance gate at the National Highway No.1 (Phahonyothin Road) to the campus area is a mountainous terrain from low (471 meters above mean sea level) to high area (541 meters above msl), the alignment in this roadway is the positive grade from low to high in the entry direction (Entry bound) and the negative grade in the opposite direction (Exit bound). The longitudinal grade in the entry direction of the roadway ranges from -1.6% to +8.5%, with a cross-section width of 10.50 meters (lane width of 3.00 meters and shoulder width of 1.50 meters). The longitudinal profile and attribution of curves including average curve radius and length, average transition length from 2 directions, left or right curve, and gradation in entry direction in this study site can be shown in Figure 2 and Table 1.

Figure 2 Study Site Research.

Table 1 Attribution in each curve.

Attribution	C1	C2	C3	C4	C5	C6	C7
Average curve radius (m)	41.0	45.6	36.2	48.9	61.6	57.2	40.4
Average curve length (m)	23.0	34.0	82.0	88.0	130.0	39.0	64.0
Approaching transition length in entry bound (m)	0.0	0.0	0.0	18.0	19.0	0.0	0.0
Ending transition length in entry bound (m)	0.0	0.0	9.0	0.0	62.0	0.0	27.0
Direction in entry bound	Left	Right	Left	Right	Left	Right	Right
Gradation in entry bound (%)	+4.3	+5.9	+8.5	+4.0	+8.5	+5.1	-1.6

2.2 Data Collection

To investigate driving behaviors, GPS devices, which were able to record in 1-second intervals and were installed in vehicles, collected driving behaviors using coordinates, speed changes, and direction information from vehicle movement. Vehicle coordinates can be identified by latitude and longitude coordination system which can be converted as a UTM system (northing and easting). Vehicle coordinates can be read from GPS devices installed at the center of vehicles. Speed change can be collected from the difference in speed information. It can be called in other words "longitudinal acceleration". Directions can detect vehicles when passing at a curve in the unit of degree from 0 to 360. Meanwhile, lateral acceleration can be calculated from speed in the perpendicular direction with longitudinal speed.

Regarding samples for collecting driving behaviors, drivers from used vehicles consisting of sedans, buses, SUVs, and pick-ups were asked to drive by samples as much as possible. These vehicle types usually pass the study site, and selected drivers were of different genders, ages, and experiences in driving.

2.3 Lateral Acceleration and Lane Overlapping Analysis

2.3.1 Lateral Acceleration

Lateral acceleration passing at a curve occurs from the transition of vehicle positions from (x_1,y_1) to (x_2,y_2) and angle directions from θ_1 degree to θ_2 degree from GPS devices as shown in Figure 3 (left).

Lateral acceleration in this research can be detected in 4 cases. Firstly, constant longitudinal speed and positions at (x_1,y_1) or (x_2,y_2) are the same as the center line in each lane. Secondly, different longitudinal speeds but positions are still the same as the center line. The third is longitudinal speeds are constant but at least one of their positions is different from the center line in each lane. The last one is both the positions are different from the center line in each lane. However, the cases that may affect lane overlapping are the third and the last. Lateral acceleration at (x_2,y_2) can be explained in Figure 3 (right).

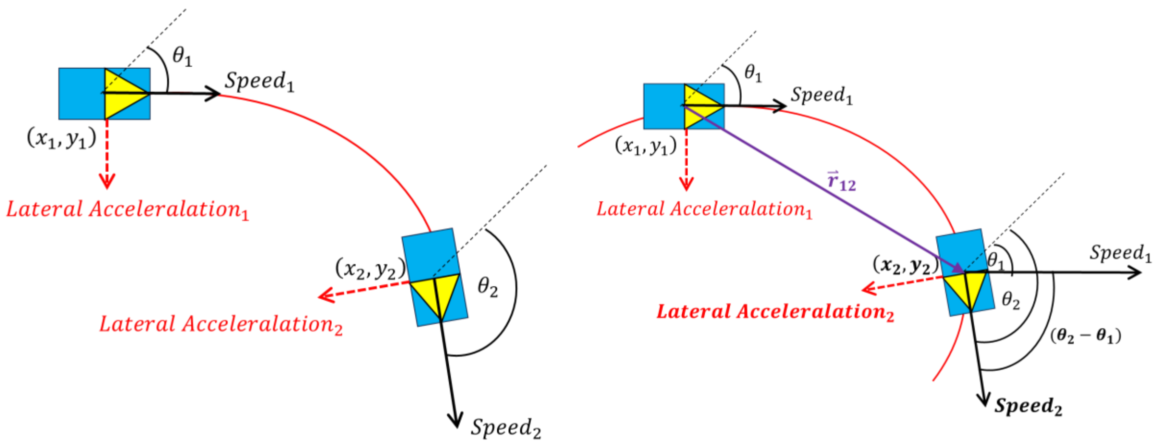

Figure 3 Transition of a vehicle passing at a curve (left) and lateral acceleration at (x_2,y_2) in all cases (right).

Refer to the kinematics of the vehicle moving in the horizontal plane with fixed coordinates (Gillespie, 1992; Abe and Manning, 2009), the models for lateral acceleration calculation at coordinate (x_2,y_2) start with position vector ($\vec{R}_{12}$) from coordinate (x_1,y_1) to (x_2,y_2) and its magnitude (R_{12}) considering from transition of vehicle positions as shown in Equation (1). Then, lateral acceleration can be calculated from the transition of angle directions from θ_1 to θ_2 degrees in 1-second intervals (rotational speed) as shown in Equation (2).

$$r_{12} = |\vec{r}_{12}| = |([x_2 - x_1]\,\vec{i})^2 + ([y_2 - y_1]\,\vec{j})^2| \tag{1}$$

Where $\vec{R}_{12}$= position vector from coordinate (x_1,y_1) to (x_2,y_2)
r_{12} = magnitude of position vector from 2 coordinates
$\vec{i}$ and $\vec{j}$ = unit vector according to x and y axis, respectively

$$Lat.Acc. = \frac{\theta_2 - \theta_1}{t_2 - t_1}\left(\frac{r_{12}}{t_2 - t_1}\right) \tag{2}$$

Where $Lat.Acc.$ = lateral acceleration (m/sec^2)
r_{12} = magnitude of position vector from 2 coordinates
θ_1 and θ_2 = angle directions in the unit of radian of a vehicle at coordinate (x_1,y_1) and (x_2,y_2), Respectively
t_1 and t_2 = time stamped at coordinate (x_1,y_1) and (x_2,y_2), respectively

2.3.2 Lane Overlapping

Lane overlapping of vehicles can be indicated by (1) the distance gap between the center of the vehicle and the centerline of roadway alignment and (2) the difference in angle direction between actual driving and the curve (Dijksterhuis et al., 2011, Jeong, H. & Liu, 2019). In this research, lane overlapping was measured by the distance gap between the center of the vehicle and the centerline of the roadway alignment using GPS coordination. However, the measurement from GPS coordination must be adjusted to correct the discrepancy by testing the vehicle in each direction.

Collecting the discrepancy, tested vehicles were asked to run on the same lane along the roadway in each direction, and drivers must try to keep the center position of the lane with a low speed of around 40 km/hr as much as possible. Then, the discrepancy values in each direction were found and implemented for adjustment after receiving GPS coordination.

GPS coordination discrepancies in this research can be calibrated by driving tests many times while maintaining driving on the left and right lanes. For each maintained driving, GPS coordination differed from the center positions of each lane and direction (downslope and upslope), as shown in an example at curve C3 (from station distance 0+750 to 0+900) in Figure 4. Therefore, the average gap distance between them in each lane was implemented to adjust in each curve.

(a) left lane maintaining driving in downslope direction

(b) right lane maintaining driving in downslope direction

(c) left lane maintaining driving in upslope direction

(d) right lane maintaining driving in upslope direction

Figure 4 The gap distance between GPS coordination and the center positions in 4 cases.

From Figure 4, the average gap distance between GPS coordination and the center positions was investigated in all cases, as shown in the yellow shaded area. Overall, the gap distance values between them are not much different at approaching (from 0+750 to 0+800) and following curve positions (from 0+875 to 0+900). On the other hand, they are different at the center position of the curve. When left-lane maintaining driving is compared with a right lane both in downslope and upslope direction, the gap distances between their lanes are different due to the discrepancy of receiving data from satellites. So, the discrepancy should be considered and adjusted. Because the gap distances were measured many times and days, they can be collected and implemented as the reference for calibration in each curve. The example of the calibration table at curve C3 can be summarized in Table 2.

Table 2 The example of the gap distance calibration table at curve C3**.**

Station Distance	The Gap Distance in Downslope Direction (m)		The Gap Distance in Upslope Direction (m)	
	Left Lane	Right Lane	Left Lane	Right Lane
0+750	1.5	1.6	-1.5	-2.0
0+800	-0.8	0.1	-2.0	-2.5
0+825	-3.0	-1.5	-4.5	-3.0
0+850	-2.9	-1.5	-3.0	-1.0
0+875	-3.0	-1.4	-1.6	-0.5
0+900	-3.0	-1.5	-1.5	-0.5

Remark: Positive and negative values mean GPS coordination is on the left and right side of the vehicle, respectively.

For vehicle lateral position measurement and refer to the study of Dijksterhuis et al. (2011), the lateral position is defined as the distance between the center of the vehicle and the center of the driving lane using the simulator to measure. Then, they detected lateral position by traffic simulator that is easy to measure lateral position. If the edge of a vehicle is near the edge line of the roadway, that means vehicle lane keeping is low. However, lane overlapping in this research without the simulator should be detected directly by human sight and errors of detection by human sight can occur. So, using GPS devices would be better for overlapping measurements.

Because considering various vehicle types in this study and having two lanes in each direction, the method from the research of Dijksterhuis et al. (2011) considered only sedans, lane keeping, and one lane in each direction. Therefore, considering efficient width limits for all vehicle types is necessary in this research. Examples of lane overlapping and keeping of a vehicle indicated in all cases can be shown in Figures 5 and 6.

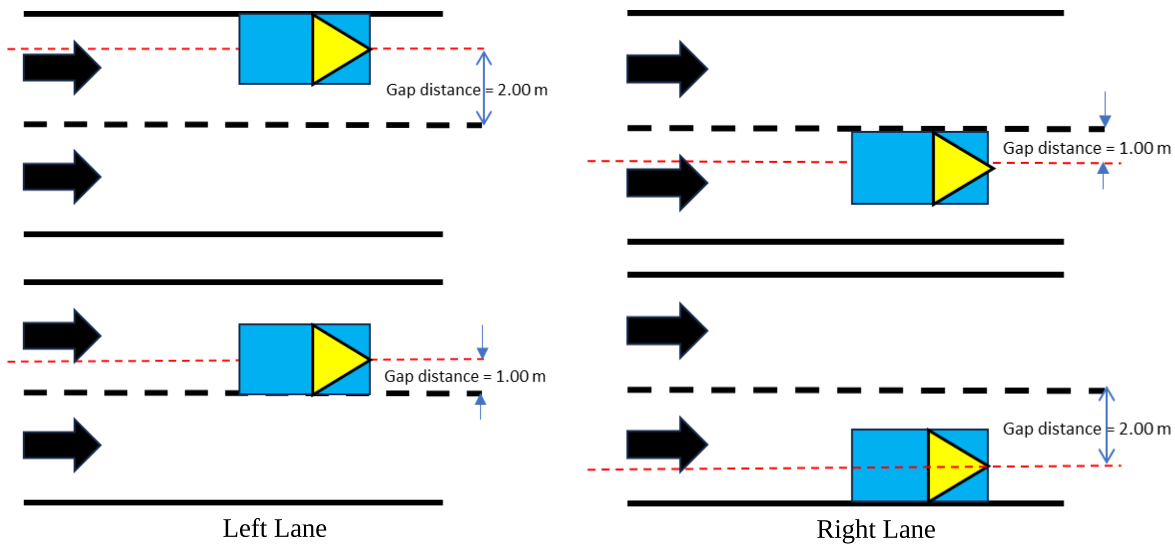

Figure 5 Examples of lane overlapping and keeping of a vehicle indicated in this research in lane keeping case.

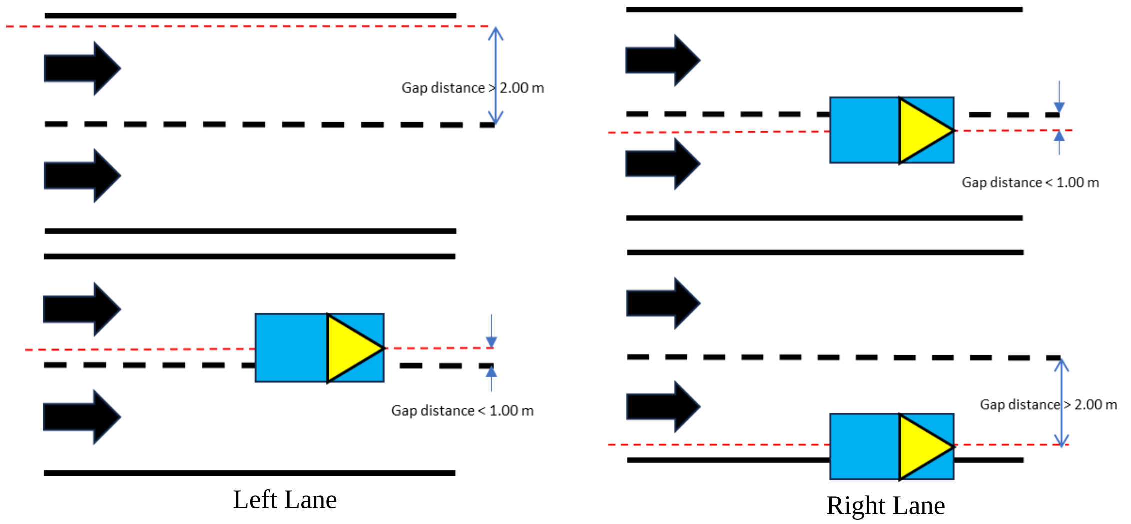

Figure 6 Examples of lane overlapping and keeping of a vehicle indicated in this research in lane overlapping case.

From Figures 5 and 6, lane keeping and overlapping can be indicated in this research. Due to having two lanes in each direction, the 3.00 meter-lane width in the study site, and the efficient 2.00-meter width limit for all vehicle types, if the gap of coordinate distance between the vehicle and the centerline of the roadway alignment is less than 1.00 meters or greater than 2.00 meters, that means vehicles have overlapped the lane. Then, vehicles overlapping in each curve can be indicated by their overlapping percentage by the distance of the curve length.

2.4 Participants

To receive several participants in this research, the target population of the volunteers is the personnel of the University of Phayao aged 20 years and above who regularly use the road at the University of Phayao. Then, the researcher tried to convince them to join the research in the greatest possible amount. As a result, 40 participants were selected as drivers by different gender, age, and driving experience. Although the sample size seems too small compared to traffic volume, using Yamane's statistical principles, the number of samples would be greater than the research duration and some related previous studies (Wang & Wang, 2018; Jeong, H. & Liu, 2019; Wang et al., 2019) did not have many participants (less than 40).

24 males and 16 females participated in this research. Males accounted for 60% of all drivers who had received private driving licenses in Thailand from the Department of Land Transport, Ministry of Transport as of 24 April 2024 (Department of Land Transport, 2024). The age of participants ranged from 23 to 48 years (mean = 31.5; SD = 7.3). All drivers were required to have driven at least 10,000 total kilometers and to have averaged at least 3000 km annually (Wang & Wang, 2018). Drivers from sedans, buses, SUVs, pick-ups, and vans are 18, 10, 6, 2, and 2, respectively. These numbers of drivers in each vehicle type were according to the fraction of vehicle type considered by the traffic volume survey at the study site.

3. RESULTS AND DISCUSSION

3.1 Descriptive Analysis

The initial descriptive analysis starts with a sedan vehicle's speed and lateral acceleration profiles by distance can be shown in Figure 7 and Figure 8 in entry (upslope) and exit (downslope) directions, respectively. Their profiles are compared with the roadway alignment and its elevation.

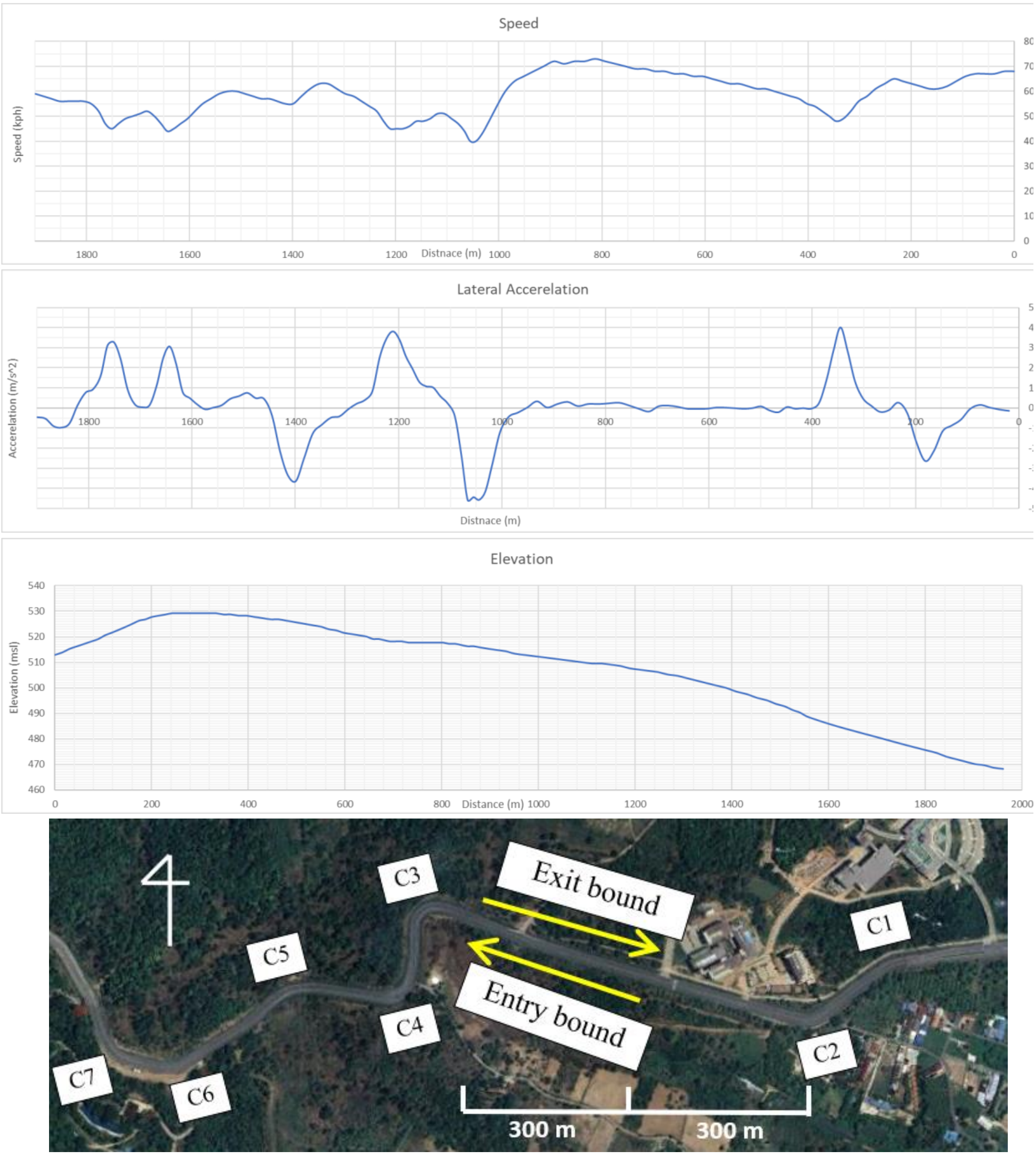

Figure 7 A vehicle's speed and lateral acceleration profiles in entry bound (Upslope).

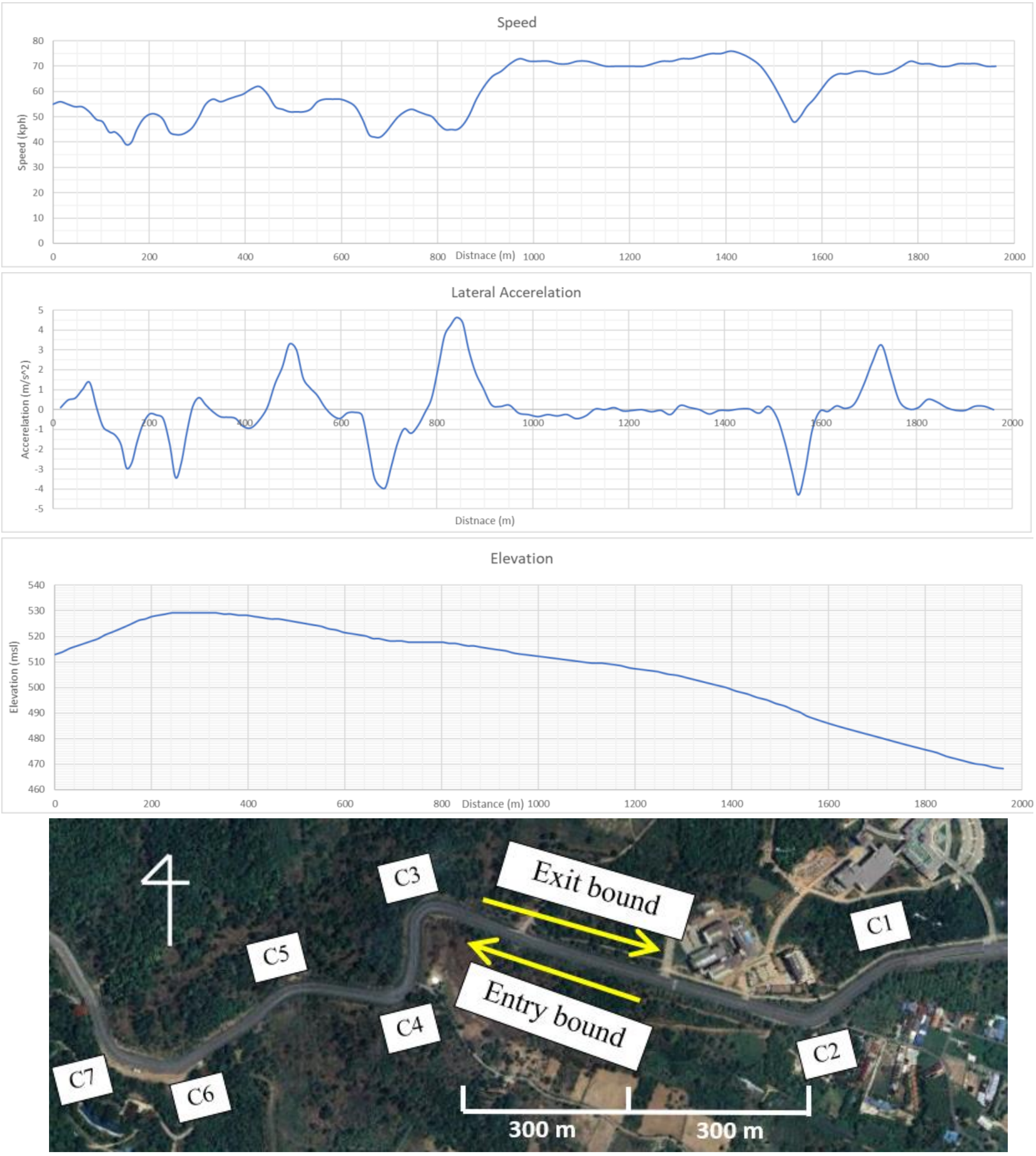

Figure 8 A vehicle's speed and lateral acceleration profiles in exit bound (Downslope).

From a vehicle's profile, vehicle speeds are in the range of 40 and 70 km/h in the upslope bound and 40 and 80 in the downslope bound. Vehicle speed in both upslope and downslope directions decreases when it moves through the curves. Lateral acceleration values are more or less than 0 depending on the curve direction data. The positive and negative acceleration values mean left and right curves, respectively. Consequently, these results can be summarized that the roadway curves affect lower vehicle speed and fluctuate lateral acceleration. The results are consistent with the research of Abele and Molter (2011) and Munzilah et al. (2015) of whose speeds were low and high lateral positions at the curves.

3.2 Investigation of Vehicle Lane Overlapping by Gap Distance

Driving behavior can be obviously investigated by the gap distance between the vehicle and the alignment of roadways. Examples of one sedan moving at curves C3 and C5, which are the lowest and highest curve radius, respectively, can be shown in Figure 9 in both 2 directions (upslope and downslope).

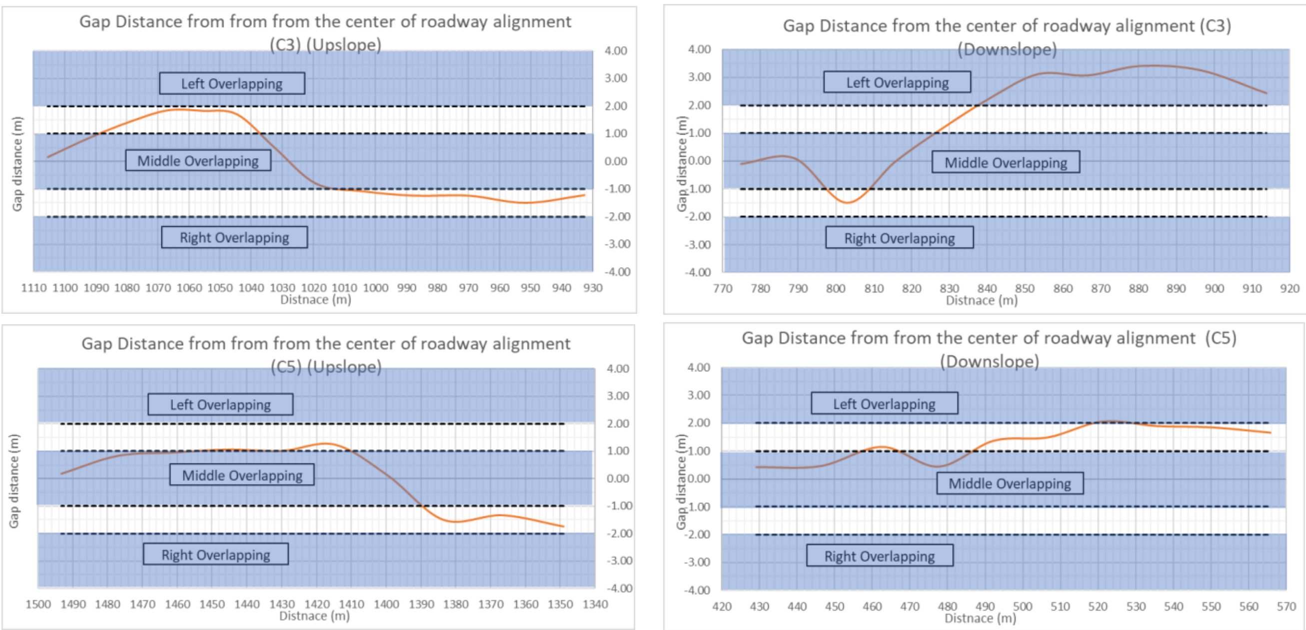

Figure 9 The gap distance at curve C3 (above) and C5 (below) in each vehicle.

From vehicle gap distance at 2 curves, side (left or right) and middle (between left and right lane) overlapping are investigated. Lane overlapping in the downslope direction can be seen at the middle and the ending position of the curve. This can be explained by the fact that when the vehicle is in the middle of the curve, the driver has difficulty controlling his vehicle and desires to overlap the lane for his comfort. This fact can vary depending on driving behaviors and traffic law enforcement in different countries. In some countries, drivers cannot change lanes because of the solid lines on the curve and can only reduce their speed as much as possible to maintain their lane (Abele and Molter, 2011; Munzilah et al., 2015). In Thailand, however, drivers can change lanes, especially private vehicles.

While in the upslope direction, lane overlapping can be slightly seen at the beginning and the middle position of the curve. This can be explained that drivers can control their vehicles easier than in the downslope direction before moving out of the curve.

3.3 Investigation and Analysis of Driving Behaviors and Lane Overlapping of Sedans

All curves of traffic characteristics of sedans including average approaching speed, following speed, speed change, lateral acceleration, and the lane overlapping percentage by distance in each direction can be shown in Table 3 in entry bound (upslope) and Table 4 in exit bound (downslope).

Table 3 Traffic characteristics of sedans in entry bound (upslope).

Traffic Characteristics	Entry bound (Upslope)						
	C1	**C2**	**C3**	**C4**	**C5**	**C6**	**C7**
Approaching speed (km/h)	62	58	58	46	58	55	46
Following speed (km/h)	60	52	41	54	54	47	51
Approaching speed change (km/h/sec)	-1.5	-2.4	-3.8	-1.2	-2.7	-2.0	-1.4
Following speed change (km/h/sec)	1.0	1.8	2.8	2.3	0.8	2.7	2.8
Lateral acceleration (m/sec^2)	-0.89	1.08	-1.88	1.65	-1.23	0.93	1.49
Lane overlapping by distance (%)	17%	60%	49%	50%	51%	45%	68%

Table 4 Traffic characteristics of sedans in exit bound (downslope).

Traffic Characteristics	Exit bound (Downslope)						
	C1	**C2**	**C3**	**C4**	**C5**	**C6**	**C7**
Approaching speed (km/h)	63	65	41	51	57	46	49
Following speed (km/h)	66	60	46	47	52	52	51
Approaching speed change (km/h/sec)	-0.3	-5.7	-1.8	-3.0	-1.8	-2.7	-2.1
Following speed change (km/h/sec)	0.8	3.4	4.2	2.2	1.7	2.8	3.0
Lateral acceleration (m/sec^2)	1.13	-1.38	2.34	-1.76	1.29	-0.87	-0.89
Lane overlapping by distance (%)	47%	30%	75%	76%	71%	67%	53%

From Tables 3 and 4, regarding average approaching and following speeds of most curves, different speeds from approaching to following in the upslope bound decrease except in curves C4 and C7. On the other hand, different speeds in the downslope bound vary between decreasing and increasing (Curve C2, C4, and C5 are decreasing).

Speed change in the approaching section decreases, and speed change in the following section increases. In the upslope bound, the maximum speed changes in the approaching and the following sections are curves C3 and C3+C7, respectively. In the downslope section, the maximum speed changes in the approaching section and the following section are C2 and C3, respectively. Also, speed changes in the downslope bound are stronger than those in the upslope bound indicated by the maximum absolute value in curve C2 due to the long straight downslope section before approaching this curve. These results are consistent with the research of Wang & Wang (2018), whose speed difference distributions in the downslope bound were wider than those in the upslope bound.

The maximum absolute lateral accelerations in the upslope and downslope bound are 1.88 m/s^2 and 2.34 m/s^2 at curve C3, respectively. The possible reason is the lowest curve radius of all 7 curves.

For the lane overlapping percentage by distance results, the maximum percent is 68 at the curve C7 in the entry bound, and 76 at the curve C4 in the exit bound. This result indicates that the vehicle moving in the downslope direction overlaps the traffic lane rather than the upslope direction due to possible reasons for the negative gradation of the 2 curves. When comparing each curve, the percentage of lane overlapping in the downslope direction is higher than in the upslope direction (6 in 7 curves).

In addition, the relationship between lane overlapping of sedans and components of the curve including curve radius, curve length, and absolute gradation can be shown in Figure

10-12. The components of the curves were sorted from lowest to highest.

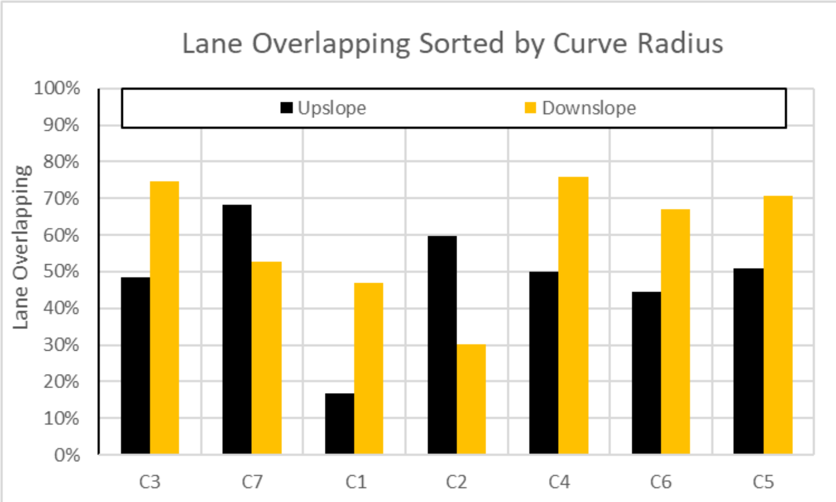

Figure 10 The relationship between lane overlapping percentage sorted by curve radius.

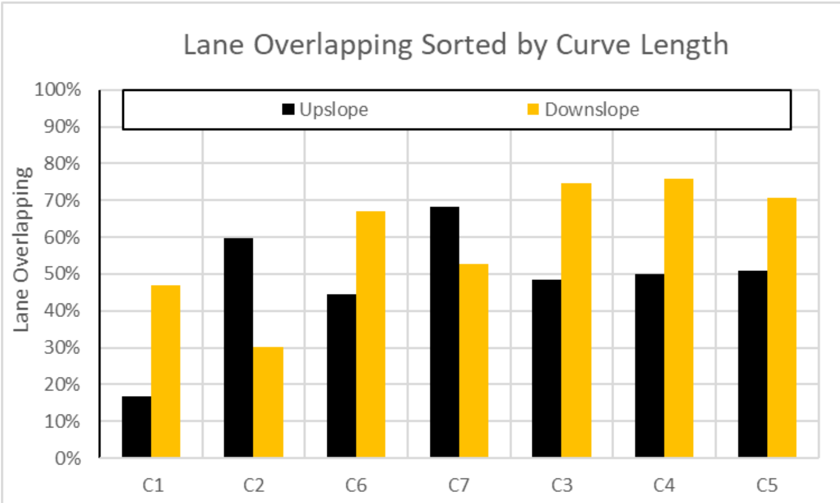

Figure 11 The relationship between lane overlapping percentage sorted by absolute gradation.

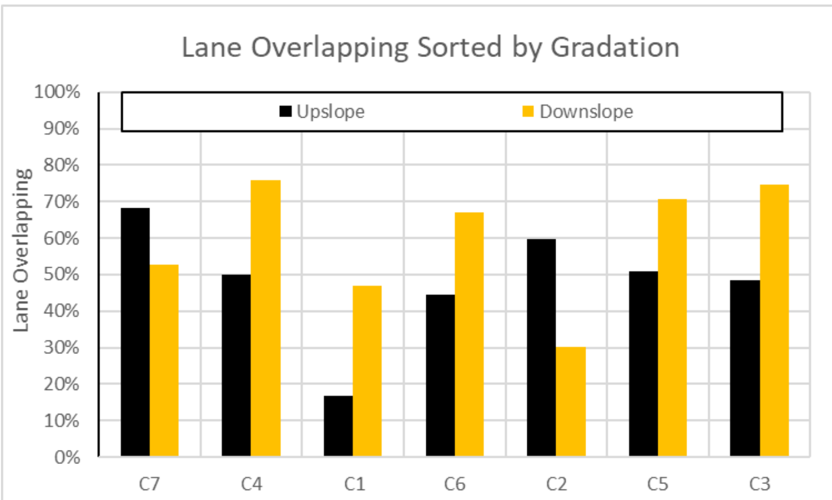

Figure 12 The relationship between lane overlapping percentage sorted by curve length.

From the relationship between lane overlapping and components of the curve, curve radius and absolute gradation are difficult to explain the relationship. However, only curve length is slightly related to lane overlapping. The lane overlapping percentages both upslope and downslope directions are higher when the curve length is longer. These results are consistent with the research of Wang & Wang (2018). Because the curve length increased, the probability of a large speed reduction also increased. That means drivers have difficulty to control their vehicles. Therefore, road geometric design of curves in case of curve length may be a concern for lane overlapping prevention.

3.4 Investigation and Analysis of Driving Behaviors and Lane Overlapping of All Vehicle Types

Considering each vehicle type, the average traffic characteristics results can be shown in Figure 13 in 2 directions by an examples of curve C3 which is the lowest curve radius.

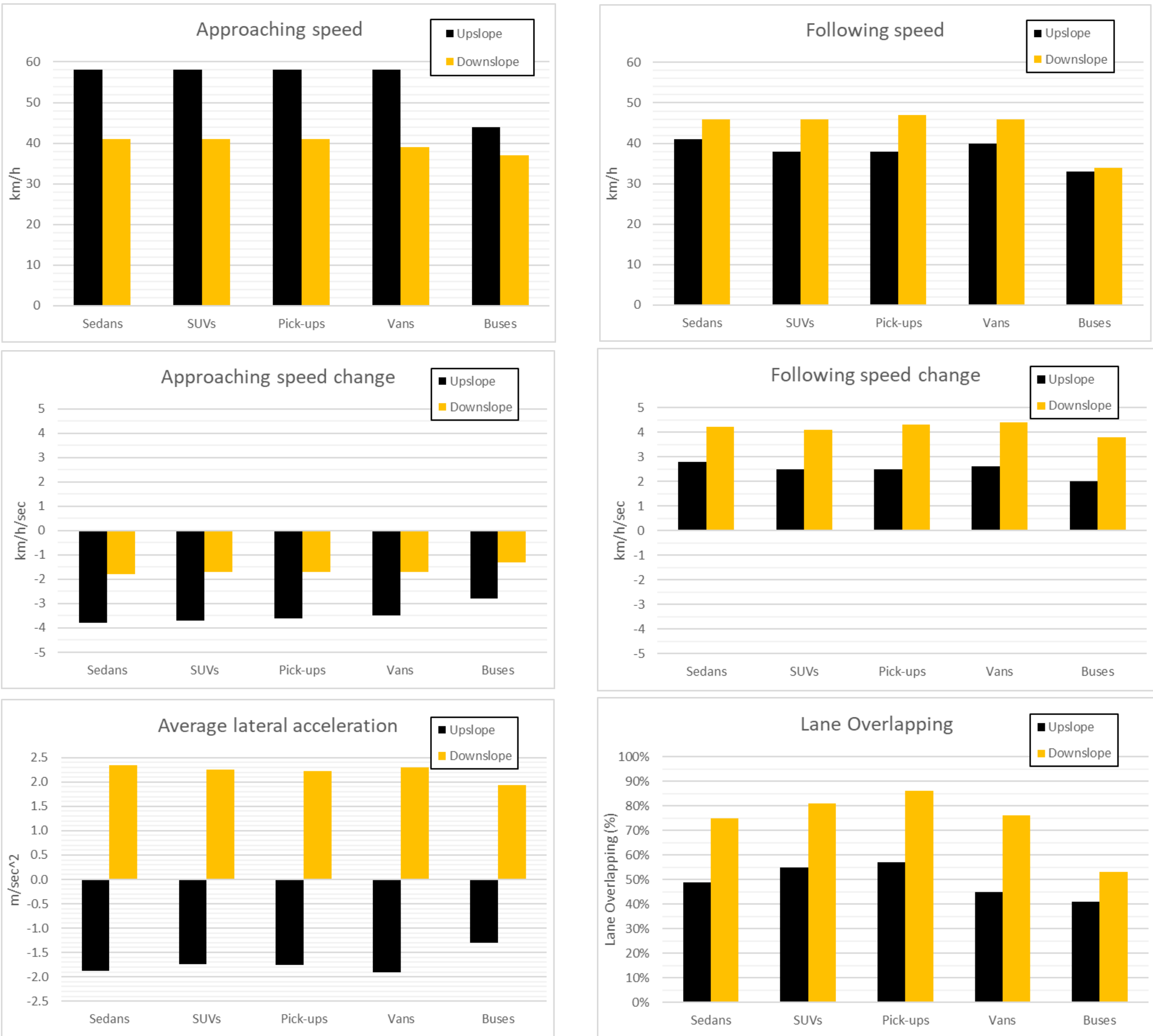

Figure 13 Traffic characteristics in each vehicle type at curve C3.

From traffic characteristic analysis in each vehicle type, approaching speed, following speed, and approaching and following speed change are not more different in both 2 directions. There are only buses whose traffic characteristics are different because of lower approaching speed, following speed, and approaching and following speed change than other vehicle types.

On the other hand, the results of lateral acceleration and lane overlapping percentages in each vehicle type can be seen. The maximum lateral accelerations both in the upslope and the downslope bounds are vans, and the second are sedans, but the 2 vehicle types are slightly different. The lateral accelerations of pick-ups and SUVs and the third and the fourth, but their values are not much different from vans and sedans. Finally, the lowest lateral accelerations are buses. These values can be seen clearly.

According to lane overlapping percentages, their percentages in the upslope bound are lower than those in the downslope bound in all vehicle types. The maximum lane overlapping percentages both in the upslope and the downslope bounds are pick-ups, and the second is SUVs. The third and the fourth are sedans and vans, but their values are not much different. Then, the lowest lane overlapping percentages are buses.

From the analysis of the relationship between lateral acceleration and lane overlapping, lower lateral acceleration affects higher lane overlapping in personal vehicles like sedans, SUVs, and pick-ups. Because these vehicle types move at higher speeds, they attempt to overlap the lane to cut shorter alignments when they move through the curve.

On the other hand, public vehicles like buses have the lowest lateral accelerations and lane overlapping percentages. These vehicles must have disciplined driving to protect passengers by lower speed and lane-keeping performance.

3.5 Applications of the Findings

The results of investigation and analysis showed that driving behaviors in Thailand, especially lane overlapping at the curve, have a significant effect in cases where the vehicles are moving at the downslope and the long curve length. In addition, private vehicles were more likely to overlap traffic lanes on curves than public vehicles. Therefore, applications from these findings in this research considered lane widening on the horizontal curve indicated in the topic 3.3.10 of the Greenbook (AASHTO, 2018) for lane overlapping prevention.

Lane widening on a horizontal curve explains the design values of the curve for lane widening in different curve radii and initial traveled way (2 lanes) width. For 3.0-lane width and 2 lanes in each direction (6.0-meter traveled way) in this study, lane widening can be identified by interpolation from equations received from the power regression model, as shown in Figure 14. Because speeds investigated from GPS data for all curves are in the range of 50-70 km/hr and curve radius are in the range of 35–60 meters, lane widening in each curve can be calculated around 4.0-6.5 meters (2.0-3.5 meters per lane).

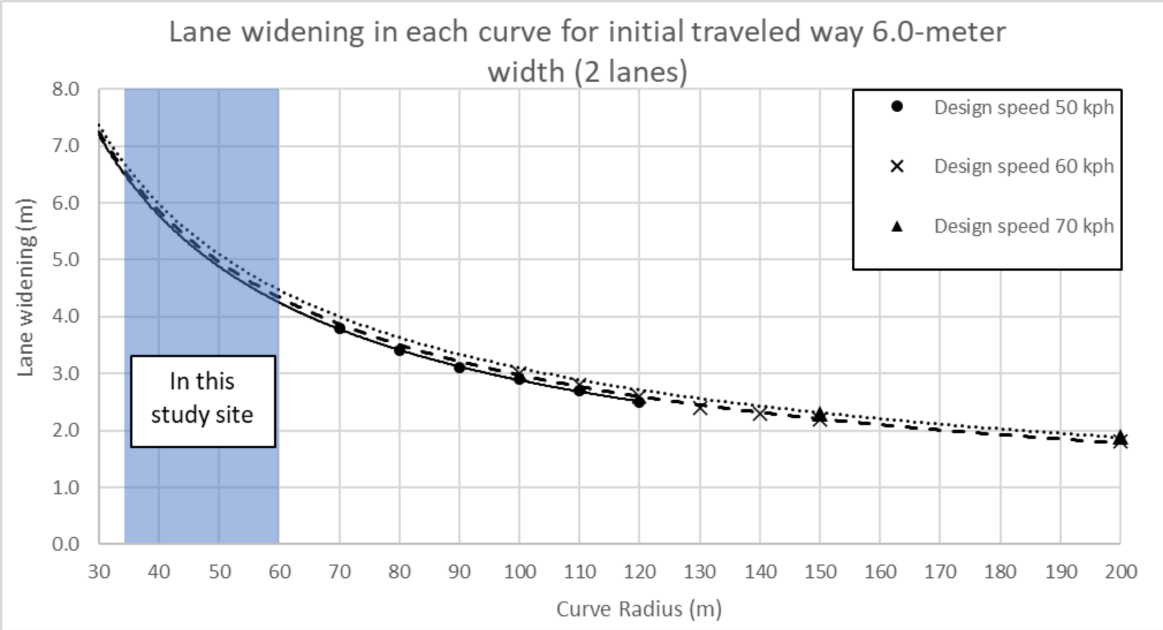

Figure 14 Power regression model for lane widening calculation.

Because lane overlapping has a significant effect in cases where the vehicles are moving at the downslope and the long curve length in this research, there is an idea for different lane widening in each direction. In addition, lane widening can be adjusted due to long or short curve length and different directions by linear regression model analysis. As shown in Figure 15, the relationship between lane overlapping percentage and curve length received from the study site can be explained by two models of downslope and upslope directions.

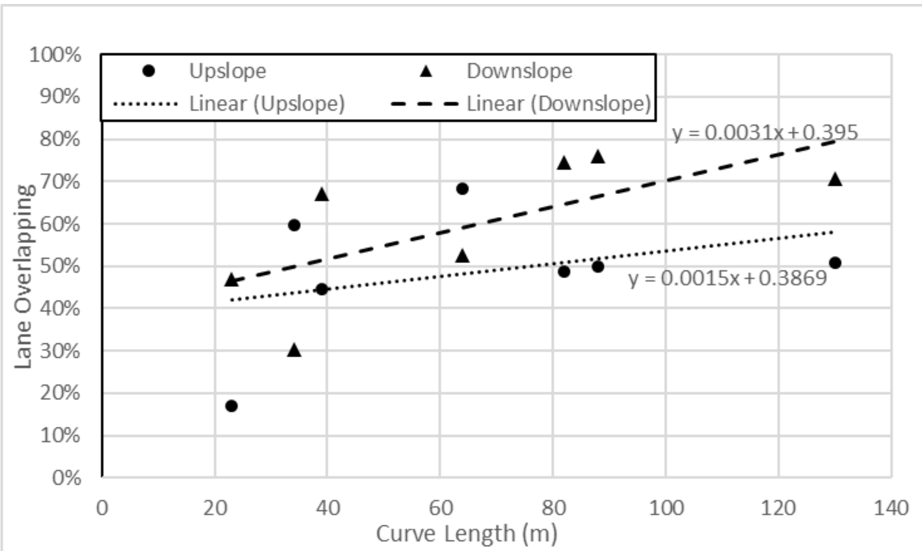

Figure 15 The relationship between lane overlapping percentage and curve length.

Figure 15 indicates that if the curve is longer, the chance of lane overlapping is higher. If this curve is in a downslope direction, the chance of lane overlapping is much higher. Therefore, by the combination of analysis from Figures 14 and 15, lane widening in the downslope direction and at a longer curve can be wider than the upslope direction by different overlapping percentages in each curve from the analysis for lane overlapping prevention.

4. CONCLUSIONS

The objective of this research is to investigate and analyze driving behaviors when drivers drive through combined curves (horizontal and vertical alignment at the same curve) on a 4-lane highway expanded from 2-lane highways. Driving behaviors were collected by GPS devices using coordinate, speed, and direction information from vehicle movement. Moreover, vehicle lane overlapping was an additional traffic characteristic in this research except typical characteristics such as approaching and following speed, speed change, and lateral acceleration.

The results investigated that lane overlapping can be seen at the middle and the ending position in each curve. Most drivers of personal vehicles (sedans, SUVs, and pick-ups) overlapped traffic lanes at curves due to high approaching and following speed. They attempted to cut shorter alignment to avoid high lateral acceleration. On the other hand, drivers of public buses vehicles had disciplined driving to protect passengers by lower speed and lane-keeping performance. Importantly, lane overlapping at the curve has a significant effect in cases where the vehicles are moving at the downslope and the long curve length. These results may be different from previous studies depending on driving behaviors and traffic law enforcement in each country.

The findings in this research, especially lane overlapping at the curve, can consider lane widening on the horizontal curve indicated in the Greenbook for lane overlapping prevention. Different gradations (downslope and upslope) and curve lengths can adjust lane widening which the Greenbook did not consider.

However, there were limitations in terms of the smaller number of samples and curves in the study site, GPS coordination discrepancy, and too short a curve radius. For further study, more than 40 drivers for testing, more covering analysis, such as crest and sag curves, and longer curve radius and increasing number of curves in the study site, should be considered. In addition, the models for lane widening by consideration of gradation and curve length should be more developed.

5. REFERENCES

Abe, M. & Manning, W. (2009) Vehicle Handling Dynamics: Theory and Application. Elsevier.

Abele, L. and Møller, M. (2011) The Relationship Between Road Design and Driving Behavior: A Simulator Study. In the 3rd International Conference on Road Safety and Simulation.

American Association of State Highway and Transportation Officials (AASHTO). (2018). A Policy on Geometric Design of Highways and Streets 2018, 7st Edition. Washington, DC.

Dijksterhuis, C., Brookhuis, K. A., & De Waard, D. (2011). Effects of steering demand on lane keeping behaviour, self-reports, and physiology. A simulator study. Accident Analysis & Prevention, 43(3), 1074–1081.

Gillespie, T.D. (1992). Fundamentals of Vehicle Dynamics. Society of Automotive Engineers, Inc.

Gong, H. & Stamatiadis, N. (2008). Operating speed prediction models for horizontal curves on rural four-lane highways. Transportation Research Record 2075(1), 1-7.

Jeong, H. & Liu, Y. (2019). Effects of non-driving-related-task modality and road geometry on eye movements, lane-keeping performance, and workload while driving. Transportation Research Part F: Traffic Psychology and Behaviour. 60, 157-171. https://doi.org/10.1016/j.trf.2018.10.015.

Munzilah, M.R., Rosnawati, B., Basil, D.D., Joewono, P., Kamarudin, A., Norsabahiah, A.S., and Sitti Asma, H. (2015). Car Driving Behaviour on Road Curves : A study Case in Universiti Tun Hussein Onn Malaysia. Applied Mechanics and Materials. 773-774, 990-995.

Nama, S., Maurya, A.K., Maji, A. (2016). Vehicle Speed Characteristics and Alignment Design Consistency for Mountainous Roads. Transp. in Dev. Econ. 2, 23. https://doi.org/10.1007/s40890-016-0028-3

Noomwongs, N., Thitipatanapong, R., Chantranuwathana, S., Klognaivai, S. (2014). Driver Behavior Detection Based on Multi-GNSS Precise Point Positioning Technology. Applied Mechanics and Materials, 619, 327-331.

Ozkan, T., Lajunen, T., Chliaoutakis, J., Parker, D. Summala, H. (2006). Cross-cultural differences in driving behaviours: A comparison of six countries. Transportation Research Part F-traffic Psychology and Behaviour. 9(3), 227-242, https://doi.org/10.1016/j.trf.2006.01.002.

PIARC (World Road Association) (2019). Road Safety Manual. 3rd Edition.

Said, D., Halim, A.E., Hassan, Y. (2009) Methodology for Driver Behaviour Data Collection and Analysis for Integration in Geometric Design of Highways, the 4th International Symposium on Highway Geometric Design, November.

Sil, G., Maji, A., Nama, S., Maurya, A. K. (2019). Operating speed prediction model as a tool for consistency based geometric design of four-lane divided highways. Transport, 34(4), 425-436. https://doi.org/10.3846/transport.2019.10715

Torbic, D. J., Harwood, D. W., Richard, K. R., & Glauz, W. D. (2004). Determining critical length of grade for geometric design of vertical alignments. Transportation research record. 1881(1), 36-45.

Wang, X., & Wang, X. (2018). Speed change behavior on combined horizontal and vertical curves: driving simulator-based analysis. Accident Analysis & Prevention 119, 215-224.

Wang, X., Wang, X., Cai, B., Liu, J. (2019). Combined alignment effects on deceleration and acceleration: A driving simulator study, Transportation Research Part C: Emerging Technologies. 104, 172-183. https://doi.org/10.1016/j.trc.2019.04.027.

Urban Road Maintenance in Taoyuan City, Taiwan: Exploring the Benefits of Performance-based Contracting

Yi-Shain Chiou [1], Pin-Yu Song [2], Min-Che Ho [3], Li-Ling Huang [4], Cheng-Ju Huang [5,*], Ping-Jen Song [6]

[1]National Central University, Taiwan / lettermail64@gmail.com
[2] National Central University, Taiwan / 110382002@cc.ncu.edu.tw
[3] National Central University, Taiwan / b1231520002000@hotmail.com
[4] National Central University, Taiwan / irenahf@gmail.com
[5] National Central University, Taiwan / q1w4e7r8@gmail.com
[6] National Taiwan University, Taiwan / pollysong921217@gmail.com

ABSTRACT

Taoyuan City's embrace of performance-based contracts for urban road maintenance since 2020 marks a significant advancement in Taiwan's administrative approach. With over three years of maintenance operations post-construction completion in 2021, analyzing the impact of these contracts is crucial for refining their execution and maximizing their benefits. This study focuses on evaluating road deterioration trends during the maintenance phase following the adoption of performance-based contracts in Taoyuan City. Through meticulous data collection and analysis, researchers have observed a notable decline in both the frequency and severity of road deterioration incidents, underscoring the positive impact of these contracts on infrastructure quality and maintenance effectiveness. Clear performance indicators and thresholds have been instrumental in enabling proactive intervention and timely remediation efforts. Regular tracking reports facilitate ongoing performance assessment, empowering stakeholders to make data-driven decisions and optimize maintenance efforts. Furthermore, the streamlined administrative processes associated with performance-based contracts have led to more efficient resource allocation and utilization, enhancing transparency, accountability, and cost-effectiveness in maintenance operations. The adoption of performance-based contracts has created a win-win-win scenario for all stakeholders involved. The organizing authority benefits from improved infrastructure quality and reduced administrative burden, while contracting companies gain incentives for delivering high-quality services. Most importantly, the public enjoys safer and more reliable roads, enhancing mobility and quality of life. Looking ahead, the insights gleaned from Taoyuan City's experience with performance-based contracts offer valuable lessons for other jurisdictions aiming to optimize infrastructure maintenance efforts and deliver better outcomes for communities. Sharing best practices and lessons learned can empower governments and businesses to achieve greater efficiency and effectiveness in their maintenance operations.

Keywords: Performance-based contracts, Performance indicators, Urban road maintenance.

1. INTRODUCTION

Performance-Based Contracts (PBCs) focus on output and performance targets instead of traditional technology and process-oriented measures. When applied to road maintenance, PBCs entail payments to contractors upon meeting or exceeding set performance indicators. This approach encourages contractor innovation, benefiting owners, contractors, and public users. Clear performance indicators are essential to minimize disputes and ensure contract execution.

Globally, PBCs have been used for over two decades, showing advantages such as:

- Clear maintenance standards
- Reduced workload for maintenance units
- Fewer claims and changes
- Encouraging contractor innovation and R&D
- Enhanced quality
- Cost savings

This study examines the "2019 Taoyuan City Road Maintenance PBC Project" (PBC 1.0), covering roads around the Qingpu Special District. Initial tasks included road inspections, defining contract sections, performance indicators, maintenance pricing methods, and verification mechanisms, alongside organizing briefings and drafting bidding documents. The contractor began road design and construction in July 2020, with a five-year maintenance period starting in April 2021 and ending in April 2026. Continuous monitoring of maintenance activities through performance indicators is in place.

As the project nears three years into the maintenance period, this study aims to analyze the trends of performance indicators collected over this period. The goal is to assess the rationality of verification mechanisms and performance indicators to improve PBC applications in road maintenance.

2. LITERATURE REVIEW AND CURRENT STATUS

2.1 Principles For Setting Performance Indicators In Performance-Based Contracts

The U.S. Department of Defense's 2000 "Guidebook for Performance-Based Services Acquisition (PBSA)" outlines PBCs as contracts that specify clear goals for outcomes and service levels, measured by various strategies and techniques. Performance is assessed based on results, not processes, to foster innovation, enhance competition, save costs, and transfer risks to contractors.

Key Elements of PBCs:

- Performance Work Statement (PWS): Defines required measurable outcomes rather than methods.
- Measurable Performance Standards: Sets clear, acceptable service standards.
- Remedies: Includes penalties for underperformance and rewards for exceeding expectations.
- Performance Assessment Plan: Details how the public sector will evaluate contractor performance, using methods like sampling, trend analysis, customer feedback, and third-party oversight.

Performance indicators must adhere to the SMART principles:

- Specific: Clear and unambiguous

- Measurable: Quantifiable and assessable
- Achievable: Realistically attainable
- Realistic: Practical within the project context
- Time-bound: Defined within a specific timeframe

Considerations:

- Clarity and Measurability: Indicators should be clear and operable.
- Threshold Values: Set initial and target thresholds based on project specifics.
- Measurement Procedures: Define reliable measurement methods.
- Response Time (TOR): Consider expected response times for both owner and contractor.

2.2 Introduction To PBC 1.0 In Qingpu Special District, Taoyuan City

In August 2019, the Taoyuan City Government launched the PBC 1.0 project for road maintenance. After three contractor workshops and two investment briefings, the project was awarded in July 2020. Design and construction began immediately, with the completion report submitted in January 2021. The five-year maintenance period started in April 2021.

The project covers several key road segments in the Qingpu Special District:

- (A) Linghang North Road
- (B) High-Speed Rail South Road
- (C) High-Speed Rail North Road
- (D) Gongyuan Road
- (E) Qingpu Road
- (F) High-Speed Rail Station Front East Road

The total area is 263,332 square meters, with 80,000 square meters of severely damaged sections repaved, the basic information of the road segments is shown in Table 1.

Table 1 Basic information of the road segments.

Road Name		Road Length (m)	Number of Lanes	Maintenance Area (m²)
A	Linghang North Road	4,349.89	6	143,779.65
B	High-Speed Rail South Road	1,585.69	6~7	58,096.28
C	High-Speed Rail North Road	1,566.98	6	36,325.91
D	Gongyuan Road	561.02	4	6,171.22
E	Qingpu Road	553.74	6	12,182.28
F	High-Speed Rail Station Front East Road	484.1	4	6,777.4
Total		9,101.41	-	263,332.74

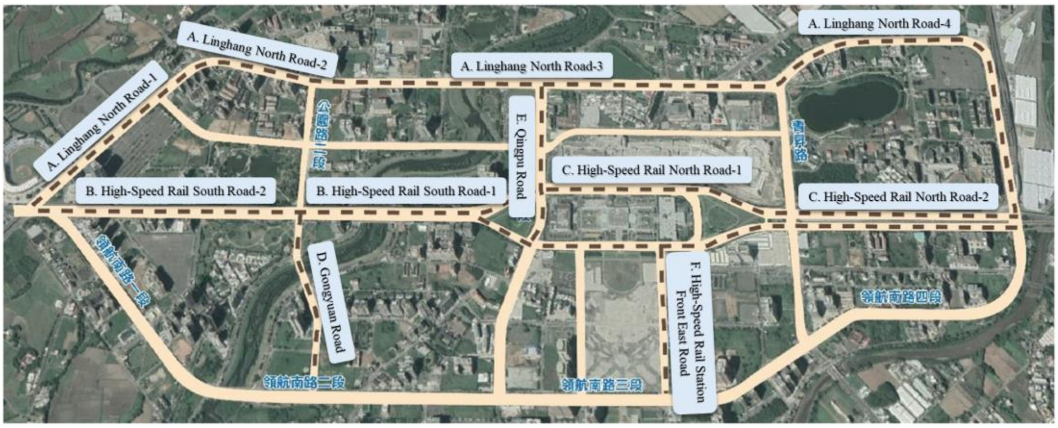

Figure 1 The range of patrol sections for PBC 1.0 in Qingpu Special District, Taoyuan City.

2.3 The Performance Indicators And Verification Mechanisms For PBC 1.0 In Qingpu Special District, Taoyuan City

Road quality inspection encompasses various aspects such as pavement smoothness, road markings, cleanliness, etc. The execution team has carefully studied and selected appropriate quality aspects to establish clear, quantifiable, easily measurable, and unambiguous performance indicators. The verification mechanisms for these indicators are based on the following principles:

- Establish Clear, Quantifiable, Easily Measurable, and Unambiguous Performance Indicators: Focus primarily on pavement and road markings, excluding vegetation and traffic signs.
- Develop Effective Performance Verification Mechanisms: Include penalties or deductions for underperformance.
- Guide PBC Contractors towards Achieving Established Road Maintenance Goals: Encourage contractors to meet the road maintenance objectives set by the authorities.

As the first project in Taiwan to introduce PBC in road maintenance, prior to awarding the PBC contract, a Professional Construction Management (PCM) unit was commissioned to conduct road surveys and asset inspections. 14 performance indicators were established (including 10 technical indicators and 4 managerial indicators) for subsequent acceptance and performance tracking. Additionally, AI-integrated inspection equipment was introduced for seamless patrol and repair operations, facilitating automatic reporting and eliminating manual processing time by integrating all maintenance data, including maintenance reports and construction inspection forms, into the cloud for storage.

The project incorporates 10 technical indicators (PI-1.1 to PI-1.10) and 4 managerial indicators (PI-2.1 to PI-2.4). The verification methods are as follows:

- For the first 9 technical indicators (PI-1.1 to PI-1.9), asset inventory and maintenance effectiveness reports are checked monthly.
- For the 10th technical indicator (PI-1.10) and the 5th to 8th managerial indicators (PI-2.1 to PI-2.4), semi-annual IRI (International Roughness Index) testing and maintenance performance reports are utilized for verification.

The 14 indicators and their respective criteria, measurement methods, and Time of Response (TOR) regulations are detailed in Tables 2 and 3.

Table 2 The list of the 10 technical indicators.

Performance Indicator (PI)	Criteria	Measurement Method	Tolerance or Time of Response (TOR)
Potholes (PI-1.1)	(1) Diameter not exceeding 150mm. (2) Number of pits with a diameter exceeding 100mm does not exceed 3.	Visual inspection, ruler.	Immediate improvement.
Patches (PI-1.2)	(1) Should be square or rectangular. (2) Flush with the adjoining pavement. (3) Material used is the same as the adjoining pavement. (4) Width does not exceed 5 mm. (5) Height difference with adjoining pavement does not exceed ± 6 mm.	Visual inspection, ruler, transparent ruler.	Within 3 days.
Single Cracks (PI-1.3)	Linear opening width does not exceed 5mm.	Transparent ruler.	Within 7 days.

Composite Cracks (PI-1.4)	Area of composite cracks does not exceed 50 m^2.	Length and width product within the area.	Composite cracks must be filled and sealed within 7 days of discovery. For composite cracks exceeding 50m^2, the affected area should be milled to a depth of at least 3 cm.
Ruts (PI-1.5)	(1) Depth does not exceed 20mm. (2) Continuous length of depth exceeding 10mm does not exceed 30 m.	Three-meter straight edge.	Within 14 days.
Loose and Peeling (PI-1.6)	No loose or peeling material.	Visual observation.	Within 7 days.
Edge Material Loose (PI-1.7)	No loose or detached blocks.	Detached blocks.Visual observation.	Within 7 days.
Pavement-to-Manhole Height Difference (PI-1.8)	Height difference between pavement and manhole does not exceed 6 mm.	Three-meter straight edge, ruler.	Within 7 days.
Pavement Heaves or Depressions (PI-1.9)	Diameter does not exceed 300 mm.	Three-meter straight edge, ruler.	Within 7 days.
International Roughness Index (IRI) (PI-1.10)	(1) The qualified value after milling is 3.5. (2) During maintenance, the International Roughness Index (IRI) qualified value increases by 0.1 every six months, starting at 3.6 for the first period and reaching a maximum of 4.2.	Inspection vehicle, half-yearly inspection.	After an unqualified inspection, milling of at least 3cm must be carried out within 14 days of notification from the authority, and the qualified standard must be met.

Table 3 The list of the 4 managerial indicators.

Performance Indicator (PI)	Criteria	Measurement Method	Tolerance or Time of Response (TOR)
Pothole Reporting (PI-2.1)	No records of reporting later than the month or other forms after 1999.	Monthly record inventory.	Payment suspension, improvement to be submitted within 7 days.
Emergency Road Damage Repair (PI-2.2)	Emergency repairs must be completed within 4 hours after notification.	Monthly record inventory.	Payment suspension, improvement to be submitted within 7 days.
Inaccurate Inspection (PI-2.3)	Daily inspections must be conducted.	Monthly record inventory, ad-hoc checks.	Payment suspension, improvement to be submitted within 7 days.
Asset Inventory and Management Inaccuracy (PI-2.4)	No records of inaccurate inventory or falsification.	Monthly record inventory, ad-hoc checks.	Payment suspension, improvement to be submitted within 7 days.

3. RESEARCH METHODOLOGY AND DATA COLLECTION PROCESS

3.1 The Pre-Construction Survey For Roadworks

According to the contract, the PBC contractor is responsible for warranty maintenance for milled sections, while they handle inspection and reporting for the remaining areas. To improve road service quality and ensure precise material selection, this study conducted an IRI survey. From 260,000 square meters, segments with an IRI over 4 were selected, totaling 140,000 square meters. We prioritized contiguous sections to avoid fragmented repairs, excluded areas around developments and public projects, and referenced PCI values and on-site surveys. This led to the final selection of 80,000 square meters for milling and repair. The pre-construction IRI survey results (partial) are summarized in Table 4.

Table 4 Pre-construction IRI survey results (partial).

Section	CL-1 High-Speed Rail North Road Sections 1 & 2	Graph of IRI Survey Results (Red Box Indicates Continuous Selection Range)
Length (m)	804	
Mileage	**IRI**	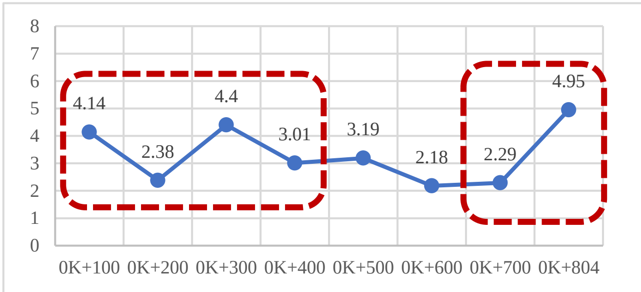
0K+100	4.14	
0K+200	2.38	
0K+300	4.40	
0K+400	3.01	
0K+500	3.19	
0K+600	2.18	
0K+700	2.29	
0K+804	4.95	

3.2 Road Maintenance Period Inspection Operations And Performance Evaluation

The project divided the road into units of 100 meters each, totaling 786 units, and collected data for each unit. It employed a fully electric AI smart inspection vehicle equipped with detection equipment (E-PCI, E-IRI, and 360-degree panoramic imaging). The vehicle's positioning system had an error margin of only 10-20 centimeters, enabling precise monthly tracking and accurate location for asset inventory. Through precise positioning and data analysis based on indicators, the data could be effectively integrated into a network platform for lifecycle analysis of the entire road network. This platform can display the pavement condition of each unit separately and further facilitate inquiries and comparisons of inspection data between years and between sections.

The road inspection utilizes an AI smart inspection vehicle for daily checks. When the vehicle detects urgent potholes, a standby road repair vehicle is dispatched promptly for repairs. The equipment of the inspection vehicle and the interface of the road maintenance platform are shown in Figure 3 below.

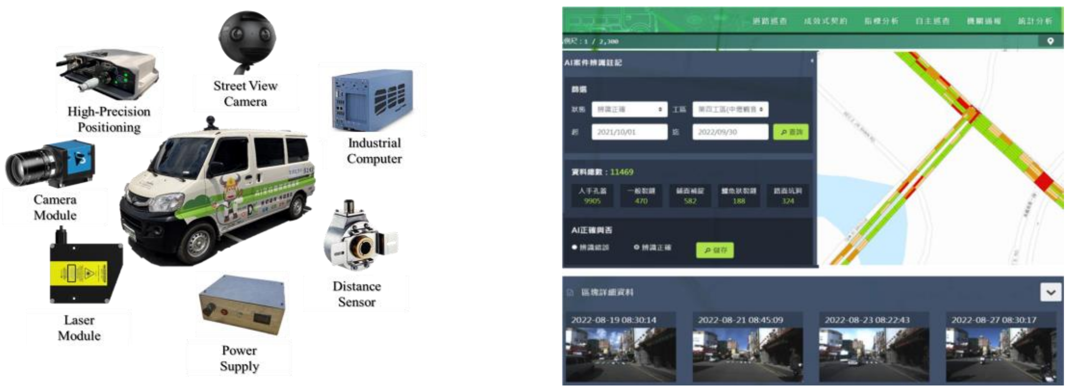

Figure 3 The equipment of the inspection vehicle and the interface of the road maintenance platform.

4. RESULTS AND DISCUSSION

4.1 Consolidation Of Inspection Results

Based on the semi-annual review reports from the PBC contractor, covering the first to fifth periods of maintenance, spanning from April 2021 to September 2023, totaling 30 months, the effectiveness indicators during the maintenance period are summarized in Table 6 below.

Table 6 Maintenance period performance indicator statistical table.

First Period (Monthly Damage Quantity)						
2021-4	2021-5	2021-6	2021-7	2021-8	2021-9	**Total**
32	96	101	53	75	70	427
Second Period (Monthly Damage Quantity)						
2021-10	2021-11	2021-12	2022-1	2022-2	2022-3	**Total**
75	66	77	32	31	54	335
Third Period (Monthly Damage Quantity)						
2022-4	2022-5	2022-6	2022-7	2022-8	2022-9	**Total**
51	39	42	71	42	87	332
Fourth Period (Monthly Damage Quantity)						
2022-10	2022-11	2022-12	2023-1	2023-2	2023-3	**Total**
62	78	41	37	56	49	323
Fifth Period (Monthly Damage Quantity)						
2023-4	2023-5	2023-6	2023-7	2023-8	2023-9	**Total**
50	39	60	65	61	53	328

Breaking down the types of damages for each month further into the statistics of each indicator, as shown in Figure 4 below.

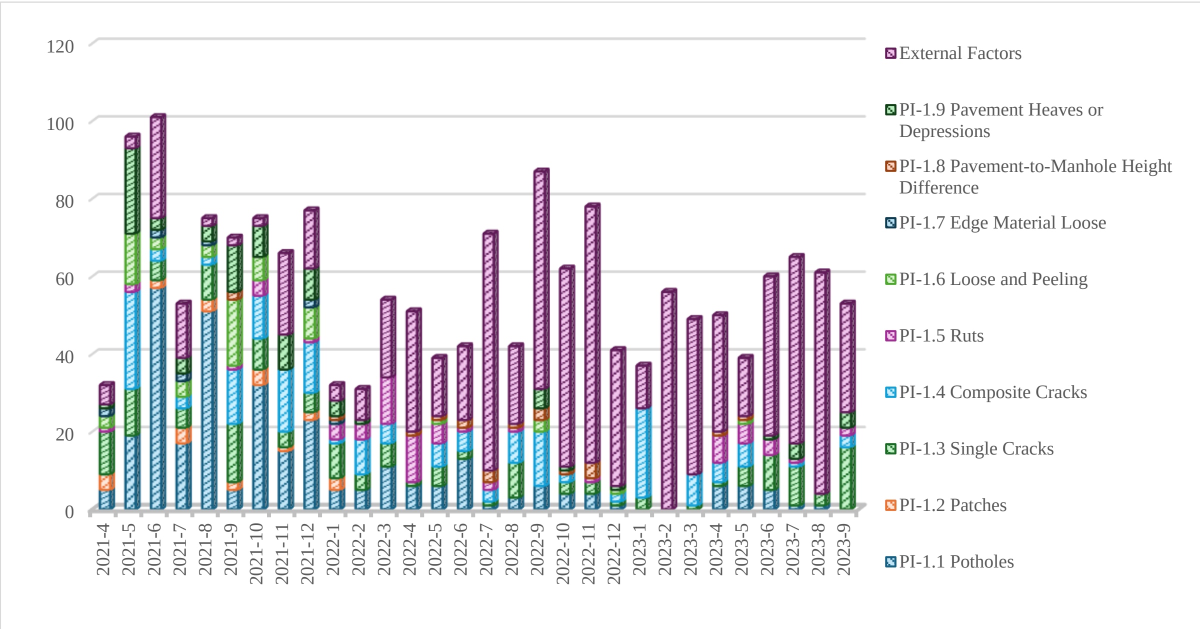

Figure 4 Maintenance period performance indicator statistics chart.

4.2 Discussion Of Inspection Results

- The benefits of the preliminary investigation help identify areas with severe road damage, allowing for focused repairs and ongoing monitoring. Additionally, it assists in observing road damage caused by surrounding construction projects, enabling timely reporting to the authorities.
- When grouped by semi-annual totals, the total number of damages for each period was: 427, 335, 332, 323, and 328, respectively. There was a significant decrease of approximately 21.55% in total damages when entering the second period, with subsequent periods showing a stable trend.
- Observing the bar chart, it's noticeable that the number of "External Factors" caused by surrounding construction and pipeline excavation operations increased significantly. If these "external factors" are excluded from each month's calculation, and only damages responsible for maintenance by the PBC contractor are considered, the total damages for each period were: 375, 265, 130, 64, and 109, respectively, showing a more significant reduction.
- In the statistics for the first maintenance period, the number of damages was mainly concentrated in May and June of 2021, with 97 and 101 occurrences, respectively, primarily consisting of potholes (PI-1.1), composite pavement cracks (PI-1.4), and pavement heaves or depressions (PI-1.9).
- When comparing the fifth maintenance period with the first, there was a significant decrease in the number of severe damage types such as potholes (PI-1.1) and pavement heaves or depressions (PI-1.9), reduced by 87.66% and 100%, respectively.
- Observing each year individually, during the summer months, the number of items such as potholes (PI-1.1) and composite pavement cracks (PI-1.4) tends to be higher compared to other months. This may be due to Taiwan's rainy season from May to June, as well as typhoons and afternoon thunderstorms in July and August, along with nearby construction and pipeline projects, all contributing to frequent road damage during this time.
- With each maintenance period, the proportion of potholes (PI-1.1) and pavement heaves or depressions (PI-1.9) to the total damage decreases gradually, transitioning to pavement single cracks (PI-1.3) and pavement composite cracks (PI-1.4). This downgrade in severity helps to slow down the deterioration rate and reduce the need for repair expenses, ultimately enhancing road safety.
- For the IRI survey results are shown in Figure 5 below, tracking was conducted based on the 10th technical indicators (PI-1.10). Initially, after the completion of construction, there was a significant improvement in the IRI values. Throughout the subsequent maintenance period, the IRI values consistently remained within the set standards, indicating effective maintenance performance.

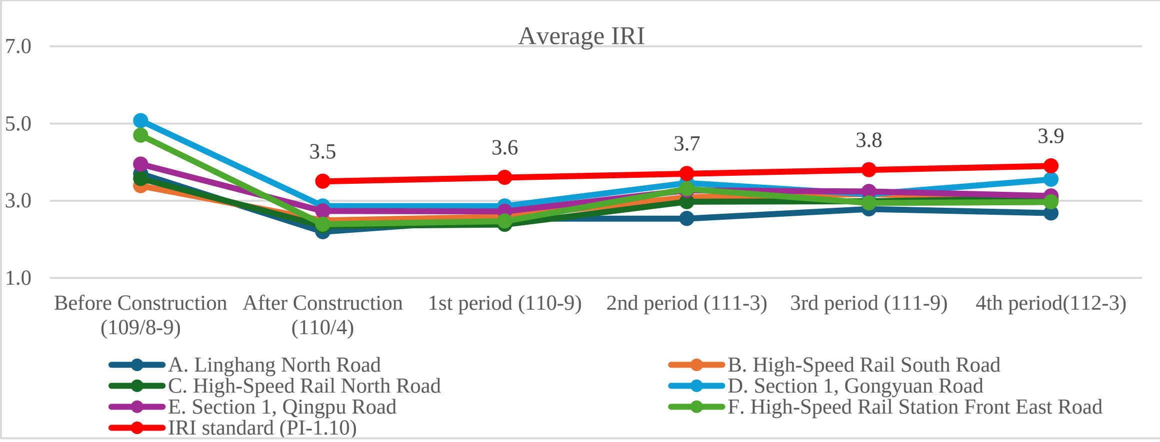

Figure 5 IRI Survey Results

- The PCI survey results are shown in Figure 6 below. Similarly, there is a noticeable improvement after construction. During the maintenance period, all segments exhibit similar PCI trends. However, it is observed that the PCI of segment B, High-Speed Rail South Road, remains relatively low. This is likely due to the significant traffic volume on this road, as it is a major route for accessing the high-speed rail, resulting in more pronounced damage.

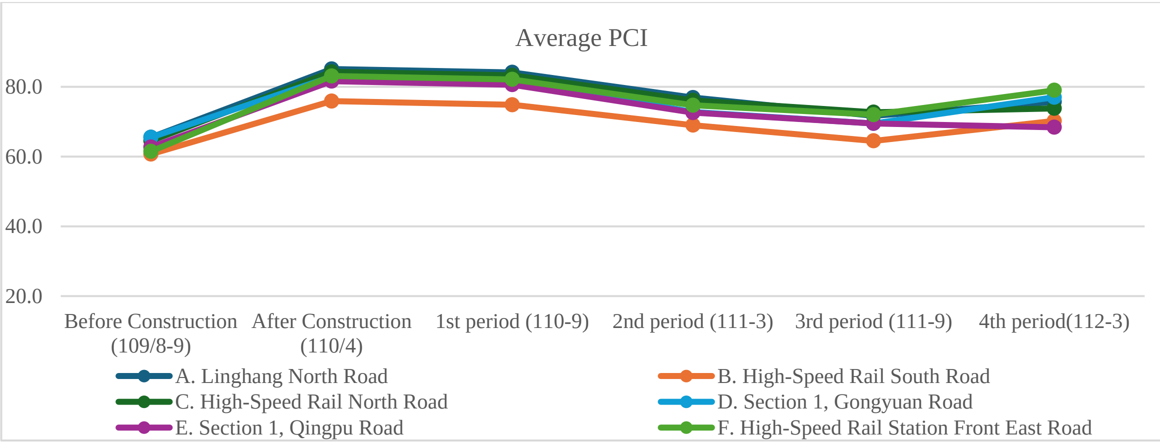

Figure 6 PCI Survey Results

4.3 Extended Benefits of Performance-Based Contracts

(1) Roads and Auxiliary Facilities

The maintenance contractor in 2022 collected datas to compare the differences before and after implementing performance-based contract maintenance. The items collected include the block dispatch area, number of pothole repairs, number of auxiliary facility repairs, number of traffic accidents, and number of national compensation cases.

a. Block Dispatch Area

The annual block dispatch areas for road maintenance are shown in the following chart. After implementing the performance-based contract, the area decreased from 94,588 m² to 7,855 m², a reduction of 92%, and has remained at a more stable level.

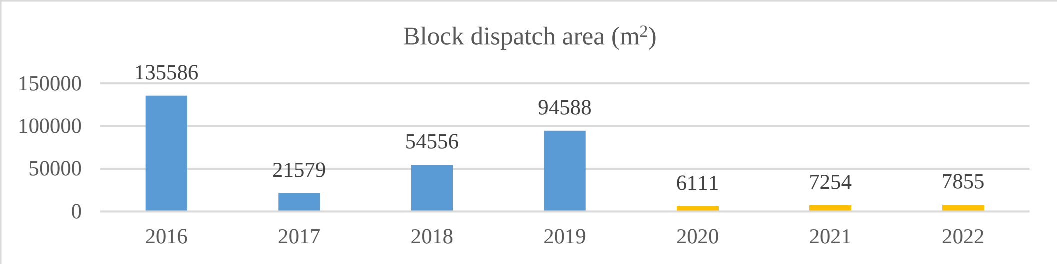

Figure 7 Block Dispatch Area Statistical Results

b. Number of Pothole Repairs

The annual number of pothole repairs is shown in the following chart. After implementing the performance-based contract, the number decreased from 533 to 182, a reduction of 66%.

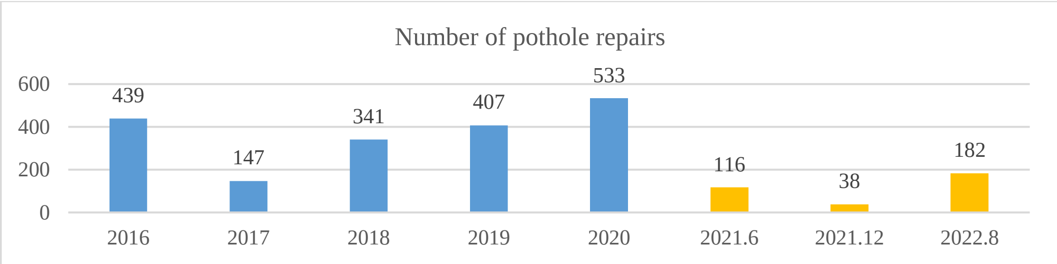

Figure 8 Number of Pothole Repairs Statistical Results

c. Number of Auxiliary Facility Repairs

The annual number of auxiliary facility repairs is shown in the following chart. After implementing the performance-based contract, the number decreased from 114 to 17, a reduction of 85%, with a clear trend of further reduction each year.

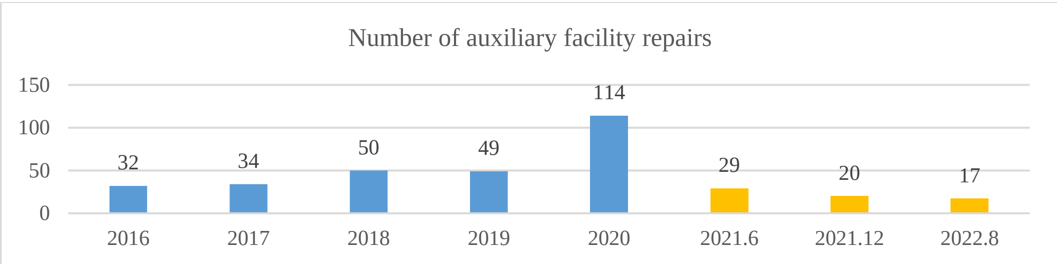

Figure 9 Number of Auxiliary Facility Repairs Statistical Results

d. Number of Traffic Accidents

The annual number of traffic accidents is shown in the following chart. After implementing the performance-based contract, the number decreased from 91 to 20, a reduction of 75%, and a clear trend of further reduction each year is observed.

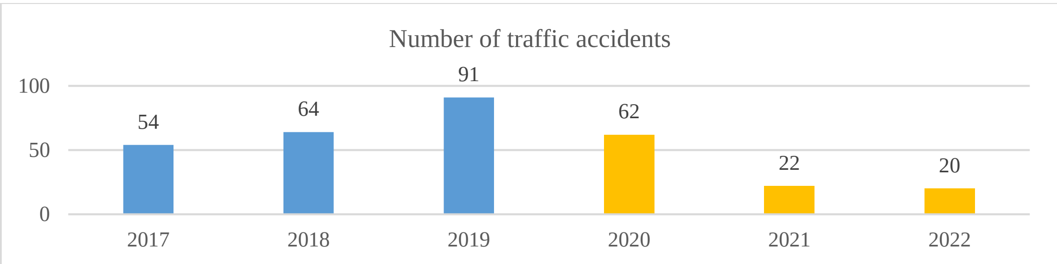

Figure 10 Number of Traffic Accidents Statistical Results

e. Number of National Compensation Cases

The annual number of national compensation cases is shown in the following chart. After implementing the performance-based contract, there have been no new national compensation cases.

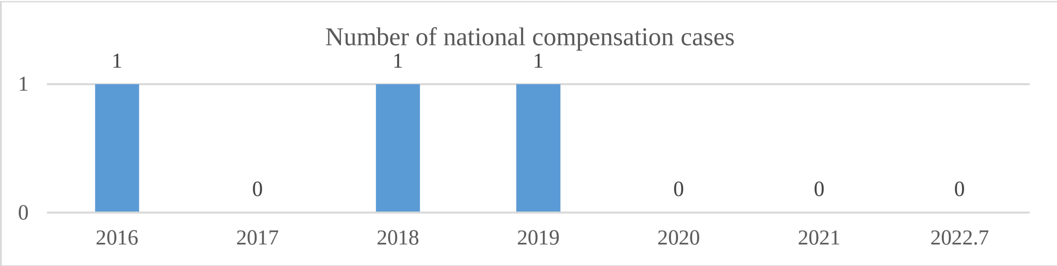

Figure 11 Number of National Compensation Cases Statistical Results

(2) Road Maintenance Costs

The project also conducted a cost comparison between performance-based contracts and traditional road maintenance contracts. Under the same maintenance period, this project not only inspected road conditions but also conducted inspections, inventory, and tracking of auxiliary facilities, sidewalks, street trees, and surrounding construction projects. These efforts, along with assisting in repair notifications, not only improved the response speed of maintenance work but also reduced indirect costs and administrative processes associated with performing different tasks separately. It is estimated that the road maintenance agency could save approximately 28% of its budget annually.

5. CONCLUSIONS

- This study investigates the application of Performance-Based Contracting (PBC) for road maintenance in the Qingpu High-Speed Rail Special Zone in Taoyuan City, Taiwan. This project is Taiwan's first PBC implementation in road engineering, covering approximately three years of maintenance. By compiling and analyzing the performance indicators during the maintenance period, it is evident that PBC effectively optimizes road conditions, maintaining them at a superior standard.
- The discussion of the survey results shows that the total number of damages per period were 427, 335, 332, 323, and 328, respectively. There was a significant reduction of approximately 21.55% from the first to the second period, with numbers stabilizing thereafter. When excluding "external factors" for each month and considering only the damages for which the PBC contractor is responsible, the total damages per period were 375, 265, 130, 64, and 109, respectively, showing a more pronounced decrease.
- Due to Taiwan's seasonal climate factors, road damages such as potholes (PI-1.1) and composite pavement cracks (PI-1.4) occur more frequently during the summer months. The heavy rains from the monsoon season in May and June,

typhoons, and afternoon thunderstorms in July and August, along with shallow-buried pipelines and ongoing construction projects, contribute to these damages.

- The PBC road maintenance approach effectively reduces severe damage types such as potholes (PI-1.1) and pavement heaves or depressions (PI-1.9) by 87.66% and 100%, respectively. The primary issues shift to single pavement cracks (PI-1.3) and composite pavement cracks (PI-1.4), reducing the severity of damage. This transition helps slow down the rate of deterioration, lowers maintenance costs, and enhances road safety.
- Regarding road maintenance costs, the project not only maintains the road surface but also integrates the inspection and reporting of surrounding public facilities, sidewalks, and street trees. Additionally, the downgrade in damage types results in cost savings for maintenance. The overall annual savings for the road management authority are estimated to be around 28% of the budget.
- In terms of road safety, the PBC maintenance approach reduces the number of potholes significantly. The frequency of pothole repairs has decreased by 66% compared to the pre-construction period. Moreover, the occurrence of traffic accidents has dropped by 75%, demonstrating significant benefits for road safety.

6. REFERENCES

Yang, Z., Yu, W., et al. (2012). Strengthening Road Surface Quality Integration Program - Establishment of Road Maintenance Effectiveness Contract Specifications. Transportation Research Institute, Ministry of Transportation.

Wu, Y. (2015). Analysis of Key Success Factors in Implementing Performance-Based Contracts. Graduate Institute of Construction Management, National Central University.

Xie, D. (2016). Application of Performance-Based Contracts in Technical Project Management Services. Graduate Institute of Construction Management, National Central University.

United States General Accounting. (2002). Guidance Needed for Using Performance-Based Service Contracting.

Gansler, J. S. (2000). Guidebook for Performance-Based Services Acquisition (PBSA) in the Department of Defense. Retrieved from: http://www.acq.osd.mil/dpap/Docs/pbsaguide010201.pdf

Queiroz, C. (2007). Recent Experience and Lessons Learned with the Use of Performance Based Contracts. Regional Workshop on Public-Private Partnership in Transport, Transport and Telecommunication Institute, Riga, Latvia.

Public Construction Commission, Executive Yuan. (Accessed 2024). Tender Notice Template. http://www.pcc.gov.tw/upload/article/970709-1(1).pdf

Performance-based Road Rehabilitation and Maintenance Contracts (CREMA) in Argentina.

Chen, Y. (2004). Application of Life Cycle Cost Analysis in Highway Pavement Maintenance Programs. Master's Thesis, Chung Hua University.

Teng, Z., Zeng, G. (1989). Connotation, Characteristics, and Application of Analytic Hierarchy Process (AHP) (Part 1). Chinese Journal of Statistics, 27(6), 13707-13724.

A Survey and Analysis of User Perceptions Towards the M-Flow Toll Collection System

Thitima Wasanapitranont[1,*], Arnon Phuekfhon[2], Agachai Sumalee[2], Thanasak Wongtanakitcharoen[3]

[1]Department of Logistics Management, King Mongkut's Institute of Technology Ladkrabang, Bangkok, Thailand, name_thitima@hotmail.com
[2]Transcode Co.,Ltd., Bangkok, Thailand, asumalee@gmail.com
[3]Department of Highways, Ministry of Transportation (Thailand), Bangkok, Thailand, wongtanakitcharoen@gmail.com

ABSTRACT

The introduction of the Multi-Lane Free Flow (M-Flow) toll collection system by the Department of Highways on Intercity Highway No. 9, encompassing toll gates such as Thap Chang 1, Thap Chang 2, Thanyaburi 1, and Thanyaburi 2, aims to mitigate traffic congestion, a significant challenge faced by the logistics industry, impacting delivery schedules and transportation expenses. Despite its potential benefits, the adoption of the M-Flow system among drivers remains subdued, with many opting for traditional cash payments or alternative systems like M-Pass/ Easy Pass. In response, this study employs statistical analysis, particularly the Independent Samples F-Test, to discern key factors influencing user preferences. Through an examination of gender and payment method differentiations, this research scrutinizes concerns during the transition from non-user status to M-Flow adoption, highlighting issues such as complex payment mechanisms, insufficient system information, regulatory ambiguities, challenges in non-subscriber usage, and mobile phone compatibility issues. Additionally, observations on the cumbersome membership application process, toll collection inaccuracies, and limited access to historical toll payment data are presented. Insights gleaned from focus group interviews, particularly on promotional strategies and advertisements for M-Flow, further inform the study. Recommendations include leveraging social marketing campaigns and implementing the 4Ps marketing mix framework to enhance user attraction and engagement.

Keywords: Free-Flow tolling, Expressway, Motorway, Customer, Marketing strategies

1. INTRODUCTION

The Intercity Motorways initiative is a key project for the Department of Highways, serving as a significant strategic endeavor. These motorways are engineered to circumvent urban areas in each province, enabling travelers to reach their destinations with greater speed and safety. The development of these motorways contributes not only to the enhancement of the country's logistics infrastructure but also to the growth of Thailand's tourism industry. Below are some examples of Intercity Motorways managed by the Department of Highways:

1. Special Highway No. 7, which is the new Bangkok - Chonburi - Pattaya route (Motorway).
2. Special Highway No. 9, which is the eastern outer ring road (Bang Pa-in - Bang Phli section).

With special highways, drivers are obligated to pay toll fees, a process that can cause delays. Initially, the Department of Highways implemented the Manual Toll Collection System (MTC), leading to delays in toll fee preparation and resulting in traffic congestion. To address these issues, the Electronic Toll Collection System (ETC) was introduced to work alongside the Manual Toll Collection System. The ETC system uses an RFID tag placed at the front of the vehicle, removing the need for drivers to prepare fees in advance. However, there are instances when the RFID tag is not detected by the RFID reader, causing traffic congestion at toll checkpoints. Consequently, traffic congestion remains a recurring issue.

To address these concerns, in 2022, the Department of Highways has introduced the Multi-Lane Free Flow (M-Flow), a free-flow toll collection system on Intercity Highway No. 9, with toll gates at Thap Chang 1, Thap Chang 2, Thanyaburi 1, and Thanyaburi 2. This system has the capability to effectively eliminate the stop-and-go traffic at toll plazas. Despite its introduction, several issues have been identified with the M-Flow system including a complex and unclear registration process, a lacking public relations strategy, and ineffective marketing campaigns and promotions.

The authors have thus initiated a survey to examine user behavior and other factors impacting the M-Flow system on Intercity Highway No. 9, in addition to conducting focus group interviews, to identify and address the most critical issues in using the M-Flow system. This initiative is being undertaken in conjunction with marketing campaigns that offer promotional incentives and an appealing solution to encourage more users to contribute to the elimination of stop-and-go traffic at toll plazas.

2. PURPOSES OF THE STUDY

1) To examine demographic variables such as gender and payment methods, aiming to determine general information regarding customer behavior and attitudes towards the M-Flow system among individuals aged 18 to over 60 years who drive cars.

2) To identify the elements related to the development and implementation of M-Flow in collaboration with new users.

3) To deploy promotional strategies to attract new users.

3. LITERATURE REVIEW

3.1 The Multi-Lane Free-Flow Toll Collection System in Thailand

(Department of Highways, 2024) In the past, Thailand relied exclusively on the Manual Toll Collection System for toll collection. Due to delays in toll fee preparation and the resultant stop-and-go traffic at toll plazas, the Electronic Toll Collection System (ETC) was introduced to operate alongside the Manual Toll Collection System. However, issues such as the failure of RFID readers have been observed with this system. To address these challenges, the Department of Highways has developed the Multi-Lane Free-Flow system (M-Flow), the latest advancement in toll collection technology that incorporates Artificial Intelligence (AI). This system integrates Video Tolling and Automatic Vehicle Identification (AVI), with the AVI component using Radio Frequency Identification (RFID) to monitor and identify vehicles. Vehicles can pass through toll checkpoints without stopping for toll payments. M-Flow supports speeds of up to 160 km/hour and accommodates various types of vehicles, including four-wheel, six-wheel, and over-six-wheel vehicles. Additionally, users have the convenience of postpaid toll payments, providing a significant level of flexibility and ease of use.

M-Flow membership is classified into three groups: Member Tier 1, Tier 2, and non-members. To become a Tier 1 member, users must register through a website or mobile application, whereas Tier 2 members must register via the Line Official Account. Non-members refer to users who utilize the M-Flow system but choose not to enroll as members. These distinctions highlight the variations among the different types of membership.

Table 1 Differences among each type of member.

Types of members	Registration	Verification	Functions
Tier 1 member	Website/Mobile application	Waiting for SMS	• Access to usage records is provided • Information on payment transactions is accessible • The payment method is changeable • Users can obtain receipts • Additional vehicles can be included
Tier 2 member	Line Official Account	The process can be used immediately	• The user receives the Line notification upon passing through the M-Flow
Non-member	-	-	• All functions are not accessible to both Tier 1 and Tier 2 members

(Transcode, 2023)

3.2 The Toll Collection Systems in International Countries

(National Payments Corporation of India, n.d.) The earliest toll collection method was the Manual Tolling System, which required significant cash handling and manual labor. This method employed single-lane free flow with barriers. Over time, operators improved the system by integrating modern technologies such as Dedicated Short-Range Communications (DSRC), Radio-Frequency Identification (RFID), and Global Navigation Satellite Systems (GNSS), while maintaining the single-lane free flow setup. These advancements are now key elements in current toll collection systems, which include multi-lane free-flow methods used internationally. For example, Malaysia's Electronic Toll Collection (ETC) system, "Touch 'n Go" (TNG), uses RFID technology to support a free-flow tolling approach. Vehicles are fitted with RFID tags or stickers for tracking. This system also provides users with the convenience of pre-loading credit onto the RFID tags or linking them to credit or debit cards for automatic top-ups.

3.3 F-Test Analysis

(Salehi et al., 2019) examined various multiple testing methods commonly encountered in the literature. They employed null statistics derived from null permuted samples to attain more accurate p-value estimates. While some statistical tests can be adapted to null statistics for scenarios involving two independent groups, the authors introduced a novel statistic and its corresponding F-test tailored for analyzing three or more groups. Simulation results demonstrated that their proposed method yielded a narrower interquartile range (IQR) compared to the conventional permutation method, resulting in more precise p-value estimates than alternative approaches.

3.2.1 F-Test Formula

(CUEMATH, n.d.) discussed that the F-Test is employed to analysis the equality of variances through hypothesis testing. The formula for the F-Test varies depending on the type of hypothesis test being conducted, as illustrated below.

- **Left Tailed Test**

  Null Hypothesis: $H_0 : \sigma_1^2 = \sigma_2^2$

  Alternate Hypothesis: $H_1 : \sigma_1^2 < \sigma_2^2$

  Decision Criteria: The null hypothesis is rejected if the F statistic is less than the critical F value.

- **Right Tailed Test**

  Null Hypothesis: $H_0 : \sigma_1^2 = \sigma_2^2$

  Alternate Hypothesis: $H_1 : \sigma_1^2 > \sigma_2^2$

  Decision Criteria: The null hypothesis is rejected if the F statistic is greater than the critical F value.

- **Two Tailed Test**

  Null Hypothesis: $H_0 : \sigma_1^2 = \sigma_2^2$

  Alternate Hypothesis: $H_1 : \sigma_1^2 \neq \sigma_2^2$

  Decision Criteria: The null hypothesis is rejected if the F statistic is greater than the critical F value.

4. MATERIAL AND METHODS

This research relies on data from surveys and focus group interviews. Data obtained from the survey will be analyzed using SPSS, a statistical software program, to conduct Independent Samples F-Test analysis, which aims to identify specific factors for developing a marketing campaign. Moreover, data from focus group interviews serves to further support the design of effective marketing campaigns intended to attract new users as well.

4.1 Collection of Survey Data

The survey was conducted to gather insights from both users and non-users of the M-Flow system. The authors plan to use Taro Yamane's sample size calculation table, which specifies a sample size of 400 for populations exceeding 100,000. However, to minimize data error and align with the defined project scope, the consultant will collect data from a sample of 3,000, significantly exceeding the sample size indicated in Taro Yamane's calculation table. Information was gathered through online channels via Google Forms and onsite at rest areas. The questionnaire is divided into three sections:

Section 1: Demographic characteristics of drivers

Section 2: Experiences, issues, satisfaction, and recommendations from users and non-users of the M-Flow system

Section 3: User's media consumption patterns and their preferred media channels

4.2 Data Collection for Focus Group Interviews

The focus group interviews were conducted at King Mongkut's Institute of Technology Ladkrabang between March 23rd and 24th, 2024. These interviews were divided into three groups: current users, potential users, and non-users of the M-Flow system. The interviews were conducted in six rounds, with each group participating in two rounds. Each round included approximately six to seven participants. The aim was to gather insights into user behaviors and obtain recommendations, such as promotional campaigns, for increasing the number of M-Flow users in the future.

4.3 Variables in Research

This study aims to identify the factors related to the development and implementation of M-Flow in collaboration with new users. The variables included in the research are as follows:

1. Independent variables
    - Factors that if non-users switch to the M-Flow system, to what extent are they concerned about the following issues?
2. Dependent variables
    - Gender
    - Type of payment

5. RESULTS

Using a dataset comprising 3,000 participants, the analysis includes both users and non-users of M-Flow, regardless of vehicle ownership. However, recognizing that data from current M-Flow users may not be relevant to the topic of attracting new users, the focus shifts to 952 individuals who neither utilize M-Flow nor own cars. Additionally, the research examined only sections 1 and 2 of the survey data. The author aims to devise effective marketing strategies to attract new users to M-Flow. Subsequently, two datasets are used to examine the factors influencing the adoption of the M-Flow system, as described below.

5.1 Demographic Factors of Non-Users

5.1.1 Gender

Based on the data, there are 742 individuals, constituting 77.9 percent, who are male. In contrast, there are 210 individuals, making up 22.1 percent, who are female.

Table 2 Number and percentage of genders.

Gender				
	Frequency	**Percent**	**Valid Percent**	**Cumulative Percent**
Male	742	77.9	77.9	77.9
Female	210	22.1	22.1	100.0
Total	952	100.0	100.0	

(Thitima & Nattanon, 2024)

5.1.2 Type of Payment

According to the data, 441 individuals, accounting for 46.3 percent, use M-Pass or Easy Pass for fee payment, while 511 individuals, comprising 53.7 percent, pay by cash.

Table 3 The number and percentage of each type of payment.

Type of Payment				
	Frequency	**Percent**	**Valid Percent**	**Cumulative Percent**
M-Pass/ Easy Pass	441	46.3	46.3	46.3
Cash	511	53.7	53.7	100.0
Total	952	100.0	100.0	

(Thitima & Nattanon, 2024)

5.2 The Analyzed Results of Relationships Between Demographic Factors of Drivers and Their Level of Concern when Transitioning from Non-Users to the M-Flow System

The author examined how demographic factors among drivers influence their level of concern regarding specific issues when transitioning from non-users to the M-Flow system.

Table 4 Statistical values to compare the differences in the level of concern regarding specific issues when transitioning from non-users to the M-Flow system between male and female groups by the Independent Samples F-Test.

Independent Samples Test									
Factors	**Levene's Test for Equality of Variances**		**T-Test for Equality of Means**						
Complicated payment method	**F**	**Sig.**	**t**	**df.**	**Sig. (2-Tailed)**	**Mean Difference**	**Std Error**	**95% confidence**	
								Lower	**Upper**
Equal variances assumed	18.509	<.001	-2.033	950	.042	-.127	.063	-.250	-.004
Equal variances not assumed			-2.201	380.928	.028	-.127	.058	-.241	-.014
Unclear system information									
Equal variances assumed	11.995	<.001	-2.687	950	.007	-.154	.057	-.267	-.042
Equal variances not assumed			-2.873	372.768	.004	-.154	.054	-.260	-.049
Inappropriate usage regulations									
Equal variances assumed	7.912	.005	-2.842	950	.005	-.150	.053	-.254	-.046
Equal variances not assumed			-2.869	341.015	.004	-.150	.052	-.253	-.047
Difficulty using the system without a subscription									
Equal variances assumed	4.065	.044	-.922	950	.357	-.055	.060	-.172	.062
Equal variances not assumed			-.945	348.704	.345	-.055	.058	-.170	.060
Compatibility issues with mobile phone models									
Equal variances assumed	3.674	.056	-4.392	950	<.001	-.239	.055	-.346	-.132
Equal variances not assumed			-4.381	335.290	<.001	-.239	.055	-.347	-.132

(Thitima & Nattanon, 2024)

The statistical analysis, utilizing the Independent Samples F-Test as depicted in Table 4, focused on factors with a significance level below 0.05. It identified four primary concerns: complicated payment methods, unclear system information, inappropriate usage regulations, and difficulty using the system without a subscription. Consequently, the study prioritized the top 5 factors based on their F-Test values, revealing one additional significant factor: compatibility issues with mobile phone models. Addressing this identified concern could effectively alleviate drivers' worries about the M-Flow system.

Table 5 Statistical values to compare the differences in the level of concern regarding specific issues when transitioning from non-users to the M-Flow system in each type of payment by the Independent Samples F-Test.

Independent Samples Test									
Factors	**Levene's Test for Equality of Variances**		**T-Test for Equality of Means**						
Complicated and lengthy membership application process	**F**	**Sig.**	**t**	**df.**	**Sig. (2-Tailed)**	**Mean Difference**	**Std Error**	**95% confidence**	
								Lower	**Upper**
Equal variances assumed	3.918	.048	.217	950	.829	.011	.051	-.090	.112
Equal variances not assumed			.217	941.602	.828	.011	.051	-.089	.112
Inaccuracies in toll collection									
Equal variances assumed	3.425	.065	1.819	950	.069	.090	.050	-.007	.188
Equal variances not assumed			1.812	914.206	.070	.090	.050	-.008	.188
Inability to access past toll payment information									
Equal variances assumed	3.208	.074	.940	950	.347	.048	.051	-.052	.147
Equal variances not assumed			.938	920.666	.348	.048	.051	-.052	.147

(Thitima & Nattanon, 2024)

The analysis conducted using the Independent Samples F-Test, as presented in Table 5, focused on factors with a significance level below 0.05. The results highlighted concerns regarding the complex and time-consuming membership application process. However, only one factor exhibited a significant value below 0.05. Consequently, attention was directed to two additional factors based on their highest F-Test values. This approach revealed two more significant factors: inaccuracies in toll collection and the inability to access past toll payment information. Addressing these identified issues could effectively mitigate drivers' concerns about the M-Flow system.

5.3 Additional Marketing Campaigns and Suggestion to Attract New Users from the Focus Group Interviews

The focus group interviews aimed to directly gather insights from M9 users. The data obtained from these interviews is valuable for the M-Flow operator as it provides insights that can be used to develop effective marketing campaigns and choose appropriate advertisement channels to promote the adoption of M-Flow.

5.3.1 Place

There is a lack of awareness among certain individuals regarding M-Flow related information such as its introduction, promotional activities, and registration procedures.

To address these issues, interviewees recommended that the M-Flow operator enhance its advertising efforts through both online and offline channels. They also suggested collaborating with well-known influencers and setting up M-Flow booths in business areas such as office buildings or Department of Land Transport premises to reach a broader target audience.

5.3.2 Price and Promotion

The majority of interviewees anticipate promotions such as fee discounts, a "10 times free for 1 time" offer, and a point collection system. Regarding the point collection system, interviewees suggested that the M-Flow operator collaborate with hotels, restaurants, or gas stations to allow users to redeem points for benefits such as hotel room discounts, gas vouchers, and buffet coupons. Additionally, some interviewees proposed that M-Flow provide souvenirs to users, such as tumblers, umbrellas, bags, and screens bearing the M-Flow logo, as a means to attract new users and foster customer loyalty.

6. CONCLUSIONS

According to the statistical findings comparing the level of concern about specific issues when transitioning from non-users to the M-Flow system between male and female groups, effective marketing campaigns, such as the use of the 4Ps marketing mix and social marketing, are essential. The main concerns arise from inadequate advertising related to the M-Flow system. For example, users are not provided with clear information about the system, and misleading signage at the entrance to M-Flow lanes contributes to confusion. These signs suggest that only registered vehicles can use the lanes, leading many drivers to believe that non-members are not allowed. However, it's not widely known that non-members can still pay a fee through various channels. Furthermore, system efficiency and usage regulations present additional obstacles to the adoption of M-Flow. To address these challenges, the author suggests that the M-Flow operator focus on enhancing the system's public perception.

According to the results from statistical values to compare the differences in the level of concern regarding specific issues when transitioning from non-users to the M-Flow system in each type of payment, the key challenges mainly arise from specific functionalities of the M-Flow system, including the complex and lengthy membership application process. This hurdle inhibits the broader adoption of M-Flow. To overcome this, the system should provide a more streamlined and user-friendly application process. Furthermore, emphasizing the advantages of becoming a Tier 1 member could encourage more users to upgrade their membership status, thereby boosting the number of Tier 1 memberships and the overall user base.

The outcomes from focus group interviews are substantially connected to public relations, pricing, and promotional activities for attracting new users. To tackle these issues, the author recommends that the M-Flow operator work on improving the system's public image and initiate a promotional campaign to expand the user base.

The data from the analyzed results, insights from focus group interviewees, and my personal perspective can be consolidated into the 4Ps marketing mix to attract new users, as outlined in the following table:

Table 6 4Ps marketing mix to attract new users derived from analyzed results, focus group interviewees, and my perspective.

Product	Price	Place	Promotion
Expanding partnerships with more payment application providers such as True Money Wallet.	Fee discounts can be offered in the form of cash deductions or as a percentage off the total amount.	Partnering with a diverse range of online and offline platforms to improve the public perception and streamline the registration process for M-Flow.	Using 10 times free for 1 time.
Utilizing the annual sticker tag fees for tolling or implementing the vignette, which is an adhesive sticker valid for one year, for frequent users.	Offering discounts during special holidays such as free passes or weekend discounts.	Partnering with popular influencers, such as teaming up with "อู๋ Spin 9," to promote the M-Flow system through his channel.	Point accumulation system. Subsequently, accumulated points can be exchanged for hotel room discounts, vouchers for gasoline, and coupons for buffets.
The application should be compatible with a wide range of mobile phone types, including those operating on Android or iOS systems.		Setting up M-Flow booths in business areas such as office buildings or Department of Land Transport premises to reach a broader target audience.	Providing souvenirs for users.
The M-Flow operator should enhance the system's efficiency to dispatch bills to users within 15 minutes of toll collection.		Producing brief video clips about the M-Flow system, such as creating a clip in line with the current social trends at the time.	Invite-a-Friend campaign aimed at attracting new users by encouraging current users to invite new users, with both parties receiving special benefits from the campaign.
The Thai National Identification Card number could potentially be integrated with vital information from the Department of Land Transportation, such as vehicle ownership details or license plate numbers.			Once registered as Tier 1 members, M-Flow users can enjoy toll-free round trips for the first time.
All toll collection systems in Thailand should be unified into a single system.			

(Thitima & Nattanon, 2024)

These outcomes may offer compelling solutions for operators to develop strategies that increase user participation and facilitate the elimination of intermittent traffic congestion at toll plazas in the future.

7. ACKNOWLEDGEMENTS

I would like to extend my sincere gratitude to my advisor, Dr. Arnon Phuekfhon, for his invaluable insights and guidance throughout this work. Additionally, I wish to express my sincere thanks to the dedicated instructors from Transcode Co., Ltd., who offered crucial advice and support during this project. These instructors include Miss Doungporn Thatree, Miss Veerapattra Sakulamporn, and Miss Thanaporn Thanlawan. Their contributions have been instrumental to the success of this work, and I am deeply grateful for their expertise and assistance.

8. REFERENCES

Department of Highways. (2024). *Project to study guidelines and measures to promote the use of the automatic toll collection system without barriers (M-Flow system)*.

F test. (n.d.). Cuemath. https://www.cuemath.com/data/f-test/

M-Flow. (n.d.). *M-flow*. https://mflowthai.com/mflow/knowledge

National Payments Corporation of India. (n.d.). *Evolution and Innovations in the Tolling Industry*. https://www.npci.org.in/PDF/npci/knowledge-center/partner-whitepapers/Evolution-and-Innovations-in-the-Tolling-Industry.pdf

Salehi, M., Mohammadpour, A., & Mengersen, K. (2019). A new F-test applicable to large-scale data. *Journal of Statistical Theory and Applications*. https://doi.org/10.2991/jsta.d.191217.001

Wasanapitranont, T., & Rodthong, N. (2024). *Reviewing guidelines and strategies to promote the implementation of the Free-Flow tolling (M-Flow system) in Thailand* [Unpublished bachelor's thesis]. King Mongkut's Institute of Technology Ladkrabang.

Inspection and Rehabilitation Design of Teluk Baru Cantilever Concrete Bridge

Andrew Nugraha Standyarto[1*], Eko Hartono[2], Eko Yuniarsyah[3]

[1]National Road Implementation Agency of East Kalimantan, Directorate General of Highways, Ministry of Public Works & Housing, Republic of Indonesia, andrew.standyarto@pu.go.id
[2]National Road Implementation Agency of Lampung, Directorate General of Highways, Ministry of Public Works & Housing, Republic of Indonesia, ehartono@pu.go.id
[3]PT Wira Widyatama, eko.yuniarsyah@gmail.com

ABSTRACT

A comprehensive inspection was carried out on the Teluk Baru cantilever concrete bridge to assess its structural integrity and ensure its long-term functionality. The assessment included visual inspections, geometric measurements, and non-destructive testing (NDT) to evaluate the bridge's current condition. In addition, dynamic load tests were performed to determine the bridge's natural frequencies and damping characteristics. The data gathered from these inspections and tests were utilized to develop a detailed bridge model, which served as the foundation for rehabilitation planning. The bridge's evaluation was conducted in accordance with the current Indonesian standard for bridge loadings, SNI 1725:2016. Based on this evaluation, several rehabilitation measures were proposed. These included crack repairs using epoxy injection, the replacement of expansion joints, and the strengthening of the concrete box girder web with carbon fiber reinforced polymer (CFRP) composites, among other interventions. While it is acknowledged that the bridge's original condition cannot be fully restored, the rehabilitation efforts are aimed at ensuring the bridge operates reliably under its intended loads and within its design life.

Keywords: Cantilever concrete bridge, bridge inspection, rehabilitation, dynamic load test

1. INTRODUCTION

Bridges are crucial infrastructure for the mobility of people and goods, especially in developing countries like Indonesia, where they play a key role in boosting economic activities. The Teluk Baru Bridge is a significant structure located on a national road network in South Sumatra, Indonesia, serving as a vital link between the cities of Palembang and Musi Banyuasin (Muba) as shown in Figure 1. Built in 2013, the bridge has a total length of 214 meters, with a 104-meter main span and two 55-meter side spans. It features a 10-meter-wide deck and a cross-section of segmental box girder (SBG) with an architectural steel arch, as shown in Figure 2. The foundation consists of a combination of 60 cm diameter round piles and 40 cm x 40 cm square driven piles.

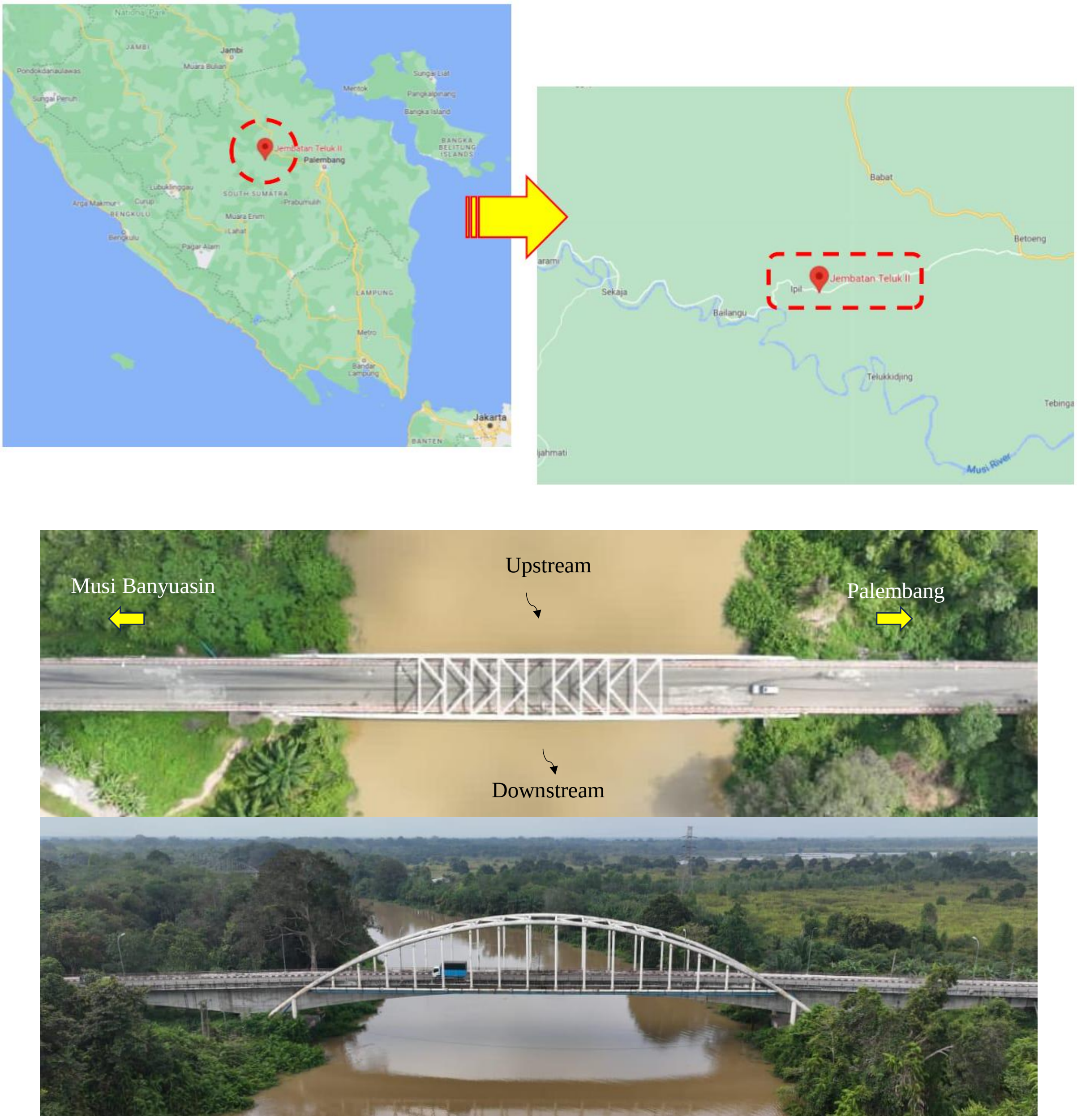

Figure 1. Location and Actual Photo of Teluk Baru Bridge in Palembang, South Sumatera, Indonesia

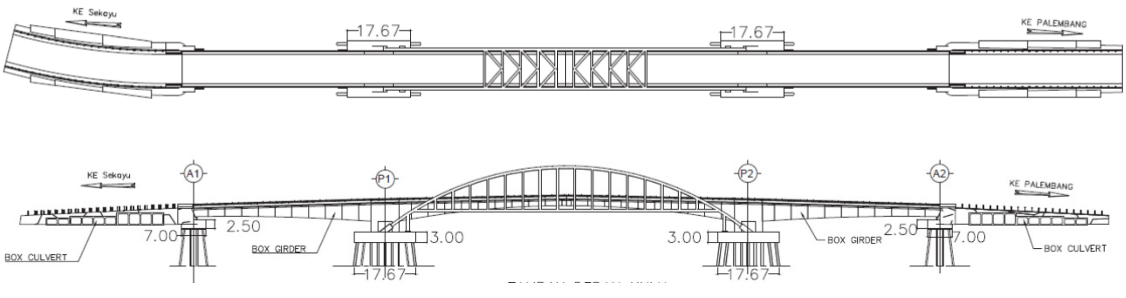

Figure 2. Plan View and Long Section of Teluk Baru Bridge (National Road Planning and Supervision Division of South Sumatera, 2023)

The bridge was originally designed as a rigid frame structure using the balanced cantilever construction method. However, for unknown reasons, the central span of the bridge was constructed without a closure segment and was instead equipped with an expansion joint (EJ), leading to settlements at both ends of the cantilever element. To address this issue and ensure the bridge's long-term functionality, a thorough inspection and non-destructive testing (NDT) were conducted to assess its structural condition. Additionally, dynamic load tests were carried out to determine the natural frequencies and damping characteristics of the bridge. Based on these findings, a rehabilitation design was proposed to ensure the bridge functions reliably under its intended loads and design life.

2. LITERATURE REVIEW

2.1 Segmental Box Girder

Segmental Box Girder (SBG) is a type of bridge structure that utilizes a rectangular cross section with part of bottom slab, web, top slab and flange or cantilever wing. It can be erected using various methods such as Span by Span Method using Shoring or Launching Gantry (LG), Incremental Launching with Pulling Jack or Balanced Cantilever Method using Form Traveler for Cast-in-Situ type and Lifter for the precasted one. The precast type usually comes as post tensioned segmental segments for easier mobilization from factory to site and the segments are jointed with internal tendon at the top slab in balanced cantilever method or external tendon that goes from EJ or link slab (LS) segment at both ends where the anchors are and then to the deviator segments to simulate the chamber. Post tension tendons can be designed as unbonded, bonded or a combination. This type of bridge is more economical with span of more than 50 m than the common Precast Concrete I (PCI) Girder which has less stability during erection, has higher torsional resistance, minor maintenance cost and more aesthetic shape especially in the city area. Important segment of a balanced cantilever bridge is the closure that connects the 2 spans, it can be connected using reinforced concrete segment or expansion joint (EJ).

In Indonesia, there are some Balanced Cantilever SBG bridge such as Rajamandala Bridge in West Java, Rantau Berangin in Riau, Kuningan Long Span and Cililitan Long Span of Light Rail Transit (LRT) Jabodebek which is erected using Form Traveler (Tirnawardana et al. 2021). Other projects from 2016 to 2020 such as Mass Rapid Transit (MRT) Jakarta Package CP 101, 102 and 103, LRT Jakarta: Kelapa Gading - Velodrome and Bogor Outer Ring Road (BORR) Section 2B and 3A (Widiantoro et al. 2020). The section single-cell and multi-cell of SBG are shown on Figure 3 as follow:

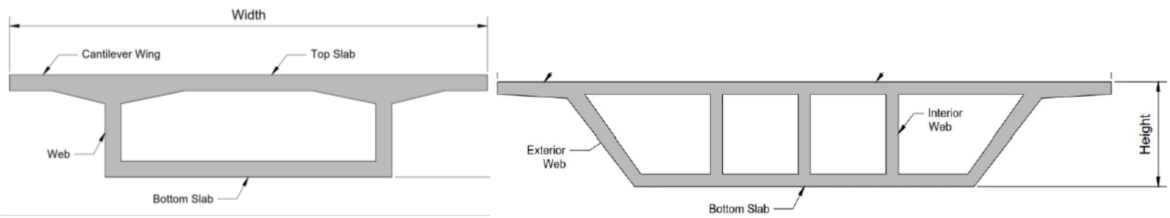

Figure 3. Typical Cross Section of SBG for Single-Cell and Multi-Section

(Midas Bridge, 2021)

2.2 Dynamic Loading Test

There are 2 types of loading test to check the condition of existing bridge which are Static loading and dynamic loading test. Dynamic loading test aims to obtain the dynamic parameters of the structure in the form of natural frequency or period and damping ratio. There are 2 vibration sources used in the test. These dynamic loads are: (1) Truck impulse loads (truck wheels dropped from certain height or wooden blocks for this case) that creates free vibration and (2) Brake load of truck, which is the speed of the truck before braking, namely 20-30 km/hour that produces forced vibration to bridge slab and then distributed to the lower structural element. Vibration from the test which is time domain is then transformed to frequency domain using peak picking of several amplitudes from the conducted test. The vibration is transformed with Fast Fourier Transform (FFT) analysis to obtain the natural frequency (fn). The natural frequency is then compared with the modal analysis of the existing bridge to check if the bridge condition is still safe or need any reinforcement (Standyarto & Hartono, 2022).

The tools used in dynamic load test are accelerometer sensor for measuring acceleration or vibrations and a data logger to record vibration data from the accelerometer sensor. The illustration of both devices is shown on Figure 4 below:

Figure 4. Illustration of Accelerometer Sensor and Data Logger (National Road Planning and Supervision Division of South Sumatera, 2023)

Damping ratio describes how oscillations in a system subdue after disturbance force is applied. It is calculated with formula on Figure 5 below:

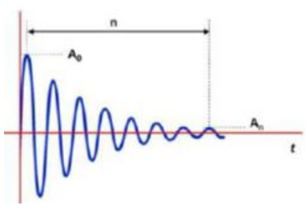

$$\zeta = \frac{\delta}{2\pi} = \frac{1}{n} \cdot \frac{1}{(2\pi)} \cdot ln\left(\frac{A_0}{A_n}\right) . 100\ [\%]$$

Figure 5. Damping Ratio Graph and Formula

3. MATERIAL AND METHODS

The materials and methods of this study is conducted based on the steps below:

a. Initial Data Collection (Survey Data, Shop Drawing, etc) from Project Team in South

Sumatera

b. Literature Review of SBG structure and Dynamic Loading Test method
c. Detailed survey on the field including geometry and elevation of the bridge
d. Dynamic Loading Test using a 15 tons Truck, 6 accelerometer sensors, data logger and laptop equipped with Matlab software for FFT Analysis
e. Structural Analysis using the surveyed model using Midas Civil
f. Result Analysis of all surveys and modellings
g. Future Rehabilitation plan to preserve the structure
h. Conclusion and Report writing as paper

4. RESULTS

Several results from some analyses conducted on the field are acquired as shown below:

4.1 Detailed Survey Result

Figure 6 shows the results of a visual inspection. The following findings are from comprehensive surveys of the bridge, which were conducted to measure its structural geometry and assess its condition:

1) Crack on SBG web that can decrease the section inertia and spalling on some concrete structural element.

(a) Sub-structure condition of bridge

(b) Crack on concrete box girder web

(c) Expansion joint on middle span

(d) Flexible Pavement condition of bridge

Figure 6. Bridge Visual Inspection Result

2) Expansion joint (EJ) at the center is damaged, filled with sand and appears to have leakage on the drainage system

3) Corrosion on architectural steel arch
4) There is no access ladder to check substructure condition from the bridge floor level
5) Geometry inspection shows deflection or asymmetrical chamber occurs on the EJ side based on collected data of shop drawing in 2004, survey data in 2021 and latest survey in 2023 as follow on Figure 7 and 8:

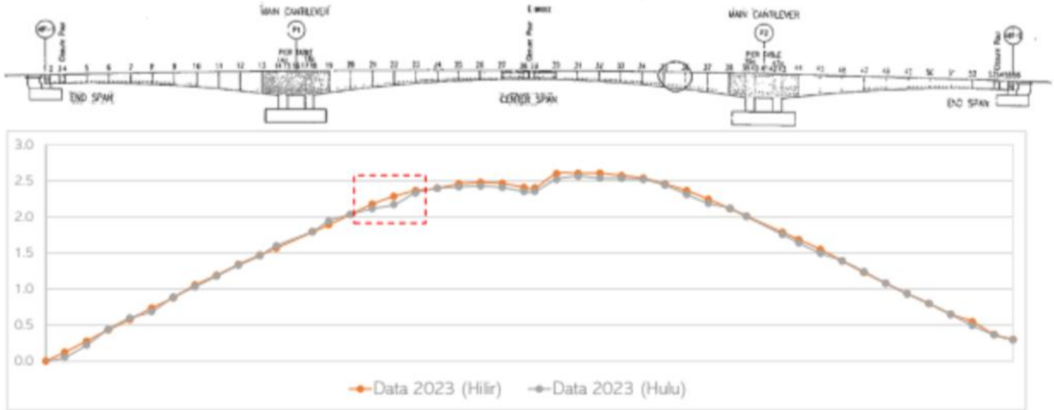

Figure 7. Chamber Data of 2023 Geometry Inspection

It can be seen that there is a slight chamber difference between upstream and downstream sides, with a maximum value at Segment 22, which is approximately 100 mm downward.

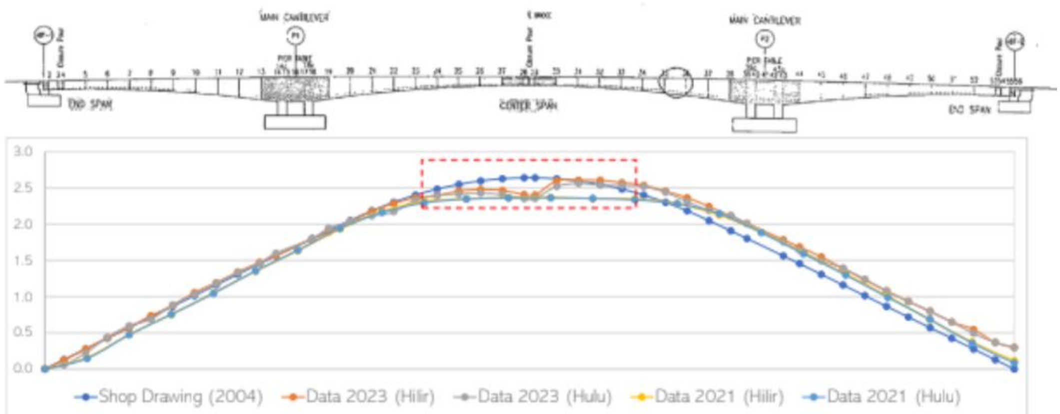

Figure 8. Chamber Data Comparison of 2004 Shop Drawing, 2021 Survey Result and 2023 Geometry Inspection

It can be seen that at the cantilever span, there has been a significant decrease around 231 - 287 mm at the joint (compared to shop drawing data in 2004). Although there is settlement at both ends of the cantilever, the elastic deflection caused by the Live Load remains within the allowable limits. One approach to address this situation is to conduct annual camber measurements to monitor whether the deflection is increasing or not. If the deflection does increase, further evaluation and reinforcement may be necessary such as adding a support column at the cantilever tip.

4.2 Dynamic Loading Test Result

Dynamic loading test was chosen to assess the condition of the old bridge due to its simplicity and minor disturbance to the crowded national road in South Sumatera. The total weight of the trucks used is around 15 tons and placed. Accelerometers (Acc) are placed on 8 locations along the bridge, 6 on the bridge floor or top slab (2 sensors without vibration sources) and 2 on the pier table. Sensor 3 axis is numbered as 1, 2, 3 and 5 (highlighted in blue) while sensor 1 axis are 4, 6, 7, 8 (highlighted in orange). Dynamic load tests were carried out 3 times at each location based on analysis, impact load on P1-EJ, A1-P1, P2-EJ and A2-P2 and brake load on P1 and P2. From the conducted tests, FFT analysis is done with Matlab program to gain the natural frequency. Layout of all sensors for each loading scheme are shown below on Figure 9 while Natural frequency and damping ratio are as shown follow on Table 1:

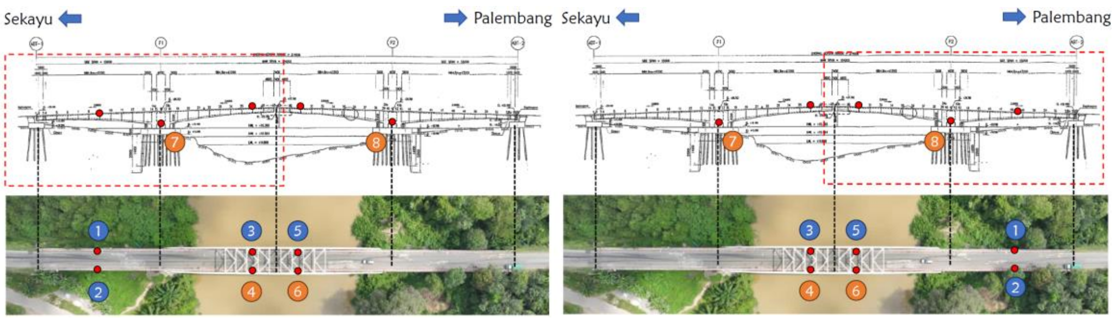

Figure 9. Layout of Accelerometers on Span A1-P1-EJ (Sekayu Side) and A2-P2-EJ (Palembang Side)

Table 1. Dynamic Parameter of Teluk Baru Bridge Spans

No	Span	Freq (Hz)	Damping Ratio (%)		
			Test	Limit	Result
1	A1-P1	3.45	2.42	3.20	OK
2	P1-EJ	1.45	2.50	3.20	OK
3	EJ-P2	1.44	2.73	3.20	OK
4	A2-P2	3.00	2.32	3.20	OK

According to the table, frequency results are similar for each type of span which are abutment to pier table span (3 - 3.45 Hz) and pier table to EJ span (1.44 - 1.45 Hz). Based on European Commission's project D5.2-S2, damping ratio for reinforced and prestressed concrete bridges is around 3.20% which is higher than the actual test results for all spans.

3.3 Structural Analysis

To get the right model to be compared with dynamic loading test result, natural frequency of the Teluk Baru bridge has to be predicted using modal analysis or modeling the existing condition of bridge with the latest detailed survey. The bridge is divided into 2 spans by EJ which are A1-P1-EJ or Sekayu side and A2-P2-EJ or Palembang side respectively. Due to its identicality, only Sekayu side is 3D modeled with beam element for SBG and pier table. Because the pile cap is large enough, the fixed point is assumed at the bottom of pier. Structural element dimension and material properties are based on field survey (Hammer test and UPV for concrete element) as follow:

Concrete: Reinforced Bar: Strand: ASTM A416 (7-wire low relaxation)

Pier: 35 MPa	fy: 313.8 MPa	fpu: 1860 MPa
SBG: 41.5 MPa	E: 200 GPa	fpy: 1670 MPa

Model loadings and load combinations are based on the latest National Standard of Indonesia (SNI): 1725-2016 for Bridge Loading which are:

a. Self Weight (MS)
b. Superimposed Dead Load (SIDL)
c. Traffic Load
d. Truck Load
e. Brake Load
f. Live Load (LL)
g. Prestressed Load (PR)
h. Wind Load on Structure (EWS)
i. Wind Load on Vehicle (EWL)
j. Temperature Load (Eun)
k. Gradient Temperature Load (ET)
l. Earthquake Load (EQ) with SE soil for conservative result based on SPT data

3.3.1 Modal Analysis

Superstructure of the bridge is modeled using Midas Civil program as shown on Figure 10:

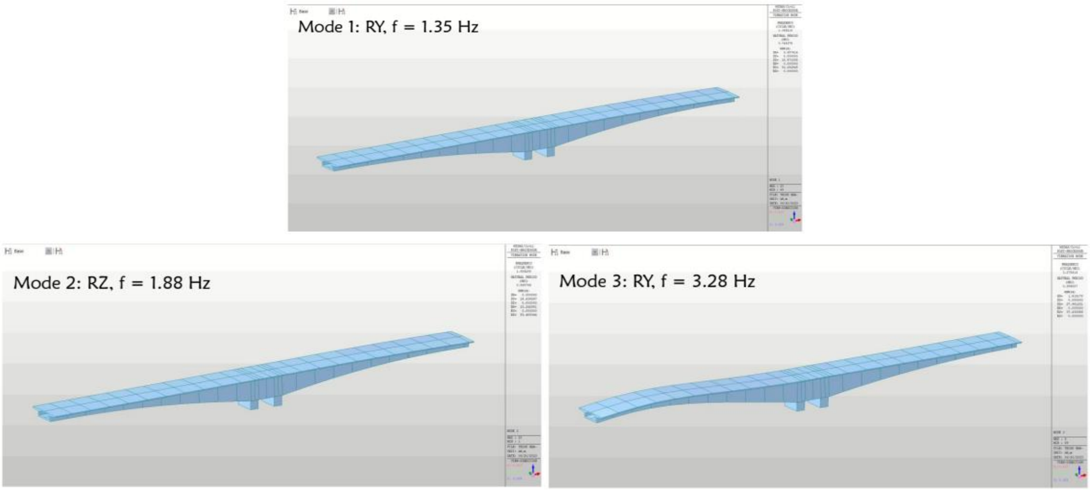

Figure 10. Natural Frequency of 3 Dominant Mode Shapes of A1-P1-EJ Span

From the Midas Civil result, it can be seen that the natural frequency for span A1-P1 is 3.28 Hz while span P1-EJ is 1.35 Hz which is similar to the loading test result and thus the model is validated and can be used for further analysis of internal forces. The ratios of modal analysis/field loading test natural frequency of bridge spans are shown below on Table 2:

Table 2. Natural Frequency Comparison of Modal Analysis and Loading Test

Span	Natural Frequency Result (Hz)		
	Modal Analysis	Loading Test	Ratio
A1 - P1	3.28	3.45	0.95
P1 - EJ	1.35	1.45	0.93

EJ - P2	1.35	1.44	0.94
P2 - A2	3.28	3.00	1.09

Based on the comparison table of natural frequencies, the ratio for each span is close to 1.00, which validates both the model and the loading test.

3.3.1 Force Result

With modal analysis, occurring internal forces of moment (Mu) and shear (Vu) on each structural element can be inspected and moment capacity (Mn) and shear force capacity (Vn) can be calculated and then compared. Moment capacity of the pier is calculated using PCA Column software. The force results on each structural element of SBG and pier table can be seen as follow on Figure 11 and Table 3 as follow:

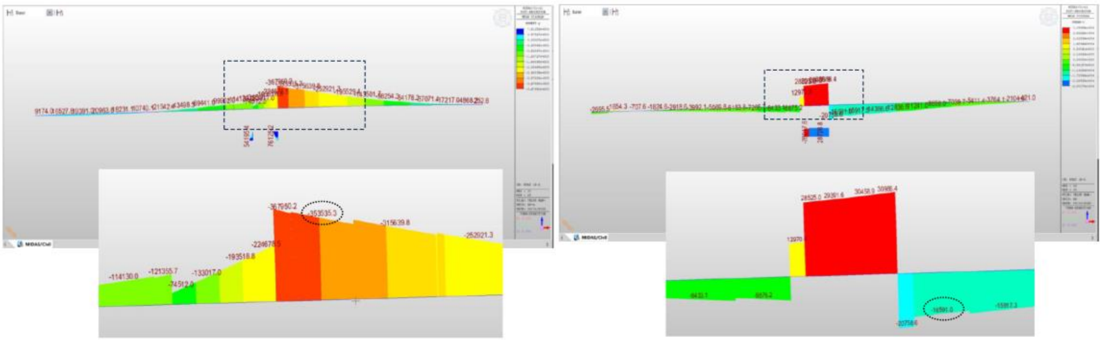

Figure 11. Example of Moment and Shear Force on SBG Structural Element

Table 3. Force Result of Structural Elements

No	Structural Element	Moment (kNm)			Shear (kN)		
		Mu	ΦMn	Result	Vu	ΦVn	Result
1	SBG	353,535	400,700	1.133	16,591	16,520	0.996
2	Pier Table	367,950	400,700	1.089	30,986	33,250	1.073
3	Pier (X Direction)	76,125	80,395	1.056	31,994	33,620	1.051
4	Pier (Y Direction)	7,414	58,858	7.939	4,693	17,950	3.825

According to the table, almost all structural elements have bigger moment and shear force capacity except SBG's shear capacity where it's less than the actual shear force. Therefore, structural reinforcement has to be applied to SBG's shear capacity to withstand the actual load working on the bridge.

3.3.1 Deflection Result

From the modal analysis, deflection can also be gained using Midas Civil. Permanent displacement uses a load combination of MS + MA + PR. Due to crack on SBG's web that is found during detailed survey in 2023, section inertia is decreased to 0.7 Ig for more actual result. Deflection of each span due to live load of traffic and pedestrian that are applied specifically on each span can be acquired as follow on Figure 12 and Table 3:

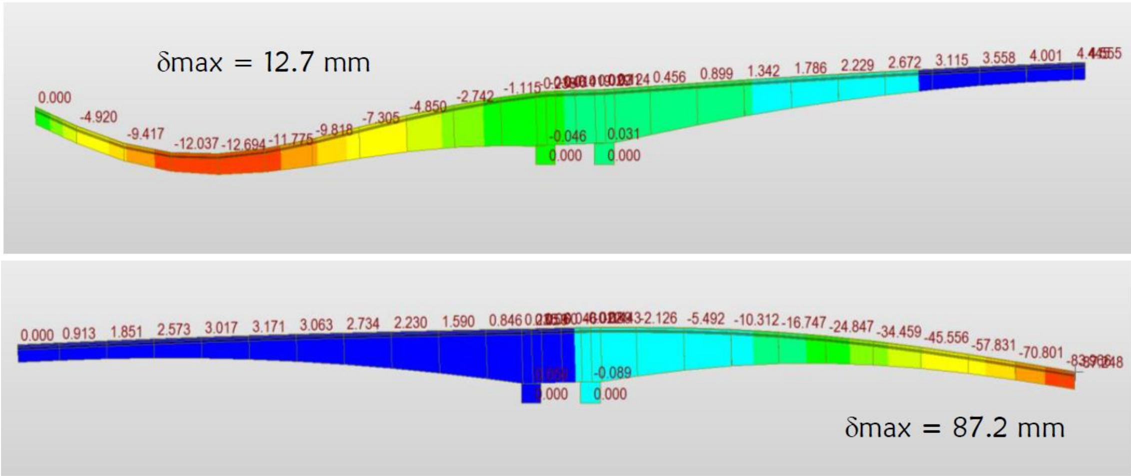

Figure 12. Deflection due to Live Load on A1-P1 / A2-P2 and P1-EJ / P2 / EJ

Table 3. Deflection Result of The Spans

No	Span	δ (mm)	Limit (mm)	Result
1	A1-P1 / A2-P2	12.7	55.0	OK
2	P1-EJ / P2-EJ	87.2	138.7	OK

It can be seen that the actual deflection is still smaller than the allowable deflection as per AASHTO LRFD standards. For the cantilever segment, the allowable deflection is L/375 = 52,000/375 = 138.7 mm for Spans P1-EJ and P2-EJ, and L/1000 = 55,000/1000 = 55 mm for Spans A1-P1 and A2-P2. The deflection limit is consistent with that specified in SNI 1725-2016 for Live Load (LL).

3.4 Rehabilitation Plan

Based on the survey and analysis conducted, there are several damages that occurred on Teluk Baru Bridge, therefore a rehabilitation work has to be planned and performed in order to restore the condition of the bridge to serve its original purpose. Figure 14 shows the location and the exact number of repair work for the Teluk Baru bridge:

1) Concrete crack injection
2) Patching for concrete spalling
3) Reinforcement with 1 layer, 0.508 mm thickness and 1.2 GPa fu CFRP on SBG main span interior and exterior webs are calculated based on ACI 440.2R-17. The illustration and details of shear strengthening using CFRP can be seen below on Figure 13:

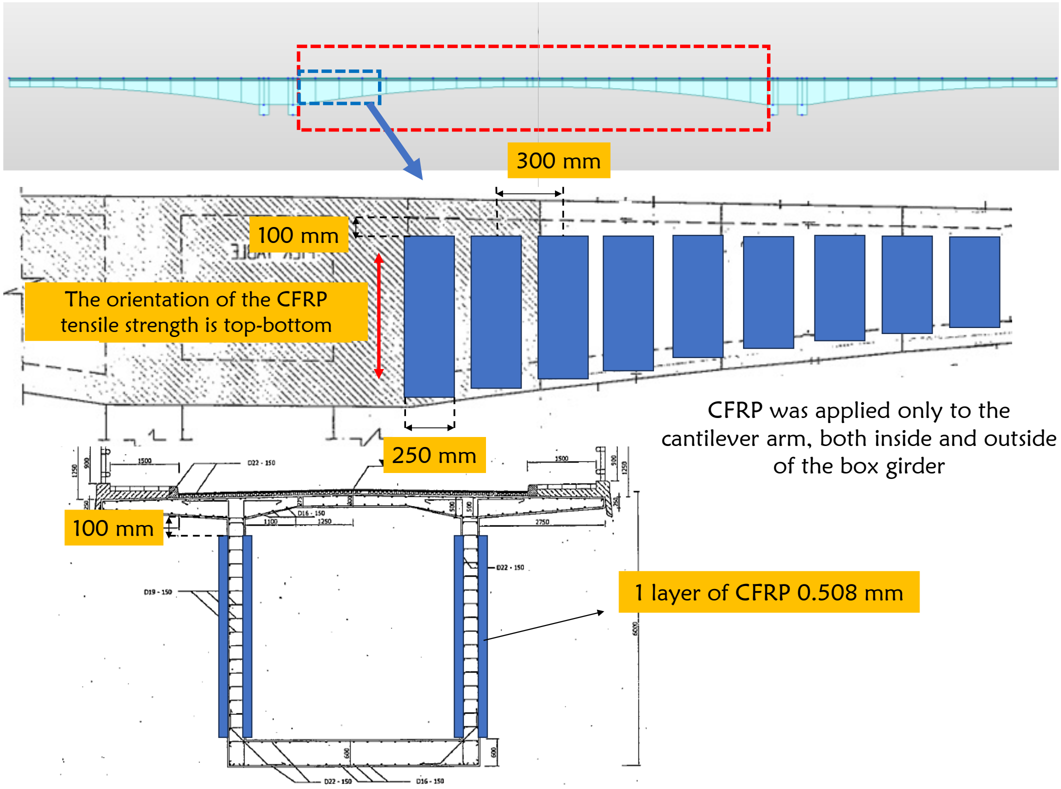

Figure 13. Shear Strengthening using CFRP on SBG

4) Expansion Joint Replacement with Strip Seal Type with respect to the existing top slab tendon while chipping to install EJ steel plates and anchors
5) Architectural Steel Arch Repaint to avoid corrosion
6) Cleaning for bearing and drainage
7) Asphalt Repair to improve safety and additional impact load from passing vehicles
8) Access Ladder installation to ease survey to substructure and repair work

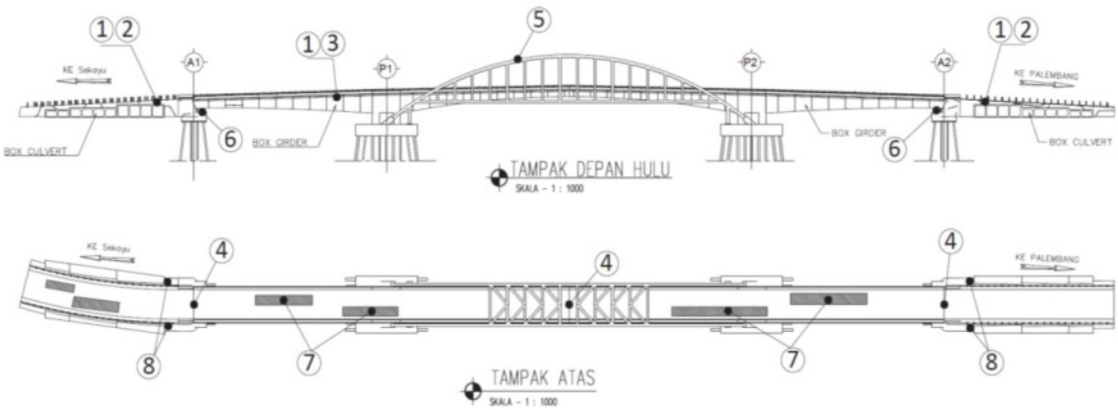

Figure 14. Longitudinal and Plan View of Teluk Baru Bridge Rehabilitation Work

5. CONCLUSIONS

To conclude, the inspection and analysis results conducted on Teluk Baru Bridge are:

a. Detailed survey shows damage on EJ, crack on SBG web, concrete spalling and asphalt degradation
b. Structural analysis shows shear capacity of SBG is less than the actual load by 71 kN

c. Rehabilitation for Teluk Baru Bridge are crack repairs using injection, EJ replacement, and SBG strengthening using Carbon Fiber Reinforced Polymer (CFRP) composites.
d. Frequent chamber inspection is needed to monitor the cantilever integrity.

6. ACKNOWLEDGMENTS

In writing the paper, the writers would give the utmost appreciation to Ministry of Public Works and Housing of Indonesia, PT. Wira Widyatama, PT. Daya Cipta Dianrancana and people in South Sumatera for the opportunity, sharing of data and continuous support for the realization of this specific paper.

7. REFERENCES

Akbar, M.; Dirawan, H. G. D. & Rahman, M. J. (2020). ANALISIS PEMODELAN BEBAN PADA STRUKTUR JEMBATAN BOX GIRDER MENGGUNAKAN SOFTWARE CSI BRIDGE. Pendidikan Teknik Sipil dan Perencanaan, Program Studi Pendidikan Teknik Bangunan, Fakultas Teknik, Universitas Negeri Makassar, Makassar.

Midas Bridge. (2021). PSC Segmental Box Girder Bridge Design. Accessed on December 3rd, 2023(https://www.midasbridge.com/en/blog/bridgeinsight/psc-segmental-box-girder-bridge-design)

National Road Planning and Supervision Division of South Sumatera. (2023). Final Report PR-04 Special Bridge Structural Evaluation in South Sumatera Province, September 2023.

Standyarto, A. N. & Hartono, E. (2022). Tinjauan Struktur Bangunan Atas Jembatan Rangka Baja Belanda Air Tkl Peninggalan. Live and Applied Science, Volume 2 Prosiding National Seminar And Call For Paper Civil Engineering 2022 Diselenggarakan di Malang, 12 September 2022 e-ISSN (2964-772X).

Tirnawardana, M. R.; Piscesa, B. & Suprobo, P. (2021). Evaluasi Perancangan Jembatan Longspan Cililitan Proyek LRT Jabodebek Menggunakan Balanced Cantilever Precast Post-Tensioned Box Girder. JURNAL TEKNIK ITS Vol. 10, No. 1, (2021) ISSN: 2337-3539 (2301-9271 Print).

Widiantoro, V; Ichsan, M. & Saputra, P. D. (2020). Measurement Analysis of Box Girder Production Cycle Times in Indonesia Infrastructure Projects. Advances in Engineering Research, volume 203 Proceedings of the 2nd Borobudur International Symposium on Science and Technology (BIS-STE 2020).

Improvement of Pavement Surface Conditions on Expressways According to the Mental Stress of Road Users

Kazuya Tomiyama[1,*], Masamitsu Ito[2], Kenichi Meguro[3], Taichi Nakamura[4], Masakazu Sato[5]

[1] Kitami Institute of Technology, tomiyama@mail.kitami-it.ac.jp
[2] Kitami Institute of Technology, m3235200062@std.kitami-it.ac.jp
[3] East Nippon Expressway Company Co., Ltd., k.meguro.aa@e-nexco.co.jp
[4] East Nippon Expressway Company Co., Ltd., t.nakamura.ao@e-nexco.co.jp
[5] East Nippon Expressway Company Co., Ltd., m.sato.af@e-nexco.co.jp

ABSTRACT

One of the most prominent indicators for pavement conditions of expressways is surface roughness which affects the safety and comfort of road users. The roughness of expressways in Japan are evaluated and controlled with the International Roughness Index (IRI). However, the relationship of IRI with the wavelengths related to the mental stress of road users is still unclear, which results in the gap between the maintenance criteria and road user ratings in terms of the ride quality. Indeed, hundreds of complaints from road users have so far been filed against the surface conditions of pavement surfaces even though the IRI values have been acceptable in terms of the maintenance threshold. This study conducts field survey measuring surface roughness on in-service expressways with which user complaints were reported, and then performs driving experiments using a motion base driving simulator with reproducing the roughness data. In the experiments, two physiological measures which are heart rate variability (HRV) and the skin conductance response (SCR) are employed for the quantitative evaluation of road user rating in terms of mental stress against surface roughness. The driving scenario is developed to investigate the impact of surface roughness with different degrees of prominence for surface wavelengths on the physiological signals. As a result, the mental stress measured by the physiological signals increases with increasing the amplitude of specific wavelengths which are 4 to 8 meters in the surface profile. Finally, this study reveals the mechanism of arising user complaints by the mental stress measured with physiological responses. The outcomes of this study contribute to the improvement of pavement management of expressways with objective measures which fill the gap between the maintenance criteria and user ratings in terms of the ride quality.

Keywords: Pavement roughness, Physiological signal, Road safety and comfort, International Roughness Index, Driving simulator

1. INTRODUCTION

One of the most prominent indicators for pavement conditions of expressways is surface roughness which has a great impact on the safety and comfort of road users, vehicle operating costs, and environmental issues (Descornet, 1989). In terms of the ride quality of a vehicle, the International Roughness Index (IRI) is widely used as a standard roughness indicator in many countries (Múčka, 2017). In Japan, the roughness of expressway pavements is controlled with IRI against the huge demand for improving ride quality under high travel speed (Kumada, et al., 2002). However, since the IRI focuses on average roughness condition for an entire road segment, it tends to underestimate localized irregularities (Eguchi, et al., 2015). This issue has especially emerged after introducing porous asphalt pavements for the surface layer (Kawamura & Kamiya, 2007). Although IRI with a fixed interval of 10 meters for localized irregularities has been proposed, the conventional maintenance criteria have been difficult to respond the condition evaluation for localized irregularities (Inagi, et al., 2022a). Accordingly, more than hundreds of complaints from road users have been recorde to the expressway agency in a year against the ride quality of pavement surfaces even though the IRI values are less than the maintenance threshold (Inagi, et al., 2023). It proves the gap between the user rating and current maintenance criteria with IRI for expressway pavements in terms of the ride quality.

Distinct approaches such as physical (Fujita, et al., 2016; Chanjun & Seung-Ki, 2019), psychological (Ishida, et al., 2004) and physiological (Jennifer & Rosalind, 2005; Tomiyama, et al., 2019) have so far been proposed for road user rating. However, few studies dealt with user complaint against road surface properties with quantitative measures of mental stress. The purpose of this study is to improve the pavement surface management of expressways with objective measures which fill the gap between the maintenance criteria and user ratings in terms of the ride quality. For this purpose, first, this study conducts field survey measuring surface roughness on in-service expressways with which user complaints were reported. Then, it performs driving experiments involving road users by use of a motion base driving simulator with reproducing the roughness data obtained. In the experiments, two physiological measures which are heart rate variability (HRV) and the skin conductance response (SCR) are employed for the quantitative evaluation road user rating in terms of mental stress against surface roughness. Finally, this study reveals the mechanism of arising user complaints by the mental stress measured with physiological responses.

2. FIELD SURVEY FOR ROUGHNESS DATA ACQUISITION

2.1 Surveying area

As mentioned earlier, hundreds of complaints from road users have so far been filed against the ride quality in expressways even though the roughness have been acceptable in terms of the IRI. Figure 1 represents the geographical distribution of user complaints recorded in the control area of the Kanto branch of East Nippon Expressway Company Limited in the fiscal year of 2021. In the figure, the complaints were plotted with the following manners (Tomiyama et al., 2023):

- Only the complaints related to the ride quality are selected.
- Only the complaints which can be tracked within the accuracy of one kilometer post

(kp) are involved. The longitude and latitude are then identified for the mapping.

- The secondary partition mesh of the Geospatial Information Authority of Japan of Ministry of Land, Infrastructure, Transport and Tourism (MLIT) is assigned to the map.
- The number of complaints included in a mesh is counted and color-coded according to the numbers.

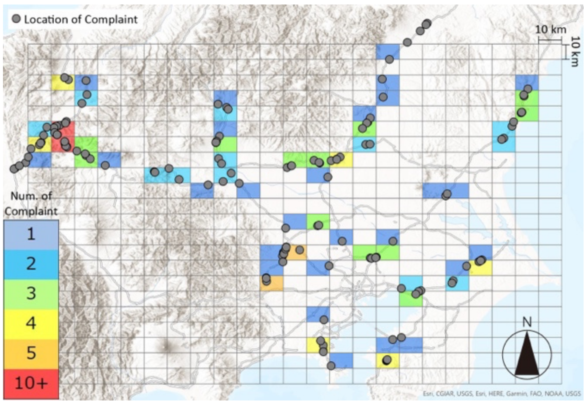

Figure 1 Distribution of Complaints in FY2021.

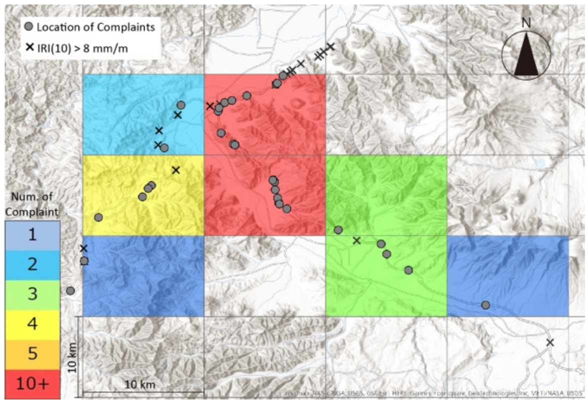

Figure 2 The most Complaint Region.

According to Figure 1, the complaints were concentrated around a mountainous region in the west side of which details are shown in Figure 2. In Figure 2, spots where the IRIs with a fixed interval of 10 meters exceeded the maintenance threshold of 8.0 mm/m are also plotted. Here, no surfaces were over the maintenance threshold in terms of the IRI with a fixed interval of 200 meters. As shown in Figure 2, the complaints were recorded even though the IRI values are less than the maintenance threshold, which ensures the gap between the user rating and maintenance criteria with IRI. In light of this situation, this study performed roughness measurement survey on the expressways located in the area shown in Figure 2

2.2 Data acquisition protocol

A survey was performed in the road segment complained by drivers within a month after the complaint were recorded by following the protocol shown in Figure 3. In the survey, the following items corresponding to Figure 3 were investigated:

- Vehicle motion: it records vehicle translational acceleration and angular velocity as well as geographic coordinates to obtain the vibration induced by roughness, and locations surveyed.
- Physiological signals: it includes the heart rate and skin conductance response of a driver to monitor the mental stress.
- Surface characteristics: it measures surface profiles and IRIs which are used for the subsequent driving simulator experiment described later.
- Video image: it records the surface image and surrounding environment during the survey.

- Pavement Diagnosis: it rates the surface condition with visual and sensory inspection to categorize the pavement distresses.

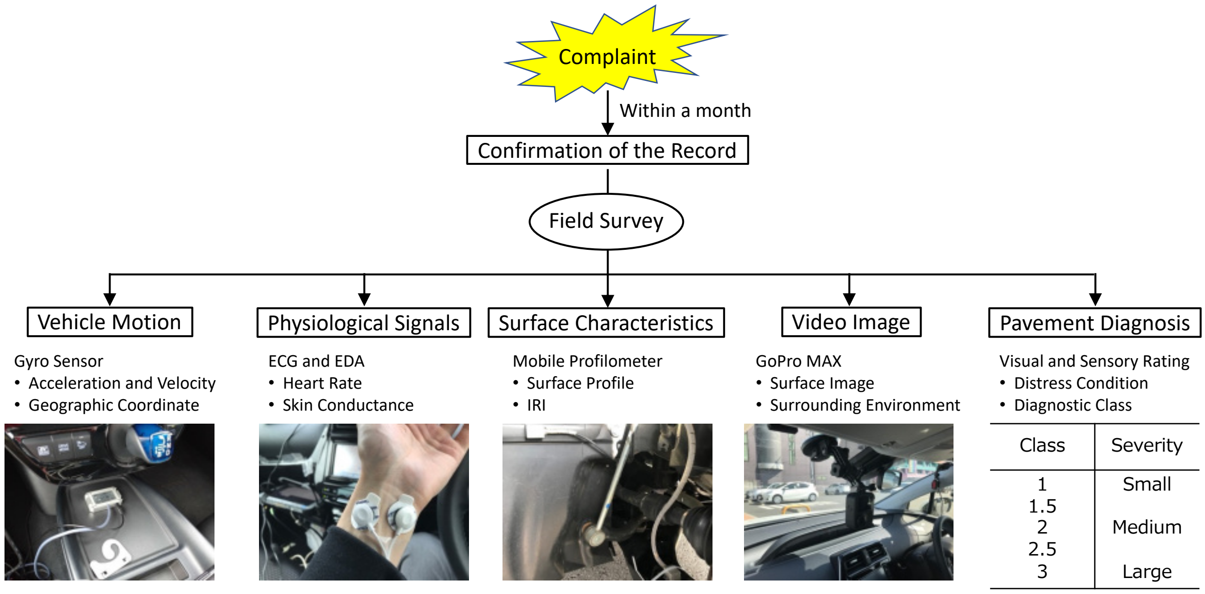

Figure 3 Data Acquisition Protocol.

3. DRIVING SIMULATOR EXPERIMENT

3.1 Apparatus

▪ ***Driving simulator***

A driving experiment were conducted to estimate physiologically the mental stress against surface roughness by use of the Kitami Institute of Technology Driving Simulator (KITDS) involving road users. The KITDS has an ability to generate the vehicle vibration induced by surface roughness by a six-axis motion base system which consists of a cockpit with six cylinders activated by electric motors. It allows loading actual road surface data directly into the simulator to perform a full vehicle simulation with the front view of computer graphics provided by the screen. The overview of KITDS in an actual experiment is shown in Figure 4.

▪ ***Physiological measure***

For physiological measures, (1) heart rate variability (HRV) was measured by an electrocardiogram (ECG) using the chest dielectric method, and (2) electrodermal activity (EDA) which is related to human emotional states, cognitive activities, and information processing processes was measured using the skin conductance response. Figure 5 shows sensors measuring physiological signals.

Figure 4 Overview of the KITDS.

Figure 5 Sensors Measuring Physiological Signals.

3.2 Interpretation of physiological measures

HRV referrers to beat-to-beat fluctuations in heart rate, which is a time series of the interval between R waves in ECG waveform shown in Figure 6. It reflects the activity of the autonomic nervous system correlated to the mental stress. In the frequency domain, HRV has different spectral components in the high-frequency (HF) and low-frequency (LF) ranges that are 0.15-0.4Hz and 0.04-0.15Hz, respectively, as shown in Figure 7. Here, HF components increase in relaxed states whereas LF/HF components increase under stressed states (Task Force of the European Society of Cardiology, and the North American Society of Pacing, and Electrophysiology, 1996). Since the HF rather than the LF oscillation is easier to interpret in respect to the physiological approach, the HF spectral oscillations were used as a stress marker regarding mental stress. This study especially focuses on the percentile variations for log-transformed HF (lnHF) considering the sensitivity variance in human body vibration.

EDA referrers to the perspiration secretion alters the electrical properties of the skin. By applying constant voltage, the change in skin conductance (SC) can be measured non-invasively (Fowles et al., 1981). As a promising measure of EDA, skin conductance response (SCR) with a unit of micro siemens (μS) is employed in this study. An example of typical waveform of EDA signal and SCRs are shown in Figure 8. This study measured the frequency of SCRs to find stressful surface irregularities.

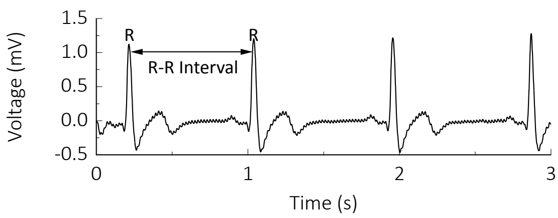

(a) ECG Waveform

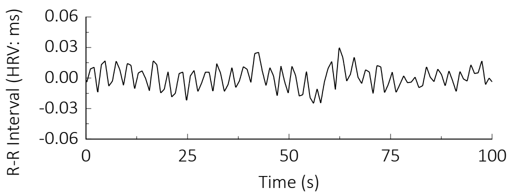

(b) Heart Rate Variability (HRV)

Figure 6. An example of Heart Rate Signal and its Variability

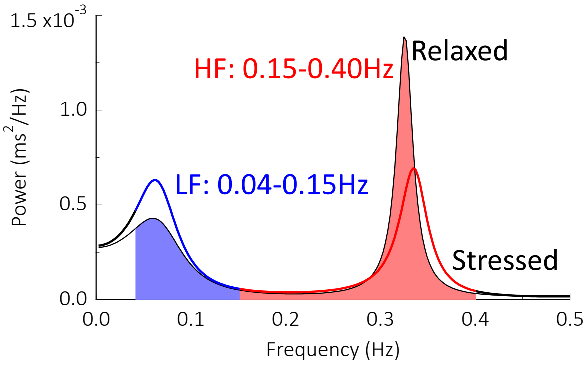

Figure 7 A HRV in the Frequency Domain.

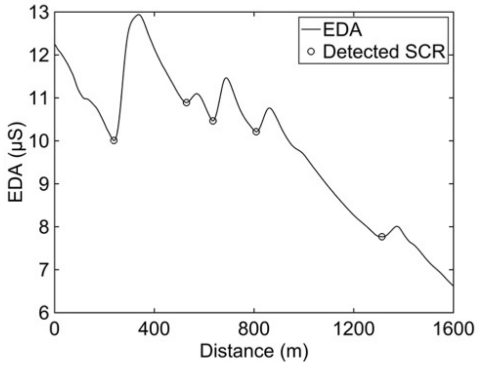

Figure 8 A Typical Waveform of EDA and SCRs.

3.3 Experimental scenario

- ***Surface profiles***

The driving scenario was developed to investigate the impact of surface roughness involved with user complaints on the physiologically measured mental stress. In this experiment, tested surfaces were considered in response to the data acquisition protocol mentioned earlier by the following criteria (Inagi, et al., 2022b):

- Roughness is under the maintenance criteria in terms of the IRI.
- No distresses requiring emergency repair such as a pothole are included.
- An extension of the road profile is 1,600 m to acquire sufficient physiological signals and to avoid giving fatigue to participants.

Finally, three surfaces were selected as shown in Table 1 of which characteristics were described as follows.

Table 1. Surface profiles and the iris for the driving experiment.

Surface	Profile	Fixed Interval IRI	Contiguous IRI
A	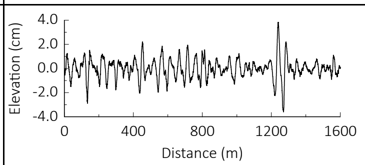	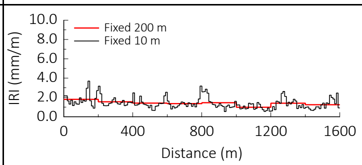	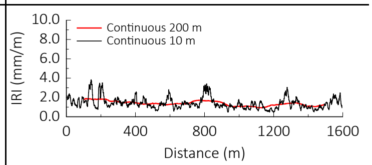
B	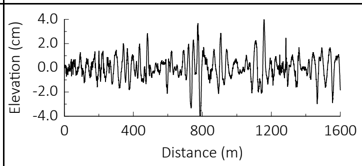	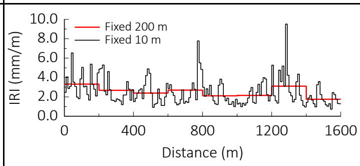	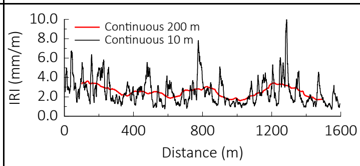
C	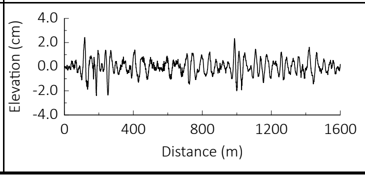	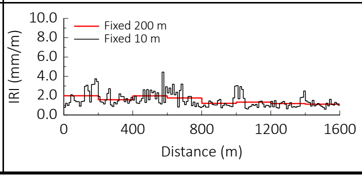	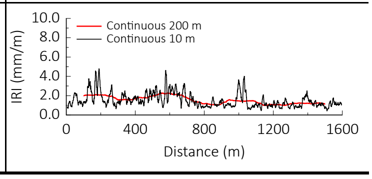

- Surface A: It included some moderate localized irregularities causing a lack of smoothness, which potentially leads user complaints in terms of ride quality.
- Surface B: it was observed with successive severe localized irregularities of which complaints were reported.
- Surface C: it appeared sinusoidal and cyclic in the profile which brought the decline of ride quality.

▪ ***Test track***

Test tracks for the experiment were designed with the combination of surface profiles shown in Table 1 and preliminary sections of which IRIs were 1.0, 2.7, and 3.5 mm/m assuming the actual conditions of expressways in Japan listed in Table 2. The purpose of preliminary section is to avoid the expectation and to refresh the memory of participants, and then the profiles included no localized irregularities. In addition, acceleration and deceleration sections of which IRI was an average of in-service expressways, that is 1.7 mm/m, were arranged at the beginning and ending points, respectively. A schematic illustration of the test track is shown in Figure 9.

Table 2 IRI values of preliminary section.

Surface	IRI (200 m fixed)	Condition
a	1.0 mm/m	An average of newly constructed pavement of expressways in Japan (Eguchi et al., 2015)
b	2.7 mm/m	Subjectively evaluated as "good" or "very good" from more than half of experimental participants (Kumada, et al., 2005)
c	3.5 mm/m	Maintenance threshold of expressway pavements in Japan

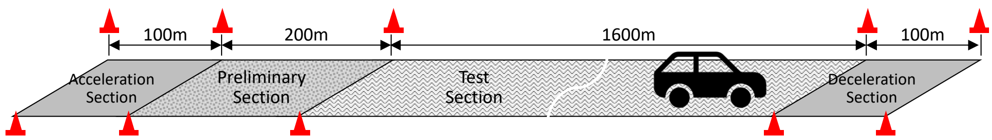

Figure 9 Schematic illustration of the test track.

▪ ***Participants***

Seventeen participants in their 20's to 50's who have various driving experiences were voluntary involved in the experiment. Two participants were tested once more in a different day due to an error of the measurement. Finally, a total of 18 and 17 data for ECG and EDA, respectively, were analyzed for this study. In the experiment, participants were asked to experience each surface as a passenger, that is free from driving, at a travel speed of 80 km/h. Each driving scenario was presented randomly to a participant for making the counterbalance. No participant suffered a motion sickness.

4. RESULT OF THE EXPERIMENT

In the experiments, two physiological measures which were HRV and SCR were recorded to evaluate the mental stress of participants against surface roughness with the dedicated experimental scenario. This chapter analyzes the response of two measures toward road surface characteristics especially in terms of the wavelengths of the profile.

4.1 HRV analysis in terms of HF components

As early mentioned, the HF component in a HRV signal increases in relaxed states, in other words, decreases with mental stress. In this analysis, the percentile variations for log-transformed HF (lnHF) are calculated for identifying the locations of surface irregularities which lead higher mental stress of participants. Figure 10 shows the variation in lnHF caused by the surface roughness.

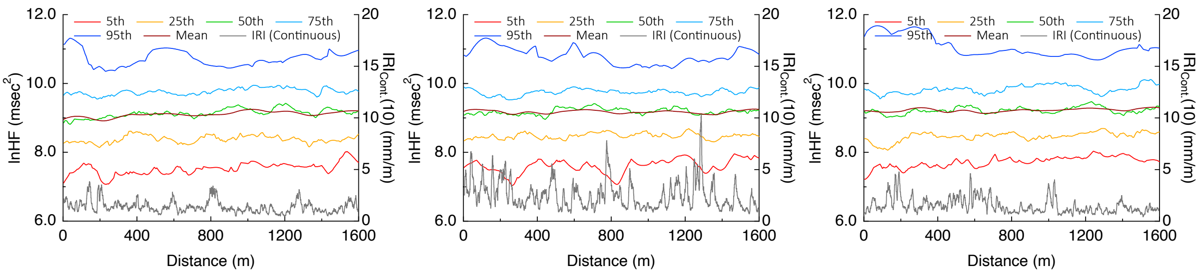

(a) Surface A (b) Surface B (c) Surface C

Figure 10 Variation in lnHF caused by the surface roughness

As shown in Figure 10, the following findings can be acquired with focusing on the instant decline of lnHF.

- Surface A: A high mental stress response was observed in the participants below the 5th percentile who were sensitive to the vibration at the location of 200 m whereas no stress responses were detected at the locations of 800 m and 1,300 m in spite of the similar IRI value.
- Surface B: In particular, a higher mental stress response was identified in the participants not only on the 5th percentile but on the first quartile at the location of 1,200 m where the IRI exceeded the maintenance threshold.
- Surface C: Although slight mental stress responses can be seen at the locations of 200 m and 500 m, it was not clear even though the degree of IRI was similar to that of Surface A.

From the above findings with considering individual variations of heart rate, the HRV of the participants below the 5th percentile responds to the mental stress against surface roughness less than the maintenance threshold whereas it is inconsistent with the degree of IRI.

4.2 EDA analysis in terms of SCR

Since SCRs appear with responding to the transient mental stress, the occurrence frequency corresponds to the mental stress caused by localized surface irregularities. Figure 11 shows the variation of SCR against the roughness as well as the lnHF components of HRV.

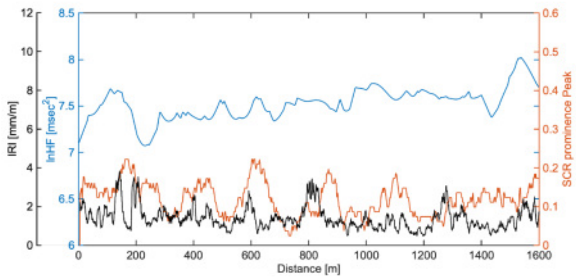

(a) Surface A

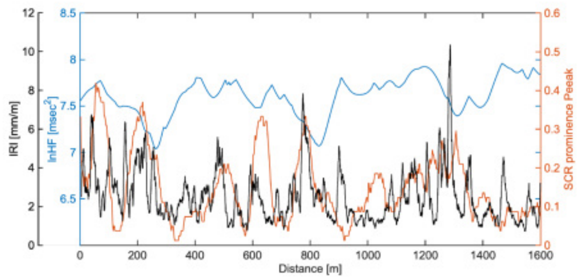

(b) Surface B

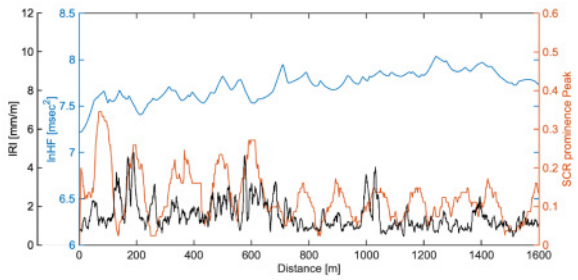

(c) Surface C

Figure 11 Variation of SCR against the roughness and lnHF.

As shown in Figure 11, the following findings for average drivers can be made by paying attention to the locations of SCR occurrence.

- SCR occurrence fluctuates with the same trend for the variance of IRI, and then, it is consistent with the evaluation by the IRI in terms of ride quality.
- The frequency of SCR occurrence increases with decreasing HF components in HRV, which suggests some surface irregularities associated with mental stress are underestimated by the evaluation with IRI.

Those findings proves the SCR reflects the mental stress associated with surface irregularities in terms of the ride quality. As a result, the combination of HRV and SCR is possible to detect the mental stress due to surface irregularities bringing user complaints which are difficult for the IRI to evaluate.

4.3 Analysis of surface characteristics

This section analyzes the profiles shown in Table 1 by the continuous wavelet transform (Mallat, 1999) to identify the relationship in terms of the surface wavelength with mental stress causing user complaints regarding ride quality. Figure 12 shows the wavelet transform result of the profiles of which corresponding continuous IRI, HF variation of the participants below the 5th percentile, and the 5% significance level are shown in Figure 13.

As shown in Figure 12, wavelength ranging from 4 to 8 m are dominated at the locations where the mental stress responses are observed in the HF fluctuations shown in Figure 13. Here, the response of quarter-car model used of the IRI calculation is less sensitive to the wavelengths between 4 and 8 m (Sayers & Karamihas, 1998). In addition, human response to whole-body vibration for the vertical acceleration (ISO, 1998) is strongly sensitive to the vibration frequencies ranging from 4 to 8Hz corresponding to the wavelength ranging from 2.8 to 5.6 m at traveling speed of 80 km/h, which overlaps with the wavelength ranges related to the mental stress. As a result, it can be concluded that user complaints occurs in responsible for the discrepancies of sensitive wavelengths between the physiological responses of road users and IRI.

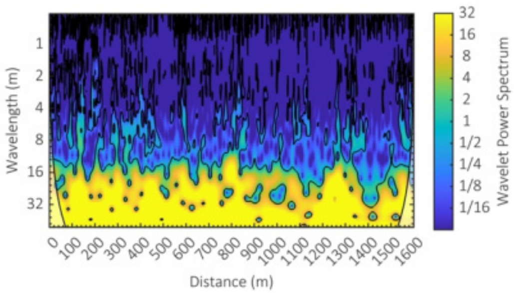

(a) Surface A

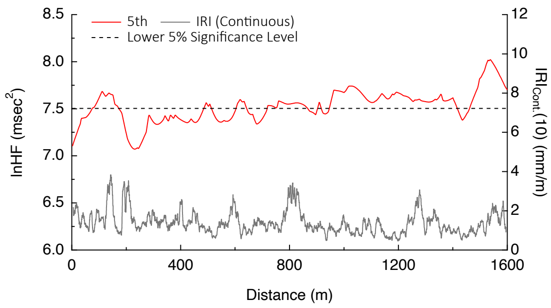

(a) Surface A

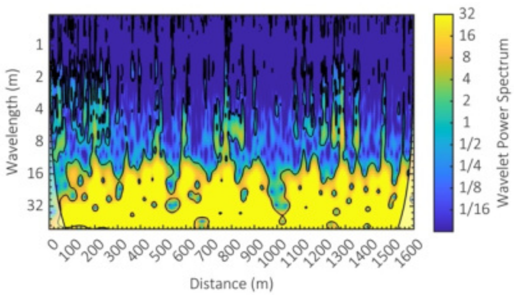

(b) Surface B

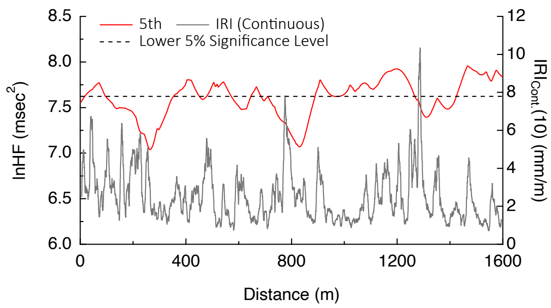

(b) Surface B

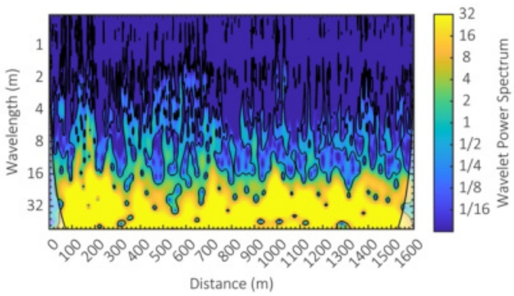

(c) Surface C

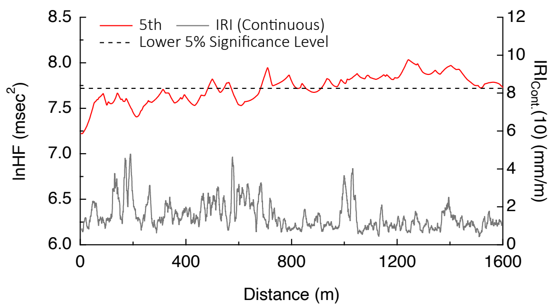

(c) Surface C

Figure 12 Wavelet transform result.

Figure 13 IRI and HF variation.

5. DISCUSSION AND CONCLUSIONS

This study has confirmed the distinct surface irregularities affecting the mental stress which causes user complaints even though the roughness level was less than the maintenance criteria. This result has been proved by the discrepancies of sensitive wavelengths between the physiological responses of road users and IRI. From those results, the mechanism of arising user complaints can be considered from viewpoints of road surface characteristics and physiological measures as follows:

- First, Localized surface irregularities with predominant wavelengths ranging from 4 to

8 m, which are underestimated in the IRI, induce vehicle vibrations sensitive to the human body when a car travel at the driving speed of 80 km/h.

- Then, mental stress due to the localized surface irregularities can be observed in road users sensitive to the vehicle vibrations.
- Finally, user complaints occurs at the locations where the mental stress significantly increases against the surface irregularities with wavelengths ranging from 4 to 8 m which are difficult to evaluate with IRI.

For the reasons above, the improvement of ride quality in expressway pavements caused especially by localized irregularities requires the maintenance considering surface wavelengths ranging from 4 to 8 m. The evidence can be supported by the following outcomes obtained in this study.

Actual surface irregularities involving user complaints which occurred on in-service expressways in a mountainous region were collected by the field survey. The result of the wavelet analysis then indicated that the profiles particularly included the unique wavelengths ranging from 4 to 8 m. This study further investigated the impact of surface irregularities on the mental stress of participants with two physiological measures such as HRV and EDA to investigate by performing a driving simulator experiment involving various drivers with actual profile data measured in the field survey. As a result, the mental stress of the participants sensitive to the vibration of which HRV response occurred below the 5th percentile was observed for the stimuli due to surface irregularities involving the wavelengths ranging from 4 to 8 m. In addition, the SCR in EDA responded to the tentative mental stress toward the ride quality for localized irregularities. Those physiological responses appeared even against the surface irregularities which were under the maintenance threshold in terms of the IRI. This was due to the discrepancies of sensitive wavelengths between the physiological responses of road users and IRI. In conclusion, the treatment of surface irregularities including predominant wavelengths between 4 and 8 m was possible to improve the ride quality of expressways by filling the gap between the maintenance criteria and user ratings. Although the predominant wavelengths depend on the traveling speed of a vehicle, the approach has a potential to be applied to other categories of roadways by considering the homeostasis of human physiological perception.

6. ACKNOWLEDGEMENTS

The authors would like to thank Ms. Marei Inagi who was a graduate student at the graduate school of engineering, Kitami Institute of Technology for her assistance to this study.

7. REFERENCES

Chanjun, C., & Seung-Ki, R. (2019). Road Surface Damage Detection Using Fully Convolutional Neural Networks and Semi-Supervised Learning. Sensors,19(24).

Descornet, G. (1989). A Criterion for Optimizing Surface Characteristics. Transportation Research Record, 1215, 173-177.

Eguchi, M., Tanaka, Y., Kawamura, A., & Tomiyama, K. (2015). A new IRI-based Assessment for Detecting Spotted Surface Defects. Journal of Japan Society of Civil

Engineers, Ser. E1 (Pavement Engineering), 71(3), I_17-I_23.
Fowles, D.C, Christie, M.J., Edelberg, R, Grings, W.W., Lykken, D.T., & Venables. P.H. (1981). Publication Recommendations for Electrodermal Measurements. Psychophysiology, 18(3): pp.232-239.
Fujita, S., Tomiyama, K., Abliz, N. & Kawamura, A. (2013). Development of a Roughness Data Collection System for Urban Roads by use of a Mobile Profilometer and GIS. Journal of Japan Society of Civil Engineers, Ser. F3 (Civil Engineering Informatics), 69(2), I_90-I_97.
Inagi, M., Tomiyama, K., Kohama, R. & Sato, M. (2022a). Identification and Human-centered Evaluation of Road Surface Roughness Causing Stress Focusing on Physiological Indices. Journal of Japan Society of Civil Engineers, Ser. E1 (Pavement Engineering), 78(2), I_135-I_143.
Inagi, M., Tomiyama, K., Kohama, R., Eguchi, M. & Sato, M. (2022). Human-centered Evaluation with Biosignals for Localized Surface Roughness on Expressway Pavements. Roads and Airports Pavement Surface Characteristics. https://doi.org/10.1201/9781003429258
Inagi, M., Tomiyama, K., Ito, M., & Sato, M. (2023). Human-Centered Road Surface Roughness Evaluation Considering Stress Factors based on Physiological Responses, Japanese Journal of JSCE, 79(21). https://doi.org/10.2208/jscejj.23-21019
Ishida, T., Takeomoto, H., Kawamura, A., & Shirakawa, T. (2004). Impact of Pavement Roughness on Riding Comfort and Sense of Safety Evaluated using a Driving Simulator. Journal of Pavement Engineering, JSCE, 9, 49-56.
ISO. (1998). Mechanical Vibration and Shock – Evaluation of Human Exposure to Whole-body Vibration - Part1: General Requirements, ISO2631-1:1997.
Jennifer, A., & Rosalind, P. (2005). Detecting Stress During Real-World Driving Tasks using Physiological Sensors. IEEE Transactions on Intelligent Transportation Systems, 6(2).
Kawamura, K & Kamiya, K. (2007). Current Status and Issues of Pavement Rehabilitation in NEXCO, Asphalt, 50(222), 25-30.
Kumada, K., Oono, S., & Sato, M. (2002). About the Relations between the Structure, Traffic Various Cause of the Expressway and IRI. Journal of Pavement Engineering, JSCE, 7, 10p1-10p6.
Kumada, K., Sato, M., & Kamiya, K. (2005). Study on Road Surface Properties and Ride Quality Evaluation, Nihon Doro Kodan Research Institute Report, 42, pp. 197-208.
Mallat, S. A. (1999). Wavelet Tour of Signal Processing, Academic Press, New York.
Múčka, P. (2017). International Roughness Index specifications around the world. Road Materials and Pavement Design, 18(4), 929-965.
Sayers, M. W. and Karamihas, S. M. (1998). The Little Book of Profiling, - Basic Information about Measuring and Interpreting Road Profiles. The University of Michigan.
Task Force of the European Society of Cardiology, and the North American Society of Pacing, and Electrophysiology. (1996). Heart Rate Variability: Standards of Measurement, Physiological Interpretation, and Clinical Use. Eur. Heart J., 17(3), pp.354-381.
Tomiyama, K., Kawamura, A., Rossi, R., Gastaldi, M., & Mulatti, C. (2015). Evaluation of Surface Unevenness Considering Mental Fatigue based on Heart Rate Variability Analysis. Journal of Japan Society of Civil Engineers, Ser. E1 (Pavement Engineering), 71(3), I_1-I_8.
Tomiyama, K., Inagi, M., Ito, M., Meguro, K., Eguchi, M., and Sato, M. (2023). Consistency of International Roughness Index and Vehicle Interaction in Ride Quality Evaluation for Expressway Pavements. Proceeding KRTJ, 16(1), Topic A, pp.1-10.

Determining the level of implementation and level of importance in the development of road classification in Indonesia

Herry Kurniawan[1], Latif Budi Suparma[2], Suryo Hapsoro Tri Utomo[3]
[1] BPJN Central Sulawesi, Directorate General of Highways, Ministry of Public Works and Housing, Indonesia, herry.kurniawan@pu.go.id
[2] Department of Civil and Environmental Engineering, University of Gadjah Mada,, Yogyakarta, Indonesia, lbsuparma@ugm.ac.id
[3] Department of Civil and Environmental Engineering, University of Gadjah Mada,, Yogyakarta, Indonesia, suryohapsoro@ugm.ac.id

ABSTRACT

Mismatch between the function, status, and class of the road is one of the main causes of road damage. The consistency in the implementation of theory/standards of road classification and the implementation in the provision of a road network system is allegedly one of the causes of the problem. Hypothetically, one of the reasons is the difference in viewpoints between actors. Literature reviews and questionnaire surveys were used to gather data and information. Questionnaires were conducted with resource persons who work as academics, practitioners, policy makers, associations. The results shows that there are differences in perspective between actors. The results of the study prove that the viewpoints between actors in responding to the variables of importance level and implementation level in determining the road hierarchy are relatively different based on their role. There are 13 variables (Volume of goods, Total population, Population density, Location, Travel time, Connected authority areas, Connectivity, Accessibility index, Urban system, Industrial area, Mining area, Road width, and Traffic volume) confirmed by actors as variables used to form synchronization models of road function, road status, road load class and road infrastructure class

Keywords: Road Classification, Synchronization, Important Performance Analysis

1. INTRODUCTION

Indonesia Law Number 2 of 2022 about roads states that roads function as part of transportation infrastructure that plays an important role in the economy, society, security, and the environment, as well as serving as infrastructure for the distribution of goods and services. The definition of a road according to this law is transportation infrastructure that includes all parts of the road, including supplementary and complementary buildings designated for traffic, located on the ground surface, above the ground surface, below the ground surface and/or water, and above the water surface, except for railways, tramways, and cable roads. Roads are categorized according to the system, function, status, load class and infrastructure class. The issue of conflicts related to the mismatch of road function, status, load class and infrastructure class remains one of the main causes of suboptimal road capacity and service, and it also impacts the performance of mobility for people and goods. This problem is not only prevalent in major cities but also in tier-two cities across various countries, including Indonesia (Karim et al., 2014). Various literatures explain that this issue often arises due to sub-problems on the supply and demand sides (Levinson et al., 2011). On the supply side, for example, road providers tend to plan roads following urban development trends and dynamics rather than consistently implementing phased planning according to medium and long-term road development scenarios (Tsigdinos et al., 2020). Meanwhile, on the demand side, the problem is exacerbated by the lack of awareness and discipline of developers in building and utilizing space that does not align with the designated road services, as well as the undisciplined behavior of road users in adhering to regulations related to road load (Liu et al., 2017). Besides traffic accidents, conflicts in the application of road function, status, class, and space utilization also cause road damage and ultimately lead to inefficient road preservation costs.

1.1 Road hierarchy in Indonesia

The function of determining road hierarchy is to ensure the orderly grouping of roads, thereby forming a framework that can be used by the government in planning development, maintenance, and management schemes for the road network (Eppell et al., 2001). A well-structured road hierarchy will reduce the negative impact of traffic by limiting activities that are not compatible with the dominant traffic flow, redirecting long distance traffic through less vital routes, and ensuring that the most important activities in urban development plans are given sufficient space. Road hierarchy is very important in transportation network planning. One of the main goals of road hierarchy is to optimize accessibility, connectivity, ease, and safety for all road users, including motor vehicles, bicycles, pedestrians, and public transport customers (Eppell & Zwart, 1997). From operational performance criteria, namely speed, most road segments do not have significantly different performance from each other except for the performance of toll road (Goto & Nakamura, 2016). In such situations, the reorganization of road networks with a functional hierarchy is crucial. Road hierarchy is necessary so that the suitability of management, planning technical standards, and maintenance concepts can be properly applied (Ye et al., 2015). The importance of classifying roads is also explained in a study which provides quantitative evidence on the importance of urban road hierarchy based on network analysis and traffic flow at various time scales, in preventing traffic congestion problems (Huang, 2016). The summaries for each type of road hierarchy in Indonesia are attached in Table 1.

Table 1 Hierarchy and classification of roads in Indonesia

Road classification		Source of regulation
System	Primary road	Article 7 Law 38 of 2004
	Secondary road	
Function	Arterial road	Article 8 Law 2 of 2022
	Collector road	
	Local road	
	Neighbourhood road	
Status	National Road	Article 9 Law 2 of 2022
	Provincial road	
	District/city road	
	Village Road	

Road classification		Source of regulation
Infrastructure class	Toll road	Article 10 Law 38 of 2004
	Main road	
	Medium road	
	Small road	
Load class	Class I	Article 19 Law 22 of 2009
	Class II	
	Class III	
	Special road	

(Analysis Result, 2024)

1.2 Freight transportation challenges

The current implementation of road functions, status, load class, and infrastructure class cause inefficiency in terms of terminals and handling costs (Mulyono, 2021). Although its implementation is intended to restrict vehicle loads, divide responsibilities in road provision and maintenance, and ensure safety, field facts indicate that there are still violations of the heavy freight vehicle load limits, no terminal and handling costs for inter-status road transfers, and county and provincial roads deteriorate faster with longer travel times. Implementing a single class does not immediately solve the existing problems. Implementing a single class in the road network system also has consequences in terms of financing a single class road infrastructure. Therefore, synchronization is needed between the function, status, and class of roads in the road network system. The challenges and problems of implementing the same class road between road statuses on regional/national logistics routes are illustrated in Figure 1.

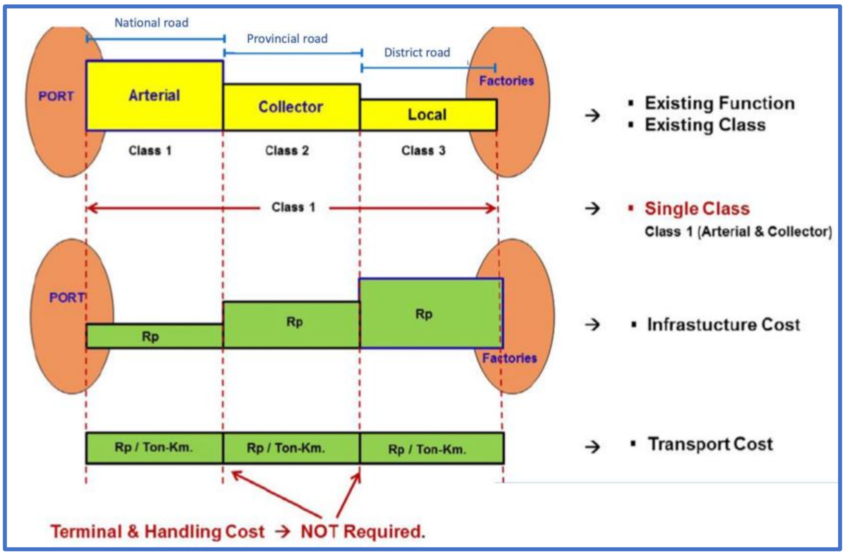

Figure 1 Challenges and problems of implementing the same road class on regional/national logistics transportation routes

2. LITERATURE REVIEW

2.1Factors considered in determining road hierarchy

Roads can enhance economic activities in a location by helping people travel and/or send goods more quickly to a destination. Commodities can flow to local markets, and the economic output of a place can be sold to markets outside the region. Additionally, roads also develop the traffic economy along their routes. The differences in resource ownership and the limited capability of an area to support the needs of its population result in the exchange of goods, people, and services between regions (Morlok, 1988). This exchange begins with the process of supply and demand. Road networks are tools to deliver supply and demand to other areas, thus enabling economic activities. There is another study used two approaches to test the performance of the road network system, which was examined with linear regression analysis, where population size and population density were the independent variables used (Parthasarathi, 2014). The higher the population, the higher the congestion, as well as the value of daily vehicle kilometers travelled. Another study demonstrated the impact of changes and developments in transportation due to changes in population patterns using the instrumental variable method (Garcia-Lopez, 2012).

The initial philosophy of road hierarchy considers the need for an area to have specific land uses that are restricted and surrounded by specific traffic flows. Regional geography becomes significant when related to transportation because spatial reach requires energy, cost, and time. The factors determining the magnitude of transportation costs are also related to the condition of the available road network such as travel time, path length, and route cost were considered to analyse performance elasticity based on road network hierarchy using a modified logit model (Zeng et al., 2018). Regional geography also impacts the road infrastructure that is built, including one of its components, the road network structure. One study used a road network matching approach, classifying the network into several structural categories, which were then assigned to each category based on appropriate parameters or criteria (Meng Zhang et al., 2010). This study was also supported by research conducted on improving highway network generalization methods by considering network geometry, topology, and traffic flow patterns. The results showed better connectivity and road functionality (Wang et al., 2020).

The road network system is structured based on spatial planning and by considering the connectivity between and within urban and rural areas. Industrial areas, warehouses, freight terminals, and multimodal transportation routes for freight are placed near the primary road network but are usually on the outskirts of city limits. This hypothesis aims to prevent freight transport from entering highways that pass through densely populated residential areas, giving the impression that they have their own transportation routes with applicable regulations to maintain the harmony of the road network functions. The generation and attraction of trips depend on the type of land use and the amount of activity on that land (Tamin, 1997). The relationships and models developed are used to better understand the relationships in a city, namely between land use (activities), transportation (network), and traffic (movement). These three components are interconnected and influence each other. Each land use system (activity) has certain types of activities that will generate movement and attract movement in the process of fulfilling needs.

Based on the explanation in the literature review regarding the concept of road hierarchy to achieve synchronization between function, status, and road class, the variables of economic, demography, geography, land use, and infrastructure will be used as determinants in this study. The consideration used is the suitability with the conditions and issues faced by road infrastructure in Indonesia.

2.2 Level of importance and implementation with Importance Performance Analysis (IPA)

Importance Performance Analysis (IPA) in research is a useful method to identify the levels of importance and performance of variables and to examine the gaps between them. This allows for determining which variables are beneficial, need improvement, or should be eliminated in the study. Initially, IPA was a quadrant analysis technique developed to examine and recommend management strategies (Martilla & James, 1977). Over time, the IPA method has been applied to various fields, including transportation. IPA was used to identify aspects of transportation at the Moncloa transport hub in Spain that needed improvement or should be maintained (Hernandez et al., 2014). Conceptually, analysis using the IPA method is a multi-attribute model (Crompton & Duray, 1985). This technique identifies the strengths and weaknesses of market offerings using two main criteria: the relative importance of attributes and customer satisfaction. Initially, IPA begins with identifying the attributes relevant to the research being conducted. This selection of attributes is based on literature and studies related to the issue at hand. These attributes are then evaluated based on their importance to consumers and how they are perceived by respondents. After determining the appropriate attributes, respondents are given two questions: the level of implementation of these attributes and the level of importance of these attributes. Using mean, median, or ranking measurements, the scores for importance and performance of attributes are collected and classified into high or low categories, then each attribute is placed into one of four quadrants of importance and performance.

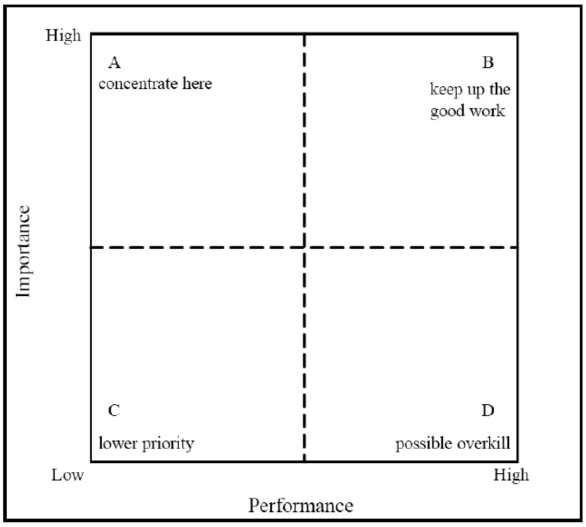

Figure 2 Importance performance analysis matrix

The main function of IPA is to display information related to service factors that respondents believe significantly affect their satisfaction levels, as well as service factors that consumers feel need improvement due to current unsatisfactory conditions. IPA combines measurements of importance and satisfaction factors into a two-dimensional graph that facilitates data explanation and practical suggestions. IPA is also used as a preferred methodology by transportation company managers because it can display results graphically in a simple way (Figler et al., 2011). IPA has been used to evaluate various public transportation services, such as Bay Area Rapid Transit in San Francisco (Weinstein, 2000), high-speed rail in Taiwan and Korea (Chou et al., 2011), airline service quality in Taiwan (Chen & Chang, 2005), and intercity passenger road transport quality in Brazil (Freitas, 2013). IPA is a graphical technique that uses levels of importance and performance as coordinates on a two-dimensional grid divided into four quadrants. The quadrant chart quantifies importance values on the vertical axis and performance values on the horizontal axis as shown in Figure 2.

3. METHODOLOGY

This study was carried out in Lampung Province, Daerah Istimewa Yogyakarta Province, South Kalimantan Province, West Papua Province, Maluku Province, and Southeast Sulawesi Province. The locations were chosen based on the major cities with significant logistics activities on each of Indonesia's main islands, covering all key islands in the country. The tool used in this research is a questionnaire.

3.1Research parameters

The survey design contains research variables and their operational definitions. This operational definition functions as a guide to finding appropriate data in the empirical world. The research variables used are as described in Table 2.

Table 2 Variables that influence the determination of road classification

No.	Factor	Variable	Operational definition
1	Economy	Economic growth	GDP growth rate
		GDP per capita	GRDP value in constant prices
		Volume of goods	Volume of goods transported by road
		Equity	Gini coefficient
		Regional fiscal capacity index	Regional fiscal capacity index
2	Demographics	Total population	The number of residents
		Population density	Comparison of the population with the area
3	Regional geography	Location	Typology of road contour
		Travel time	Time for transporting goods from origin to destination.
		Connected authority areas	Roads connect between cities/regencies
		Connectivity	The attractiveness of an area and the ease of reaching that area
4	Urban systems and spatial patterns	Accessibility index	National, regional, and local activity centre
		Urban system	The industrial area served by the road
		Industrial area	The mining area served by the road
5	Transportation infrastructure	Mining area	Connectivity between regions
		Travel cost	Costs incurred by those carrying goods
		Road width	Existing road width
		Traffic volume	Average daily traffic volume per day
		Drainage system	Roadside channel width
		Median	Road equipment and road user information (markings, lighting, sidewalks, signs)
		Signs and markings	Separated by vehicle class according to Bina Marga, Ministry of Public Works

(Analysis Result, 2024)

3.2Research procedures and analysis

The data collection stage includes data collection techniques, source, and the results achieved are summarized in Table 3.

Table 3 Data collection and processing stage

Data	Data collection techniques	Source	Result
Assessment of importance level	Questionnaire	Survey results obtained from academics, practitioners, policy makers, associations	Data on the level of importance and implementation of each variable for determining road sections in the road network system
Assessment of implementation level			
Assessment of importance level and implementation level	Importance performance analysis (IPA) matrix quadrant	Assessment and analysis result	The variables are grouped into importance performance matrix

In carrying out the analysis, the first target is to identify problems that occur due to lack of synchronization of road function, road status, road load class, and road infrastructure class and their impact on logistics mobility. At this stage, the data used are existing regulations and empirical data, while the results obtained are descriptions of conflict problems that occur due to road function, road status, road load class, and road infrastructure class that are not in sync and their impact on logistics mobility. The next stage is to identify the analytical relationship between road segment determination based on road function, road status, road load class and road infrastructure class with influencing variables. The variables utilised in the data are chosen based on their significance and applicability within the road network system, and they are subsequently inserted into the IPA matrix.

4. RESULT AND DISCUSSION

This analysis of respondent characteristics helps in understanding the diversity and perspectives they bring to the survey, which in turn will influence the results and conclusions of the analysis conducted. Figure 3 below is a general description of survey respondent data on the synchronization of road function, status and class. The general description also shows the respondent's professional group and location where the respondent works.

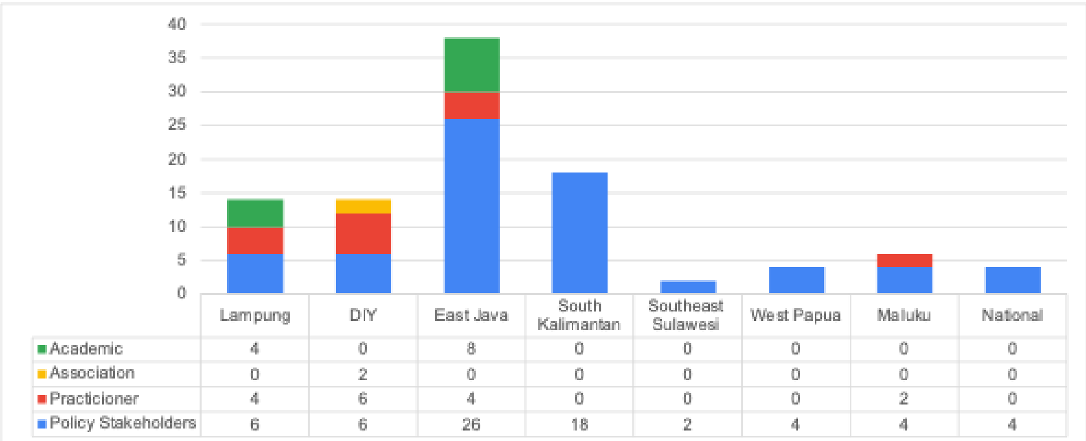

Figure 3 Description of respondents

Table 4 below explains the number of respondents who answered whether each variable is important and whether it has been implemented in determining the function, status, load class and infrastructure class of road.

Table 4 Survey results

Code	Var.	Level of importance				Level of implementation			
		Not important	**Less important**	**Important**	**Very important**	**Not implemented**	**Less implemented**	**Implemented**	**Very implemented**
V1	Economic growth	4	44	210	142	21	76	145	158
V2	GDP per capita	4	131	172	93	27	88	218	67
V3	Volume of goods	2	15	176	207	11	55	134	200
V4	Equity	4	146	150	100	39	93	211	57
V5	Regional fiscal capacity index	5	132	148	115	33	87	222	58
V6	Total population	2	35	195	168	25	64	138	173
V7	Population density	2	34	204	160	25	61	141	173
V8	Location	6	45	183	166	18	72	136	174
V9	Travel time	8	39	182	171	18	72	140	170
V10	Connected authority areas	2	15	182	201	4	59	139	198
V11	Connectivity	2	17	175	206	2	55	119	224
V12	Accessibility index	2	21	192	185	4	58	144	194
V13	Urban system	3	17	175	205	4	50	133	213
V14	Industrial area	7	32	197	164	30	65	138	167
V15	Mining area	8	48	178	166	32	73	144	151
V16	Travel cost	56	98	130	116	30	148	165	57
V17	Road width	4	19	177	200	11	48	136	205
V18	Traffic volume	2	6	165	227	9	47	119	225
V19	Drainage system	13	57	190	140	33	63	149	155
V20	Median	62	111	128	99	37	152	154	57
V21	Signs and markings	72	104	131	93	34	143	159	64
V22	Vehicle class 4	1	15	176	208	15	58	137	190
V23	Vehicle class 6a	1	16	162	221	17	54	130	199
V24	Vehicle class 6b	1	15	163	221	19	51	133	197
V25	Vehicle	1	18	173	208	20	57	140	183

Code	Var.	Level of importance				Level of implementation			
		Not important	Less important	Important	Very important	Not implemented	Less implemented	Implemented	Very implemented
	class 7a								
V26	Vehicle class 7b	2	18	183	197	19	60	135	186
V27	Vehicle class 7c	2	17	167	214	20	59	125	196

(Analysis Result, 2024)

From the survey results, the majority answer was selected to represent the level of importance and level of implementation for each variable and shown in Table 5. Most of the answers selected for each variable were considered important/very important and implemented/ very implemented. The IPA matrix as shown in Figure 4 to Figure 7, important and very important variables are both in quadrant A or B, meanwhile implemented and very implemented variables are both in quadrant B or D, therefore all variables are in quadrant B (all variables) have a high level of importance and level of implementation. Figure 4 to Figure 7 shows any different between the level of importance and the level of implementation based on the respondent's point of view. Respondents who are policy makers (Figure 4) tend to answer that all variables (except V20) are very important and fully used in the classification/hierarchy of the road. Respondents who are Association (Figure 5) tend to answer that all variables are very important and fully used in the classification/hierarchy of the road. While in Figure 6 shows that practitioners likely having view that V1 and V4 are very important but less implemented. Figure 7 shows that academic tend to answer that V4 and V5 are very important but less implemented, while V2 and V16 are less important and less implemented. It shows that there is different point of views between actors regarding the importance level of variables in the determination of road hierarchy and the level of its implementation. This result reinforces the findings of previous studies that the difficulty of developing a road network for freight transportation is influenced by the consideration of conflict of interest between actors represented by the government, the community, and the private sector (Vermote et al., 2013). Factors causing road damage are inaccuracy and inconsistency (planning, implementation, and maintenance) (Susanti, 2018).

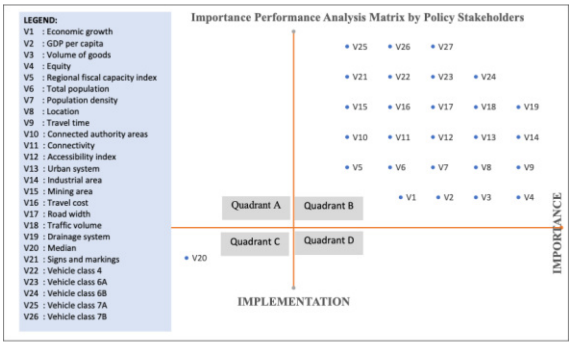

Figure 4 Importance performance analysis matrix (Policy Maker)

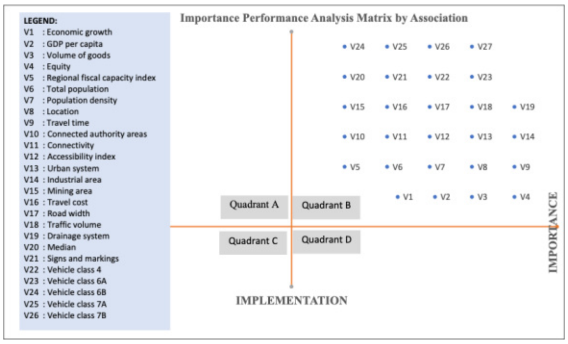

Figure 5 Importance performance analysis matrix (Association)

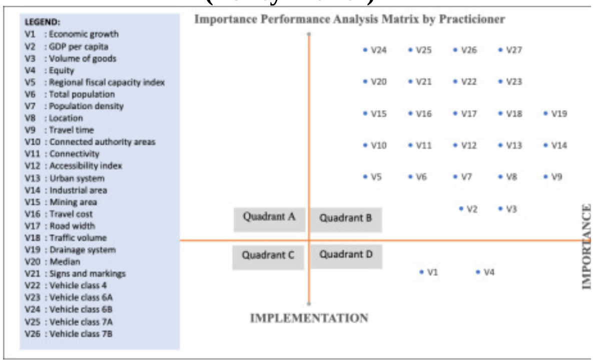

Figure 6 Importance performance analysis matrix (Practitioner)

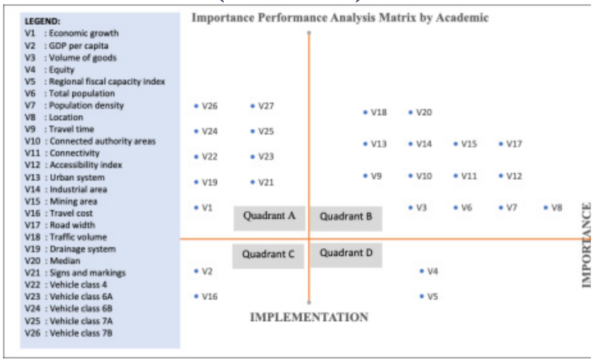

Figure 7 Importance performance analysis matrix (Academic)

However, we can differentiate respondent's answers between important and very important, or implemented and very implemented. Table 5 below explains the differences or gaps between the level of importance and the level of implementation.

Table 5 Variables that have a gap between the level of importance and the level of implementation

Code	Variable	Importance level	Implementation level
V3	Volume of goods	Very Important	Very implemented
V6	Total population	Very Important	Very implemented
V7	Population density	Very Important	Very implemented
V8	Location	Very Important	Very implemented
V9	Travel time	Very Important	Very implemented
V10	Connected authority areas	Very Important	Very implemented
V11	Connectivity	Very Important	Very implemented
V12	Accessibility index	Very Important	Very implemented
V13	Urban system	Very Important	Very implemented
V14	Industrial area	Very Important	Very implemented
V15	Mining area	Very Important	Very implemented
V17	Road width	Very Important	Very implemented
V18	Traffic volume	Very Important	Very implemented

(Analysis Result, 2024)

Based on table 5 above, it can be seen that there are 13 variables that are not only considered very important but also considered to be fully implemented as variables forming synchronization models of road function, road status, road load class and road infrastructure class.

In order to ensure the result, a short questionnaire was also distributed to several academics, practitioners and policy makers to ask whether they agreed that these variables influenced road classification. Figure 8 shows that most of respondent agreed that the 13 variables influence road classification.

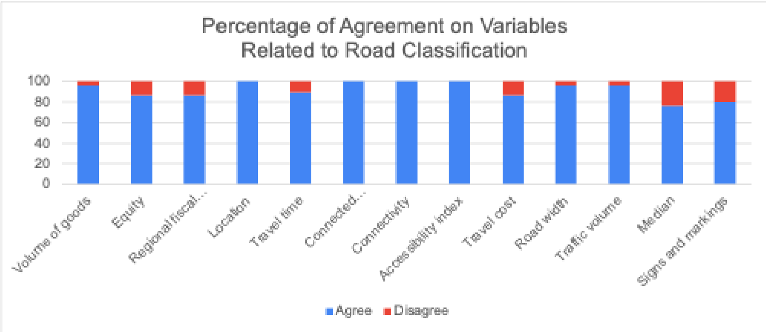

Figure 8 Percentage of Agreement on Variables Related to Road Classification

5. CONCLUSIONS

Based on the results of the analysis described in the previous chapter, two conclusions were obtained as follows:

- There are gaps between the level of importance and the level of implementation based on the respondent's point of view. Respondents who are association tend to give the answer that all variables are very important variable and full implemented. While respondents who are policy makers tend to give answer that all variables are very important variable and full implemented, except V20 (less implemented, adjusting to land availability). Respondents who are practitioners and academic more critical in assessing the level of implementation of variables in determining road hierarchy.
- There are 13 variables that are classified as very important and fully implemented as variables used in synchronization models of road function, road status, road load class and road infrastructure class.

6. REFERENCES

Chen, F.Y. and Chang, Y.H. (2005) Examining airline service quality from a process perspective. Journal of Air Transport Management, 11, 79–87.

Chou, J., Kim C., Kuo, Y. and Ou, N. (2011) Deploying effective service strategy in the operations stage of high-speed rail. Transportation Research Part E, 47(4), 507-519.

Crompton, J. L., & Duray, N. A. (1985). An Investigation of the Relative Efficiency of Four Alternative Approaches to Importance Performance Analysis. Journal of Academy of marketing Sciences.

Eppell, V., McClurg, B. A. and Bunker, J. M. (2001) "A four level road hierarchy for network planning and management", 20th ARRB Conference, p. 15. Available at: https://eprints.qut.edu.au/2349/1/2349.pdf.

Eppell, V.A.T. and Zwart, J. (1997) Hierarchy the Next Step 21st Australian Transport Research Forum Adelaide.

Figler, S.A., Sriraj, P.S., Welch, E.W. and Yavuz, N. (2011) Customer loyalty and Chicago, Illinois, transit authority buses. Transportation Research Record: Journal of the Transportation Research Board, 2216, 148-156.

Freitas, A.L.P. (2013) Assessing the quality of intercity road transportation of passengers: An exploratory study in Brazil. Transportation Research Part A: Policy and Practice. 49, 379–392.

Garcia-López, M. àngel (2012) 'Urban spatial structure, suburbanization and transportation in Barcelona', Journal of Urban Economics, 72(2–3), pp. 176–190. doi: 10.1016/j.jue.2012.05.003.

Goto, A. and Nakamura, H. (2016) 'Functionally Hierarchical Road Classification Considering the Area Characteristics for the Performance-oriented Road Planning', Transportation Research Procedia. Elsevier B.V., 15, pp. 732–748. doi: 10.1016/j.trpro.2016.06.061.

Hernandez, S., Monzon, A., & Ona, R. (2014). Urban transport interchanges: Importance-Performance analysis for Urban transport interchanges methodology for evaluating perceived quality By : Sara Hernandez , Andres Monzon and Rocío de Oña. Transportation Research Part A, 84(June), 31–43.

Huang, L. et al. (2016) 'Characterising streets hierarchies through network analysis and large-scale taxi traffic flow: a case study of Wuhan, China', Environment and Planning B: Planning and Design, 43(2), pp. 276–296. doi: 10.1177/0265813515614456

JICA. (2010). Study Report on Planning the Road Preservation Fund in The Republic of Indonesia (Inception). Ministry of Public Works.

Levinson, David & Zhu, Shanjiang (2011) "The Hierarchy of Roads, The Locality of Traffic, and Governance". Elsevier 19 October2011. TransportPolicy19(2012)147–154.

Liu, P., Mu, D., & Gong, D. (2017). Eliminating overload trucking via a modal shift to achieve intercity freight sustainability: A system dynamics approach. Sustainability (Switzerland), 9(3). https://doi.org/10.3390/su9030398

Karim, M. R., Ibrahim, N. I., Saifizul, A. A., & Yamanaka, H. (2014). Effectiveness of vehicle weight enforcement in a developing country using weigh-in-motion sorting system considering vehicle by-pass and enforcement capability. IATSS Research, 37(2), 124–129. https://doi.org/10.1016/j.iatssr.2013.06.004

Kementerian Pekerjaan Umum dan Perumahan Rakyat (2020) "Pengendalian ODOL Jaga Kemantapan Jalan dan Keselamatan Berkendara". Diunduh dari https://www.pu.go.id/berita/view/17992/pengendalian-odol-jaga-kemantapan-jalan-dan-keselamatan-berkendara pada 12 November 2020.

Martilla, J.A. and James, J.C. (1977) Importance-performance analysis. Journal of Marketing, 14(1), 77–79.

Meng Zhang, Liqiu Meng & Joachim Bobrich (2010) A road network matching approach guided by 'structure', Annals of GIS, 16:3, 165-176, DOI:10.1080/19475683.2010.513154. https://doi.org/10.1080/19475683.2010.513154

Morlok, K. E. (1988). Introduction to Transportation Engineering and Planning. Jakarta: Erlangga.

Mulyono, T.A. (2021). Assessment of the Functionality of Roads Safety and Legal Certainty. Yogyakarta. Gadjah Mada University Press.

Parthasarathi, P. (2014) 'Network structure and metropolitan mobility', Journal of Transport and Land Use, 7(2), p. 153. doi: 10.5198/jtluv7i2.494.

Susanti, Rina (2018) Analisis Terhadap Variabel yang Mempengaruhi Pemberlakuan Standar Mutu pada Pekerjaan Pemeliharaan Jalan di Propinsi Banten. Jurnal Fondasi, Volume

7 No 1.

Tamin, O.Z. (1997) "Transportation Planning and Modeling", Teknik Sipil Institut Teknologi Bandung.

Tsigdinos, S., & Vlastos, T. (2020). Exploring ways to determine an alternative strategic road network in a metropolitan city: A multi-criteria analysis approach. IATSS Research. https://doi.org/10.1016/j.iatssr.2020.06.002

Vermote, L., Macharis, C., and Putman, K. (2013) 'A Road Network for Freight Transport in Flanders: Multi-Actor Multi-Criteria Assessment of Alternative Ring Ways', Sustainability, 5, pp. 4222-4246. Doi: 10.3390/su5104222

Wang, Y., Cao, M., Liu, Y., Ye, R., Gao, X., & Ma, L. (2020). Public transport equity in Shenyang: Using structural equation modelling. Research in Transportation Business and Management, September, 100555. https://doi.org/10.1016/j.rtbm.2020.100555

Weinstein, A. (2000) Customer satisfaction among transit riders. How customer rank the relative importance of various service attributes. Transportation Research Record: Journal of the Transportation Research Board, 1735, 123-132.

Ye, P., Wu, B. & Rong, D. (2015) 'A Quantitative Method of Urban Road Hierarchy', ICTE 2015 - Proceedings of the 5th International Conference on Transportation Engineering, (December), pp. 2708–2716. doi: 10.1061/9780784479384.346.

Zeng, M., Ling, Z., Zhang, B. et al. (2018) Elasticity Analysis of Hierarchical Road Network Performance Based on Modified Logit Models. KSCE J Civ Eng 22, 4127–4135 (2018). https://doi.org.ezproxy.ugm.ac.id/10.1007/s12205-018-0905-x

Exploring The Risk Time of Fatal Injury Crash from Road Accidents in Chonburi's Urban Areas, Thailand.

Piyawan Tanudtanusilp[1], Surames Piriyawat[2,*]

[1]Department of Civil Engineering, Faculty of Engineering, Burapha University, Chonburi, THAILAND
[2]Sustainable Urban System Engineering and Transport Center (SUSET), Faculty of Engineering, Burapha University, THAILAND

*Corresponding Author, Email: suramesp@eng.buu.ac.th

ABSTRACT

Road accidents is the serious transport problems in worldly scale which affect quality and security of life in personal scale, and economic and human resource in national scale. Thailand is a country that was listed in the World recorded of high road accidents for many years. Among various factors, the happening time rule as specific characteristics of road accidents in each area's environments. On the behavior perspective, the happening time of road accidents reflect the lifestyles, activities, and driving behaviors of the most people in communities. In order to put the suitable control measures to manage negative driving behaviors in the risk duration time and reduce the possibility of road accidents and the losses from these happenings, studying and exploring risk times of accidents are the first necessary task for transport planners. As describe above, this article presents the study results from analyzing the road accident data of Chonburi, one of the most important provinces in Thailand's eastern region. The outstanding of Chonburi's urban areas, Mueang, Sriracha, and Bang-Lamung district, were selected as the studied areas. To reveal the risk time characteristics, 1,010 data set of fatal injury crash cases of provincial police region 2 Chonburi's official traffic accident reports between 2015 – 2024 was used as the case studies. Time series analysis was employed as the statistical mean for solving the data. The interest finding present the distinctions from the previous accident reports for daily and annually timeframe. Almost death cases of road accident in Chonburi's urban areas were happened during the late nighttime, 12.00 a.m. – 03.00 a.m. (21.49%) and in July (10.40%). However, the results found deathly road accident cases in studied areas were occurred during Saturday – Sunday (30.50%) by considering weekly timeframe that consist of the previous reports of Department of Highway.

Keywords: Road accident, Accident risk time, Fatal injury crash, Chonburi, Thailand

1. INTRODUCTION

Traffic accidents present a significant global transportation challenge, contributing to over 1.35 million deaths annually, which has substantial economic implications. On average, these accidents constitute approximately 3% Gross Domestic Product (GDP) (World Health Organization, 2020). Thailand ranks the ninth worldwide in terms of road accident rates (World Health Organization, 2018), which has substantial economic implications. To address this issue, a collective road safety objective has been established, aligning with the principles of sustainable development by overcoming the aim of reducing the road accident fatality rate to 12 individuals per 100,000 populations. This target is outlined in the Road Safety Master Plan 2022 – 2027, part of the 20 years National Strategy from 2018 –2037. The plan focuses on addressing infrastructure, logistics, and digital systems with the goal of achieving this target within the next three years (2027).

Among the road accident's risk areas in Thailand, Chonburi is one of those areas. Chonburi province is strong economic, offering significant potential at the national level. With a Gross Provincial Product (GPP) of 1,059,797 million Baht, it contributes 6.27% to the nation's GDP (Office of the National Economic and Social Development Council, 2022). This economic prominence is primarily due to its status as a major industrial center and a modern hub in Southeast Asia, particularly within the Association of Southeast Asian Nations (ASEAN). Additionally, Chonburi has emerged as a vital region within the Eastern Economic Corridor (EEC). Besides its economic importance, Chonburi boasts 114 significant and picturesque tourist destinations, drawing around 2.3 million Thai and international visitors (Ministry of Tourism and Sports, 2024). However, the step-up growth leads to the other side of developments, road accident. The large numbers of travelers and good movements increase the possibility of vehicles' accidents, especially, in the major cities in Chonburi, Mueang, Sriracha, and Bang-Lamung district. According to data from the Accident Information Center (2023), there were 11,456, 8,925, and 10,525 reported road incidents respectively. This surge in tourism also brings about several urban problems, such as traffic congestion and road accidents (Piriyawat & Intanu, 2018). Particularly concerning is the province's recent report of a high mortality rate due to road accidents, standing at 42.44 fatalities per 100,000 individuals, ranking second in the nation (Department of Land Transport, 2023).

In fact, there are a lot of factors causing the road accidents, such as, age, gender, road type, lighting, and speed limit (Eboli et al., 2019; Chen et al., 2012; Ghandour et al., 2020; Wood et al., 2019; Clarke et al., 2010). Among those various factors, the happening time rule as specific characteristics of road accidents in each area's environments. On the behavior perspective, the happening time of road accidents reflect the lifestyles, activities, and driving behaviors of the most people in communities. In order to put the suitable control measures to manage negative driving behaviors in the risk time and reduce the possibility of road accidents and the losses from road accidents, studying and exploring risk times of accidents are the first necessary task for transport planners. As describe above, this article presents the study results from analyzing the road accident data of the outstanding Chonburi's urban areas, Mueang, Sriracha, and Bang-Lamung district, by using time-series analysis. To reveal the risk time characteristics, 1,010 data set of fatal injury crash cases of provincial police region 2 Chonburi's official traffic accident reports between 2015 – 2024 were used as the case studies. The details of the study are presented in the following section.

2. LITERATURE REVIEW

A review of fatal road accident data in Thailand for 2023 indicates that Chonburi Province ranks second in accident statistics, following Bangkok. The top ten provinces with the highest road accident rates are Bangkok, Chonburi, Samut Prakan, Chiang Mai, Nakhon Ratchasima, Phuket, Pathum Thani, Ubon Ratchathani, Nakhon Si Thammarat, and Surat Thani, in that order (Road Safety Collaboration, 2024). An analysis of road accident statistics in Chonburi Province over the past four years reveals that the districts of Sriracha, Bang-Lamung, and Mueang consistently have the highest fatality rates each year, with a combined accident rate of 63%, as shown in Table 1.

Table 1 The fatality cases of road accident statistics in Chonburi Province between 2020-2023.

No.	District	2020	2021	2022	2023	Frequency	Percentage
1	Sriracha	84	116	145	131	476	23.55%
2	Bang-Lamung	98	84	114	115	411	20.34%
3	Mueang	106	72	105	102	385	19.05%
4	Ban-Bueng	29	59	65	53	206	10.19%
5	Phan-Thong	43	42	40	29	154	7.62%
6	Phanat-Nikhom	52	31	32	30	145	7.17%
7	Sattahip	27	23	37	30	117	5.79%
8	Bo-Thong	24	11	11	13	59	2.92%
9	Ko-Chan	13	6	9	12	40	1.98%
10	Nang-Yai	6	8	8	6	28	1.39%

(Source: Road Safety Collaboration, 2023)

A review of fatal road accidents across the regions of the Americas, Europe, Africa, South-East Asia, South Asia, and East Asia found that road traffic fatalities remain a major global concern, with varying trends observed in each region, as shown in Table 2.

Table 2 The fatality cases of road accident statistics in other Region between 2020-2023.

Country	Times of day	Days of week	Months of year	Source
The United States	12.00 A.M. – 04.00 A.M.	Saturday	October	National Safety Council, 2024
The European Union	12.00 A.M. – 06.00 A.M.	Saturday	August	SWOV Institute for Road Safety Research, 2023
Kenya	06.00 P.M. – 08.00 P.M.	Saturday	June	Kinyanjui, 2024
Taiwan	12.00 A.M. – 04.00 A.M	--	--	Ming-Heng, 2022
India	06.00 P.M. – 09.00 P.M.	--	May	Ministry of Road Transport and Highways, 2023
Pakistan	09.00 P.M. – 06.00 A.M.	Saturday & Sunday	--	Amjad et al., 2021
Taipei	04.00 P.M. – 08.00 P.M.	--	--	Heng-Yu et al., 2022

A review of fatal road accident statistics from Thailand's road accident reports reveals that these incidents often spike during periods that include New Year celebrations and the Songkran festival, as shown in Table 3 – Table 5.

Table 3 The fatality road accident statistics in Thailand between 2018-2023.

Item	Times of day	Days of week	Months of year	Source
1	07.00 P.M. – 08.00 P.M.	Friday	April	Department of Highway, 2018, 2021
2	07.00 P.M. – 08.00 P.M.	Sunday	April	Department of Highway, 2019
3	07.00 P.M. – 08.00 P.M.	Wednesday	December	Department of Highway, 2020
4	07.00 P.M. – 08.00 P.M.	Saturday	April	Department of Highway, 2022
5	12.00 A.M. – 01.00 A.M.	Sunday	April	Department of Highway, 2023
6	06.00 P.M. – 10.00 P.M.	Sunday	December	Road Safety Collaboration, 2021, 2023
7	06.00 P.M. – 10.00 P.M.	Sunday	May	Road Safety Collaboration, 2022
8	10.00 P.M. – 02.00 A.M.	Sunday	October	Road Safety Collaboration, 2020
9	--	--	January	Ministry of Public Health, 2019 Road Safety Thailand, 2020
10	--	--	March	Ministry of Public Health, 2018, 2021, 2023
11	--	--	December	Ministry of Public Health, 2020, 2022 Department of Land Transport, 2020-2023

Table 4 The fatality road accident statistics on New Year celebrations in Thailand between 2018-2023.

Item	Times of day	Days of week	Months of year	Source
1	07.00 P.M. – 08.00 P.M.	Saturday	December & January	Department of Highway, 2018
2	08.00 P.M. – 09.00 P.M.	Saturday	December & January	Department of Highway, 2019
3	10.00 P.M. – 11.00 P.M.	Saturday	December & January	Department of Highway, 2020
4	07.00 P.M. – 08.00 P.M.	Saturday	December & January	Department of Highway, 2021
5	07.00 P.M. – 08.00 P.M.	Saturday	December & January	Department of Highway, 2022
6	12.00 A.M. – 01.00 A.M.	Sunday	December & January	Department of Highway, 2023

Table 5 The fatality road accident statistics on Songkran Festival in Thailand between 2018-2023.

Item	Times of day	Days of week	Months of year	Source
1	07.00 P.M. – 08.00 P.M.	Friday	April	Department of Highway, 2018
2	08.00 P.M. – 09.00 P.M.	Saturday	April	Department of Highway, 2019
3	11.00 P.M. – 12.00 P.M.	Monday	April	Department of Highway, 2021
4	11.00 P.M. – 12.00 P.M.	Tuesday	April	Department of Highway, 2022
5	12.00 A.M. – 01.00 A.M.	Friday	April	Department of Highway, 2023

3. MATERIAL AND METHODS

3.1 Data

Chonburi Province is a significant hub for economic growth in eastern Thailand, characterized by its numerous industrial estates and large manufacturing industries. The province boasts a commercial port, a robust product delivery system, and popular tourist attractions. Covering a total area of 4,363 square kilometers, Chonburi has a population of approximately 1.6 million people and additional hidden population of about 1.1 million (Chonburi Provincial Administration Organization, 2022), many of whom are migrants working in the continuously expanding industrial sectors. Consequently, Chonburi has the highest highway travel volume in the eastern region, totaling 16,593 million vehicle-kilometers. The province also has a highway accident rate of 5.63 per 100 million vehicle-kilometers (Department of Highways, 2023) and a road accident death rate of 42.44 per 100,000 people, ranking second in the country (Department of Land Transport, 2023).

This study collected six years' worth of road accident data, from 2015 - 2023, excluding the Covid-19 pandemic between 2019-2021, using official traffic accident reports from the Provincial Police Region 2 in Chonburi. The dataset comprised 1,010 instances of fatal injury crashes, selected through purposive sampling. The districts with the highest number of road accidents were Muang, Siracha and Bang-Lamung, as shown in Figure 1. The variables from traffic accident reports were converted into numerical codes and compiled into a database. This data was then processed using Statistical Package for the Social Sciences and descriptive statistics were applied for analysis.

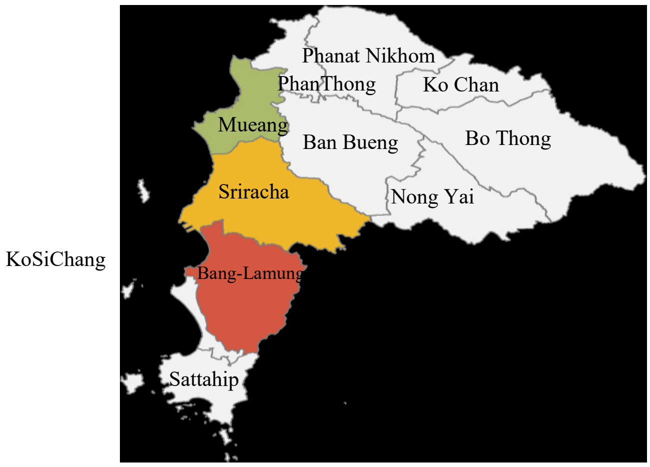

Figure 1 The studied areas of Chonburi's urban areas, which includes Mueang, Sriracha, and Bang Lamung Districts.

3.2 Time series analysis

The study employed time series analysis to examine the trends and occurrences of road accidents in the studied areas. The analysis focused three categories of time durations, including times of day, days of week, and months of year.

Times of day

In this category, road accident data were organized based on the time of day. The 24-hour period was divided into eight intervals, each lasting three hours: 12.01 a.m. – 03.00 a.m., 03.01 a.m. – 06.00 a.m., 06.01 a.m. – 09.00 a.m., 09.01 a.m. – 12.00 p.m., 12.01 p.m. – 03.00 p.m., 03.01 p.m. – 06.00 p.m., 06.01 p.m. – 09.00 p.m., and 09.01 p.m. – 12.00 a.m.

Days of week

For the next category, the accident data were grouped by days of week. The weekly accident data (Monday – Sunday) between 2015 – 2023 were considered to observe the accident rate in each day.

Months of year

The last group is analyzing by months of year. The road accident data in each month (January – December) between 2015 – 2023 were explored to finding the critical months of the accident in each year and overview.

4. RESULTS

4.1 The overviews of road accidents

In Chonburi's urban areas, there were 1,010 fatal road accidents. These incidents were distributed across three districts: Muang Chonburi with 308 cases (30.50%), Si Racha also with 352 cases (34.85%), and Bang Lamung also with 350 cases (34.65%).

The highest number of accidents occurred between 12.00 A.M. – 3.00 A.M. Saturdays and Sundays consistently showed the highest average accident rates, with fatal accidents peaking in July. The data, categorized by accident time periods, are presented in Table 6 – Table 9 and Figure 2 – Figure 7.

4.2 The trends of fatality cases of road accidents classifying by times of day

The road accident rates analyzed by times of day between 2015 – 2023 are listed in the Table 6 and depicted as trend lines for each year in Figure 2 and Figure 3.

Table 6 The trends of fatality cases of road accidents in studied areas classifying by times of day between 2015-2023 (Excluding Covid-19 pandemic between 2019-2021).

Time period	Time interval	Mean (Cases/hour)	SD (Cases/hour)	Frequency (Cases)	Percentage (Cases)
1	12.01 A.M. – 03.00 A.M.	36.17	11.87	217	21.49%
2	03.01 A.M. – 06.00 A.M.	24.67	9.67	148	14.65%
3	06.01 A.M. – 09.00 A.M.	19.17	5.71	115	11.39%
4	09.01 A.M. – 12.00 A.M.	16.00	6.63	96	9.50%
5	12.01 P.M. – 03.00 P.M.	12.33	4.55	74	7.33%
6	03.01 P.M. – 06.00 P.M.	13.67	4.27	82	8.12%
7	06.01 P.M. – 09.00 P.M.	17.33	5.09	104	10.30%
8	09.01 P.M. – 12.00 P.M.	29.00	11.52	174	17.23%

The data from Table 6 indicates a clear trend in the occurrence of fatal road accidents based on the time of day. The daytime's results, from 06.00 A.M. – 06.00 P.M., show lower frequency of fatal accidents, (36.34%). The times between 12.01 P.M. – 03.00 P.M. shown the lowest rate with 12.33 cases per hour (7.33%)

Conversely, fatal road accidents are more prevalent during the nighttime, accounting for 63.67% the number of accidents starts to increase in the evening, particularly from 06.01 P.M. – 09.00 P.M., and reaches its peak between 12.00 A.M. – 03.00 A.M. with the highest rate of 36.77 accidents per hour, or 21.49%. After 03.01 A.M., the frequency of accidents decreases, although it remains within the nighttime period.

This data underscores the importance of considering time of day when implementing road safety measures and enforcing traffic regulations.

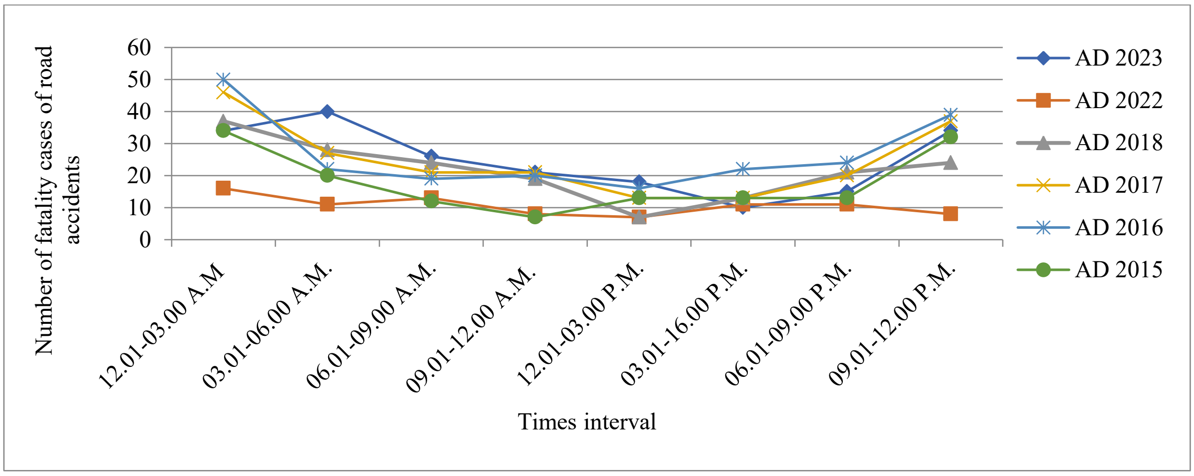

Figure 2 The numbers of fatality cases of road accidents in studied areas classifying by times of day between 2015-2023. (Excluding Covid-19 pandemic years 2019-2021)

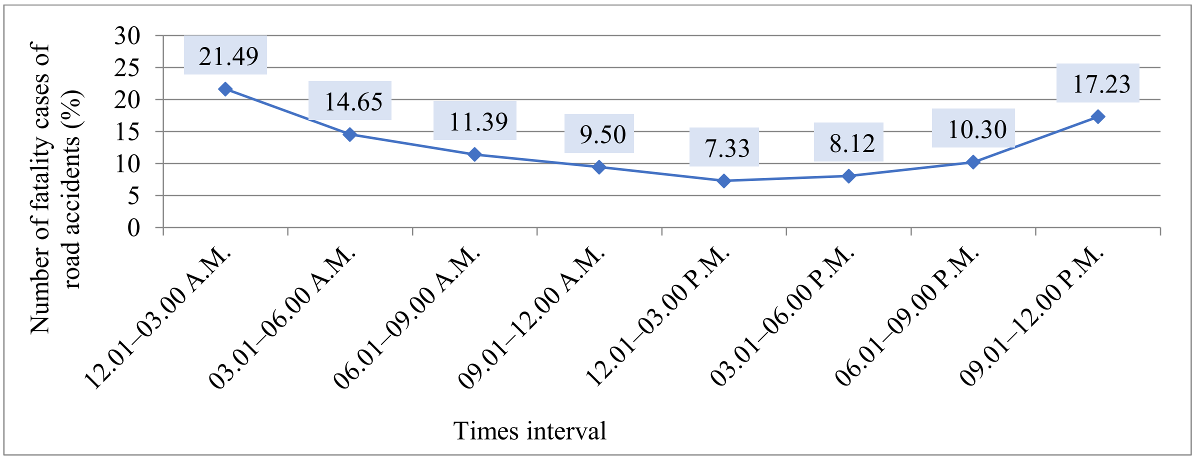

Figure 3 The trends of fatality cases of road accidents in studied areas classifying by times of day between 2015-2023. (Excluding Covid-19 pandemic between 2019-2021).

Figures 2 and 3 illustrate the annual trends in fatal road accidents, showing a consistent pattern during typical travel conditions and behaviors observed from 2015 – 2018. This consistency indicates that, under normal circumstances, fatal road accidents in Chonburi's urban areas follow a predictable pattern.

However, following the COVID-19 pandemic, specifically in 2022 and 2023, there was a marked deviation from this trend. The patterns of fatal road accidents during these years, particularly concerning the time of day, were significantly different from those observed in the pre-pandemic years. This variation highlights how the pandemic altered travel behaviors and conditions, resulting in notable changes in the frequency of fatal road accidents.

4.3 The trends of fatality cases of road accidents classifying by days of week

The occurrences of road accidents are categorized into seven days of the week, comprising five working days (Monday – Friday) and two weekend days (Saturday and Sunday), as depicted in Table 7 and were constructed as the trend lines for each year in Figure 4 and Figure 5.

Table 7 The trends of fatality cases of road accidents in studied areas classifying by days of week between 2015-2023. (Excluding Covid-19 pandemic between 2019-2021).

Time period	Days of Week	Mean (Cases/ day)	SD (Cases/ day)	Frequency (Cases)	Percentage (Cases)
1	Monday	23.50	7.69	141	13.96%
2	Tuesday	23.33	6.89	140	13.86%
3	Wednesday	23.17	6.79	139	13.76%
4	Thursday	23.83	8.68	143	14.16%
5	Friday	23.17	8.11	139	13.76%
6	Saturday	25.83	6.79	155	15.35%
7	Sunday	25.50	10.03	153	15.15%

According to Table 7, the overall analysis of fatal road accidents between 2015 –2023 reveals a consistent trend in the average number and proportion of accidents per week, broken down by day (Monday – Sunday).

Interestingly, Saturday and Sunday consistently exhibit the highest average number and proportion of accidents, with 25.83 and 25.50 accidents per day, respectively, totaling 30.50% this finding suggests that weekends tend to experience a higher frequency of fatal road accidents compared to weekdays.

Conversely, the weekdays (Monday – Friday) display relatively similar accident rates, indicating a more consistent pattern of accidents during the workweek.

This data underscores the importance of considering day of week variations when implementing road safety measures and enforcing traffic regulations, particularly focusing on strategies to mitigate the higher incidence of accidents during weekends.

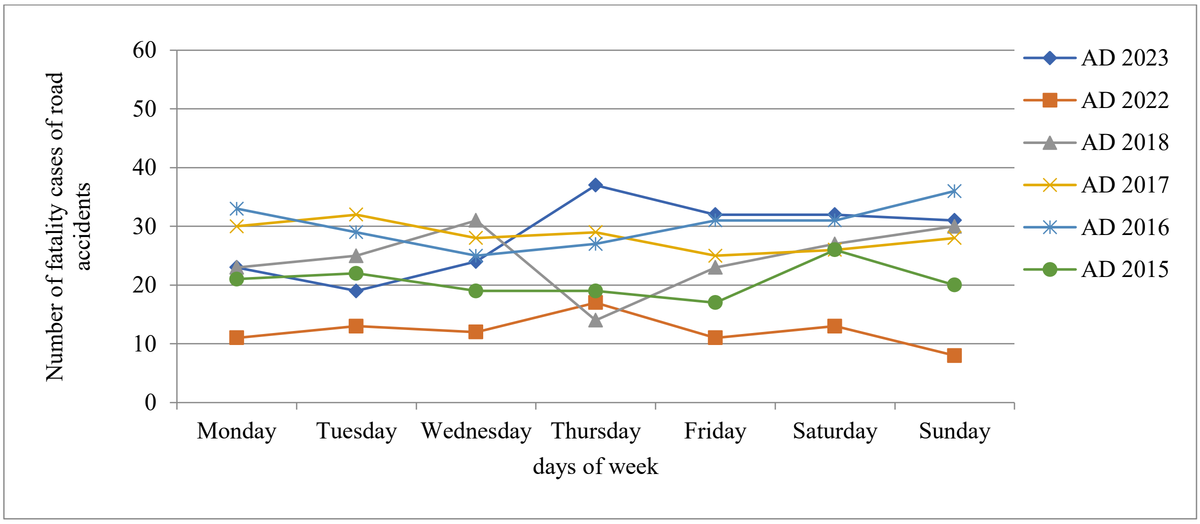

Figure 4 The numbers of fatality cases of road accidents in studied areas classifying by days of week between 2015-2023. (Excluding Covid-19 pandemic between 2019-2021).

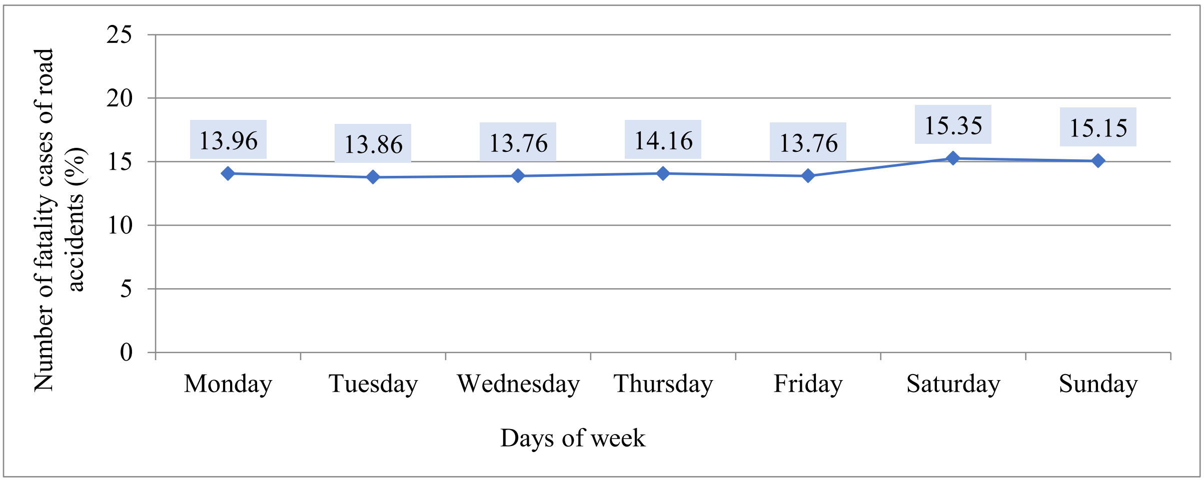

Figure 5 The trends of fatality cases of road accidents in studied areas classifying by days of week between 2015-2023. (Excluding Covid-19 pandemic between 2019-2021).

Figures 4 and 5 illustrate trends in serious road accidents by day of the week, revealing different patterns from year to year. These variations reflect changes in travel behavior and socio-economic conditions over time, emphasizing the evolving nature of road accident trends and the impact of various factors on road safety. Notably, the accident patterns by day of the week after from the COVID-19 pandemic (2019-2021) show significant differences.

These findings underscore the importance of accounting for annual changes when analyzing trends in serious road accidents. They also highlight the necessity of implementing adaptive and context-specific measures to effectively address the changing challenges in road safety.

4.4 The trends of fatality cases of road accidents classifying by months of year

The timing of road fatalities is categorized by month, covering all twelve months of the year, from January to December. This data is illustrated in Table 8 and were constructed as the trend lines for each year in Figure 6 and Figure 7.

Table 8 The trends of fatality cases of road accidents in studied areas classifying by months of year between 2015-2023. (Excluding Covid-19 pandemic between 2019-2021).

Time period	Months of year	Mean (Cases/month)	SD (Cases/ month)	Frequency (Cases)	Percentage (Cases)
1	January	9.50	7.34	57	5.64%
2	February	12.50	9.75	75	7.43%
3	March	13.33	11.55	80	7.92%
4	April	11.67	6.56	70	6.93%
5	May	17.00	7.72	102	10.10%
6	June	14.00	5.73	84	8.32%
7	July	17.50	1.87	105	10.40%
8	August	15.50	3.51	93	9.21%
9	September	15.33	3.27	92	9.11%
10	October	15.50	5.13	93	9.21%
11	November	12.50	2.81	75	7.43%
12	December	14.00	8.39	84	8.32%

According to Table 8, the overall trend between 2015 – 2023 indicates a pattern in fatal road accidents throughout the year. Starting from January, the number of fatal accidents tends to increase, averaging 9.50 incidents per month or 5.64% this upward trend reaches its peak in July, with an average of 17.50 incidents per month, constituting 10.40%

After July, there is a steady decline in the frequency of fatal accidents, continuing until December. During this period, the average number of accidents per month stands at 14.00, representing 8.32%

The analysis also indicates a higher average and proportion of fatal accidents during Thailand's transitional and rainy seasons, from May to October, compared to other times of the year. This discrepancy may be attributed to Chonburi Province's unique weather patterns, influenced by two primary monsoon seasons. The Northeastern Monsoon, from mid-October to mid-February, brings cooler temperatures and moderate winds, while the Southwest Monsoon, from mid-May to mid-October, results in heavy rain and strong winds (Thai Meteorological Department, 2024). This is supported by rainfall data from the Laem-Chabang Meteorological Station, which recorded 964.91 millimeters of rainfall from May to October 2022, contributing to a total rainfall of 2,557.95 millimeters (Smart Water Operation Center, 2024). This data highlights the significant impact of the Southwest Monsoon on Chonburi Province's weather during the rainy season.

These findings highlight the critical need for enhanced road safety measures, particularly during high-risk periods like the transitional and rainy seasons, to reduce the occurrence of fatal accidents.

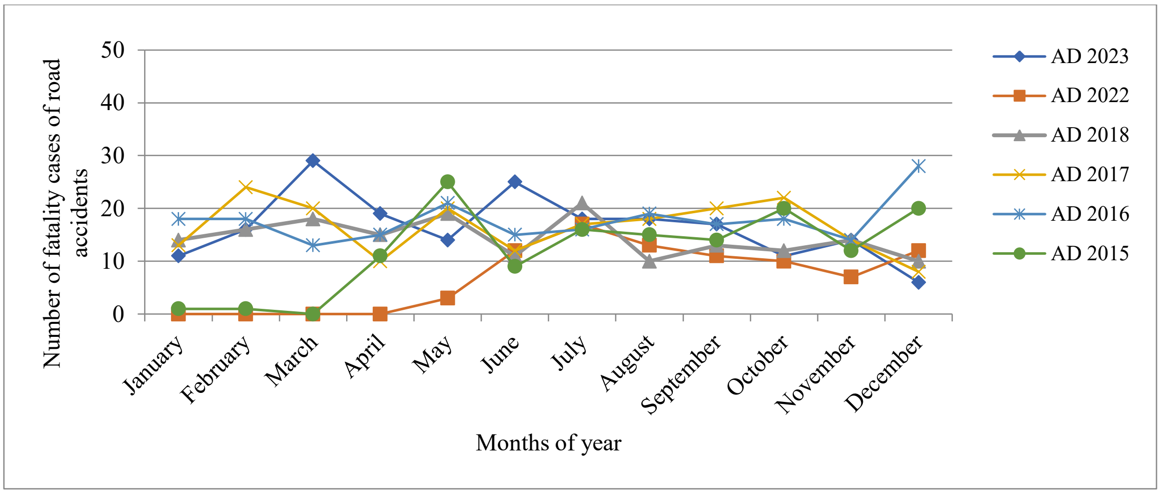

Figure 6 The numbers of fatality cases of road accidents in studied areas classifying by months of year between 2015-2023. (Excluding Covid-19 pandemic between 2019-2021).

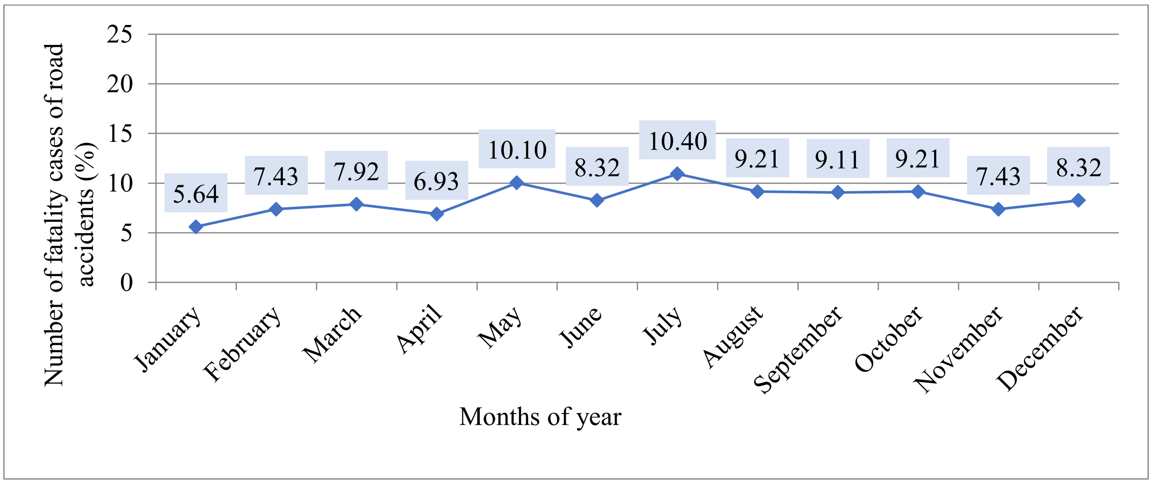

Figure 7 The trends of fatality cases of road accidents in studied areas classifying by months of year between 2015-2023. (Excluding Covid-19 pandemic between 2019-2021).

Figures 6 and 7 illustrate the monthly trends in road accidents resulting in fatalities throughout the year, revealing distinct patterns for each year due to varying travel behaviors. This variability and irregularity in the monthly accident trends highlight the dynamic nature of road accident patterns, influenced by factors such as travel behaviors and external conditions. Notably, after the COVID-19 outbreak (2022-2023), the patterns of accidents diverged from those seen in typical years, consistent with previous analyses that indicated the pandemic's impact on travel behaviors and road accident trends.

A significant finding from the analysis is that, while accident trends by time of day showed consistency and clear patterns across different years, reflecting commuters' risk behaviors depending on the time of day, the patterns varied significantly when considering the risk of accidents by day of the week and month of the year. This variability emphasizes the importance of a nuanced understanding of road accident patterns and the factors that influence them.

Despite fluctuations in patterns across individual years, an overall trend in accidents can be discerned when considering all the years studied. However, it is crucial to recognize that the accident pattern for any single year cannot reliably be used to predict incident behavior on an annual basis, unlike the more stable analysis based on time of day. These insights underscore the complexity of road accident patterns and the need for comprehensive analyses that consider the various factors affecting road safety.

4.5 The trends of fatality cases of road accidents classifying by study area

The data, categorized by accident time period and study area, are presented in Table 9. This table summarizes the peak times for fatality cases in road accidents across different districts, specifying the most critical hours, days, and months based on data from 2015 – 2023.

Table 9 The trends of fatality cases of road accidents in studied areas classifying between 2015-2023. (Excluding Covid-19 pandemic between 2019-2021).

District	Times of day	Days of week	Months of year
Mueang	12.00 A.M. – 03.00 A.M.	Saturday	September
Sriracha	09.00 P.M. – 12.00 P.M.	Friday	July
Bang-Lamung	03.00 A.M. – 06.00 A.M.	Sunday	May and August

Mueang: A tourist hub and provincial center

Road accidents in tourist areas such as Chonburi often exhibit unique characteristics due to the nature of traffic and tourist activities. Contributing factors include drivers who are unfamiliar with local routes, reckless driving in scenic areas where views can be distracting, and increased traffic density and parking difficulties during festivals or peak tourist seasons. Additionally, the risk of accidents is heightened by alcohol consumption while traveling and driving. The majority of fatal accidents occur on Saturdays, between 12.00 A.M. – 3.00 A.M., particularly in September.

Sriracha: Industrial and logistics zones

Road accidents in industrial areas like Sriracha are influenced by the types of vehicles, the environment, and the nature of activities within these zones. These areas often host factories, warehouses, and businesses requiring the transport of heavy goods, leading to frequent movement of large vehicles. Common accidents include collisions between trucks, trailers, or other large vehicles, as well as incidents involving vehicles and workers, particularly during shift changes or while goods are being transported. Despite speed limits, high-speed driving remains a concern, as drivers may exceed these limits. The risk of accidents is further heightened during nighttime operations due to reduced visibility, making it harder to detect obstacles or other road users. Most fatal accidents in this area occur on Fridays, during the daytime hours between 9.00 A.M. – 12.00 P.M., with a particular increase in September.

Bang-Lamung: Residential areas

Road accidents in residential areas often differ from those on busy highways or in urban zones. Common incidents include speeding, ignoring traffic signals, stop signs, or warning signs, and parking in no-parking zones. Drunk driving is also a major issue, significantly impairing driving ability. Additionally, poor road conditions such as potholes, slippery surfaces, and the absence of stop signs or traffic lights further increase the risk of accidents. Most serious accidents occur during the early hours of Sunday mornings, between 3.00 – 6.00 A.M., with a notable increase in May and August.

5. CONCLUSIONS

The objective of the research was to identify risk periods for fatal road accidents in urban areas of Chonburi, Thailand, The analysis utilized 1,010 official traffic accident reports from the Provincial Police Region 2, covering the years 2015 – 2023, with the exception of the Covid-19 pandemic years (2019–2021). The study found that the majority of fatal road accidents occurred during late-night hours, notably between 12.00 A.M. – 03.00 A.M., constituting 21.49% This aligns with prior research by various entities (National Safety Council, 2024; SWOV Institute for Road Safety Research, 2023; Ming-Heng, 2022; Department of Highway, 2023; Road Safety Collaboration, 2020), but contrasts with results from other studies (Department of Highway, 2018–2022; Kinyanjui, 2024; Road Safety Collaboration, 2021–2023).

Additionally, the research identified July as a high-risk month for fatal road accidents, accounting for 10.40% these finding contrasts with many prior studies, such as those by the National Safety Council (2024), SWOV Institute for Road Safety Research (2023), and the Department of Highway (2018–2023). This discrepancy may be influenced the Southwest Monsoon, from mid-May to mid-October, results Chonburi Province's in heavy rain and strong winds, with increased rainfall correlating with a higher incidence of accidents (Bergel-Hayat et al., 2013) and adverse weather conditions generally leading to more accidents (Koetse, 2009). Climate change further impacts road safety, with various studies indicating its influence on accident rates (Amin et al., 2014; Andersson and Chapman, 2011; Hambly, 2013; Malin et al., 2019).

However, road traffic accidents on highways and infrastructure, including environmental conditions, can be attributed to several factors. These include excessive speed, loss of control, and neglecting of road safety (Goss et al., 2008; Jeffrey, 2010). Other contributing factors are the use of mobile phones while driving (Jeffrey, 2010; Abiodun, 2011), high traffic volume, road rage, drunk driving, work-related stress, lack of driving experience, and insufficient attention to the road (Goss et al., 2008; Jeffrey, 2010; Odero, 2003).

Overall, the research indicates that the period between 12.00 A.M. – 03.00 A.M. is the most hazardous for fatal road accidents, despite lower traffic volume during these hours. This underscores the importance of increased caution during nighttime driving. Additionally, the highest number of fatalities occurring on Saturdays and Sundays suggests a need for heightened awareness and vigilance during weekends.

Findings in the study time of day, day of the week, and month of year can be used to guide road traffic control measures and regulations in Chonburi's urban areas. Although, legislation is also a vital area for addressing the factors that contribute to fatalities from road traffic accident such as not wearing seat belts, drink-driving, not using helmets, violating speed limits, and using mobile phones while driving. These laws regulating these issues exist in the country, they are often not effectively enforced. Hence, it is essential for Thailand to establish stringent laws and impose severe penalties, as road traffic accidents continue to be a significant cause of death worldwide.

6. SUGGESTIONS

The applications for safety measures

Speed checkpoints

Implementing speed checkpoints is an effective strategy to enhance road safety by reducing accidents caused by speeding. This measure encourages drivers to exercise caution and improves overall traffic safety.

Establishing speed checkpoints during the highest-risk periods in Chonburi, Sriracha, and Bang-Lamung, specifically between 12.00 A.M. – 3.00 A.M., with a focus on Saturdays and Sundays, especially in July, when the risk of accidents is highest, is recommended.

Alcohol checkpoints

The New Year and Songkran festivals, known for their celebration, joy, and social gatherings, often involve the consumption of alcoholic beverages. This factor has become a leading cause of traffic accidents during these periods. Patterns show that drinking and driving lead to a higher incidence of accidents, resulting in injuries, disabilities, and fatalities more frequently than at other times. This is supported by a 7-day accident statistics report highlighting the New Year and Songkran festivals, which indicate that the peak number of fatalities occurs between 00.00 A.M. – 01.00 A.M. (Department of Highways, 2023). Additionally, of the 2,440 reported accidents, over 96% were attributed to drunk driving (Office of the Alcoholic Beverage Control Board, Department of Disease Control, Ministry of Public Health, 2023). A study also revealed that 60% of those injured in traffic accidents, whether fatal or non-fatal, had blood alcohol levels exceeding the legal limit of 50 milligrams per percent when tested (Office of the Alcoholic Beverage Control Board, Department of Disease Control, Ministry of Public Health, 2022).

Setting up alcohol checkpoints is crucial for identifying drivers who may be under the influence of alcohol. This method effectively reduces accidents related to drunk driving. Such checkpoints not only help prevent accidents but also serve as a reminder for drivers to adhere to laws regarding alcohol consumption and driving. They raise awareness about the importance of safe driving practices and support campaigns highlighting the dangers of drunk driving.

Alcohol checkpoints should be strategically placed to align with the closing times of entertainment venues and the peak risk period, particularly during major festivals. During regular periods, alcohol checkpoints should operate between 9.00 P.M. – 3.00 A.M., and during festivals, they should extend their operation hours from 9.00 P.M. – 6.00 A.M.

7. ACKNOWLEDGMENTS

This study was financially supported by graduated student's scholarship program, Faculty of Engineering, Burapha University, Thailand. The accident data were provided from the Provincial Police Station Region 2, Chonburi.

8. REFERENCES

Abiodun, O., Legall, G., & Odekunle, A. (2011). Mobile phone use by drivers in Trinidad and Tobago, West Indies. *Journal of Public Health and Epidemiology*, 3(4), 115–120.

Amin, M. S. R., Zareie, A., & Amador-Jiménez, L. E. (2014). Climate change modeling and the weather-related road accidents in Canada. *Transportation Research Part D: Transport and Environment*, 32, 171–183.

Andersson, A. K., & Chapman, L. (2011). The impact of climate change on winter road maintenance and traffic accidents in West Midlands, UK. *Accident Analysis & Prevention*, 43(1), 284–289.

Bergel-Hayat, R., Debbarh, M., Antoniou, C., & Yannis, G. (2013). Explaining the road accident risk: Weather effects. *Accident Analysis & Prevention*, 60, 456–465.

Bureau of Traffic Safety. (2015). *Traffic accident on national highways 2015*. Department of Highways, Ministry of Transport, Thailand. https://bhs.doh.go.th/files/accident/58/report_accident_2558.pdf

Bureau of Traffic Safety. (2016). *Traffic accident on national highways 2016*. Department of Highways, Ministry of Transport, Thailand. https://bhs.doh.go.th/files/accident/59/report_accident_2559.pdf

Bureau of Traffic Safety. (2017). *Traffic accident on national highways 2017*. Department of Highways, Ministry of Transport, Thailand. https://bhs.doh.go.th/files/accident/60/report_accident_2560.pdf

Bureau of Traffic Safety. (2018). *Traffic accident on national highways 2018*. Department of Highways, Ministry of Transport, Thailand. https://bhs.doh.go.th/files/accident/61/report_accident_2561.pdf

Bureau of Traffic Safety. (2019). *Traffic accident on national highways 2019*. Department of Highways, Ministry of Transport, Thailand. https://bhs.doh.go.th/files/accident/62/report_accident_2562.pdf

Bureau of Traffic Safety. (2020). *Traffic accident on national highways 2020*. Department of Highways, Ministry of Transport, Thailand. https://bhs.doh.go.th/files/accident/63/report_accident_2563.pdf

Bureau of Traffic Safety. (2021). *Traffic accident on national highways 2021*. Department of Highways, Ministry of Transport, Thailand. https://bhs.doh.go.th/files/accident/64/report_accident_2564.pdf

Bureau of Traffic Safety. (2022). *Traffic accident on national highways 2022*. Department of Highways, Ministry of Transport, Thailand. https://bhs.doh.go.th/files/accident/65/report_accident_2565.pdf

Bureau of Traffic Safety. (2023). *Traffic accident on national highways 2023*. Department of Highways, Ministry of Transport, Thailand. https://bhs.doh.go.th/files/accident/66/report_accident_2566.pdf

Bureau of Highway Safety. (2023). *Travelled vehicle-kilometers on highways report | 2023*. Department of Highways, Ministry of Transport, Thailand. https://bhs.doh.go.th/files/VK/VK2566.pdf

Chen, H., Cao, L., & Logan, D. B. (2012). Analysis of risk factors affecting the severity of intersection crashes. *Accident Analysis & Prevention, 43*(3), 670–677. https://doi.org/10.1016/j.aap.2011.10.019

Chen, H., Cao, L., & Logan, D. B. (2013). Analysis of risk factors affecting the severity of intersection crashes by logistic regression. *Traffic Injury Prevention, 13*(3), 300–307. https://doi.org/10.1080/15389588.2012.710761

Chia, C. H. (2024, March 4). Reducing traffic accidents and deaths. *The Sun*. https://thesun.my/opinion_news/reducing-traffic-accidents-and-deaths-JF12171338

Chonburi Provincial Administration Organization. (2022). Basic information for development planning of local government organizations in Chonburi Province 1-7 Year 2022. http://www.chonburi.go.th/website/about_chonburi/about440

Clarke, D., Ward, P., Bartle, C., & Truman, W. (2010). Killer crashes: Fatal road traffic accidents in the UK. *Accident Analysis & Prevention, 42*(2), 764–770. https://doi.org/10.1016/j.aap.2009.09.011

Department of Disease Control, Ministry of Public Health. (2023). Project to study alcohol content to look at road accidents during the New Year Festival and Songkran Festival 2023. https://ddc.moph.go.th/

Department of Highways. (2015). *Traffic accident on national highways 2015*. https://bhs.doh.go.th/files/accident/66/report_accident_2015.pdf

Department of Highway. (2016). *Traffic accident on national highways 2016*. https://bhs.doh.go.th/files/accident/65/report_accident_2016.pdf

Department of Highway. (2017). *Traffic accident on national highways 2017*. https://bhs.doh.go.th/files/accident/64/report_accident_2017.pdf

Department of Highway. (2018). *Traffic accident on national highways 2018*. https://bhs.doh.go.th/files/accident/63/report_accident_2018.pdf

Department of Highway. (2019). *Traffic accident on national highways 2019*. https://bhs.doh.go.th/files/accident/62/report_accident_2019.pdf

Department of Highway. (2020). *Traffic accident on national highways 2020*. https://bhs.doh.go.th/files/accident/61/report_accident_2020.pdf

Department of Highway. (2021). *Traffic accident on national highways 2021*. https://bhs.doh.go.th/files/accident/60/report_accident_2021.pdf

Department of Highway. (2022). *Traffic accident on national highways 2022*. https://bhs.doh.go.th/files/accident/59/report_accident_2022.pdf

Department of Highway. (2023). *Traffic accident on national highways 2023*. https://bhs.doh.go.th/files/accident/58/report_accident_2023.pdf

Department of Highway. (2023). *Travelled vehicle-kilometers on highways report | 2023*. https://bhs.doh.go.th/files/VK/VK2023.pdf

Department of Land Transport. (2018). *Report on analysis of deaths from road accidents and the death rate from road accidents per 100,000 people in fiscal year 2018*. https://web.dlt.go.th/statistics/

Department of Land Transport. (2019). *Report on analysis of deaths from road accidents and the death rate from road accidents per 100,000 people in fiscal year 2019*. https://web.dlt.go.th/statistics/

Department of Land Transport. (2020). *Report on analysis of deaths from road accidents and the death rate from road accidents per 100,000 people in fiscal year 2020*. https://web.dlt.go.th/statistics/

Department of Land Transport. (2021). *Report on analysis of deaths from road accidents and the death rate from road accidents per 100,000 people in fiscal year 2021*. https://web.dlt.go.th/statistics/

Department of Land Transport. (2022). *Report on analysis of deaths from road accidents and the death rate from road accidents per 100,000 people in fiscal year 2022*. https://web.dlt.go.th/statistics/

Department of Land Transport. (2023). *Report on analysis of deaths from road accidents and the death rate from road accidents per 100,000 people in fiscal year 2023*. https://web.dlt.go.th/statistics/

Department of Provincial Administration, Ministry of Interior. (2023). Announcement from the Central Registration Office, Department of Provincial Administration, regarding the number of citizens throughout the Kingdom, separated into Bangkok & various provinces according to evidence of civil registration as of December 31, 2023. http://stat.bora.dopa.go.th/stat/pk/pk_66.pdf

Eboli, L., Forciniti, C., & Mazzulla, G. (2019). The influence of road characteristics on road safety: *A driving simulation study. Transportation Research Part F: Traffic Psychology and Behaviour, 62,* 505–519. https://doi.org/10.1016/j.trf.2019.02.006

Goss, C. W., Van Bramer, L. D., Gliner, J. A., Porter, T. R., Roberts, I. G., & Diguiseppi, C. (2008). Increased police patrols for preventing alcohol-impaired driving. Cochrane Database of Systematic Reviews, 2008(5), 005241. https://doi.org/10.1002/14651858.CDC005241.pub2

Ghandour, W., Al-Ghandour, L. A., & Karli, A. (2020). Analysis of factors contributing to road traffic accidents in Jordan. *Accident Analysis & Prevention, 144*, 105661. https://doi.org/10.1016/j.aap.2020.105661

Ghandour, A., Hammoud, H., & Al-Hajj, S. (2020). Analyzing factors associated with fatal road crashes: A machine learning approach. International Journal of Environmental Research and Public Health, 17(1), 1–13. https://doi.org/10.3390/ijerph17010391

Hambly, D., Andrey, J., Mills, B., & Fletcher, C. (2013). Projected implications of climate change for road safety in Greater Vancouver, Canada. Climatic Change, 116(3–4), 613–629.

Jeffrey, S. K. E. (2010). Epidemiology, cost and prevention of road traffic crash injuries in Strathclyde, Scotland (PhD thesis). University of Glasgow.

Koetse, M. J., & Rietveld, P. (2009). The impact of climate change and weather on transport: An overview of empirical findings. Transportation Research Part D: Transport and Environment, 14(3), 205–221.

Lin, H. Y., et al. (2022). Environmental factors associated with severe motorcycle crash injury in university neighborhoods: A multicenter study in Taiwan. *International Journal of Environmental Research and Public Health, 19*(10), 10274. https://doi.org/10.3390/ijerph191610274

Malin, F., Norros, I., & Innamaa, S. (2019). Accident risk of road and weather conditions on different road types. Accident Analysis & Prevention, 122, 181–188.

Maureen, K. (2024, February 13). Saturday was most dangerous day to travel in 2023 – NTSA. *The Star*. https://www.the-star.co.ke/news/2024-02-13-saturday-was-most-dangerous-day-to-travel-in-2023-ntsa/

Ministry of Public Health. (2020). *Situation of deaths from road accidents in Thailand*. Department of Disease Control, Ministry of Public Health. https://dip.ddc.moph.go.th/new/3base_status_new

Ministry of Public Health. (2021). *Situation of deaths from road accidents in Thailand*. Department of Disease Control, Ministry of Public Health. https://dip.ddc.moph.go.th/new/3base_status_new

Ministry of Public Health. (2022). *Situation of deaths from road accidents in Thailand*. Department of Disease Control, Ministry of Public Health. https://dip.ddc.moph.go.th/new/3base_status_new

Ministry of Road Transport and Highways. (2023). *Road accident in India 2022*. https://morth.nic.in/sites/default/files/RA_2022_30_Oct.pdf

Ministry of Public Health. (2023). *Situation of road accidents in Thailand 2023*. Department of Disease Control, Ministry of Public Health. https://www.roadsafetythai.org/edoc/doc_20221219100929.pdf

Ministry of Tourism and Sports. (2024). *Domestic tourism statistics (Classify by region and province 2024)*. https://www.mots.go.th/news/category/758

National Safety Council (NSC). (2024). *Motor vehicle crashes by time of day and day of week*. https://injuryfacts.nsc.org/motor-vehicle/overview/crashes-by-time-of-day-and-day-of-week/

Novoa, A. M., Perez, K., Santamarina-Rubio, E., Marí-Dell'Olmo, M., Cozar, R., & Ferrando, J. (2011). Road safety in the political agenda: The impact on road traffic injuries. Journal of Epidemiology and Community Health, 65(3), 218–225.

Odero, W., Khayesi, M., & Heda, P. M. (2003). Road traffic injuries: Magnitude, causes and status of intervention. Injury Control and Safety Promotion, 10(1–2), 53–61.

Office of the Alcoholic Beverage Control Board, Department of Disease Control, Ministry of Public Health. (2023). *Annual report 2023*. https://ddc.moph.go.th/uploads/files/4323020240524073051.pdf

Office of the National Economic and Social Development Council. (2022). *Gross regional and provincial product chain*. https://www.nesdc.go.th/main.php?filename=gross_regional

Pervez, A., Lee, J., & Huang, H. (2021). Identifying factors contributing to the motorcycle crash severity in Pakistan. *Journal of Advanced Transportation*, *2021*, Article ID 6636130, 1–10. https://doi.org/10.1155/2021/6636130

Piriyawat, S., & Intanu, C. (2018). Past behavior, attitudes, subjective norm and positive anticipated emotions as determinants of using bicycle in daily life: Bangkhla District, Chachoengsao case study. In *Proceedings of the 23rd National Convention on Civil Engineering*. Nakhon Nayok, Thailand.

Provincial Administration Organization. (2022). *Basic information for development planning of local government organizations in Chonburi Province 1-7 Year 2022*. http://www.chonburi.go.th/website/about_chonburi/about4

Road Safety Collaboration. (2020–2023). *Comparison of road accident statistics in Thailand*. https://www.thairsc.com/data-compare

Road Safety Collaboration. (2024). *Statistics of deaths and injuries*. https://www.thairsc.com/

Road Safety Authority (RSA). (2024, January 01). Road safety. Road deaths in 2023 increase by 19%. https://www.rsa.ie/news-events/news/details/2024/01/01/road-deaths-in-2023-increase-by-19

St Bernard, G., & Matthews, W. (2003). A contemporary analysis of road traffic crashes, fatalities, and injuries in Trinidad and Tobago. Injury Control and Safety Promotion, 10(1–2), 21–27.

Strategic and Information for Provincial Development Section. (2018). A study for developing implementation and action plans for sustainable improving and reducing transport problems under Eastern Development Master Plans (Final Report). Chonburi Provincial Office, Chonburi, Thailand.

Smart Water Operation Center. (n.d.). *SMART Water Operation*. https://swocrf.rid.go.th/

South African Government News Agency. (2024, January 24). Decline of 2.3% in fatal road crashes during 2023/24 festive season. https://www.sanews.gov.za/south-africa/decline-23-fatal-road-crashes-during-202324-festive-season

SWOV Institute for Road Safety Research. (2023). *European Road Safety Observatory*. https://road-safety.transport.ec.europa.eu/system/files/2023-03/ff_single_vehicle_crashes_20230221.pdf

Thai Meteorological Department. (2024). *Weather characteristics by province*. Publisher. http://climate.tmd.go.th

Wood, J. M., Lacherez, P. F., & Tyrrell, R. A. (2019). Aging drivers and the impact of visual and cognitive factors on their driving performance. *Accident Analysis & Prevention*, 41(4), 768–773. https://doi.org/10.1016/j.aap.2019.01.019

Wood, J. M. (2019). Nighttime driving: Visual, lighting and visibility challenges. *Ophthalmic and Physiological Optics, 40*(2), 187–201. https://doi.org/10.1111/opo.12665

World Health Organization. (2015). Global status report on road safety. Geneva: World Health Organization.

World Health Organization. (2018). *Global status report on road safety*. Retrieved from https://iris.who.int/bitstream/handle/10665/277370/WHO-NMH-NVI-18.20-eng.pdf?sequence=1

World Health Organization. (2020). *Road traffic injuries*. Retrieved from https://www.who.int/news-room/fact-sheets/detail/road-traffic-injuries

iRAP Star Rating Implementation on Soedijatmo and Dalam Kota Toll Road, Indonesia by PT Jasamarga Tollroad Maintenance

Yonathan Elia Munthe[1,*], Ahmad Saleh Lubis[2] and Selvira Salsabila[3]

[1]PT Jasamarga Tollroad Maintenance, Jakarta, Indonesia, yonathan.munthe@jasamarga.co.id
[2]PT Jasamarga Tollroad Maintenance, Jakarta, Indonesia, salehlubis@rocketmail.com
[3]PT Jasamarga Tollroad Maintenance, Jakarta, Indonesia, selvira030103@gmail.com

ABSTRACT

Currently, there are various methods to assess road safety, and one was developed in the UK for over two decades called iRAP Star Rating. International Road Assessment Program / iRAP Star Rating is a method to assess road safety by evaluating its physical asset, thus this method has the advantage of being able to be carried out before crash occurs and creates trend. Thailand, a country concerns with the safety of road users, has developed a star rating method which has been adapted to the characteristics of Thailand society, vehicles, roads, speeds, and socio-cultural conditions, known as ThaiRAP. Following Thailand, Indonesian Ministry of Public Works and Housing has been formulating and developing InaRAP for the last decade, yet it is not finalized. In spite of this stagnant development, PT Jasamarga Tollroad Maintenance / PT JMTM has started conducting iRAP Star Rating assessment since 2020, with help of Hawkeye 2000, iRAP accredited Survey Vehicle from Australian Road Research Board / ARRB and iRAP accredited personnels. PT JMTM has carried out iRAP Star Rating assessment on 5 toll roads in Java Island, they are Cipularang, Jagorawi, Soedijatmo, Dalam Kota, and Pondok Aren-Ulujami Toll Road – totalling 831.40 kilometres long. We believe PT JMTM, a subsidiary company of PT Jasa Marga (Persero) Tbk, was the pioneer in conducting iRAP Star Rating assessment in Indonesia. Soedijatmo and Dalam Kota Toll Road has achieved 3-Star Rating, ensuring the safety of road users travelling from Soekarno-Hatta International Airport to the heart of Jakarta. There was a significant reduction in the crash rate by 42% after implementing Safer Roads Investment Plan. This paper will explain details of the process, the impacts and benefits, as well as the challenges of conducting iRAP assessment on Soedijatmo and Dalam Kota Toll Road.

Keywords: International Road Assessment Program, iRAP Star Rating, road safety assessment, Soedijatmo Toll Road, Dalam Kota Toll Road

1. INTRODUCTION

International Road Assessment Program / iRAP is the umbrella programme for Road Assessment Programmes (RAPs) worldwide that are working to save lives. Like many life-saving charities working in the public health arena, iRAP uses robust, evidence-based approach to prevent unnecessary deaths and suffering. iRAP was formed in 2006 as a global umbrella organisation for EuroRAP, usRAP and AusRAP and also to facilitate work in low and middle-income countries. iRAP partners with organisations in more than 100 countries and is the umbrella organisation for a number of official 'x'RAPs including : AusRAP, BrazilRAP, BrazilRAP Sao Paulo, ChinaRAP, IndiaRAP, KiwiRAP, KSARAP, MexiRAP, MyRAP, SARAP, TanRAP, ThaiRAP, United KingdomRAP, usRAP. See iRAP Metrics Infographic below.

Figure 1 iRAP Metrics Infographic.
(irap.org, 2024)

PT Jasa Marga (Persero) Tbk is a state-owned company engaged in the toll road business, encompassing the entire process from design and construction to operation. PT Jasa Marga (Persero) Tbk has the responsibility to ensure safety aspects across all business lines for stakeholders, especially toll road users as corporate consumers.

PT Jasamarga Tollroad Maintenance / PT JMTM, a subsidiary company of PT Jasa Marga (Persero) Tbk, manages the maintenance of physical toll road assets as a Service Provider. PT JMTM has the capability to conduct iRAP Star Rating assessment and has started conducting iRAP Star Rating assessment since 2020, with help of Hawkeye 2000, iRAP accredited Survey Vehicle from Australian Road Research Board / ARRB and iRAP accredited personnels. PT JMTM has carried out iRAP Star Rating assessment on 5 toll roads in Java Island, they are Cipularang, Jagorawi, Soedijatmo, Dalam Kota, and Pondok Aren-Ulujami Toll Road – totalling 831,40 kilometres long.

Prof. Dr. Ir. Soedijatmo Toll Road has been operating since 1984. This toll road stretches for approximately 13 kilometres and connects Jakarta with Soekarno – Hatta International Airport. Currently, it is connected to JORR 2 Toll Road, namely Cengkareng - Batu Ceper – Kunciran Toll Road. This toll road was named after the late Prof. Dr. Ir. Soedijatmo as a tribute to his services in the field of infrastructure construction in Indonesia. He invented the "Chicken Claw Construction", also known as the "cakar ayam" system. It is a foundation technique designed for building on soft or unstable ground. It involves using a reinforced concrete slab as the base, with pipes (resembling chicken claws) inserted into the ground at regular intervals to provide additional support and stability. This method is particularly effective in areas with challenging soil conditions, such as swamps or soft soil layers.

Cawang – Tomang – Pluit Toll Road, better known as Jakarta Inner Ring Road / Lingkar Dalam Jakarta or Dalam Kota, a "VIP" toll road that connects city centers in the capital city of Jakarta. This 20 – kilometres toll road links Eastern and Western region of Jakarta, from Cawang to Pluit. It is integrated with 5 (five) toll road sections: Prof. Dr. Ir. Soedijatmo Toll Road (to Soekarno – Hatta Airport), Jakarta – Tangerang (Janger) Toll Road, Jakarta – Bogor – Ciawi (Jagorawi) Toll Road, Jakarta – Cikampek (Japek) Toll Road and Cawang – Tanjung Priok – East Ancol – Jembatan Tiga / Pluit Toll Road.

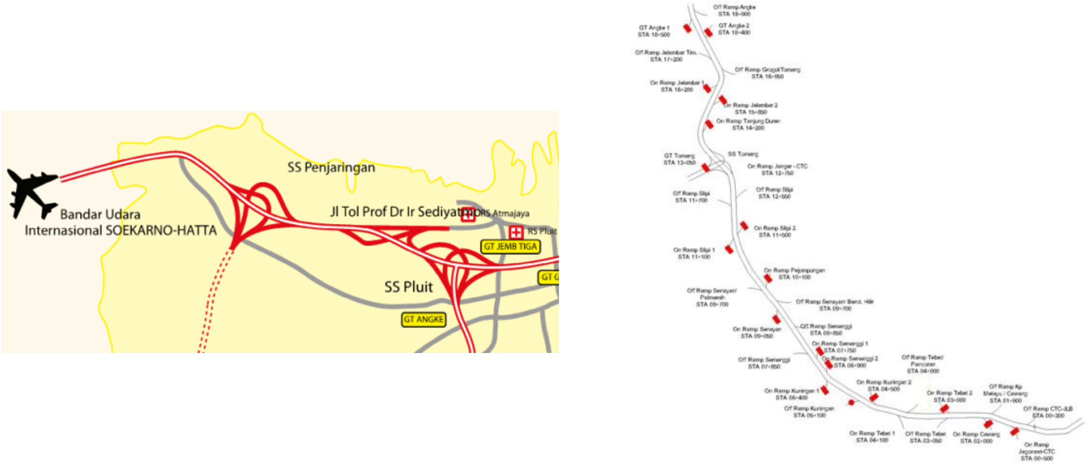

Figure 2 Map of Soedijatmo Toll Road and Dalam Kota Toll Road.
(PT JMTM, 2024)

2. MATERIAL AND METHODS

2.1 Safe System Approach

In general, road safety is a condition where no crash occur, or where the risk of serious injuries or death when an crash occurs can be minimized. Road safety conditions can be achieved by applying Safe System Approach. The Safety System Approach was developed based on the principle that serious injuries and deaths occurring in road crash are unacceptable and avoidable (PIARC, 2015). The key Safe System Approach principles are that:

1. Human beings have limitations and tend to make mistakes;
2. Humans have limitations in receiving kinetic energy during crash. Humans will suffer serious injury or death when the kinetic energy exceeds these limitations;
3. A well – designed system can ensure that the kinetic energy received by humans will not be excessive in the event of crash;
4. The main focus of this principle is to eliminate serious injuries and deaths in the event of crash; and
5. Road safety is a shared responsibility between the system designer and road users.

2.2 Background International Road Assessment Programme (iRAP)

iRAP method is a method for assessing road safety performance at the road network, based on the condition of existing or planned physical infrastructure, even if it is still in the design and construction phases. iRAP assessment can be conducted before any crash occurs, as it is based solely on the condition of physical infrastructure. The targets for iRAP assessment are: all new roads are built to a 3-star or better standard for all road users; and more than 75% of travel is on the equivalent of 3-star or better for all road users by 2030.

2.3 iRAP Assessment Process

Road Survey

There are three primary survey data needed to do iRAP Assessment: geo-referenced images of the roads, speed data, and flow data (average annual daily traffic). PT JMTM utilizes Road Survey Vehicle, Hawkeye 2000 produced by Australian Road Research Board, to acquire geo-referenced images of the roads; Speed Gun, LTI 20/20 TruCAM, to acquire speed data; and Manual Counting (if the data is not available from traffic operation unit) to acquire flow data.

Figure 3 Road survey vehicle Hawkeye 2000.
(PT JMTM, 2021)

Road Coding

Coding is a stage in which codes are assigned to the road network according to the attributes – total 78 attributes of the road based on surveyed images; attributes recorded for each 100 metres segment. The coding process is essential to ensure that the road attributes have become codes that can be processed by computer applications with algorithms developed by iRAP.

To ensure the quality of the coding results, there is a Quality Assurance / QA process according to the procedures set by iRAP. Each region worldwide has a Regional Project Manager from iRAP who is in charge of running QA for coding results performed by surveyors using ViDA computer applications provided by the iRAP Organization.

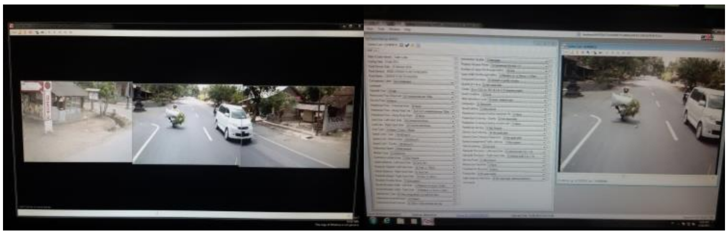

Figure 4 Images of survey results and coding process on the Hawkeye 2000 Application.
(PT JMTM, 2015)

Analysis and Reporting

The coding results will be entered into ViDA application and will generate Star Rating Score / SRS. The measure that iRAP uses in conducting road safety performance assessments is the number of crash risk factors of the elements under various conditions. SRS represents the magnitude of the risk of various types of collisions that are considered to cause serious crash with serious injuries and death.

SRS is calculated for 4 (four) road users: motor vehicles, motorcycles, bicycles, and pedestrians. For the assessment of road safety performance on toll roads, the assessment will focus on motor vehicle road users. Here's the basic formula of SRS:

$$SRS = \sum Crash\ Type\ Scores \quad (1)$$

Where:

$$Crash\ Type\ Scores = likelihood \times severity \times operating\ speed \times external\ flow\ influence \times median\ traversability \quad (2)$$

Where:

a) Likelihood refers to road attribute risk factors that account for the chance that a crash will be initiated;
b) Severity refers to road attribute risk factors that account for the severity of a crash;
c) Operating speed refers to factors that account for the degree to which risk changes with speed;
d) External flow influence factors account for the degree to which a person's risk of being involved in a crash is a function of another person's use of the road; and
e) Median traversability factors account for the potential that an errant vehicle will cross a median (only applies to vehicle occupants and motorcyclist's run-off and head-on crashes).

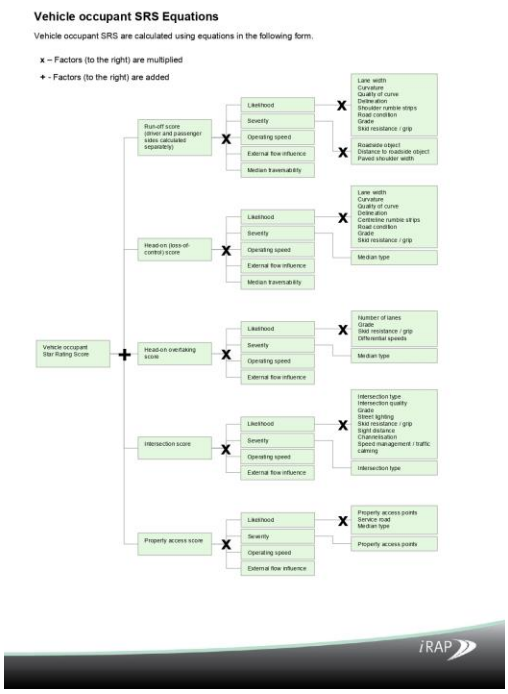

Figure 5 Vehicle Occupant SRS Equations.
(irap.org, 2014)

Table 1 Star Rating bands and colors by Star Rating Score.

Star Rating	Star Rating Score				
	Vehicle occupants and motorcyclists	Bicyclists	Pedestrians		
			Total	Along	Crossing
5	0 to < 2.5	0 to < 5	0 to < 5	0 to < 0.2	0 to < 4.8
4	2.5 to < 5	5 to < 10	5 to < 15	0.2 to < 1	4.8 to < 14
3	5 to < 12.5	10 to < 30	15 to < 40	1 to < 7.5	14 to < 32.5
2	12.5 to < 22.5	30 to < 60	40 to < 90	7.5 to < 15	32.5 to < 75
1	22.5 +	60+	90 +	15 +	75 +

(irap.org, 2020)

The next analysis process is the preparation of recommendations for Safer Roads Investment Plans, which is carried out with the ViDA computer application with the following steps:

1. Identification of types of handling / repairs of physical road assets;
2. Estimation of potential prevention of serious injuries and deaths;
3. Economic Analysis; and
4. Preparation of Investment Plans for Safer Road Investment Plans with priority scale.

2.4 ViDA Apllication

ViDA is iRAP's free-to-air online platform. It is the data processing engine for Star Ratings, FSI Estimates and Investment Plans, hosting data and analysing results, and the portal for iRAP's tools: SR4D, the Star Rating Demonstrator. ViDA is free to access and use and enables users to investigate interactive reports, create data and manage secure access to their data. ViDA can be integrated within road authority systems utilizing its API. This enables data to be transferred from asset management tools and the Star Ratings accessed.

Figure 6 ViDA Dashboard Page.
(ViDA, 2024)

2.5 Crash Rate

Crash rate is the number of observed crashes per unit of traffic volume passing through the location. This method incorporates traffic volume to augment the crash data. The crash frequency at a site is divided by the traffic volume – either the annual average daily traffic (for road segments), total entering volume (for vehicle traffic at intersections), or other volumes, such as pedestrian crossing volume. The typical unit for this method is crashes per 100 million vehicle miles traveled for road segments or crashes per 100 million entering vehicles for intersections. Crash rate in these units is calculated as:

$$CR = \frac{(C \times 100.000.000)}{(V \times 365 \times N \times L)} \tag{3}$$

CR : Crash rate per 100 million vehicle miles traveled.
C : Number of crashes in the study period.

V : Traffic volumes using average annual daily traffic (AADT) volumes.
N : Number of years of data.
L : Length of the roadway segment in miles.
(Srinivasan, R., & Carter, D, 2017)

Authors use crash rate before and after the iRAP implementation to analyze the benefit of iRAP implementation on Soedijatmo and Dalam Kota Toll Road.

3. RESULTS

3.1 iRAP Certification of Soedijatmo Toll Road

iRAP Star Rating Before

Overall, **iRAP *Star Rating Before*** achieved **2-star rating** on **Soedijatmo Toll Road.** The length of survey on Soedijatmo Toll Road stretches from 40 kilometres, which 0,9 kilometres is considered to have achieved 2-star rating: 0,1 kilometres in lane A lower section; 0,4 kilometres in lane B upper section; 0,4 kilometres in lane B lower section.

	Vehicle Occupant	
Star Ratings	Length (km)	Percent
5 Stars	5.30	80.30%
4 Stars	1.00	15.15%
3 Stars	0.30	4.55%
2 Stars	0.00	0.00%
1 Star	0.00	0.00%
Not applicable	0.00	0.00%
Totals	6.60	100.00%

	Vehicle Occupant	
Star Ratings	Length (km)	Percent
5 Stars	7.80	60.94%
4 Stars	3.90	30.47%
3 Stars	1.00	7.81%
2 Stars	0.10	0.78%
1 Star	0.00	0.00%
Not applicable	0.00	0.00%
Totals	12.80	100.00%

	Vehicle Occupant	
Star Ratings	Length (km)	Percent
5 Stars	6.30	80.77%
4 Stars	0.30	3.85%
3 Stars	0.80	10.26%
2 Stars	0.40	5.13%
1 Star	0.00	0.00%
Not applicable	0.00	0.00%
Totals	7.80	100.00%

	Vehicle Occupant	
Star Ratings	Length (km)	Percent
5 Stars	4.40	34.38%
4 Stars	5.50	42.97%
3 Stars	2.50	19.53%
2 Stars	0.40	3.13%
1 Star	0.00	0.00%
Not applicable	0.00	0.00%
Totals	12.80	100.00%

Figure 7 iRAP Star Rating before for lane A and B upper section and lower section on Soedijatmo Toll Road.
(PT JMTM , 2021)

Improvement Reccomendations

After iRAP Star Rating Before was carried out, a recommendation for Safer Roads Investment Plans / SRIP was obtained. There are recommendations for improvements to Soedijatmo Toll Road, including repairing safety barriers, repairing delineation, and installing chevron signs. The most improvements made were improvements to the safety barrier: installing safety barriers spread at **5 out of 9** points **(55.56%)**; tidying up the safety barrier spread at **4 out of 9 points (44.44%).**

Table 2 Improvement recommendations on Soedijatmo Toll Road

<table>
<tr><th>No</th><th>Findings / Before</th><th>Follow – up / After</th></tr>
<tr><td rowspan="2">1</td><td colspan="2">Location : 31+800 lane A lower section</td></tr>
<tr><td>
Figure 8 Unprotected barrier end.
(PT JMTM, 2021)</td><td>
Figure 9 Installing guardrail.
(PT JMTM, 2021)</td></tr>
</table>

2	**Location :** 21+800 lane B upper section	
	 **Figure 10 Delineation and quality of curve poor.** (PT JMTM, 2021)	 **Figure 11 MCB, chevron signs, delineation.** (PT JMTM, 2021)
3	**Location :** 21+100 lane B upper section	
	 **Figure 12 Unprotected barrier, delineation poor.** (PT JMTM, 2021)	 **Figure 13 Installing MCB and delineation.** (PT JMTM, 2021)
4	**Location :** 21+00 lane B upper section	
	 **Figure 14 Unprotected safety barrier.** (PT JMTM, 2021)	 **Figure 15 Installing MCB.** (PT JMTM, 2021)
5	**Location :** 20+900 lane B upper section	
	 **Figure 16 Unprotected safety barrier.** (PT JMTM, 2021)	 **Figure 17 Installing MCB.** (PT JMTM, 2021)
6	**Location :** 32+400 lane B lower section	
	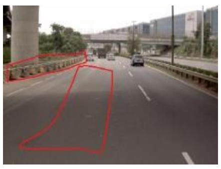 **Figure 18 Unprotected barrier, delineation poor.** (PT JMTM, 2021)	 **Figure 19 Moving out MCB and delineation.** (PT JMTM, 2021)
7	**Location :** 32+300 lane B lower section	
	 **Figure 20 Unprotected barrier, delineation poor.** (PT JMTM, 2021)	 **Figure 21 Moving out MCB and delineation.** (PT JMTM, 2021)

8	**Location :** 31+900 lane B lower section	
	 **Figure 22 Unprotected safety barrier.** (PT JMTM, 2021)	 **Figure 23 Tidying up MCB.** (PT JMTM, 2021)
9	**Location :** 31+800 lane B lower section	
	 **Figure 24 Unprotected safety barrier.** (PT JMTM, 2021)	 **Figure 25 Tidying up MCB.** (PT JMTM, 2021)

(PT JMTM, 2021)

Installing safety barriers is essential to prevent vehicles from colliding with hazardous objects along the roadside, which can lead to serious crash. Road delination is crucial to guide driver to drive inside lane. Inadequate or unclear delineation can cause confusion, particularly at night or in adverse weather conditions, increasing the likelihood of crash. Additionally, installing chevron sign provides visual warning to driver about road curve, help driver to slow down and navigate road curve safely, decreasing the likelihood of crash.

iRAP Star Rating After

Overall, **iRAP Star Rating After** achieved **3-star rating** on **Soedijatmo Toll Road.** The length of survey on Soedijatmo Toll Road stretches from 40 kilometres, which 1,8 kilometres is considered to have achieved 3-star rating in lane B upper section.

	Vehicle Occupant	
Star Ratings	Length (km)	Percent
3 star or better	6.60	100.00%
5 Stars	3.60	54.55%
4 Stars	3.00	45.45%
3 Stars	0.00	0.00%
2 Stars	0.00	0.00%
1 Star	0.00	0.00%
Not applicable	0.00	0.00%
Totals	6.60	100.00%

	Vehicle Occupant	
Star Ratings	Length (km)	Percent
3 star or better	12.80	100.00%
5 Stars	5.00	39.06%
4 Stars	7.80	60.94%
3 Stars	0.00	0.00%
2 Stars	0.00	0.00%
1 Star	0.00	0.00%
Not applicable	0.00	0.00%
Totals	12.80	100.00%

	Vehicle Occupant	
Star Ratings	Length (km)	Percent
3 star or better	7.80	100.00%
5 Stars	3.00	38.46%
4 Stars	3.00	38.46%
3 Stars	1.80	23.08%
2 Stars	0.00	0.00%
1 Star	0.00	0.00%
Not applicable	0.00	0.00%
Totals	7.80	100.00%

	Vehicle Occupant	
Star Ratings	Length (km)	Percent
3 star or better	12.80	100.00%
5 Stars	1.00	7.81%
4 Stars	11.80	92.19%
3 Stars	0.00	0.00%
2 Stars	0.00	0.00%
1 Star	0.00	0.00%
Not applicable	0.00	0.00%
Totals	12.80	100.00%

Figure 26 iRAP Star Rating after for lane A and B upper section and lower section on Soedijatmo Toll Road.
(PT JMTM, 2021)

Figure 27 iRAP Star Rating Certificate on Soedijatmo Toll Road.
(irap.org and PT JMTM, 2021)

3.2 iRAP Certification of Dalam Kota Toll Road

iRAP Star Rating Before

Overall, **iRAP *Star Rating Before*** achieved **2-star rating** on **Dalam Kota Toll Road.** The length of survey on Dalam Kota Toll Road stretches from 44,4 kilometres, which 0,4 kilometres is considered to have achieved 2-star rating: 0,2 kilometres in lane A; 0,2 kilometres in lane B.

	Vehicle Occupant	
Star Ratings	Length (km)	Percent
3 star or better	22.00	99.10%
5 Stars	12.80	57.66%
4 Stars	5.40	24.32%
3 Stars	3.80	17.12%
2 Stars	0.20	0.90%
1 Star	0.00	0.00%
Not applicable	0.00	0.00%
Totals	22.20	100.00%

	Vehicle Occupant	
Star Ratings	Length (km)	Percent
3 star or better	22.00	99.10%
5 Stars	12.90	58.11%
4 Stars	6.70	30.18%
3 Stars	2.40	10.81%
2 Stars	0.20	0.90%
1 Star	0.00	0.00%
Not applicable	0.00	0.00%
Totals	22.20	100.00%

Figure 28 iRAP Star Rating before for lane A and lane B on Dalam Kota Toll Road.
(PT JMTM, 2022)

Improvement Recommendations

After iRAP Star Rating Before was carried out, a recommendation for Safer Roads Investment Plans / SRIP was obtained. There are recommendations for improvements to Dalam Kota Toll Road, including installing safety barriers, repairing markings, repairing road pavements, and tidying up the installation MCB. The most improvements made were improvements to installing safety barriers spread to **3 out of 4** points **(75%)**.

Table 3 Improvement recommendations on Dalam Kota Toll Road.

No	Findings / Before	Follow – up / After
1	**Location :** 1+400 lane A	
	 **Figure 29 Unprotected safety barrier end.** (PT JMTM, 2022)	 **Figure 30 Installing guardrail.** (PT JMTM, 2022)

<table>
<tr><td></td><td>
Figure 31 Unprotected safety barrier end.
(PT JMTM, 2022)</td><td>
Figure 32 Road conditions and MCB good.
(PT JMTM, 2022)</td></tr>
<tr><td rowspan="2">2</td><td colspan="2">**Location :** 1+500 lane A</td></tr>
<tr><td>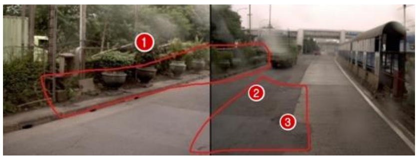
Figure 33 Road condition and delineation poor.
(PT JMTM, 2022)</td><td>
Figure 34 Road conditions, delineation good.
(PT JMTM, 2022)</td></tr>
<tr><td rowspan="2">3</td><td colspan="2">**Location :** 14+700 lane B</td></tr>
<tr><td>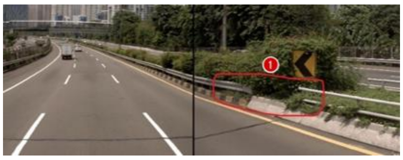
Figure 35 Unprotected safety barrier end.
(PT JMTM, 2022)</td><td>
Figure 36 Installing safety barrier – metal.
(PT JMTM, 2022)</td></tr>
<tr><td rowspan="2">4</td><td colspan="2">**Location :** 00+500 lane B</td></tr>
<tr><td>
Figure 37 Unprotected safety barrier.
(PT JMTM, 2022)</td><td>

Figure 38 Installing guardrail.
(PT JMTM, 2022)</td></tr>
</table>

(PT JMTM, 2022)

Installing safety barriers is essential to prevent vehicles from colliding with hazardous objects along the roadside, which can lead to serious crash. Good road condition is crucial for the comfort and safety of driver. Pothole or uneven road can cause driver to lose control of their vehicle, increasing the likelihood of crash. Road delination is crucial to guide driver to drive inside lane. Inadequate or unclear delineation can cause confusion, particularly at night or in adverse weather conditions, increasing the likelihood of crash.

iRAP Star Rating After

Overall, **iRAP *Star Rating After*** achieved **3-star rating** on **Dalam Kota Toll Road.** The length of survey on Dalam Kota Toll Road stretches from 44,4 kilometres, which 2 kilometres is considered to have achieved 3-star rating: 1 kilometres in lane A; 1 kilometres in lane B.

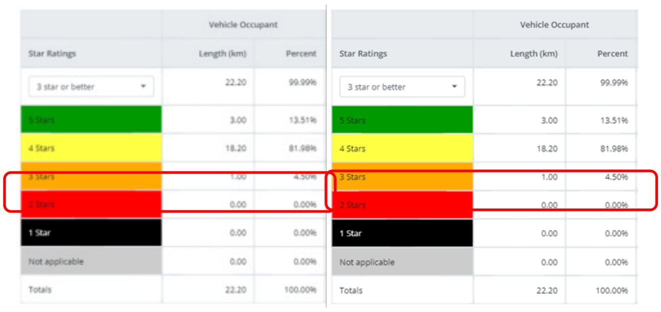

Star Ratings	Vehicle Occupant Length (km)	Vehicle Occupant Percent
3 star or better	22.20	99.99%
5 Stars	3.00	13.51%
4 Stars	18.20	81.98%
3 Stars	1.00	4.50%
2 Stars	0.00	0.00%
1 Star	0.00	0.00%
Not applicable	0.00	0.00%
Totals	22.20	100.00%

Star Ratings	Vehicle Occupant Length (km)	Vehicle Occupant Percent
3 star or better	22.20	99.99%
5 Stars	3.00	13.51%
4 Stars	18.20	81.98%
3 Stars	1.00	4.50%
2 Stars	0.00	0.00%
1 Star	0.00	0.00%
Not applicable	0.00	0.00%
Totals	22.20	100.00%

Figure 39 iRAP Star Rating after for lane A and lane B on Dalam Kota Toll Road.
(PT JMTM, 2023)

Figure 40 iRAP Star Rating Certificate on Dalam Kota Toll Road.
(irap.org and PT JMTM, 2023)

3.3 Crash Rate

In 2022, crash rate on Soedijatmo and Dalam Kota Toll Road reached 87 crashes per 100 million vehicles. However, in 2023, the crash rate fell about 42% to 50 crashes per 100 million vehicles. This decline reflects the success of iRAP implementation on Soedijatmo and Dalam Kota Toll Road.

2022

$$CR_{2022} = \frac{(154 \times 100.000.000)}{(484.643 \times 365 \times 1)} = 87$$

2023

$$CR_{2023} = \frac{(94 \times 100.000.000)}{(514.244 \times 365 \times 1)} = 50$$

Table 4 Crash rate on Soedijatmo Toll Road and Dalam Kota Toll Road in 2022-2023.

Crash rate Soedijatmo & Dalam Kota Toll Road	2022	2023	Percentage change
	87	50	42%

(PT JMTM, 2024)

3.4 Number of Crashes

In 2022, there were 64 crashes on Soedijatmo Toll Road. The number of crashes decreased by 32, or 50%, to 32 crashes in 2023. In 2022, there were 90 crashes on Dalam Kota Toll Road. The number of crashes decreased by 28, or 31%, to 62 crashes in 2023. This decreased numbers show that efforts to improve safety or the iRAP Star Rating on both toll roads have been successful.

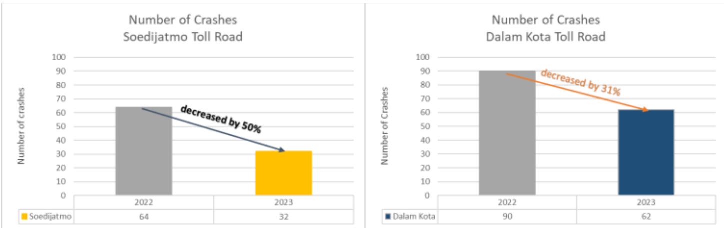

Figure 41 Number of crashes on Soedijatmo Toll Road and Dalam Kota Toll Road.
(PT JMTM, 2024)

3.5 Crash Distribution

The distribution of crashes on Soedijatmo Toll Road and Dalam Kota Toll Road during the 2022 – 2023 period shows a downward trend in crashes at almost all kilometres points. This reflects the effectiveness of preventive and safety measures undertaken during the period.

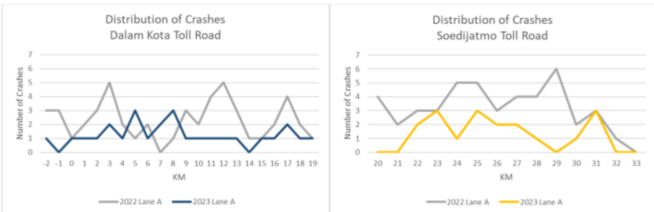

Figure 42 Distribution of crashes on Dalam Kota Toll Road and Soedijatmo Toll Road on line A.
(PT JMTM, 2024)

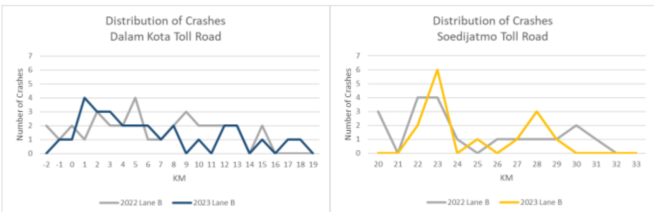

Figure 43 Distribution of crashes on Dalam Kota Toll Road and Soedijatmo Toll Road on line B.
(PT JMTM, 2024)

3.6 Factor Causing Crashes

The main contributing factor to crashes on Soedijatmo and Dalam Kota Toll Road in 2022 was the behavior of the drivers, which accounted for 130 crashes or 85%. Meanwhile, crashes caused by vehicle conditions accounted for 22 crashes, or 14%, while environmental factors such as the condition of road assets (e.g., potholes) accounted for 2 crashes, or 1%.

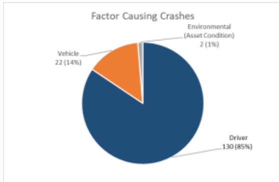

Figure 44 Factor causing crashes on Soedijatmo Toll Road and Dalam Kota Toll Road.
(PT JMTM, 2024)

4. CONCLUSIONS

1. Soedijatmo Toll Road has received a 3-Star iRAP certificate on December 15, 2021 and Dalam Kota Toll Road has received a 3-Star iRAP certificate on January 16, 2023;
2. In 2022 – 2023, there was a decrease in crash rate from 87 to 50 crashes;
3. In 2022 – 2023, there was a decrease in crash number on Soedijatmo Toll Road by 50% and Dalam Kota Toll Road by 31%;
4. In 2022 – 2023, there was a downward trend in crash number at almost all road segments;
5. The main causes of crashes in 2022 are behavior of the drivers (85%); and
6. Authors hope Indonesia can evaluate and maintain effort to improve the quality of road safety and achieve iRAP certification for other toll roads.

5. ACKNOWLEDGMENTS

Yonathan Elia Munthe, Ahmad Saleh Lubis, and Selvira Salsabila of the PT Jasamarga Tollroad Maintenance / JMTM, prepared this journal article based on the report iRAP Star Rating Implementation on Soedijatmo and Dalam Kota Toll Road, Indonesia by PT Jasamarga Tollroad Maintenance. This work has been funded by PT Jasa Marga (Persero) Tbk under management contract between PT JMTM and PT Jasa Marga (Persero) Tbk. The opinions expresses here in are those of the authors and do not necessarily reflect the views of funding agency.

6. REFERENCES

iRAP. (2019). iRAP Inspection System - Accreditation Specification. https://irap.org/specifications/

iRAP. (2019). iRAP Survey Manual. https://irap.org/specifications/

iRAP. (2019). iRAP Star Rating and Investment Plan Manual. https://irap.org/specifications/

Srinivasan, R., & Carter, D. (2017, November). Road Safety Fundamentals - Unit 4 : Solving Safety Problems. https://highways.dot.gov/safety/learn-safety/road-safety-fundamentals-html-version/unit-4-solving-safety-problems

PT Jasamarga Tollroad Maintenance. PT Jasamarga Tollroad Maintenance https://jmtm.co.id/

World Health Organization. *Decade of action for road safety 2011-2020*. World Health Organization. https://www.who.int/groups/united-nations-road-safety-collaboration/decade-of-action-for-road-safety-2011-2020

World Health Organization. *Decade of Action for Road Safety 2021-2030*. World Health Organization. https://www.who.int/teams/social-determinants-of-health/safety-and-mobility/decade-of-action-for-road-safety-2021-2030

Operational and Safety Analysis of Temporary Median U-Turn Intersection Design: A Case Study of Highways No. 121 and No. 1317

Moe Sandi Zaw[1,*], Nopadon Kronprasert[2], Pongthep Pisetsit[3]

[1]Department of Civil Engineering, Faculty of Engineering, Chiang Mai University,
emmamoe1523@gmail.com
[2]Department of Civil Engineering, Faculty of Engineering, Chiang Mai University,
nopkron@eng.cmu.ac.th
[3]Department of Civil Engineering, Faculty of Engineering, Chiang Mai University,
pongthep.pisetsit@gmail.com

ABSTRACT

A median U-turn (MUT) intersection is an alternative design prohibiting right turns at major intersections. The design guides drivers to proceed through the intersection, but make a U-turn downstream, travel back toward the intersection, and execute to a left turn. The concept of MUT intersection configuration has been widely implemented, especially during construing interchange projects where the intersection area is temporarily closed for all vehicles. This study aims to evaluate the operational performance of this temporary MUT intersection design using microscopic traffic simulation. The results indicate that the key to this design is the median U-turn offset, which influences the operational and safety efficiency. A short offset may result in harsh lane change conflicts with minor road traffic, while a long offset may increase vehicle travel time. The sensitivity analysis of recommended median U-turn offsets with respect to various factors, including offset length and traffic volumes, is performed. The simulation-based evaluation applies to the real-world intersection improvement at the San-Klang Intersection project, which is located between Highways No. 121 and Highways No. 1317 in Chiang Mai Province. Two simulation models for signalized intersection and MUT intersection are compared. This study offers a practical approach to mitigate congestion and enhance mobility during construction periods at major interchanges.

Keywords: Median U-turn intersection, Work-zone traffic management, Traffic operations, Microscopic traffic simulation, Intersection improvement

1. INTRODUCTION

Managing traffic mobility and safety at intersections has become a very complex task for highway and traffic engineers. Various alternative intersection or interchange designs have been proposed to improve operational and safety efficiency by separating different traffic movements, providing more uninterrupted flow, and reducing severe traffic conflicts. A median U-turn (MUT) intersection is one of the most accepted alternative intersection designs that are being implemented to manage traffic flow at intersections. The design restricts the use of the major intersection areas. It prohibits drivers from crossing the intersection area but guides them to go around by making a U-turn at the downstream median U-turn, opening and returning to the intersection from another approach. The concept of MUT intersection configuration has been widely implemented at intersections along high-speed major arterials where minor roads intersect, as shown in Figure 1.

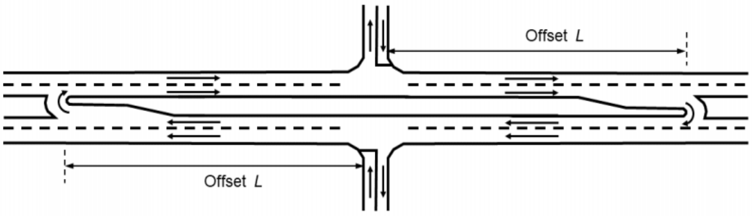

Figure 1 Typical Median U-Turn (MUT) Intersection Design

However, managing traffic mobility and safety of work zone intersection improvement projects can become even more complex, where existing at-grade unsignalized or signalized intersections might be temporarily disrupted and the intersection area is closed for all vehicles (Göçmen Demir & Demir, 2020; Wided, 2023). They can create bottlenecks, especially during peak hours or with high traffic volumes leading to congestion and delays.

In Thailand, the MUT intersection design concept has been adapted to circulate traffic during the construction of intersection/interchange projects. This study aims to investigate the operational performance, traffic flow characteristics, and safety implications of temporary work-zone traffic management schemes. Figure 2 presents an example of traffic management during the construction of an intersection project in Chiang Mai Province. This study will guide highway engineers in developing, implementing, and managing MUT intersections on highways.

Figure 2 An Example of Median U-Turn Intersection Design for Work Zone Traffic Management
(Department of Highways, 2024)

2. LITERATURE REVIEW

A median U-turn (MUT) intersection design is an alternative intersection design that can reduce conflict points and improve traffic flow. It restricts the need for vehicles across crossing traffic and guides them to make U-turns at a designated median opening (*FHWA MEDIAN U-TURN INTERSECTION*, 2014). Several studies explored the performance and design of MUTs (Alhadidi et al., 2024; Jagannathan, 2007; Nopadon et al., 2020). They found that MUTs can improve traffic flow and reduce congestion. They also found that MUTs can reduce crash rates by 20-50%, especially severe head-on and angle collisions, and reduce conflicts at intersections. The offset distance in a MUT design significantly impacts its effectiveness. MUTs can be cost-effective for enhancing intersection capacity necessitating only minor adjustments to infrastructure and enabling swift implementation.

Research on the operational and safety analysis of MUTIs in Thailand is in its early stages. While some studies have been conducted, there are still significant research gaps that need to be addressed (Kronprasert et al., 2021; Lueanpech et al., 2023). While MUT designs can improve traffic efficiency, they may raise safety concerns due to drivers' unfamiliarity with the layout. This could lead to unsafe maneuvers like sudden turns or collisions. Moreover, the MUT design may not be suitable for large vehicles, such as trucks or buses, due to the limited turning radius (Shao et al., 2019). By addressing these research gaps and considerations, policymakers, transportation planners, and engineers can make informed decisions regarding the planning, design, and operation of temporary MUTs. Ultimately, these efforts will contribute to the enhancement of traffic efficiency, safety, and sustainability in the highway network, benefiting both local communities and road users.

Techniques commonly employed for evaluating the operational and safety performance of alternative design and control and highway networks are observational studies and traffic simulation modeling. Microscopic simulation models provide detailed representations of individual vehicle behaviors, movements, and interactions within the intersection, allowing for the assessment of factors like queuing, delay, and congestion (Barcelo, 2011; Hasan et al., 2019; Nasuha & Rohani, 2018; Shirke et al., 2019).

Traffic flow analysis techniques examine vehicle movement, evaluating parameters like flow rates, speeds, densities, delays, and queue lengths to understand intersection efficiency. Capacity analysis determines a maximum vehicle flow rate by evaluating lane configurations, geometric design, signal timings, and driver behavior, while performance metrics assess intersection delay, level of service, and travel time reliability.

The Surrogate Safety Assessment Model (SSAM) analyzes the safety performance of highway facilities. It uses vehicle trajectory data to identify and classify potential conflict points between vehicles, estimating the risk of collisions (FHWA, 2008). Two frequently used indicators in surrogate safety assessment are Time-to-Collision (TTC)—the time for two vehicles to collide if they continue at their present speed and on the same trajectory, and Post-Encroachment Time (PET)—the time between the moment the first vehicle leaves the conflict area and the moment the second vehicle reaches the same conflict area. Using vehicle trajectory data, three types of conflict events can be identified: crossing conflict, rear-end conflict, and lane-change conflict (He et al., 2018).

3. MATERIAL AND METHODS

In this study, the data were collected from the real-world case study of the highway intersection improvement project. Traffic simulation models were developed to analyze data on operational and safety performance measures of the temporary Median U-turn (MUT) intersection design.

3.1 Data Collection

A case study of the San-Klang Intersection in Chiang Mai was selected for evaluation of the temporary MUT intersection (TMUT). This study area is located in the San Sai district of Chiang Mai, connecting between major highways: No. 121 and No. 1317 as illustrated in Figure 2. The intersection is near several residential neighborhoods, educational institutions, housing estates, and commercial establishments. These areas are home to both local residents and expatriates, highlighting the intersection's role in local commuting and transportation, contributing to high traffic volumes during peak periods. The San-Klang Intersection project is a currently undergoing highway intersection improvement project to handle increased traffic volume more efficiently and safely. This project includes expanding the roadways, installing new traffic signals, even flyovers to ensure smoother transit, and implementing advanced traffic management systems. However, construction and upgrading activities can cause temporary disruptions. Figure 3 illustrates the current layout and the proposed upgraded configuration of the intersection.

(a) Existing (Signalized)

(b) Final design

Figure 3 Existing and final design of the San-Klang intersection

Field data were collected on Highway No.121 and Highway No.1317 before and during the construction. They include road geometry (i.e. the configuration of intersection and U-turn openings) and traffic data (i.e. traffic volume, speed, traffic composition, and gap acceptance). Detailed field data are shown in Table 1.

Table 1 Field Data and Parameters used in simulation models.

Parameter	Approach			
	Major road (Highway no. 121)		Minor road (Highway no. 1317)	
	Northbound	Southbound	Eastbound	Westbound
Field data				
Traffic volume (pcu/h)	1,280	1,121	1,068	2,076
Turning movement (%) (Left/Through/Right)	35/33/32	29/44/27	34/50/16	37/56/7
Traffic composition (%)	Motorcycle 28% / Car 70% / Truck 2%			
Signal phasing and cycle time	4 Phase (Split Phase), 366 sec			
Signal time (s) (Green/Amber/All-red)	78/3/5	65/3/5	68/3/5	123/3/5
Microscopic Traffic Simulation				
Median U-turn offset (meter)	250 – 1,000			
Roundabout diameter (meter)	60			
Accepted gap (sec)	Motorcycle 3 sec / Car 4 sec / Truck 6 sec			
Desire speed (kph)	Motorcycle 50 kph / Car 70 kph / Truck 50 kph			
Surrogate Safety Assessment Model				
Time to collision (sec)	1.5 sec			
Post Encroachment Time (sec)	5 sec			
Conflicting speed (kph)	> 30 kph			

3.2 Model Development and Analysis

This study developed the simulation models for the base scenario (existing signalized intersection), and two work-zone traffic management scenarios including the roundabout (RAB) design, and the median U-turn (MUT) intersection design as shown in Figure 4. The models were developed using the PTV Vissim microscopic traffic simulation package and surrogate safety assessment model (SSAM) for evaluating operational and safety performances, respectively. The simulation models were calibrated by using observed data on traffic movement.

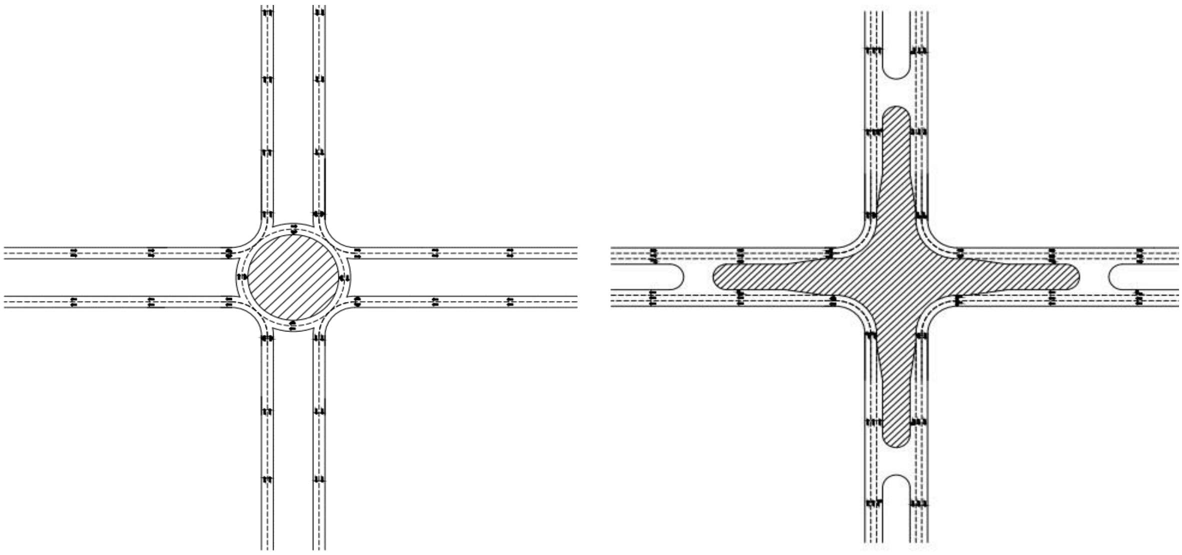

(a) Roundabout design (b) MUT intersection design

Figure 4 Alternative Intersection Designs for Work-Zone Traffic Management

The model analyses were performed on both operational and safety performance. The operational performance is analyzed in terms of vehicle delays, travel time, and average travel speed. The safety performance is analyzed in terms of the number of vehicle conflicts. A surrogate safety assessment model is used to record the number of possible conflicts by conflict types (i.e., rear-end conflicts and lane-change conflicts) that vehicles encounter when proceeding through the intersection. The simulation model and the surrogate safety assessment model for both temporary roundabout and temporary MUT intersection designs are shown in Figure 5 and Figure 6.

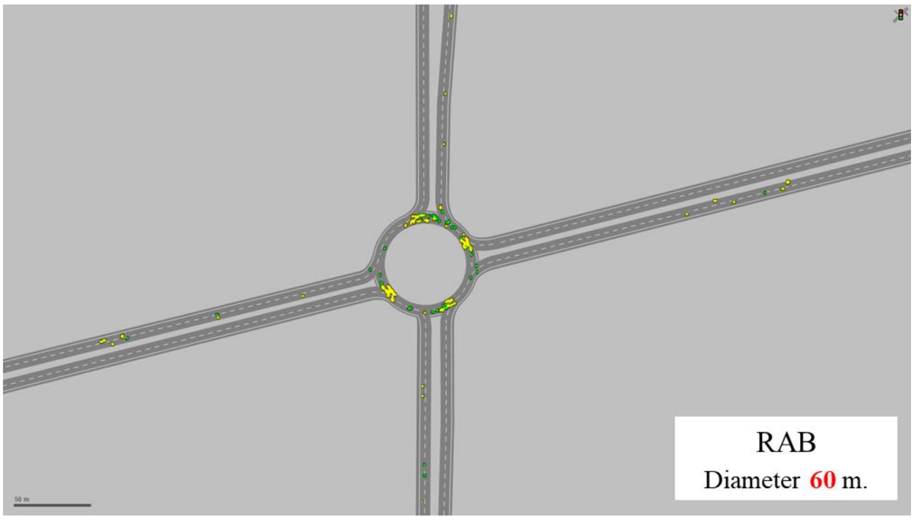

(a) Simulation model

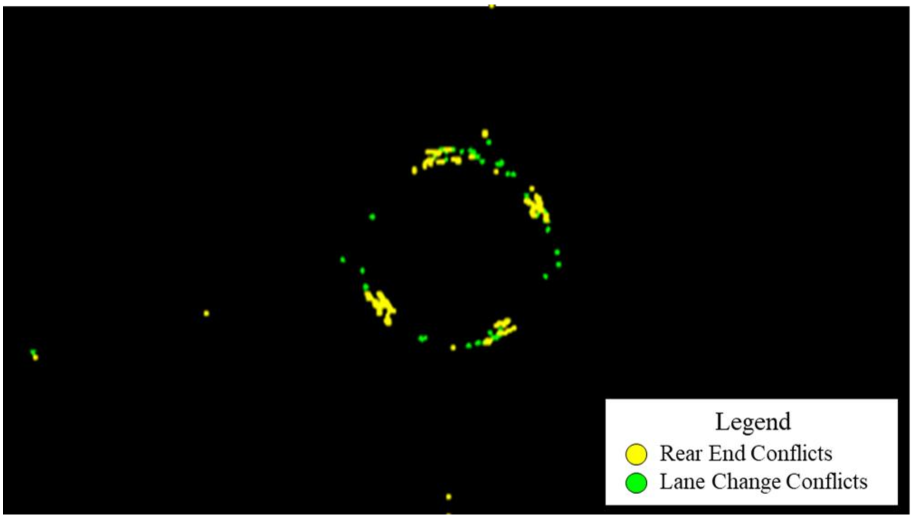

(b) Surrogate safety assessment model

Figure 5 Model Development for Temporary Roundabout Design

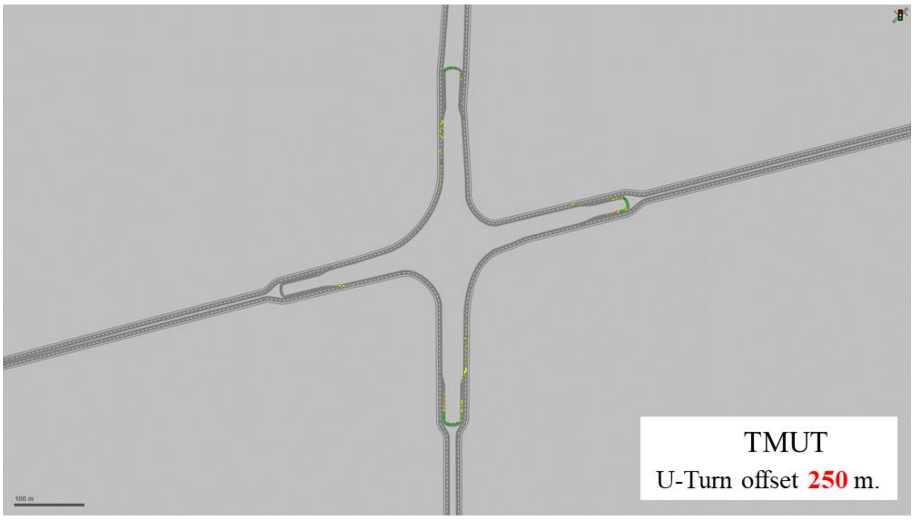

(a) Simulation model

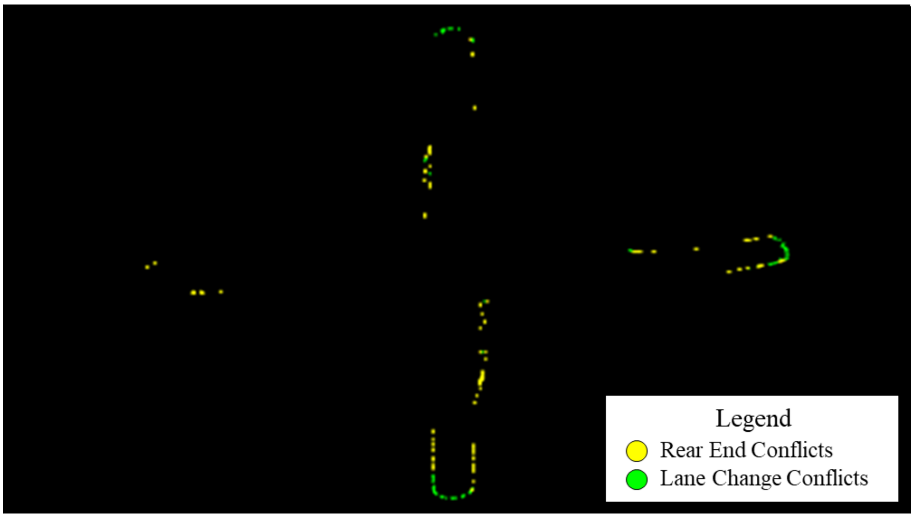

(b) Surrogate safety assessment model

Figure 6 Model Development for Temporary MUT Intersection Design

4. RESULTS

The results are presented in two sections. The first section analyzes design performance by comparing a baseline scenario with various work-zone traffic management scenarios, evaluating factors like speed, delay, and conflict rate. The second section presents a sensitivity analysis to recommend suitable U-turn offsets for intersections with varying traffic volumes. This study utilized PTV Vissim software to design and evaluate road improvement and transition schemes for the work zone area.

4.1 Design Performance

The results of the operational analysis indicated that the travel speed at the roundabout (RAB) was low, and the delay experienced by vehicles was high. This was attributed to the existing traffic volume being too high for the roundabout design, leading to significant traffic congestion at the intersection. On the other hand, the median U-turn (MUT) design demonstrated acceptable operational performance, particularly when the U-turn offset was minimized at 250 meters. The operational performance of the traffic management scenarios is shown in Table 2.

Table 2 Comparison of operational performance measures among different scenarios

Approach	Volume	Speed (kph)	Avg. Speed (kph)	Delay (s/veh)	Avg. Delay (s/veh)	%Change in Speed
Signalized Intersection						
NB	1,280	33.6	33.9	81.9	90.2	-
SB	1,121	31.1		96.3		
EB	1,068	36.7		86.6		
WB	2,076	33.9		93.9		
Roundabout						
NB	1,280	8.0	8.9	601.4	567.8	-73%
SB	1,121	7.9		607.4		
EB	1,068	10.9		447.4		
WB	2,076	9.1		611.1		
MUT @250 m offset						
NB	1,280	56.9	55.5	13.0	17.1	+64%
SB	1,121	55.5		16.6		
EB	1,068	54.8		20.7		
WB	2,076	55.1		17.9		
MUT @500 m offset						
NB	1,280	58.0	55.4	12.3	20.2	+64%
SB	1,121	54.5		23.2		
EB	1,068	56.2		19.0		
WB	2,076	53.8		23.9		
MUT @750 m offset						
NB	1,280	59.4	55.8	10.2	22.5	+65%
SB	1,121	54.1		30.7		
EB	1,068	57.8		15.6		
WB	2,076	53.5		29.2		
MUT @1,0000 m offset						
NB	1,280	58.3	56.3	18.2	26.4	+66%
SB	1,121	55.9		30.4		
EB	1,068	56.1		27.7		
WB	2,076	55.4		28.6		

In terms of safety performance, this study found that the MUT design with longer U-turn offsets led to fewer traffic conflicts than shorter U-turn offsets. The long U-turn offsets effectively reduced potential conflicts. It suggests that this design feature can be effective in improving safety at intersections. With the existing high traffic volume, the traffic conflicts at the RAB were low due to the congestion, indicating a positive safety performance. The safety performance of the traffic management scenarios is shown in Table 3.

Table 3 Comparison of safety performance measures among different scenarios

Approach	Volume	Conflict Rate by Approach			Conflict Rate by Intersection		
		Rear-end Conflict	Lane Change Conflict	Total	Rear-end Conflict	Lane Change Conflict	Total
Roundabout							
NB	1,280	0.014	0.028	0.042	0.011	0.017	0.027
SB	1,121	0.013	0.029	0.042			
EB	1,068	0.012	0.009	0.022			
WB	2,076	0.005	0.006	0.011			
MUT @250 m offset							
NB	1,280	0.031	0.026	0.057	0.022	0.019	0.040
SB	1,121	0.024	0.019	0.043			
EB	1,068	0.024	0.013	0.037			
WB	2,076	0.014	0.016	0.030			
MUT @500 m offset							
NB	1,280	0.029	0.025	0.054	0.017	0.016	0.034
SB	1,121	0.021	0.017	0.038			
EB	1,068	0.016	0.014	0.029			
WB	2,076	0.009	0.013	0.022			
MUT @750 m offset							
NB	1,280	0.028	0.022	0.050	0.016	0.014	0.030
SB	1,121	0.019	0.014	0.033			
EB	1,068	0.015	0.012	0.027			
WB	2,076	0.009	0.010	0.019			
MUT @1,0000 m offset							
NB	1,280	0.023	0.018	0.041	0.013	0.012	0.025
SB	1,121	0.017	0.013	0.030			
EB	1,068	0.008	0.010	0.018			
WB	2,076	0.007	0.009	0.016			

4.2 Sensitivity Analysis

The study conducted a sensitivity analysis on Median U-Turn (MUT) intersection models. The MUT intersection models were developed with four-lane major and minor roads, and the analysis considered different combinations of traffic volumes and U-turn offsets. Specifically, the traffic volumes ranged from 1,000 to 2,000 vehicles per hour per approach, and the U-turn offsets ranged from 250 to 1,000 meters. A total of 120 simulation tests were performed, which involved three sets of traffic volumes, four U-turn offsets, and ten simulation runs for each combination. According to Figure 7, the study found that longer U-turn offsets generally resulted in higher travel speeds and fewer conflicts, except for the 250-meter offset scenario. In this scenario, the traffic volume was particularly high, reaching 2,000 vehicles per hour per approach. This high traffic volume led to traffic congestion, which in turn resulted in low travel speeds and a high conflict rate. These findings suggest the significant impact of U-turn offset length on intersection performance. Furthermore, the study emphasizes the importance of considering both traffic volume and U-turn offset in intersection planning to mitigate congestion and enhance overall traffic flow dynamics.

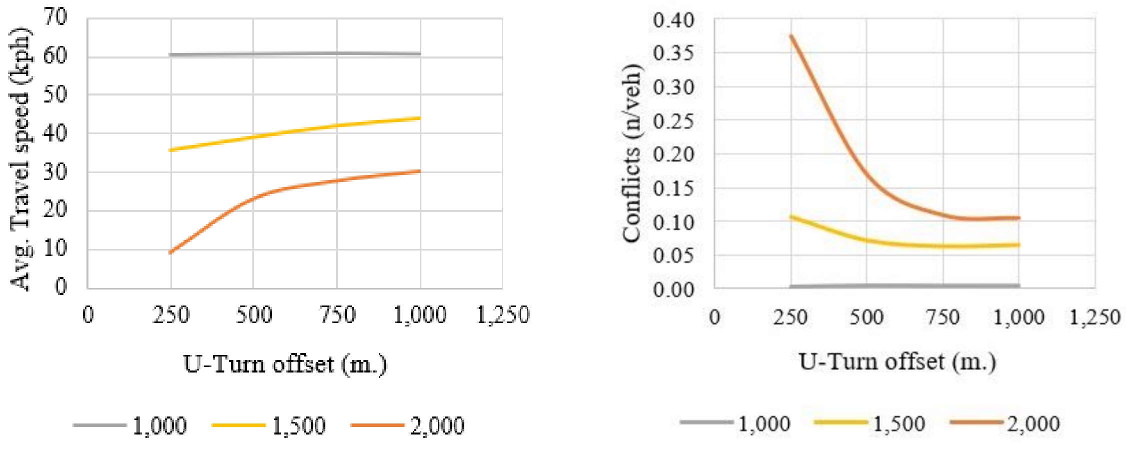

(a) Average travel speed

(b) Conflict rate

Figure 7 Sensitivity analysis of operational and safety performance with respect to U-Turn offsets

5. CONCLUSIONS

Managing traffic mobility and safety at major intersections during construction is a very challenging issue. When the intersection area is closed to traffic, all vehicles need to deviate from their routes. A temporary median U-turn intersection design, used as an alternative work-zone traffic management strategy, can enhance safety and mobility by redirecting all vehicles to the downstream median U-turn and traveling back to the intersection. This design provides longer spaces for merging and lane-changing conflicts.

This paper evaluates the operational and safety effects of the temporary MUT intersection at a real-world highway construction project using simulation analysis. The model analysis considers the trade-off between the increase in travel distance and the decrease in traffic conflicts. The study recommends the MUT intersection design to accommodate medium-to-high traffic volumes at major intersections, compared to the roundabout design. Additionally, the study proposes the locations of median U-turn openings, which can affect the cost of road users. This study will contribute valuable insights to the field of intersection design and work-zone traffic management, providing actionable recommendations for optimizing MUT intersections.

This study demonstrates the operational and safety analysis at a certain traffic composition and vehicle types including motorcycles and trucks. The assumption about the impact of these vehicle types is related to gap time. The motorcycles require less gap time to merge into traffic and change lanes compared to large vehicles albeit in a risky maneuver. A high proportion of motorcycles in mixed traffic suggests that the median U-turn offset should be shorter than what is typically proposed. Smaller gaps time can lead to more conflicts in terms of safety. In contrast, trucks require more gap time than other vehicles, leading to longer delay compared to the motorcycle. However, these assumptions require further study.

Moreover, this temporary MUT design is suitable for intersections where the highway has enough space between the medians (including raised and depressed medians) for both the temporary U-turn area and storage. If space in the median is limited, one lane may need to be designated for U-turn storage, potentially causing traffic bottlenecks. A narrow median width requires additional space for U-turn maneuvers, which can adversely affect overall traffic flow. In addition, the locations of existing median U-turn opening should be compromised in order to determine the cost-effective and near-optimal MUT intersection design.

6. ACKNOWLEDGMENTS

The authors would like to express their sincere gratitude to the Office of Highways (Chiang Mai) and the Department of Highways for their invaluable support and cooperation for the data.

7. REFERENCES

Alhadidi, T., Matarneh, S., & Tahoon, A. (2024). *The Feasibility and Operational Performance of Median U-Turn Intersections: A CRITIC Method*.

Barcelo, J. (2011). Models, Traffic Models, Simulation, and Traffic Simulation. In (pp. 1-62). https://doi.org/10.1007/978-1-4419-6142-6_1

FHWA. (2008). *Surrogate Safety Assessment Model and Validation: Final Report* (FHWA-HRT-08-051).

FHWA MEDIAN U-TURN INTERSECTION. (2014). (FHWA-SA-14-069).

Hasan, A., Jamal, A., Reza, I., Assi, K., & Anees, S. (2019). Using Microscopic Simulation-Based Analysis to Model Driving Behavior: A Case Study of Khobar-Dammam in Saudi Arabia. *Sustainability*, *11*. https://doi.org/10.3390/su11113018

He, Z., Zheng, L., Lu, L., & Guan, W. (2018). Erasing Lane Changes From Roads: A Design of Future Road Intersections. *IEEE Transactions on Intelligent Vehicles*, *3*(2), 173-184. https://doi.org/10.1109/TIV.2018.2804164

Jagannathan, R. (2007). Synthesis of the median U-turn intersection treatment, safety, and operational benefits.

Kronprasert, N., Sutheerakul, C., Satiennam, T., & Luathep, P. (2021). Intersection Safety Assessment Using Video-Based Traffic Conflict Analysis: The Case Study of Thailand. *Sustainability*, *13*, 12722. https://doi.org/10.3390/su132212722

Lueanpech, P., Buasap, A., & Masmek, S. (2023). *Traffic Impact Analysis of Temporary Median U-Turn on Highway No. 35 during The Motorway No. 82 (M82) Construction Project, Thailand*.

Nasuha, N., & Rohani, M. (2018). Overview Of Application Of Traffic Simulation Model. *MATEC Web of Conferences*, *150*, 03006. https://doi.org/10.1051/matecconf/201815003006

Nopadon, K., Pavee, K., & Wachira, W. (2020). SAFETY AND OPERATIONAL ANALYSIS FOR MEDIAN U-TURN INTERSECTIONS IN THAILAND. *GEOMATE Journal*, *18*(68), 156-163. https://geomatejournal.com/geomate/article/view/557

Shao, Y., Han, X., Wu, H., Shan, H., Yang, S., & Claudel, C. G. (2019). Evaluating the sustainable traffic flow operational features of an exclusive spur dike U-turn lane design. *PLoS One*, *14*(4), e0214759. https://doi.org/10.1371/journal.pone.0214759

Shirke, C., Bhaskar, A., & Chung, E. (2019). Macroscopic modelling of arterial traffic: An extension to the cell transmission model. *Transportation Research Part C: Emerging Technologies*, *105*, 54-80. https://doi.org/https://doi.org/10.1016/j.trc.2019.05.033

iCHE
BANGKOK 2024

iCHE
BANGKOK 2024